Practical Food Rheology

Practical Food Rheology: An Interpretive Approach
Edited by Ian T. Norton, Fotios Spyropoulos and Philip Cox
 ISBN: 978-1-405-19978-0

Practical Food Rheology

An Interpretive Approach

Edited by

Ian T. Norton, Fotios Spyropoulos and Philip Cox

Chemical Engineering
University of Birmingham
Edgbaston, Birmingham
B15 2TT, UK

WILEY-BLACKWELL

A John Wiley & Sons, Ltd., Publication

This edition first published 2011 © 2011 by Blackwell Publishing Ltd.

Blackwell Publishing was acquired by John Wiley & Sons in February 2007. Blackwell's publishing programme has been merged with Wiley's global Scientific, Technical, and Medical business to form Wiley-Blackwell.

Registered office
John Wiley & Sons Ltd, The Atrium, Southern Gate, Chichester, West Sussex, PO19 8SQ, UK

Editorial offices
9600 Garsington Road, Oxford, OX4 2DQ, UK
The Atrium, Southern Gate, Chichester, West Sussex, PO19 8SQ, UK
2121 State Avenue, Ames, Iowa 50014-8300, USA

For details of our global editorial offices, for customer services and for information about how to apply for permission to reuse the copyright material in this book please see our website at www.wiley.com/wiley-blackwell.

Library of Congress Cataloging-in-Publication Data

Practical food rheology : an interpretive approach / edited by Ian T. Norton, Fotios Spyropoulos and Philip Cox.
p. cm.
Includes bibliographical references and index.
ISBN 978-1-4051-9978-0 (hardback : alk. paper)
1. Food. 2. Rheology. I. Norton, Ian T. II. Spyropoulos, Fotios. III. Cox, Philip.
TP370.P62 2011
664.02–dc22

2010022798

A catalogue record for this book is available from the British Library.

This book is published in the following electronic formats:
ePDF (9781444391046);
Wiley Online Library (9781444391060);
ePub (9781444391053)

Set in 11/13 pt Times by Aptara® Inc., New Delhi, India

1 2011

Contents

Preface xi
Contributors xiii

1 Introduction – Why the Interpretive Approach? 1
Niall W. G. Young
1.1 Rheology – What is in it for me? 1
1.1.1 Case study 3
References 6

2 Viscosity and Oscillatory Rheology 7
Taghi Miri
2.1 Introduction 7
2.2 Food rheology 8
2.3 Directions of rheological research 8
2.3.1 Phenomenological rheology or macrorheology 9
2.3.2 Structural rheology or microrheology 9
2.3.3 Rheometry 9
2.3.4 Applied rheology 10
2.4 Steady-state shear flow behaviour: viscosity 10
2.4.1 Rheological models for shear flow 11
2.4.2 Wall slip 15
2.5 Viscoelasticity and oscillation 16
2.5.1 Oscillatory testing 18
2.6 Process, rheology and microstructural interactions 20
2.7 Rheology of soft solids 20
2.7.1 Capillary rheometer 21
2.7.2 Squeeze flow rheometer 22
2.8 Measuring instruments – practical aspects 23
2.8.1 Choosing the right measuring system 23
References 26

3 Doppler Ultrasound-Based Rheology 29
Beat Birkhofer
3.1 Introduction 29
3.1.1 Overview 29
3.1.2 History of ultrasonic velocimetry 30
3.1.3 Existing literature on UVP-based rheometry 31
3.2 Ultrasound transducers 38

3.3 Flow adapter 39
3.3.1 Doppler angle 40
3.4 Acoustic properties 41
3.4.1 Propagation 41
3.4.2 Attenuation 42
3.4.3 Sound velocity 42
3.4.4 Scattering 43
3.4.5 Backscattering 43
3.5 Electronics, signal processing and software 45
3.5.1 Electronics 45
3.5.2 Signal processing and profile estimation 45
3.5.3 Software 45
3.6 Pipe flow and fluid models 46
3.6.1 Gradient method or point-wise rheological characterisation 46
3.6.2 Power law fluid model 47
3.6.3 Herschel–Bulkley fluid model 48
3.6.4 Other models 48
3.7 Rheometry 49
3.7.1 Averaging effects at the pipe wall 49
3.7.2 Fitting 49
3.7.3 Gradient method 50
3.8 Examples 50
3.8.1 Carbopol solution 50
3.8.2 Suspension of polyamide in rapeseed oil 52
3.9 Summary 54
References 54

4 Hydrocolloid Gums – Their Role and Interactions in Foods 61
Tim Foster and Bettina Wolf
4.1 Introduction 61
4.2 Behaviour of hydrocolloid gums in solution 61
4.3 Hydrocolloid gelation and gel rheology 68
4.4 Hydrocolloid–hydrocolloid interactions 69
4.5 Hydrocolloids in foods – role and interactions 77
References 79

5 Xanthan Gum – Functionality and Application 85
Graham Sworn
5.1 Introduction 85
5.2 Xanthan molecular structure and its influence on functionality 85
5.3 The conformational states of xanthan gum 91
5.4 Food ingredients and their effects on xanthan gum functionality 93
5.4.1 Salts 93
5.4.2 Acids (pH) 95
5.4.3 Xanthan and proteins 99
5.4.4 Xanthan and starch 101

5.5 Food processing and its impact on xanthan gum functionality 101
5.5.1 Thermal treatment 101
5.5.2 Homogenisation 102
5.5.3 Freezing 103
5.6 Food structures 104
5.6.1 Emulsions 104
5.6.2 Gels 105
5.7 Applications 106
5.8 Future trends 108
Acknowledgements 110
References 110

6 Alginates in Foods 113
Alan M. Smith and Taghi Miri
6.1 Alginate source and molecular structure 113
6.2 Alginate hydrogels 115
6.3 Alginic acid 119
6.4 Alginate solutions 120
6.5 Enzymatically tailored alginate 121
6.6 Alginates as food additive 122
6.6.1 Gelling agent 123
6.6.2 Thickening agent 124
6.6.3 Film-forming agent 125
6.6.4 Encapsulation and immobilisation 125
6.6.5 Texturisation of vegetative materials 126
6.6.6 Stabiliser 126
6.6.7 Appetite control 127
6.6.8 Summary 128
References 129

7 Dairy Systems 133
E. Allen Foegeding, Bongkosh Vardhanabhuti and Xin Yang
7.1 Introduction 133
7.2 Fluid milk 134
7.2.1 Rheological properties of milk 134
7.2.2 Measurements of the rheological properties of milk 139
7.2.3 Factors influencing milk rheological properties 141
7.2.4 Correlating rheological properties of milk to sensory perceptions 145
7.2.5 Process engineering calculation 146
7.3 Solid cheese 147
7.3.1 Small amplitude oscillatory tests 148
7.3.2 Large strain rheological analysis 152
7.3.3 Creep and stress relaxation 157
7.4 Rheological properties of semi-solid dairy foods 159
7.4.1 Flow properties 159

7.4.2 Yield stress 163
7.4.3 Viscoelastic properties of semi-solid dairy products 164
7.5 Effect of oral processing on interpretation of rheological measurement 165
References 167

8 Relationship between Food Rheology and Perception 173
John R. Mitchell and Bettina Wolf
8.1 Introduction 173
8.2 Rheology and thickness perception 174
8.3 Rheology and flavour perception 176
8.4 Mixing, microstructure, gels and mouthfeel 179
8.4.1 Mixing 179
8.4.2 Microstructure 181
8.4.3 Mouthfeel 184
8.4.4 Gels 185
8.5 Beyond shear rheology 187
8.6 Conclusions 190
Acknowledgements 190
References 190

9 Protein-Stabilised Emulsions and Rheological Aspects of Structure and Mouthfeel 193
Fotios Spyropoulos, Ernest Alexander K. Heuer, Tom B. Mills and Serafim Bakalis
9.1 Introduction 193
9.2 Processing and stability of emulsions 194
9.2.1 Instabilities in emulsions 194
9.2.2 Protein functionality at liquid interfaces 196
9.2.3 Protein-stabilised oil-in-water emulsions – Effect of aqueous phase composition 200
9.2.4 Effect of processing 203
9.3 Oral processes 203
9.3.1 Different stages and phenomena during oral processing 204
9.3.2 Fluid dynamics during oral processing 206
9.3.3 Interactions with saliva 207
9.3.4 Interaction with oral surfaces 208
9.4 *In vitro* measurements of sensory perception 209
9.5 Future perspectives 213
References 214

10 Rheological Control and Understanding Necessary to Formulate Healthy Everyday Foods 219
Ian T. Norton, Abigail B. Norton, Fotios Spyropoulos, Benjamin J. D. Le Révérend and Philip Cox
10.1 Introduction 219

10.2 Design and control of material properties of foods inside people 221
10.2.1 Oral perception of foods 221
10.2.2 Food in the stomach 226
10.2.3 Food in the intestine 228
10.3 Reconstructing foods to be healthy and control dietary intake 230
10.3.1 Use of emulsions as partial fat replacement 231
10.3.2 Duplex emulsions 232
10.3.3 Fat replacement with air-filled emulsion 235
10.3.4 Sheared gels (fluid gels) 238
10.3.5 Water-in-water emulsions 241
10.3.6 Self-structuring systems 245
10.4 Conclusions 249
References 249

Index 254

A colour plate section falls between pages 146 and 147

Preface

For many decades the interplay between the rheology, texture and overall structure of foods and their functionality has been extensively studied. Recently, research in this area has received increasing interest not only because of the consumer-driven need to 're-invent' certain foods labelled as 'unhealthy' (high fat, sugar, salt) but also because of industrial desire to introduce foods with 'novel' functionalities. Consequently, there have been a growing number of studies focusing on the complex interplay between food structure and rheological and textural behaviour and food functionality. In addition, besides its huge potential to change the way we design and formulate foods in the future, this research field has proved to be extremely exciting as it brings together scientists from a wide range of different disciplines, including food engineering, chemistry, physics, sensory sciences, physiology, nutrition and even medicine.

Many of the current food rheology books tend to be aimed either at the beginner or at the specialist, leaving practitioners either short of the information they require, or feeling rather confused by an overwhelming display of equations and mathematics. On the other hand, many food rheology books approach the subject from the individual food ingredient standpoint, fitting data to various mathematical models to then extrapolate the behaviour to that of the overall food structure. Often, what is required is a simpler approach, i.e. a practical interpretative look at food rheology and how it relates to a given system. This approach will guide the reader, regardless of whether he/she is an industrial food developer/rheologist, student, or academic, through the interpretation of rheological data in a clear and concise manner and link these to the actual perceived functionality of the food. The functionality may relate to texture, structure and mouthfeel, and may result as a function of temperature, pH, flocculation, concentration effects and mixing. The aim of this book is to fill this gap and consider how rheology can be used to select the right ingredients and design using these as food structure having a required sensory impact. This book meets its aim by providing a comprehensive overview of some of the most important research areas currently associated with what is broadly termed as 'food rheology'. This is achieved by firstly giving an overview of those techniques used to monitor/measure rheological properties, then secondly by considering

the links between food microstructure and rheological/textural properties, and finally by discussing how such properties can be used to alter texture and product performance, thus leading to the design of functional foods. Through the collection of chapters from recognised experts in the field of food rheology, microstructure mechanics and engineering, and food texture, the reader will be guided through the interpretative 'forest' of rheological data and hopefully be led to enlightenment and inspiration for their own work.

We thank all the authors of each of the chapters in this book for taking valuable time out of their already busy schedules to contribute to this project. We also thank all the excellent, editorial and other, staff at Wiley-Blackwell for their invaluable efforts and help that have made this book possible. Lastly, we thank our families, friends and colleagues for all their support and help throughout the process of editing this book.

Contributors

Serafim Bakalis
School of Chemical Engineering
College of Engineering &
Physical Sciences
University of Birmingham
Edgbaston, Birmingham
B15 2TT, UK

Beat Birkhofer
Laboratory of Food Process
Engineering
Institute of Food Science and
Nutrition
ETH Zurich
Schmelzbergstrasse 7, 8092
Zurich, Switzerland

Philip Cox
School of Chemical Engineering
College of Engineering &
Physical Sciences
University of Birmingham
Edgbaston, Birmingham
B15 2TT, UK

E. Allen Foegeding
North Carolina State University
Raleigh
NC 27695, USA

Tim Foster
Food Sciences
University of Nottingham
Sutton Bonington
LE12 5RD, UK

Ernest Alexander K. Heuer
School of Chemical Engineering
College of Engineering &
Physical Sciences
University of Birmingham
Edgbaston, Birmingham
B15 2TT, UK

Tom B. Mills
School of Chemical Engineering
College of Engineering &
Physical Sciences
University of Birmingham
Edgbaston, Birmingham
B15 2TT, UK

Taghi Miri
School of Chemical Engineering
College of Engineering &
Physical Sciences
University of Birmingham
Edgbaston, Birmingham
B15 2TT, UK

John R. Mitchell
School of Biosciences
University of Nottingham
Division of Food Sciences
Sutton Bonington
LE12 5RD, UK

Abigail B. Norton
Ingram Building
School of Physical Sciences
University of Kent
Canterbury
CT2 7NH, UK

Ian T. Norton
School of Chemical Engineering
College of Engineering &
Physical Sciences
University of Birmingham
Edgbaston, Birmingham
B15 2TT, UK

Benjamin J. D. Le Révérend
School of Chemical Engineering
College of Engineering &
Physical Sciences
University of Birmingham
Edgbaston, Birmingham
B15 2TT, UK

Alan M. Smith
School of Chemical Engineering
College of Engineering &
Physical Sciences
University of Birmingham
Edgbaston, Birmingham
B15 2TT, UK

Fotios Spyropoulos
School of Chemical Engineering
College of Engineering &
Physical Sciences
University of Birmingham
Edgbaston, Birmingham
B15 2TT, UK

Graham Sworn
DANISCO France SAS
20 rue Brunel, 75017 Paris
France

Bongkosh Vardhanabhuti
North Carolina State University
Raleigh
NC 27695, USA

Bettina Wolf
Food Sciences
University of Nottingham
Sutton Bonington
LE12 5RD, UK

Xin Yang
North Carolina State University
Raleigh
NC 27695, USA

Niall W. G. Young
Danisco A/S, Edwin Rahrs Vej
38, DK 8220, Brabrand, Denmark

1 Introduction – Why the Interpretive Approach?

Niall W. G. Young

The interpretive approach is a new way of looking at rheology, and it stems from the benefits to be gained from the multidisciplinary approach (Wassell and Young, 2007). Sole focus on single aspects – viscosity, shear rate and shear stress – can blink the view of the data and cause either misconstrued interpretations or incomplete analysis of the system. The interpretive approach, whilst placing demands on the rheologist, however allows for a fuller interpretation and analysis of the system. The rheologists must maintain their scientific foundation, but also possess the skills of the journalist and studio presenter. In short, today's rheologists are tasked with being required to deliver their message to the professional and layman in clear, concise terms. The interpretive approach is the key to value creation for the industrial rheologist's customers, or the academic's funding applications, and as such equips the rheologist with 'alchemic' powers to turn 'worthless' rheological graphs into 'gold'. This sentiment is echoed in the analogy that, for most food ingredient and food producing companies, rheology is not a key business, but it is the key to the business. Successful implementation of the interpretive approach into the role of the industrial rheologist (Young, 2007) ultimately pays dividends for the company. But what is rheology?

1.1 RHEOLOGY – WHAT IS IN IT FOR ME?

Classically, the term 'rheology' dates back to the late 1920s and is credited to Bingham, who expanded on the ancient Greek philosophers' musings of παντα ρει or everything flows. The definition of rheology therefore came to be the study of the deformation and flow of matter. Barnes *et al*. (1989) claim, quite rightly, that rheology is a difficult subject, and one can lose one's audience quickly. Focusing on the key words of the definition in isolation – deformation, flow and matter – suggests

Practical Food Rheology: An Interpretive Approach
Edited by Ian T. Norton, Fotios Spyropoulos and Philip Cox
 ISBN: 978-1-405-19978-0

that rheology is, by nature, multidisciplinary. Hence, it is rooted in mathematics, physics, mechanics, but it is also rooted in life, and therefore everybody has fundamental experience with the basic concepts of rheology. Here, one can think of the daily non-food application of shampoo to one's hand before rubbing it into the scalp. Subconsciously, one measures the viscosity as the shampoo moves between the fingers and, quite wrongly, associates this viscosity with quality – the thicker the shampoo, the better it cleans one's hair. Hence, most shampoos on the market are viscous in nature. It is this 'human rheometer' experience, which fills us with perceptions as to what the world around us should feel like, that drives the rigorous rheological control of materials. This perception is so strong that if the rheological control fails we enter into the abnormal, and the world about us feels wrong. Demands are therefore placed on the food industry to control the flow and viscoelastic properties of all our foods as much for practical reasons as for upholding consumer perceptions.

Achieving this rheological control over the food materials requires a dialogue between the rheologist and the food developer, and for them to agree on the conditions of the measurements to be made. Therefore, this prompts a list of questions that need answers before the measurements can be started:

(i) *Why should the measurement be performed, and to what aim?* Here, the purpose and need of the measurement are established, and begin to shape the manner in which the results can be used. Decision as to small or large deformation is taken, as is holding temperature constant or varied, or stress or shear rate, or frequency of oscillation. Does the measurement require a viscosity curve or a viscoelastic profile? Essentially, the experimental set-up is founded in this stage, and competent understanding here leads to a greater degree of first-time success with the measurement.

(ii) *Are there any special criteria that should be considered?* One has probed the manner in which the material is to be tested. But now consideration of the material itself is required, i.e. does the material undergo a state change as a function of temperature? This could have implications as to the choice of measuring geometry. Other examples could include the effect of pH over time; does the material have particles (large or small) present; how fast should temperature or shear rate be ramped to reflect reality or account for temperature or shear gradients? It is worth noting that we may not be interested in obtaining measurements in the steady state, because this may not describe the 'reality' we wish to explain, and this can raise questions as to the validity of results. Thus, through additional fine-tuning to the measurement profile, positive

influence is exerted on the results. This can be thought of as an extra lens available to the magnifying glass analogy to sharpen the image.

(iii) *How will the results be used?* Here, one considers the final audience who will receive the results, should they be journal article readers, conference delegates/fellow rheologists, colleagues, customers or the layman. Whichever group, the intended audience alters the manner in which the data are presented, to what level it is discussed and which form the interpretive style will take. This requires the rheologist to possess sound and robust communication skills to be adept at presenting material in the different styles needed.

Assimilating all the information from the questions asked earlier, the rheologist should now be able predict what the outcome of the results will look like. This can be sketched out as a guide, and if the measured results match the predicted results, then the theory and set-up of the rheometer were likely correct. From these basic tenets, the rheologists are now ready to begin measuring their sample, and subsequently explore their data to explain their findings using the interpretive method. In order to demonstrate this approach, a worked case study is presented in the following section.

1.1.1 Case study

Wine gums and the art of making them are governed by the setting temperature of the system. High-ester pectin can be used to make excellent wine gums, but the setting temperature is high, typically around 70–80°C. This in itself presents possible application limits on the use of wine gum syrup, i.e. it makes filling it into chocolate cups unrealistic. How can this problem be solved, quantified and controlled?

High-ester pectin sets in the presence of a co-solute (sugar) as a function of temperature or pH (acidity). Cold setting of pectin is possible and has been documented, but has focused on low-ester pectin (Gilsenan *et al*., 2000; Lootens *et al*., 2003), typically not used in wine gums. Controlling the acidification of the wine gum mass by means of glucono-δ-lactone (GDL) allows gelation of high-ester pectin to occur over ambient temperatures (Madsen and Thulin, 2002; Young, 2007).

Discussion now, as regards the rheology, centred on how to measure this gelation profile. Small deformation oscillation is performed with constant small strain; within the linear viscoelastic region, temperature is kept constant – room temperature (23°C) – and the frequency of oscillation is kept constant, 0.5 Hz.

Predictions were made of the type of curve to be seen. Focusing on the phase angle curve against time, we expect to see a high phase angle

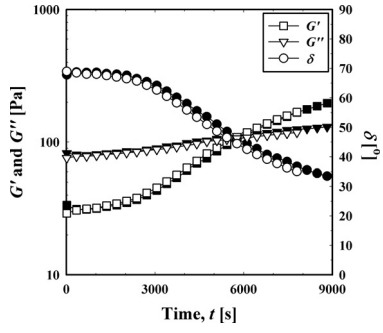

Fig. 1.1 The gelation profile of high-ester pectin with 2% GDL at 23°C. Open and closed symbols indicate replicate experiments. For a colour version of this figure, please see the colour plate section.

at time zero, forming an initial plateau – parallel to the *x*-axis – before dropping off as time progresses, and finally showing signs of levelling off, again parallel to the *x*-axis. G' will start below G' with the gap between them being constant. G' and G'' then converge and cross, and finally deviate from each other until there is again a constant gap. The real results are given in Fig. 1.1.

Immediately apparent is that the predicted results conform to the actual results obtained, suggesting good agreement between theory – measurement – and material. Interpretation of the graph allows characterisation of the gelling process: from time 0 to 1800s little or no structure formation is occurring. The 1800s mark the onset of gelation, which proceeds until 5500s, where the G' and G'' profiles cross, the phase angle value is 45°, and this is termed the gel point. After 5500s, the gel is building in structure and the graph does not extend far enough to show the gelled plateau.

In terms of the material and what this means for the customer, one can reinterpret the graph to say that between 0 and 1800s the wine gum syrup can here be pumped, moved and deposited into the chocolate cups or moulds. Between 1800s and 5500s, it is recommended that the material is not disturbed, so that the gel is allowed to form. Beyond 5500s, the system has set, and a fruit flake, chocolate bead or other material can be deposited on the surface where it will remain without sinking into the wine gum.

Questions may now arise from the customer about the time allowed for filling and depositing, namely 1800s. Could this be altered to optimise the process? The gelation process is controlled by the speed at which the pH is reduced, and therefore governed by the concentration of GDL. Hence, by varying the GDL concentration, the initial 1800s plateau can be shortened or extended. This can be monitored simply by following the pH decrease over time immediately after the addition of

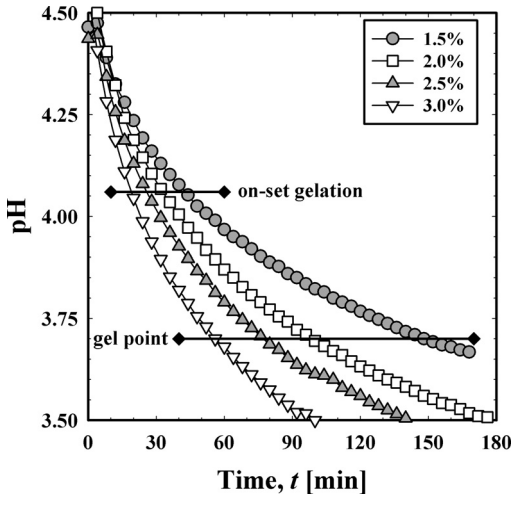

Fig. 1.2 pH curves versus time for varying GDL dosages at 23°C indicating the onset of gelation and gel point taken from rheology measurements. For a colour version of this figure, please see the colour plate section.

GDL to the system, simultaneously with the rheology measurements. Fig. 1.2 presents the pH reduction curves over time for four GDL concentrations. The beauty and simplicity of this pH reduction measurement is that, after coupling to and aligning with the rheology measurements, it allows the gelation process to be accurately followed using only a pH meter and a stopwatch – equipment every confectionery manufacturer will have access to. Thus, the need for expensive rheological equipment investments is not required.

This example demonstrates two important points, which highlight the elegance and simplicity of the interpretive approach, and how this benefits food rheology:

(i) Simple measurements can lead to extensive process characterisation and material understanding.
(ii) Rheological measurements can be monitored by simpler techniques, allowing the non-specialist to manage the process.

Step I is the initial value creation step where earnings are generated. Here, the process can be described and the response of the material under investigation during the process is explained. Such knowledge brings understanding and therefore creates flexibility, which in turn generates earnings. Step II demonstrates that simpler methods can be used to follow rheological processes – given the right conditions – which allows for ease of operation and does not require extensive investments. This is particularly beneficial in industry. Therefore, industry benefits from the

interpretive approach through increased process understanding, leading to flexibility and boosted earnings. Academia, in turn, benefits from the interpretive approach through demonstrating their ability to deliver the knowledge and the understanding to the industry, either directly or through scientific and popular publications. Indeed, a successful interpretive approach is a key to successful knowledge transfer schemes of the university.

This book, with chapters on diverse topics including ultrasound-based rheology, hydrocolloids, dairy systems, emulsions and the link between rheology control and health, aims to provide the readers with the tools and the evidence to take on the interpretive role in their own work and to see the difference.

REFERENCES

Barnes, H.A., Hutton, J.F. and Walters, K. (1989) *An Introduction to Rheology*. Amsterdam, the Netherlands: Elsevier.

Gilsenan, P.M., Richardson, R.K. and Morris, E.R. (2000) Thermally reversible acid-induced gelation of low-methoxy pectin. *Carbohydrate Polymers* **41**, 339–349.

Lootens, D., Capel, F., Durand, D., Nicolai, T., Boulenguer, P. and Langendorff, V. (2003) Influence of pH, Ca concentration, temperature and amidation on the gelation of low methoxyl pectin. *Food Hydrocolloids* **17**, 237–244.

Madsen, O.T. and Thulin, R. (2002) Cold setting of HE pectin. Patent, PCT 0242 US 60/428747.

Wassell, P. and Young, N.W.G. (2007) Food applications of trans fatty acid substitutes. *International Journal of Food Science and Technology* **42**, 503–517.

Young, N.W.G. (2007) Industrial rheology applied: the role of the rheologist. *Food Science and Technology* **21**, 21–23.

2 Viscosity and Oscillatory Rheology

Taghi Miri

2.1 INTRODUCTION

The work of the polymaths Hooke and Newton forms the basis of the field of rheology. In 1678, Hooke offered a description for an elastic solid. Nine years later, Newton's famous hypothesis on fluid behaviour appeared in his *Principia* (Walters, 1999; Barnes, 2000).

All materials have rheological properties, and the area is relevant to many fields of study such as concrete technology (Skalny, 1982; Banfill and Tattersall, 1983), soil mechanics (Keedwell, 1984; Ene and Cristescu, 1988), plastics processing (Lenk, 1968; Prentice, 1995; Shenoy and Saini, 1996), polymers and composites (Ferry, 1980; Advani, 1994; Shenoy, 1999; Gupta, 2000), blood (Ghista, 1979; Platt, 1988), bioengineering (Fryer *et al*., 1985), electrorheology (Williams *et al*., 1993), cosmetics and toiletries (Sherman, 1970) and food (Muller Hans, 1973; DeMan, 1976; Prentice, 1984; Bourne, 1992; Rao and Steffe, 1992; Shoemaker and Borwankar, 1992; Lareo *et al*., 1997; Mankad and Fryer, 1997; Rao, 1999; Kasapis *et al*., 2000). The focus of this chapter is on food rheology, where understanding of flow behaviour is crucial for optimising product development, processing methodology and final product quality (Tabilo-Munizaga and Barbosa-Cánovas, 2005).

There is a large body of general food rheology literature; examples include the work of Muller Hans (1973), Rao (1977), Baird (1981), Rao and Steffe (1992), Lareo *et al.* (1997), Mankad and Fryer (1997), Lareo and Fryer (1998), Gallegos and Franco (1999), Rao (1999), Kasapis *et al.* (2000), Tabilo-Munizaga and Barbosa-Cánovas (2005), Genovese *et al.* (2007) and Fischer *et al.* (2009).

Practical Food Rheology: An Interpretive Approach
Edited by Ian T. Norton, Fotios Spyropoulos and Philip Cox
 ISBN: 978-1-405-19978-0

2.2 FOOD RHEOLOGY

Foods can be classified in different ways, such as solids, gels, homogeneous liquids, suspensions of solids in liquids and emulsions (Gallegos and Franco, 1999; Fischer *et al.*, 2009). Foods that do not retain their shape but take the shape of their container are fluids. Such materials may contain amounts of dissolved or suspended solids, and exhibit non-Newtonian behaviour (described in detail in the later parts of the chapter), which classifies them as semi-fluids (Baird, 1981; Decindio, 1994). Many of these exhibit both viscous and elastic properties and can be described as viscoelastic materials. In contrast, if fluids contain dissolved low-molecular-weight compounds (e.g. sugars) and no polymer or insoluble solids, they may show Newtonian behaviour (Rao, 1977). However, a small amount ($\sim$1%) of a dissolved polymer can substantially increase the viscosity and alter material behaviour from Newtonian to non-Newtonian (Blair, 1954).

Rheometry helps in understanding the responses of food structure to applied forces or deformation and also provides information on the dependence of food structure on overall composition and interaction between the components (Shoemaker and Borwankar, 1992). Many approaches to rheometry are possible depending on what is expected from the measurements; i.e. is it for prediction of flow behaviour of material in a process or for characterising the material without damaging its structure?

The classification of rheological behaviour and the measurement of rheological properties of fluid foods have been reviewed by Blair (1954), Muller Hans (1973), Baird (1981), Ross-Murphy (1984), Borwankar (1992), Rao and Steffe (1992), Stanley and Taylor (1993), Decindio (1994), Steffe (1996), Lareo *et al.* (1997), Mankad and Fryer (1997), Rao (1977, 1999, Lareo and Fryer (1998), Kasapis *et al.* (2000) and many others. Techniques for measuring rheological properties, especially flow properties, are covered by Van Wazer *et al*. (1963) and those of viscoelastic properties by Whorlow (1980) and Macosko (1994). Rao (1999) in his book discussed in detail the rheological properties of fluid and semi-fluid foods.

2.3 DIRECTIONS OF RHEOLOGICAL RESEARCH

Ferguson and Kemblowski (1991) have described the focus in rheological research, in terms of four branches: (i) phenomenological rheology, (ii) structural rheology, (iii) rheometry and (iv) applied rheology.

2.3.1 Phenomenological rheology or macrorheology

This domain of rheology is concerned with real bodies on a macroscopic level, and disregards the molecular nature of the material. Therefore, the equations describing the observed phenomena contain coefficients called rheological parameters, which have to be determined experimentally. Phenomenological rheology tries to explain the complex phenomena happening during the deformation of real bodies, and to formulate rheological equations of state that define these.

2.3.2 Structural rheology or microrheology

Structural rheology is concerned with the connections between the bulk rheological properties of a substance and its actual microscopic structure. It tries to predict the properties of macromolecular compounds based on mathematical models of structure and dynamics. In microrheology, the rheological behaviour of two-phase and multiphase systems is derived from the known rheological behaviour of their elements. However, the actual composition of dispersed systems makes a mathematical approach unworkable outside the simplest of cases. In these, a mechanical model replaces the unknown structure and is assumed to behave in an analogous fashion. Such models consist of different elements such as elastic springs (Hookean springs), viscous dashpots (Newtonian dashpots) or a combination of these two, but in general these have no exact counterpart within the real material. Structural rheology has been successful in describing the behaviour of solid elastomers and dilute polymer solutions. However, it has been hardly applicable to concentrated solutions.

2.3.3 Rheometry

Rheometry is concerned with the quantitative determination of rheological properties of the investigated system in an experimental way. There are five principal types of rheometers: (i) the concentric cylinder or coaxial cylinder rotary viscometer, (ii) the rotating cylinder in an 'infinite' medium, (iii) the cone-and-plate (and plate–plate) rotary rheometer, (iv) the vane rheometer (v) and the capillary tube rheometer. The first four rheometers are usually applied to obtain rheological properties of liquids or fairly soft pastes (Nielsen, 1977). The last can be used to measure the rheology of stiffer (more rigid) pastes. In theory, fundamental rheological properties should be independent of the instruments on which they are measured, so different instruments should yield the same results. However, this is an ideal concept and different instruments rarely give identical results. Therefore, it is important to distinguish the

true rheological material properties from the subjective (empirical and generally instrument-dependent) material characterisations. Rheometry can be broadly divided into two categories:

(i) *Steady shear characterisation.* This provides viscosity data of fluid materials and/or simulates a process shear rate. It provides information about the material's response to varying flow rate regimes by measuring its viscosity, which is usually shear-rate dependent.
(ii) *Dynamic or oscillatory shear.* This provides structural information, time dependency and temperature stability/dependency of the material. It facilitates the distinction between elastic and viscous contributions to a measured stress as a function of frequency by measuring storage and loss moduli. These tests can also be non-destructive to the structure of the samples, as the amount of strain applied to the sample is very small.

2.3.4 Applied rheology

Applied rheology is concerned with deformation and flow of complex material in geometries of practical interest. Many problems of this kind occur in chemical and process engineering, such as flow of non-Newtonian fluids in channels of various geometries, flow through granular beds, mixing of non-Newtonian fluids and extrusion (Tabilo-Munizaga and Barbosa-Cánovas, 2005).

2.4 STEADY-STATE SHEAR FLOW BEHAVIOUR: VISCOSITY

By definition, rheology is the deformation and flow of matter, and rheological properties are based on the flow and deformation responses of a substance when subjected to stress (Barnes, 1999; Rao, 1999). Deformation is the relative displacement of points of a body. This deformation may be viscous flow, elastic deformation or a combination of the two. Viscous flow is an irreversible deformation, which means that when the stress is removed the material does not return to its original form; i.e. work is converted to heat. Fig. 2.1 shows common types of flow curves, plotted as shear stress against shear rate. Shear-thinning and shear-thickening flows are shown by curves and a Newtonian flow by a straight line. Any yield stress is shown by interception on the stress axis. The yield stress is the stress which must be exceeded before flow starts.

The existence of yield stresses is controversial as some authors consider them to be artefacts resulting from high Newtonian viscosity at low shear rates (De Kee and Chan, 1983; Barnes and Walters, 1985;

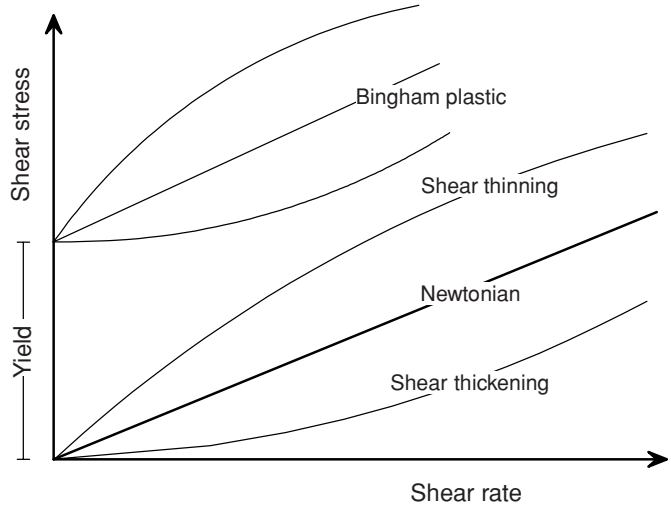

Fig. 2.1 Flow curves (shear stress vs shear rate) for different types of flow behaviour.

Evans, 1992). Barnes and Walters (1985) insisted that the yield stress is a myth, because 'if a material flows at high stresses it will also flow, however slowly, at low stresses'. Nonetheless, this viscosity in many dispersed systems is so high that the material would take years to flow. Therefore, in practice, yield stress is an engineering reality (Spaans and Williams, 1995), and this parameter can be quite useful in characterising materials, within the range of shear rates and time scales encountered in commercial processes (Papanastasiou, 1987).

2.4.1 Rheological models for shear flow

Modelling offers a means of representing a large quantity of rheological data in terms of a simple mathematical expression. Flow models are frequently encountered in the literature. They are useful for the treatment and summarising rheological data. However, none of the available models could possibly fit the rheological behaviour of a material under a wide range of conditions, for example, when using a wide range of shear rates.

2.4.1.1 *Time-independent flow models*

The flow of most materials is independent of time. For a Newtonian liquid, viscosity is equal to shear stress divided by shear rate, and it is independent of both time and shear rate; however, it may vary with temperature and pressure.

Table 2.1 Rheological models used to describe the behaviour of fluids

Flow model name	Equation[a]
Newtonian	$\sigma = \eta\dot{\gamma}$
Bingham (plastic body)	$\sigma - \sigma_0 = \eta\dot{\gamma}$
Power law	$\sigma = k\dot{\gamma}^n$
Herschel–Bulkely	$\sigma - \sigma_0 = k_H\dot{\gamma}^n$
Sisko	$\eta = \eta_\infty + k'\dot{\gamma}^{n-1}$
Casson (Casson, 1959)	$\sigma^{1/2} = k_0 + k_1\dot{\gamma}^{1/2}$
Prandtl	$\sigma = A\sin^{-1}\left(\frac{\dot{\gamma}}{C}\right)$
Eyring	$\sigma = \frac{\dot{\gamma}}{B} + C\sin\left(\frac{\sigma}{A}\right)$
Powell-Eyring	$\sigma = A\dot{\gamma} + B\sin^{-1}(C\dot{\gamma})$
Williamson	$\sigma = \frac{A\dot{\gamma}}{(B+\dot{\gamma})} + \eta_\infty\dot{\gamma}$
Ellis	$\frac{1}{\eta} = \frac{1}{\eta_0} + m^{-1/n}(\sigma^2)^{(1-n)/2n}$

[a] k, k', k_1 and n are arbitrary constants and power indices, respectively, determined from experimental data.

Table 2.1 shows some flow models among the many proposed. The simplest model is the Newtonian:

$$\eta = \frac{\sigma}{\dot{\gamma}} \tag{2.1}$$

where η is the viscosity, σ is the shear stress and $\dot{\gamma}$ is the shear rate (Goodwin and Hughes, 2008). The flow behaviour of water, fruit juice, milk, honey and vegetable oil solvents can all fit this model over a wide range of shear rates (Steffe, 1996).

The Bingham model extends the Newtonian law to include the yield value, σ_0:

$$\sigma - \sigma_0 = \eta\dot{\gamma} \tag{2.2}$$

This model predicts constant viscosity (similar to Newtonian model) above a certain yield stress. A number of dispersions, including margarine, tomato paste and chocolate paste, comply with this model.

The power law is widely used as a model for materials of non-Newtonian behaviour:

$$\sigma = k\dot{\gamma}^n \tag{2.3}$$

where k is the consistency index and n is the flow behaviour index. The model can describe a Newtonian, shear-thinning and shear-thickening

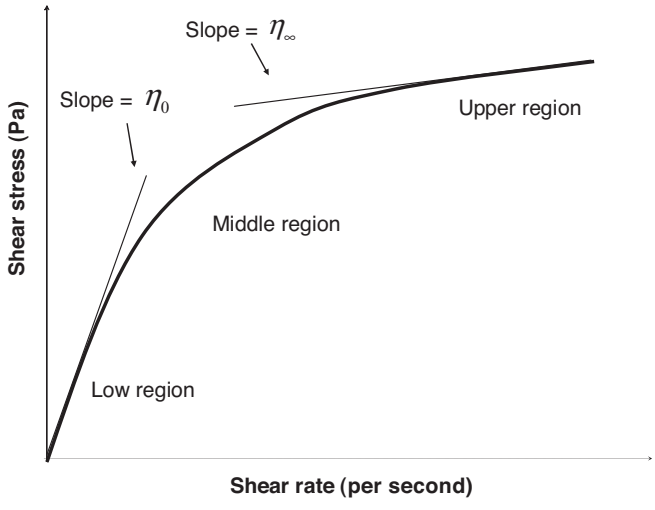

Fig. 2.2 The flow curve of a typical shear-thinning material (reproduced from Steffe, 1996).

behaviour, depending on the value of the flow behaviour index, n. For a Newtonian material, n is equal to 1, and the equation reduces to the Newtonian model. If n is less than 1, the fluid is shear thinning, whereas if it is greater than 1, then the fluid is shear thickening (dilatant).

Shear-thinning behaviour is very common in concentrated juices, vegetable products and creams. Shear-thinning materials may demonstrate three different regions during their flow, as shown in Fig. 2.2. At high shear rates, they have a tendency towards a Newtonian viscosity, η_∞, called the limiting viscosity at infinite shear rate. At low shear rates, they tend towards either a yield point or a Newtonian viscosity, η_0, called the limiting viscosity at zero shear rate. At intermediate shear rates where the apparent viscosity is changing (see decreasing for shear-thinning materials) with shear rate, the power law or the Casson model is a useful approximation.

The Herschel–Bulkley model is an extension to the power law to include the yield value, σ_0:

$$\sigma - \sigma_0 = k_{\mathrm{H}}\dot{\gamma}^n \tag{2.4}$$

This model is appropriate for many foods and is very convenient because Newtonian, power law (shear-thinning or shear-thickening) and Bingham plastic behaviour may be considered as special cases (Steffe, 1996). Other extended power law models are the Sisko model:

$$\eta = \eta_\infty + k'\dot{\gamma}^{n-1} \tag{2.5}$$

where η_∞ is the Newtonian limiting viscosity, and the Casson equation, which is useful, for example, in establishing the flow characteristic of chocolate flow behaviour (Steffe, 1996; Aguilera and Stanley, 1999):

$$\sigma^{1/2} = k_0 + k_1 \dot{\gamma}^{1/2} \tag{2.6}$$

The power law, Bingham, Herschel–Bulkley and Casson models effectively describe the rheology of a wide variety of foodstuffs (Steffe, 1996).

2.4.1.2 *Time-dependent flow models*

In addition to the non-ideal behaviour described previously, many materials exhibit time-dependent effects, which have more complex responses. There are two types of time-dependant flow: thixotropy and rheopexy. If the viscosity of the material decreases with time, when sheared at a constant shear rate, this behaviour is termed as thixotropy. On the other hand, if the viscosity of the material increases with time, again when sheared at a constant shear rate, this behaviour is called as rheopexy. These effects can occur in materials with or without yield stress. Rheopexy is a rare phenomenon, but thixotropic materials are common. Examples of thixotropic materials are starch pastes, gelatine and mayonnaise (Steffe, 1996).

Irreversible changes, such as cross-linking, coagulation, degradation and mechanical instabilities, cause the time-dependent behaviour, and so the sample does not recover when the stress is removed. However, if reversible changes occur, for example, the breakage and reformation of colloidal aggregates, the material can recover if left at rest. Models describing time-dependent behaviour are less satisfactory and more controversial than those of shear-dependent behaviour (Prentice, 1984).

Experimentally, it can be difficult to detect differences between a shear-thinning fluid, in which the viscosity decreases with increasing shear, and a thixotropic material, in which the viscosity decreases with time, because of the combined shear and time effects that occur during measurement. This is especially true if only a small number of data points are collected. In addition, most materials which are thixotropic are also shear thinning. In fact, one definition suggests that for a material to be described as thixotropic, its viscosity should be a function of both shear rate and time (Donald and Gary, 1971; Aral and Kalyon, 1994).

Constitutive models such as the Herschel–Bulkley equation may be adapted to allow for thixotropic effects by introducing a structural parameter λ (Steffe, 1996):

$$\sigma = \lambda(\tau_y + K(\dot{\gamma})^n) \tag{2.7}$$

with λ having a value of 1 at $t = 0$ and overall described by a first-order decay equation:

$$\frac{d\lambda}{dt} = -k_1(\lambda - \lambda_e) \quad \text{for } \lambda > \lambda_e \tag{2.8}$$

where λ_e is the final value for complete breakdown of the structure and k_1 is the rate constant which depends on the shear rate.

2.4.2 Wall slip

Slip happens during the flow of multiphase systems by the displacement of the disperse phase away from solid boundaries and walls. As a result, a thin layer adjacent to the wall will be rich in continuous phase, which is usually less viscous in comparison to the bulk viscosity of the system. Consequently, the fluid will flow (slip) much easier near the wall(s), as the formed thin layer will induce some lubrication effect (Barnes, 1995; Bertola *et al.*, 2003).

In terms of rheometry, if a system exhibits wall slip, then its viscosity becomes a function of the size of the measuring geometry, the gap size used as well as the magnitude of the applied stress (Meeker *et al*., 2004). A sudden 'break' in the flow curve can be an indication of slip. The presence of large particles in the fluid coupled with smooth walls and flow of small dimensions can increase the risk of slip (Barnes, 1995). Fig. 2.3 shows photographs of a sample that slips during a rheometry test. In order to see the slip effect, the sample and both upper and lower plates were marked before any shear applied (Fig. 2.3a). Fig. 2.3b shows the same sample after a few seconds of applying shear and what can be

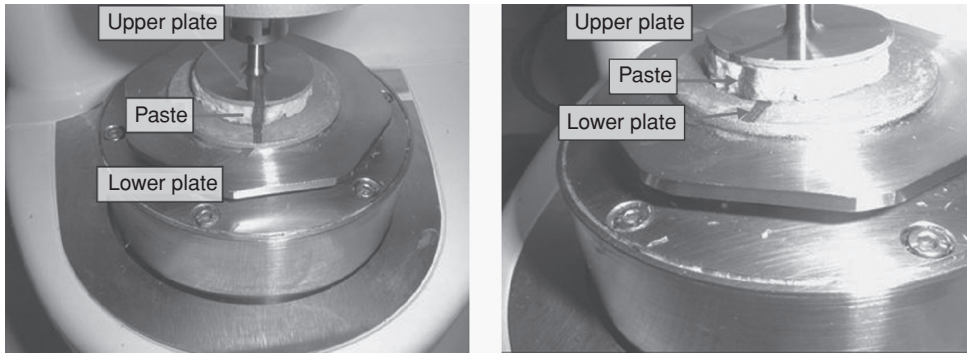

(a) (b)

Fig. 2.3 Depiction of wall slippage by tracing a mark in rheological measurement of mycoprotein paste at a shear rate of 20 per second, using 4 cm roughened parallel plates (Miri, 2003).

clearly seen is that it does not flow between the plates, but slips. The same figure also shows that the sample slips on both sides of the plates.

As such slip effects can also occur during manufacturing processes, when a smooth surface such as a pipe is used, it is necessary to characterise these by calculating the slip velocity and correcting the shear rate (Barnes, 1995). To calculate slip velocity, the size of the used geometry should be changed and obtained results should be extrapolated to a very large size (see for example Yoshimura and Prud'homme, 1988; Chakrabandhu and Singh, 2005; Ahuja and Singh, 2009).

Changing the physical or chemical characteristics of the walls, by physically roughening or profiling the surface, can be a way of eliminating or minimising slip effects. Another alternative is to use a vane system or a squeeze flow system (Barnes, 1995); both rheological systems are described later in this chapter.

2.5 VISCOELASTICITY AND OSCILLATION

The previous section focused on flow curves for non-Newtonian materials under steady shear conditions. Every food has a unique flow curve, and these data are critical to a large number of industrial applications. Clearly, from an engineering point of view, the steady flow curve is the most valuable way to characterise the rheological behaviour of foods. Steady shear viscosity is a property of all materials, irrespective of whether they do or do not demonstrate elastic behaviour. However, many phenomena cannot be described by the viscosity definition alone, and elastic behaviour must be taken into consideration (Steffe, 1996).

Elastic flow is reversible; i.e. by removing the stress, the deformed body recovers its original shape, and the applied work is mostly recovered. However viscoelastic materials, such as dough, cereal extrudates and cheese, show both flow and elasticity and, in terms of modelling, viscoelastic materials provide special challenges.

Transient experiments, such as oscillatory and creep tests, generate data, which can quantify viscoelasticity. In the oscillatory technique, a sample is subjected to harmonically varying (usually sinusoidal) small-amplitude deformations in a simple shear field. This is a non-destructive test, which is able to characterise viscoelastic behaviour. Oscillation can also be used to determine structural changes occurring in the sample. It is also a useful tool for measuring rheologically complex samples such as semi-solids and food pastes (for example, see Ferry, 1980; Tsardaka, 1990; Rao and Steffe, 1992; Steffe, 1996; Reilly, 1997).

These types of experimental testing lead to the simultaneous measurement of numerous viscoelastic properties such as complex viscosity (η^*), dynamic viscosity (η'), phase (out-of-phase) angle (δ), complex

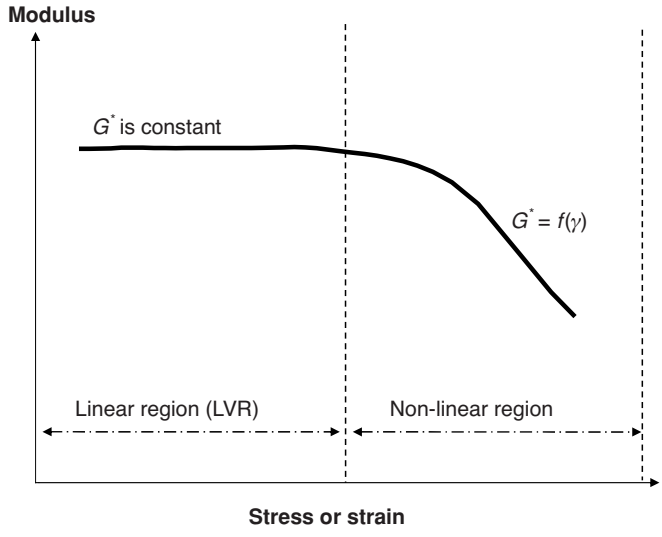

Fig. 2.4 Linear and non-linear stress–strain behaviour.

shear modulus (G^*), shear storage modulus (G'), shear loss modulus (G''), complex shear compliance (J^*), shear storage compliance (J') and shear loss compliance (J''). The ones most commonly used are the moduli terms; storage modulus is the elastic component, which indicates the amount of energy stored, and loss modulus is the viscous component, which indicates the amount of energy dissipated through a generated heat. The complex modulus is defined as $\sqrt{G''^2 + G'^2}$ and defines the overall stiffness of the sample. Another popular material function used to describe the viscoelastic behaviour is the tangent of the phase shift or phase angle (called tan delta), which is a function of frequency:

$$\tan \delta = \frac{G''}{G'} \tag{2.9}$$

The phase angle (δ) varies between 0 and 90°; it is zero in case of a purely elastic material and 90° for a purely viscous fluid.

Critical to these studies is the identification of the linear viscoelastic region (LVR), within which material properties do not depend on the magnitude of the stress, the magnitude of the deforming strain or the rate of application of the strain. Within the LVR, depicted in Fig. 2.4, an applied stress will produce a proportional strain response; therefore, for example, doubling the stress will double the strain response. The linear range of testing is determined from experimental data. Testing can easily enter the non-linear range if excessive strain (usually greater than 1%) or high deformation rates are applied to the sample.

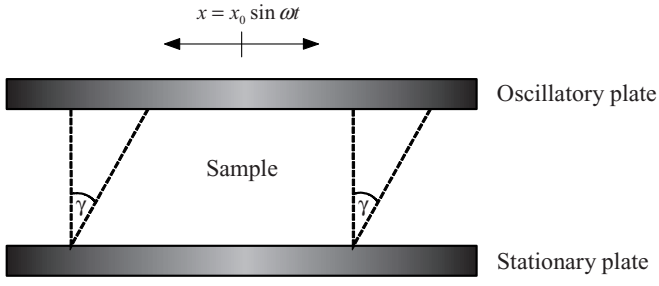

Fig. 2.5 Simplified schematic of an oscillatory test.

2.5.1 Oscillatory testing

The rheological behaviour of viscoelastic materials can be determined from dynamic testing. In rheological terms, dynamic or oscillatory testing always refers to process during which the material is subjected to either a stress or frequency that varies harmonically with time. Typically, a sinusoidal strain is applied to the sample, causing some levels of stress to be transmitted through the material. The magnitude and phase lag of the transmission will depend on the viscoelastic properties of the specimen. In viscous materials, most of the stress is dissipated by friction, whereas the stress is transmitted in highly elastic materials.

For simplicity let us consider a thin sample of material contained between two parallel plates (Fig. 2.5). As the lower plate is fixed while the upper plate oscillates horizontally in a sinusoidal mode and at an angular frequency ω (rad/second), the position of the plate at time t is given by:

$$x = x_0 \sin \omega t \tag{2.10}$$

where x is the position of the plate at the time t and x_0 is the amplitude of the plate oscillation. The sinusoidal shear strain γ, of amplitude γ_0, is imposed on the material and given by:

$$\gamma = \gamma_0 \sin \omega t \tag{2.11}$$

Using low strain amplitudes, within the LVR, an out-of-phase sinusoidal shear stress response σ is produced:

$$\sigma = \sigma_0 \sin(\omega t + \delta) \tag{2.12}$$

where σ_0 is the shear stress amplitude and δ is the phase lag.

The phase lag, δ, and the amplitude ratio depend on the material being tested; δ is 0° for purely elastic materials (no phase lag) and 90° for purely viscous materials (out of phase due to viscous losses).

Equation 2.12 can be written as follows:

$$\sigma = \sigma_0 \cos\delta \sin\omega t + \sigma_0 \sin\delta \cos\omega t \tag{2.13}$$

This allows for the following quantities to be defined:

$$G' = \frac{\sigma_0 \cos\delta}{\gamma_0} = \frac{\text{in-phase stress amplitude}}{\text{strain amplitude}} \tag{2.14}$$

$$G'' = \frac{\sigma_0 \sin\delta}{\gamma_0} = \frac{\text{out-of-phase stress amplitude}}{\text{strain amplitude}} \tag{2.15}$$

and

$$\tan\delta = \frac{G''}{G'} \tag{2.16}$$

and therefore the stress response can be written as follows:

$$\sigma = G'\gamma_0 \sin\omega t + G''\gamma_0 \cos\omega t \tag{2.17}$$

where G' is the storage modulus and G'' is the loss modulus. The storage modulus is an indicator of the degree of elasticity of the material, and G'' is a measure of the degree of viscous behaviour. A large value of G', in comparison to that for G'', indicates that the product being analysed has predominantly elastic properties. The tan δ is directly related to the energy lost, per cycle, divided by the energy stored per cycle; because this can vary from zero to infinity, $0° \leq \delta \leq 90°$.

Fig. 2.6 shows a typical viscoelastic behaviour as identified by a frequency sweep within the LVR. Frequencies are an indicator of the time scale of process, i.e. the higher the frequency, the shorter the time scale of the process and vice versa.

The crossover frequency is the frequency where the G' and G'' curves intersect, i.e. the frequency at which the elastic and viscous responses are equal. The crossover frequency is an important rheological parameter and is inversely proportional to the relaxation time (the time at rest required for the sample to relax a stress received from an external body), i.e.:

$$f_{\text{crossover}} \propto \frac{1}{\text{relaxation time}} \tag{2.18}$$

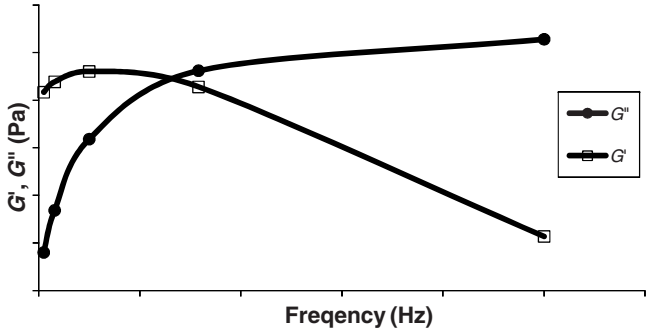

Fig. 2.6 A typical graph of viscoelastic modules and their frequency dependency.

2.6 PROCESS, RHEOLOGY AND MICROSTRUCTURAL INTERACTIONS

The microstructure of complex food products is greatly influenced by the type of processing employed, and in particular the shear processes and thermal processes, such as freezing. However, the effects are not always well understood or easily quantifiable. As food processing operations are usually designed to create a microstructure that gives the food product its characteristic properties, understanding of the microstructure and the route to its formation is imperative (Aguilera and Stanley, 1999; Aguilera, 2000). In rheometry also, the manner in which the material interacts with the testing instrument varies according to the flow configuration used. This can lead to different microstructural rearrangements that may result in different rheological responses. Therefore, a fundamental understanding of the relationship between processing, rheology and microstructure is important for the control of product quality and rheology (Guell and Papathanasiou, 1997). However, most of the work on the effects of processing on food materials has been limited to investigations of flow behaviour, without consideration of the accompanying structural changes (Cheyne *et al*., 2001).

2.7 RHEOLOGY OF SOFT SOLIDS

Concentrated pastes are used in a variety of industrial applications, such as ceramic manufacture, as well as food processing. In food manufacture, the 'ideal paste' is one that will undergo sufficient plastic or viscous flow, so that it can be formed, and yet be rigid enough to retain its shape during subsequent processing and handling. Therefore, food pastes are generally complex heterogeneous materials with microstructure that

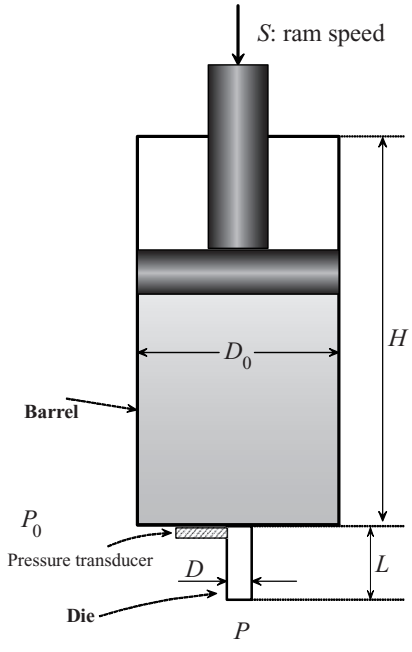

Fig. 2.7 Schematic representation of a capillary system.

specifies final product quality, and which is affected by processing. The rheological behaviour of many paste materials has not been fully characterised, due to their complexity, both in terms of bulk behaviour and of microstructure (Barnes, 1995). For characterising soft solid foods, both capillary and squeeze flow rheometers are useful. Nonetheless, these rheometers are less commonly used in food research and as such they are only briefly described here.

2.7.1 Capillary rheometer

Capillary rheometers can perform both flow and elasticity experiments (such as stress relaxation) by using a ram to force material through a die of known dimensions and measuring the pressure drop across the die by a pressure transducer. Fig. 2.7 schematically shows a capillary rheometer, where the material being measured is contained in a barrel with diameter D_0 and is forced through a die of diameter D and length L by using a ram, moving with a linear speed of S.

As the material enters from the barrel to the die, the cross-section decreases and as a result the sample extends and elongates along the flow direction. The apparent wall shear rate ($\dot{\gamma}_w$) and the wall

shear stress (σ_w) are calculated from the commonly used standard formulae:

$$\sigma_w = \frac{\Delta P \cdot D}{4L} \tag{2.19}$$

and

$$\dot{\gamma}_w = \frac{8D_0^2 \cdot S}{D^3}\left(\frac{3}{4} + \frac{1}{4}\frac{d\ln Q}{d\ln \sigma_w}\right) \tag{2.20}$$

where ΔP is the pressure drop across the die and Q is the flow rate. The term in the parenthesis is called the *Rabinowitch correction* (Reilly, 1997) and accounts for the fact that the flow profile in the die departs from a true parabolic profile as in Newtonian fluids.

The apparent viscosity (η) of the paste can be calculated as follows:

$$\eta = \frac{\sigma_w}{\dot{\gamma}_w} \tag{2.21}$$

To extract the true viscosity from the apparent viscosity, the Bagley correction has to be applied (Halliday and Smith, 1995). This correction is used to calculate the true shear stress in the capillary and corrects for the pressure losses at its entrance and exit. This correction needs to be applied if the pressure is not directly measured at the orifice. The correction requires shear rate data from at least two dies, of the same diameter but of different aspect ratios, to extrapolate pressure drop at zero die length, P_0. Then, shear stress can be corrected as follows:

$$\sigma = \frac{(\Delta P - P_0)D}{4L} \tag{2.22}$$

More details on the theory of rotational and capillary rheometry can be found in Steffe (1996).

2.7.2 Squeeze flow rheometer

Squeeze flow rheometers have long been used to study highly viscous material, such as polymer melts, food pastes and polymer composites, mainly due to their relative simplicity and the ease by which a wide range of shear rates can be realised in a single run. However, the squeeze flow geometry, whilst apparently simple, provides a complex flow field involving both shear and extensional flows as well as evolving boundary conditions (Sherwood and Durban, 1996; Gibson and Toll, 1999;

Engmann *et al.*, 2005). Squeeze flow is encountered in various processes, for example, filtration, pressing, rolling compression moulding and rheometry (Steffe, 1996).

In squeeze flow test equipment, the material is placed between rigid parallel plates, which are then moved together. The material exits radially, and the radial fluid velocity is a function of the position z between the plates at any radial position, r (Sherwood *et al.*, 1991). The plates can be driven together at constant velocity, constant load or constant strain rate. As deformation proceeds, a pressure distribution develops within the tested material, which depends on the material properties and the prevailing wall boundary conditions (Gibson and Toll, 1999; Engmann *et al.*, 2005). The force required to squeeze a thin cylindrical shaped sample between two approaching parallel circular plates depends on the material rheology and also on the friction characteristics at the material–plate interface (Laun *et al.*, 1999). As the deformation energy is transmitted to the bulk of the material via the wall, the interfacial boundary environment must be described as accurately as possible; in practice, this may be as important, if not more so, than the bulk behaviour (Corfield, 1996).

It should be noted that due to the complex nature of the flow fields produced by using this technique, there is no universal model available for application to all materials.

2.8 MEASURING INSTRUMENTS – PRACTICAL ASPECTS

2.8.1 Choosing the right measuring system

The choice of instrumentation and the measuring system requires careful consideration of the particular fluid being analysed and the rheological properties being studied. Without the knowledge of the parameters influencing the rheology of a material, measurements can easily be misleading and sometimes completely incorrect.

There are two main types of rotary rheometers, namely controlled stress and control strain rheometers (Fig. 2.8a). Here, a set of commonly used rheometers are described and compared. More detail can be found in Macosko (1994).

2.8.1.1 *Cone-and-plate rheometry*

Cone-and-plate rheometry has the benefit of having a well-defined flow, and hence accurate interpretation is possible (Fig. 2.8). It requires a small sample volume, and it is easy to clean. The main advantage is that the shear rate applied is uniform throughout the sample. However,

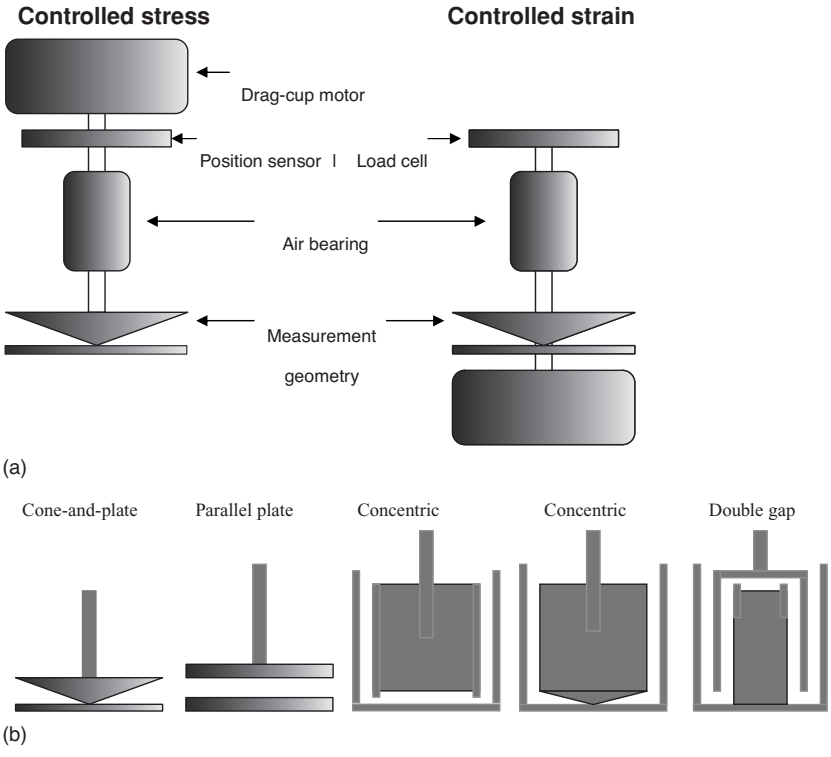

Fig. 2.8 Schematic of two types of rotary rheometers and related geometries (reproduced from Goodwin and Hughes, 2008): (a) controlled stress versus control strain and (b) cross sections of common measuring geometries.

in the cone-and-plate rheometry, the size of any particles present within the sample should be limited to 10–20% of the truncation height of this geometry; i.e. particles should typically be smaller than 5–20 μm in size to avoid jamming the gap and irregularities in the data. Care must be taken when measuring at high shear rates as material can 'escape' from between the plates. Furthermore, this geometry is very susceptible to sedimentation.

2.8.1.2 *Parallel plate rheometry*

Similar to the cone-and-plate, parallel plate geometry (Fig. 2.8) has a well-defined flow, and accurate interpretation is, in principle, possible. It requires only a small sample volume, and it is easy to clean. The main advantage of this geometry is that the user can define the gap which can be set to values considerably larger than those of typical particles in the material to be tested. This gap can also be varied to probe wall slip effects (Barnes, 1995). The parallel plate geometry has the disadvantage that the

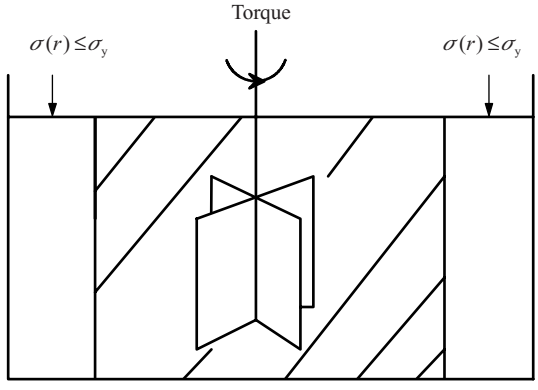

Fig. 2.9 Schematic diagram of a vane rheometer with pseudo-infinite vessel arrangement for a suspension with a yield stress (σ_y); i.e. the shear stress falls below the yield stress before the wall, which prevents slippage at the outer boundary of the rheometer.

shear field varies with radial position; therefore, the reported shear rate is an average value. This geometry is also susceptible to sedimentation.

2.8.1.3 *Concentric cylinder rheometry*

Concentric cylinder geometry (Fig. 2.9) has a well-defined flow, with small annular gaps, and accurate interpretation is possible. It does not expel suspension even at high shear rates, and it is more sensitive to low viscous material than the cone-and-plate and parallel plate systems. However, its narrow gaps are inappropriate for solid particles, as they may compact particles and jam the instrument; settling and slippage of solids may occur (Bongenaar *et al.*, 1973).

2.8.1.4 *Vane rheometry*

This approach to rheological measurements has been employed by a number of authors, and has been suggested as a reliable and largely reproducible method for characterising biological broths (Tucker and Thomas, 1993; Riley *et al.*, 2000). The success and attraction of this method lies in the use of a turbine as the moving rotor so that the suspension is forced to shear rather than slip at the moving surface (Barnes and Nguyen, 2001). For a suspension exhibiting a yield stress, or which is very shear thinning, the turbine can be contained in a vessel large enough so that the shear stress falls to below the yield stress before the wall (Fig. 2.9). Thus, it is a so-called pseudo-infinite vessel arrangement, which also prevents slippage at the outer boundary of the rheometer. This equipment has a significant disadvantage of having a poorly defined flow

field. Hence, only an approximate analysis of non-Newtonian systems is possible, which relies heavily on the method of calibration.

2.8.1.5 *Capillary rheometry*

Capillary rheometry has a well-defined flow, and it is more sensitive for high viscous material than the cone-and-plate and parallel plate systems. In addition, it can reach high shear rates, and it is possible to correct raw data to account for any wall slip. Its main disadvantage is that temperature control is difficult; hence, only approximate analysis of non-Newtonian systems is possible. This geometry is susceptible to phase separation in material, which could lead to wall slip.

REFERENCES

Advani, S.G. (1994) *Flow and Rheology in Polymer Composites Manufacturing*. Amsterdam: Elsevier.

Aguilera, J.M. (2000) Microstructure and food product engineering. *Food Technology* **54**, 56–65.

Aguilera, J.M. and Stanley, D.W. (1999) *Microstructural Principles of Food Processing and Engineering*, 2nd Edition. USA: Aspen Publishers.

Ahuja, A. and Singh, A. (2009) Slip velocity of concentrated suspensions in Couette flow. *Journal of Rheology* **53**, 1461–1485.

Aral, B.K. and Kalyon, D.M. (1994) Effects of temperature and surface roughness on time-dependent development of wall slip in steady torsional flow of concentrated suspensions. *Journal of Rheology* **38,** 957–972.

Baird, D.G. (1981) Review of food dough rheology. *Journal of Rheology* **25**, 477–478.

Banfill, P.F.G. and Tattersall, G.H. (1983) *The Rheology of Fresh Concrete*. London: Pitman.

Barnes, H.A. (1995) A review of the slip (wall depletion) of polymer solutions, emulsions and particle suspensions in viscometers: its cause, character, and cure. *Journal of Non-Newtonian Fluid Mechanics* **56**, 221–251.

Barnes, H.A. (1999) The yield stress – a review or '[pi][alpha][nu][tau][alpha] [rho][epsiv][iota]' – everything flows? *Journal of Non-Newtonian Fluid Mechanics* **81**, 133–178.

Barnes, H.A. (2000) *A Handbook of Elementary Rheology*. Aberystwyth: University of Wales Institute of Non-Newtonian Fluid Mechanics.

Barnes, H.A. and Nguyen, Q.D. (2001) Rotating vane rheometry – a review. *Journal of Non-Newtonian Fluid Mechanics* **98**, 1–14.

Barnes, H.A. and Walters, K. (1985) The yield stress myth. *Rheolgica Acta* **24**, 324–326.

Bertola, V., Bertrand, F., Tabuteau, H., Bonn, D. and Coussot, P. (2003) Wall slip and yielding in pasty materials. *Journal of Rheology* **47**, 1211–1226.

Blair, G.W.S. (1954) The rheology of fats – a review. *Journal of the Science of Food and Agriculture* **5**, 401–405.

Bongenaar, J.J.T.M., Kossen, N.W.F., Metz, B. and Meijboom, F.W. (1973) A method for characterising the rheological properties of viscous fermentation broths. *Biotechnology and Bioengineering* **15**, 201–206.

Borwankar, R.P. (1992) Food texture and rheology – a tutorial review. *Journal of Food Engineering* **16**, 1–16.

Bourne, M.C. (1992) Calibration of rheological techniques used for foods. *Journal of Food Engineering* **16**, 151–163.

Casson, N. (1959) A flow equation for pigment oil-suspensions of the printing ink type. In: Mill C.C., editor. *Rheology of Disperse Systems*. Oxford: Pergamon Press.

Chakrabandhu, K. and Singh, R.K. (2005) Wall slip determination for coarse food suspensions in tube flow at high temperatures. *Journal of Food Engineering* **70**, 73–81.

Cheyne, A., Wilson, D.L., Gedney, S., Barnes, O.J. and Scriven, F. (2001) Shear induced microstructural changes in starchy materials, *6th World Chemical Engineering Congress*, Australia.

Corfield, G.M. (1996) *The Constrained Flow of Pastes*, PhD thesis. UK: Imperial College of Science, Technology and Medicine .

Decindio, B. (1994) Rheology in fresh pasta production – a review. *Industrie Alimentari* **4**, 21–32.

De Kee, D. and Chan, C.E. (1983) A true yield stress. *Journal of Rheology* **37**, 775–776.

DeMan, J.M. (1976) *Rheology and Texture in Food Quality*. Westport: AVI Publication.

Donald, D.J. and Gary, W. (1971) Characteristics of thixotropic behavior. *Transactions of the Society of Rheology* **15**, 51–61.

Ene, H.I. and Cristescu, N. (1988) *Rock and Soil Rheology*. Berlin: European Mechanics Publication.

Engmann, J., Servais, C. and Burbidge, A.S. (2005) Squeeze flow theory and applications to rheometry: a review. *Journal of Non-Newtonian Fluid Mechanics* **132**, 1–27.

Evans, I.D. (1992) On the nature of the yield stress. *Journal of Rheology* **36**, 1313–1316.

Ferguson, J. and Kemblowski, Z. (1991) *Applied Fluid Rheology*. London: Elsevier.

Ferry, J.D. (1980) *Viscoelastic Properties of Polymers*, 3rd Edition. Chichester: Wiley.

Fischer, P., Pollard, M., Erni, P., Marti, I. and Padar, S. (2009) Rheological approaches to food systems. *Comptes Rendus Physique* **10**, 740–750.

Fryer, P.J., Slater, N.K.H. and Duddridge, J.E. (1985) Suggestions for the operation of radial flow cells in cell adhesion and biofouling studies. *Biotechnology and Bioengineering* **27**, 434–438.

Gallegos, C. and Franco, J.M. (1999) Rheology of food, cosmetics and pharmaceuticals. *Current Opinion in Colloid & Interface Science* **4**, 288–293.

Genovese, M.A., Lozano, J.E. and Rao, M.A. (2007) The rheology of colloidal and noncolloidal food dispersions. *Journal of Food Science* **72**, R11–R20.

Ghista, D.N. (1979) *Blood: Rheology, Hemolysis, Gas and Surface Interactions*. London: Wiley.

Gibson, A.G. and Toll, S. (1999) Mechanics of the squeeze flow of planar fibre suspensions. *Journal of Non-Newtonian Fluid Mechanics* **82**, 1–24.

Goodwin, J.W. and Hughes, R.W. (2008) *Rheology for Chemists: An Introduction*. Cambridge: Royal Society of Chemistry.

Guell, D.C. and Papathanasiou, T.D. (1997) *Flow-Induced Alignment in Composite Materials*. Cambridge: Woodhead Publishing Limited.

Gupta, R.K. (2000) *Polymer and Composite Rheology*. New York: Marcel Dekker.

Halliday, P.J. and Smith, A.C. (1995) Estimation of the wall slip velocity in the capillary flow of potato granule pastes. *Journal of Rheology* **39**, 139–149.

Kasapis, S., Al-Alawi, A., Guizani, N., Khan, A.J. and Mitchell, J.R. (2000) Viscoelastic properties of pectin-co-solute mixtures at iso-free-volume states. *Carbohydrate Research* **329**, 399–407.

Keedwell, M.J. (1984) *Rheology and Soil Mechanics*. London: Elsevier.

Lareo, C.A. and Fryer, P.J. (1998) Vertical flows of solid-liquid food mixtures. *Journal of Food Engineering* **36**, 417–443.

Lareo, C.A, Fryer, P.J. and Barigou, M. (1997) The fluid mechanics of two-phase solid-liquid food flows: a review. *Food and Bioproducts Processing* **75**, 73–105.

Laun, H.M., Rady, M. and Hassager, O. (1999) Analytical solutions for squeeze flow with partial wall slip. *Journal of Non-Newtonian Fluid Mechanics* **81**, 1–15.

Lenk, R.S. (1968) *Plastics Rheology*. London: Maclaren.

Macosko, C.W. (1994) *Rheology: Principles, Measurements, and Applications*. New York: VCH Publishers.

Mankad, S. and Fryer, P.J. (1997) Heterogeneous flow model for the effect of slip and flow velocities on food sterilizer design. *Chemical Engineering Science* **52**, 1835–1843.

Meeker, S.P., Bonnecaze, R.T. and Cloitre, M. (2004) Slip and flow in pastes of soft particles: direct observation and rheology. *Journal of Rheology* **48**, 1295–1320.

Miri, T. (2003) *Rheology and Microstructure of Food Materials*, PhD thesis. Birmingham: University of Birmingham.
Muller Hans, G. (1973) *An Introduction to Food Rheology*. London: Heinemann.
Nielsen, L.E. (1977) *Polymer Rheology*. New York: Marcel Dekker.
Papanastasiou, T.C. (1987) Flows of materials with yield. *Journal of Rheology* **31**, 385–404.
Platt, D. (1988) *Blood Cells, Rheology, and Aging*. London: Springer-Verlag.
Prentice, J.H. (1984) *Measurements in the Rheology of Foodstuffs*. London: Elsevier.
Prentice, P. (1995) *Rheology and Its Role in Plastics Processing*. Shrewsbury: Rapra Technology.
Rao, M.A. (1977) Rheology of liquid foods – review. *Journal of Texture Studies* **8**, 135–168.
Rao, M.A. (1999) *Rheology of Fluid and Semisolid Foods: Principles and Applications*. Gaithersburg: Aspen Publishers.
Rao, M.A. and Steffe, J.F. (1992) *Viscoelastic Properties of Foods*. London: Elsevier Applied Science.
Reilly, D.L. (1997) Food rheology. In: Fryer, P.J., Pyle, D.L. and Reilly, C.D., editors. *Chemical Engineering in the Food Industry*. London: Blackie.
Riley, G.L., Tucker, K.G., Paul, G.C. and Thomas, C.R. (2000) Effect of biomass concentration and mycelial morphology on fermentation broth rheology. *Biotechnology and Bioengineering* **68**, 160–172.
Ross-Murphy, S.B. (1984) Rheological methods. In: Chan, H.W.S., editor. *Biophysical Methods in Food Research*. Oxford: Society of Chemical Industry, pp. 138–199.
Shenoy, A.V. (1999) *Rheology of Filled Polymer Systems*. London: Kluwer.
Shenoy, A.V. and Saini, D.R. (1996) *Thermoplastic Melt Rheology and Processing*. New York: Dekker.
Sherman, P. (1970) *Industrial Rheology with Particular Reference to Foods, Pharmaceuticals, and Cosmetics*. London: Academic Press.
Sherwood, J.D. and Durban, D. (1996) Squeeze flow of a power-law viscoplastic solid. *Journal of Non-Newtonian Fluid Mechanics* **62**, 35–54.
Sherwood, J.D., Meeten, G.H., Farrow, C.A. and Alderman, N.J. (1991) Squeeze–film rheometry of non-uniform mudcakes. *Journal of Non-Newtonian Fluid Mechanics* **39**, 311–334.
Shoemaker, C.F. and Borwankar, R. (1992) *Rheology of Foods*. New York: Elsevier.
Skalny, J. (1982) *Effect of Surface and Colloid Phenomena on Properties of Fresh Concrete*. Pennsylvania: Materials Research Society.
Spaans, R.D. and Williams, M.C. (1995) Letter to the editor: at last, a true liquid-phase yield stress *Journal of Rheology* **39**, 241–246.
Stanley, N.L. and Taylor, L.J. (1993) Rheological basis of oral characteristics of fluid and semi-solid foods: a review. *Acta Psychologica* **84**, 79–92.
Steffe, J.F. (1996) *Rheological Methods in Food Process Engineering*. East Lansing, MI: Freeman Press.
Tabilo-Munizaga, G. and Barbosa-Cánovas, G.V. (2005) Rheology for the food industry. *Journal of Food Engineering* **67**, 147–156.
Tsardaka, E.D. (1990) *Viscoelastic Properties and Compaction Behaviour of Pharmaceutical Particulate Materials*, PhD thesis. Bath: University of Bath.
Tucker, K.G. and Thomas, C.R. (1993) Effect of biomass concentration and morphology on the rheological parameters of *Penicillium chrysogenum* fermentation broths. *Transactions of the Institution of Chemical Engineers – Part C* **71**, 111–117.
Van Wazer, J.R., Lyons, J.W., Kim, K.Y. and Colwell, R.E. (1963) *Viscosity and Flow Measurement: A Handbook of Rheology*. New York: Interscience.
Walters, K. (1999) Lessons from history. *Korea-Australia Rheology Journal* **11**, 265–268.
Williams, E.W., Rigby, S.G., Sproston, J.L. and Stanway, R. (1993) Electrorheological fluids applied to an automotive engine mount. *Journal of Non-Newtonian Fluid Mechanics* **47**, 221–238.
Whorlow, R.W. (1980) *Rheological Techniques*. New York: Halsted Press.
Yoshimura, A. and Prud'homme, R.K. (1988) Wall slip corrections for Couette and parallel disk viscometers. *Journal of Rheology* **32**, 53–67.

3 Doppler Ultrasound-Based Rheology

Beat Birkhofer

3.1 INTRODUCTION

3.1.1 Overview

The principle of the technique described in this chapter is simple: the shape of the symmetric velocity profile in laminar, stationary pipe flow depends on the rheological characteristics. For example, Newtonian fluids have a parabolic flow profile, while for shear-thinning fluids it is steep close to the wall and flat towards the centre (Fig. 3.1). Thus, being able to measure this velocity profile allows a characterisation of the rheological properties of the fluid. Combining the velocity profile with pressure drop results in a non-invasive in-line rheometer, which allows to measure the shear rate-dependent viscosity.

Pulsed ultrasound[1], a flow measurement method applied since the early 1970s in the medical field, can be used to obtain the velocity profile. Compared to magnetic resonance imaging, it is relatively simple and far less expensive. In contrast to laser Doppler anemometry (LDA) or particle image velocimetry (PIV), the technique can be applied in opaque fluids.

The main benefit of the combination of ultrasonic velocity profiling (UVP) and pressure drop (PD) is the applicability as in-line rheometer for complex fluids. The necessary basic installation – a straight pipe with the fluid flow – is quite ubiquitous in the relevant industries such as food, pharmaceutical, cosmetic or chemical. As the rheological properties are measured directly in-line, there are the obvious advantages of avoiding complicated measurements in the laboratory and

[1] The question as to whether pulsed Doppler ultrasound makes use of the Doppler effect depends on the definition of the Doppler effect (Cobbold, 2007, Chapter 10). For Jensen (1996, Chapter 6), the classic Doppler effect is only an artefact in pulsed systems.

Practical Food Rheology: An Interpretive Approach
Edited by Ian T. Norton, Fotios Spyropoulos and Philip Cox
 ISBN: 978-1-405-19978-0

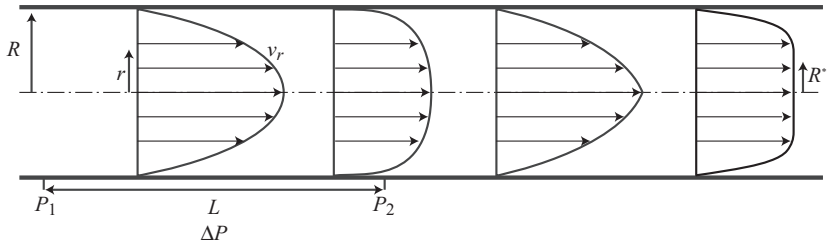

Fig. 3.1 Pipe flow velocity profiles with the geometric sizes used in Equations 3.14 to 3.23. The typical profiles for Newtonian ($n = 1$), power law shear thinning ($n < 1$), power law shear thickening ($n > 1$) and Herschel–Bulkley with plug radius R^* are shown from left to right.

having a continuous product quality monitoring. In addition, it becomes possible to measure under conditions (pressure, temperature, shear history) not reproducible in a conventional rheometer, and it allows to measure suspensions containing particles of a size that would not fit in a conventional rheometer gap.

In spite of all those advantages and four completed doctoral works on the topic since 1993, there is still no known commercial installation of a UVP-PD-based in-line rheometer in the industry. This is probably due to several reasons: the fact that many components are yet custom-made and that for a successful implementation know-how is needed in the fields of acoustics, electronics, software programming, signal processing, ultrasound transducers and of course rheology. So this chapter tries to give an overview of the technique and describes the single components of the measurement system from the transducer to the rheometry calculations.

Another interesting application of ultrasound velocimetry, not further described here, is the measurement of the flow profile in the gap of a rotational rheometer described by Manneville *et al.* (2004, 2005) and Sandrin *et al.* (2001).

3.1.2 History of ultrasonic velocimetry

Historically, the development of the Doppler velocimetry started in the medical field in the 1950s (Satomura, 1957) with continuous wave devices. The first pulsed range gate systems were introduced at the beginning of the 1970s (Wells, 1969; Baker, 1970; Brandestini, 1978; Peronneau, 1992). Outside the medical field, ultrasonic velocimetry was applied to measurements of liquid metal flow by Fowlis (1973), using continuous wave ultrasound, while Pinkel (1979) utilised pulsed ultrasound at low frequencies to measure ocean currents. Garbini *et al.* (1982a, 1982b) characterised turbulence using the spectral broadening

of the echo signal. Takeda (1986) investigated pipe and Taylor vortex flows. He also applied the UVP technique for flow mapping in mercury (Takeda, 1987).

A short overview of the UVP method including the signal processing for the Doppler shift frequency estimation and application was given by Lemmin and Rolland (1997). An extensive coverage of Doppler ultrasound can be found in three textbooks (Jensen, 1996; Evans and McDicken, 2000; Hill *et al.*, 2004) from the medical field, which describe many aspects also relevant for engineering applications of ultrasonic measurements. Also, Cobbold (2007) contains one chapter on pulsed ultrasound for velocimetry.

3.1.3 Existing literature on UVP-based rheometry

An overview of the publications on ultrasound velocimetry-based rheometry carried out by various research groups is given in the text and Tables 3.1 and 3.2.

3.1.3.1 *Polish Academy of Sciences, Warszawa, Poland*

In his often overlooked publication, Kowalewski (1980) describes measurements in suspensions and two different emulsion types with concentrations varying from 5 to 50% using a pulsed ultrasound-based machine (Nowicki, 1979). The 'blunting' of the profiles as a function of the particle concentration was characterised with a power law exponent (Equation 3.18).

3.1.3.2 *University Erlangen-Nürnberg, Germany*

The idea of combining the velocity profile measured with ultrasound and pressure drop for in-line rheometry was first mentioned by Brunn *et al.* (1993). In this publication actual rheometry data are only shown for measurements where laser Doppler is used to obtain the velocity profile. Then, Müller *et al.* (1997) calculated shear rate-dependent viscosities from simultaneous measurements of ultrasonic velocity profiles and pressure drop in a Newtonian glycerin/water solution, a non-Newtonian aqueous polyacrylamide solution and a non-Newtonian hydroxypropyl guar gum solution. The velocity profile-based flow curves (shear rate-dependent viscosity) were compared with those measured using a rheometer. Later Wunderlich and Brunn (1999) also measured a polyacrylamide solution and fitted the measured profiles with polynomial, power law and Ellis fluid functions. Brunn *et al.* (2004) presented results of UVP-PD measurements of a body lotion (concentrated surfactant solution).

Table 3.1 Fluids and suspensions used for UVP-PD measurements

References	Fluid	Shape	Particle size	c (m/second)	Concentration	Model
Kowalewski (1980)	Emulsion of glycerin and water in castor oil			1520/1580	5–50% vol	pl
	Emulsion of castor oil in glycerine and water			1580/1525	6–50% vol	pl
	Methacrylate spheres in glycerine and water	Spherical	0.1 mm	2350/1900	7–50% vol	pl
Müller *et al.* (1997)	Glycerin and water					gr
	Polyacrylamide				4000 ppm	Gr
	Hydroxypropyl guar gum				8000 ppm	Gr
Wunderlich and Brunn (1999)	Polyacrylamide				4000 wppm	polynom, Ellis, pl
Brunn *et al.* (2004)	Surfactant solution			1580		gr
Ouriev *et al.* (2000)	Fat suspension				1.6–10.7%	pl
Ouriev and Windhab (2002)	Silicon oil AK10 and native cornstarch			1010	≤40% wt	pl, HB
	Glucose syrup (50%), starch particles and water			1830	≤40% wt	pl, HB
Ouriev (2002)	Glucose syrup (50%), starch particles and water			1830	30 and 40% wt	
Ouriev *et al.* (2003)	Chocolate					
Wiklund *et al.* (2002)	Surfactant solution					pl, HB
	Cellulose fibre suspension	Fibres			1–3%	pl, HB
Birkhofer *et al.* (2008)	Cocoa butter crystal suspension			1400–1475	10–25%	pl, HB
Fischer *et al.* (2009)	Viscoelastic surfactant solution	Micelles		1830		
Wiklund *et al.* (2007)	Xanthan gum solution, pasta sauce, yoghurt, etc.					pl, HB
Wiklund and Stading (2008)	PEG400			1624		pl
Wiklund and Stading (2008)	Xanthan gum solution			1486		pl
Wiklund and Stading (2008)	Cheese sauce (8% fat)			1531		pl
Wiklund and Stading (2008)	Mayonnaise			1471		pl
Wiklund and Stading (2008)	Dairy products	Spherical	1–6 μm		8% wt	
Wiklund and Stading (2008)	Glycerol and glass beads	Spherical	4–15 μm		5% wt	
Wiklund and Stading (2008)	Mineral slurries	Agglomerative	100 nm to 80 μm		20% wt	

Wiklund and Stading (2008)	Rapeseed oil and polyamide particles	Spherical	11–90 μm		25% wt	
Wiklund and Stading (2008)	Syrup and starch particles	Spherical	30–300 μm		30% wt	
Wiklund and Stading (2008)	Tomato sauce	Fibres	1 mm		30% wt	
Wiklund and Stading (2008)	Strawberry yoghurt (<0.2% fat)	Seeds	1–1.2 mm	1540	8% wt	pl
Wiklund and Stading (2008)	Marmalades, fruit soup	Fibres	0.2–2 mm		35% wt	
Wiklund and Stading (2008)	Fruit jams	Fibres	1–4 mm		35% wt	
Wiklund and Stading (2008)	Pasta sauce	Fibres	1–4 mm	1610		pl
Wiklund and Stading (2008)	Cellulose pulp	Fibres	2–2.4 mm		8% wt	
Wiklund and Stading (2008)	Cheese sauce and carrot cubes	Cubic	2–2.4 mm		1% wt	
Wiklund and Stading (2008)	Seafood chowder	Mixture	≤30 mm	1518		
Wiklund and Stading (2008)	Vegetable sauces	Mixture	≤40 mm	1580		pl
Young *et al.* (2008)	Fat blends					
Choi *et al.* (2002)	Corn syrup solution Tomato juice suspension			1667 1420	65.7°Brix 4.3°Brix	gr gr
Dogan *et al.* (2002)	Diced tomatoes in juice	Complex	1–3 mm		8.15% wt	HB, pl, Casson
Dogan *et al.* (2003a)	Xanthan gum solution				3.5% vol	gr
Dogan *et al.* (2003b)	Tomato concentrate				8.75–17.10%	gr, pl, Casson
Dogan *et al.* (2005a)	Acid-thinned and native cornstarch		4–17 μm (average 11.4 μm)		6% vol	gr, pl
Dogan *et al.* (2005b)	Polydimethylsiloxane			1030		gr, Eyring
Choi *et al.* (2006)	Tomato concentrate			1420	5–24°Brix	pl
Pfund *et al.* (2006)	Carbopol, sodium hydroxide and glass beads		40–90 μm		0.1% wt/ 0.032% vol	gr
Haldenwang *et al.* (2006)	Bentonite and kaolin suspension				5.7–8.3%	HB
Kotzé *et al.* (2008a)	Bentonite suspension		25 μm	1560	7% wt	HB
Kotzé *et al.* (2008a)	Kaolin suspension		35 μm	1555	12% vol	HB
Kotzé *et al.* (2008b)	Carboxymethyl cellulose				6.5% wt	pl
Kotzé *et al.* (2008b)	Bentonite suspension		25 μm		7% wt	HB
Kotzé *et al.* (2008b)	Kaolin suspension		35 μm		12% vol	HB

gr, gradient method; HB, Herschel–Bulkley; pl, power law.

Table 3.2 Measurement parameters

References	Instrument	Transducer type	Transducer position	Frequency (MHz)	Pulse (Cyc)	N_{rpt}	#Prof	Angle	Pipe diameter (mm)	Flow rate (L/minute)	v_{max} (mm/second)
Kowalewski (1980)	UDP 30		Wall	5					10/14	1.2–3	300
Müller *et al.* (1997)	DOP 1000		Wall	4	4	128	1024		16.6	1–7	500
Wunderlich and Brunn (1999)	DOP 1000			4					16.6		900
Brunn *et al.* (2004)	DOP 1000			4		512			16.6		50–350
Ouriev *et al.* (2000)	UVP X3	Imasonic TN	Contact/flush	8			1024		8	0.08–0.37	50–250
Ouriev and Windhab (2002)	UVP X3	Imasonic TN	Contact/flush	4			25–50	70	23	7.3–30	500–1200
Ouriev (2002)	UVP X3	Imasonic TN	Contact/flush	4			25		23	7.3–30	500–1800
Ouriev *et al.* (2003)	UVP X3	Imasonic TN	Contact/flush	4			25	70	32	230	120
Wiklund *et al.* (2002)	UVP X3	Imasonic TN	Contact	4	4	88	1024	70	23	8.4–44	400–1800
Birkhofer *et al.* (2008)	Duo/FFT	Imasonic TN/TX	Contact	4				60	16	0.2	40
Fischer *et al.* (2009)	UVP X3	Imasonic TN	Contact/flush	4					22	0.8, 1.5, 2.1	
Wiklund *et al.* (2007)	Duo/FFT	Imasonic TN/TX	Contact/membrane/wall	4	2–4	128–512	5–300	65–71	35.5/45.5		400
Wiklund and Stading (2008)	Duo/FFT	Imasonic TN/TX	Membrane	2–4	2		20–1024	70	22.5/ 35.5/ 48.5		

Young *et al.* (2008)	Duo/FFT		Contact	4	2–4	192–256	10–40		22.5	1.1	30
Choi *et al.* (2002)	Custom/FFT	Xactex IM-HP-1/4-5	Contact/flush	5	5	512–2048	8	45	50.8	0.78–4.1	40–68
Dogan *et al.* (2002)	Custom/FFT						8	45	53.2	8–25	128–298
Dogan *et al.* (2003a)	Custom/FFT								20/53		
Dogan *et al.* (2003b)	Custom/FFT	Xactex IM-HP-1/4		5	10			45	53.2		40–120
Dogan *et al.* (2005a)	Custom/FFT			5		4096			20.4		100
Dogan *et al.* (2005b)	Custom/FFT		Wall	5	10	4096		45	20.4	0.25–0.77	160
Choi *et al.* (2006)	Duo	Xactex IM-HP-1/4-2[a]	Contact/flush	4	5–20	200	256	45			
Pfund *et al.* (2006)	Custom/FFT	Xactex IM-HP-1/4-5 XIM 1055-27	Contact/non-flush/bottom	5	5–20	1024	16	45	53.2		8–33
Haldenwang *et al.* (2006)	Duo	Imasonic TX	Wall	4	2, 4			70	42, 50	78–168	1500–3500
Kotzé *et al.* (2008a)	Duo	Imasonic TN/TX	Contact						16	30	3000
Kotzé *et al.* (2008b)	Duo	Imasonic TN/TX	Contact	4				70	16	23	3000

#Prof is the number of profiles averaged used for processing. The angle is the Doppler angle between the flow and beam direction. v_{max} is the maximum velocity in the profile.
[a] According to the naming scheme of Xactex, this would be a 2-MHz transducer, and according to the text, it is a 4-MHz transducer.

3.1.3.3 *Swiss Federal Institute of Technology (ETH) Zurich, Switzerland*

At the laboratory of food process engineering, the UVP-PD technique was developed and tested from 1994 onwards (Windhab, 1994). After finishing his PhD (Ouriev, 2000), Boris Ouriev published several articles. Ouriev *et al.* (2000) deal with measurements of fat suspensions with different solid fat concentrations and flow rates. Ouriev and Windhab (2002) applied power law and Herschel–Bulkley models to a shear-thinning suspension of cornstarch in silicon oil and a shear-thickening suspension of cornstarch in glucose syrup. Ouriev (2002) gave details on wall slip measurements of shear-thickening suspension. UVP-PD measurements in chocolate suspension and the influence of seeding with pre-crystallised cocoa butter were presented by Ouriev *et al.* (2003). Ouriev and Windhab (2004) investigated transient flows of non-Newtonian model suspensions. Ouriev *et al.* (2004) presented results on measurements in partly pulsating chocolate flow and corresponding power law fits. Fischer *et al.* (2009) compared in- and off-line measurements in a viscoelastic surfactant solution. Due to a limited spatial resolution and missing velocity profile data towards the pipe walls, it was not possible to detect the expected banding flow. During a stay at ETH Zurich, J. Wiklund and M. Johansson made measurements in shear-thinning surfactant solutions and cellulose suspension and fitted the results to power law and Herschel–Bulkley models. The results were also compared with off-line rheometer measurements. A part of the findings were presented by Wiklund *et al.* (Wiklund *et al.* 2001, 2002). In the course of his PhD work, Birkhofer (2007) made in-line measurements of the acoustic properties and rheology of cocoa butter crystal suspensions (Birkhofer *et al.*, 2004, 2008) as well as model suspensions.

3.1.3.4 *Swedish Institute for Food and Biotechnology (SIK) Gothenburg, Sweden*

Wiklund continued with a PhD work (Wiklund, 2007) at SIK developing the UVP-PD technique mainly for the food industry. Wiklund *et al.* (2006) presented a comparative LDA-UVP study on highly concentrated cellulose fibre suspensions. Results showed that the UVP-PD method can be used to determine the yield stress of such suspensions, directly in-line, and that an important concentration gradient exists close to the wall, which was confirmed later by Wiklund *et al.* (2008). Wiklund *et al.* (2007) presented results of the UVP-PD measurements of various food systems such as cheese sauce, fruit yoghurt and a vegetable sauce. The aim of those trials was to test the applicability of the UVP-PD method to highly concentrated polydisperse suspensions containing anisotropic

particles of various shapes and sizes up to several centimetres in length. Rheological and structural changes due to processing were also studied. That article also contains an overview on the UVP-PD methodology in addition to details of the signal processing and statistical methods such as low pass filtering of the velocity information obtained by the time domain algorithm and singular value decomposition methods to determine the wall position by channel correlation. Young *et al.* (2008) show measurements in fat suspensions of varying crystal content. Wiklund and Stading (2008) show measurements in many different suspension types including their acoustic properties.

3.1.3.5 *University of California Davis, USA*

The group started with magnetic resonance imaging-based flow profiling and pressure drop for in-line rheometry including power law fitting (McCarthy *et al.*, 1992), a technique described earlier by Sinton and Chow (1991) for non-Newtonian fluids. Choi *et al.* (2002) compared this technique with the UVP-PD method for corn syrup solution and tomato juice flow. Dogan *et al.* (2002) presented results on measured properties of diced tomatoes suspended in tomato juice including yield stress, consistency index and apparent wall slip. Dogan *et al.* (2003b) investigated the flow of tomato concentrates with different solid content, the shear-thinning behaviour with a yield stress being fitted to power law and Casson models. In addition, the viscosity and plug radius (yield stress) were also determined directly from the profile. Subsequently, they (Dogan *et al.*, 2005a, 2005b) investigated chemically modified and native cornstarch and polymer melt flows. Choi *et al.* (2005) described the software and data processing procedure for the UVP-PD measurements. Choi *et al.* (2006) reported on the in-line monitoring of tomato concentrate during evaporation by measuring velocity profiles and sound velocity, the latter being used for the determination of the concentration. Powell and Pfund (2005), in collaboration with the Battelle Pacific Northwest National Laboratory, applied the UVP-PD method to the flow of slurry suspensions.

3.1.3.6 *Pacific Northwest National Laboratory (U.S. Department of Energy), Richland, USA*

The UVP-related work started with Shekarriz and Sheen (1998) who characterised the shear-thinning fluids by just fitting the power law exponent n using the velocity profile and flow rate. Pfund *et al.* (2006) investigated the flow of a non-Newtonian solution of Carbopol EZ-1 with sodium hydroxide, which forms a gel.

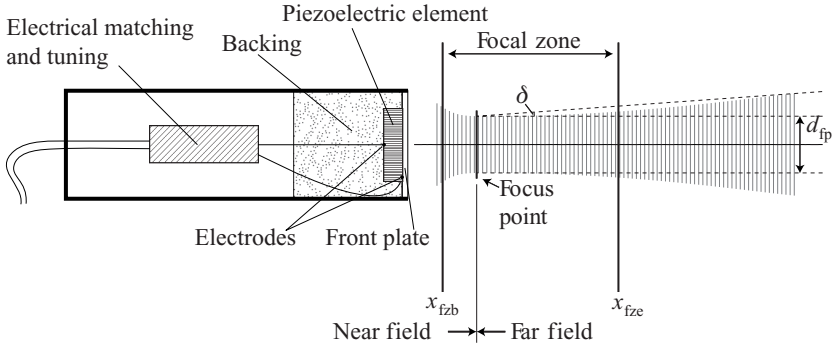

Fig. 3.2 Scheme of the transducer and the pressure field (x_{fzb} and x_{fze}, focal zone begin and end; d_{fp}, diameter of the beam at the focus point) with the divergence half angle δ.

3.1.3.7 *Cape Peninsula University of Technology, Cape Town, South Africa*

This research group applied UVP-PD mainly for the measurements in highly concentrated mineral suspensions of kaolin and bentonite (Kotzé *et al.*, 2008b).

3.2 ULTRASOUND TRANSDUCERS

The transducer is a converter between the electrical and ultrasonic signal and works in both directions. It consists, as also illustrated in Fig. 3.2, of the piezoelectric element which is usually round and has a diameter of a few millimetres, a front plate made of epoxy which has usually a thickness of $\lambda/2$ (λ is wavelength), backing material which has a damping function to avoid reverberations, the housing and the electrical connection. The main design parameters of a transducer are the central frequency f_0 and the diameter of the piezoelectric element D, also known as active diameter, which is usually smaller than the visible diameter of the front plate. These two parameters are important for the pressure field (Fig. 3.2) generated by the transducer, which consists of the near field, focal zone and the far field. The length of the near field l_N is equal to $D^2 f_0/4c$, where c is the sound velocity. Although it is possible to make measurements inside the near field, it is not advisable as the pressure field is irregular and has a not very well defined diameter. Another parameter to be considered is the half-divergence angle $\delta = \arcsin(0.51 \lambda/D)$. Thus, a large active element has the advantages of an increased sensitivity and a reduced beam divergence but the disadvantage of a long near-field length. The central frequency influences the near-field length, the beam divergence and the attenuation respectively. For most

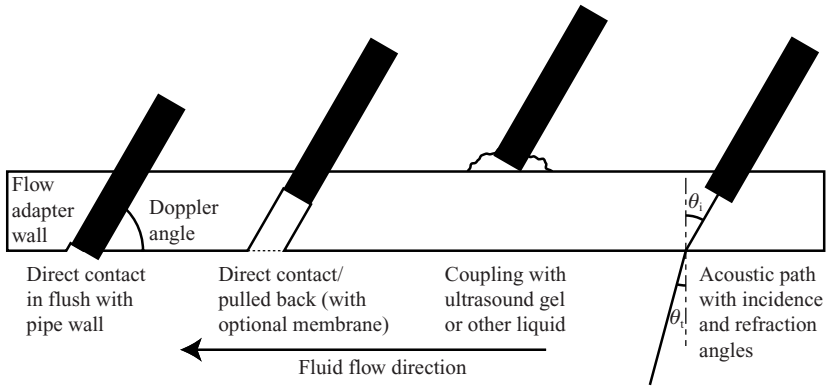

Fig. 3.3 Four different transducer installation possibilities. For the first option (from left), the transducer is in direct contact with the fluid in the pipe, for the second, only if no membrane is installed. The third alternative with a coupling fluid can be used as an ad hoc solution if no flow adapter is available. The fourth option shows the change of the beam path at the interface to the fluid with the incident angle θ_i and the transmittance angle θ_t.

fluids, the attenuation increases as the square of the frequency. Thus, for each applications those parameters have to be optimised.

An additional transducer property is the bandwidth which describes the frequency-dependent characteristics. This is interesting in cases where the same transducer should be used with different frequencies, for example 2 and 4 MHz. There is no standardised procedure for the measurement of the bandwidth of a transducer, which makes it difficult to compare the available data from the manufacturers.

In the operational temperature range, the sensitivity of a transducer can vary, usually decreasing with temperature.

For special applications also, focused transducers can be of interest as they allow to customise to a certain degree the near-field length, the focal zone and the beam diameter.

A good overview of problems and paradoxes of transducer design is given in Hunt *et al.* (1983). Also, Papadakis (1999) contains information on the different transducer types.

3.3 FLOW ADAPTER

The flow adapter or flow cell is the mechanical construction needed to fix the ultrasound transducer relative to the pipe with fluid flow inside. There exist several different approaches (Fig. 3.3), and the best solution will depend on the acoustic properties of the fluid, pipe dimensions, process conditions and other parameters.

Direct contact of the transducer with the fluid in the pipe ('wetted') was described by several authors (Shekarriz and Sheen, 1998; Choi *et al.*, 2002; Ouriev and Windhab, 2003). Mounting the transducer in flush with the pipe wall makes it usually impossible to have a realistic measurement in the wall region, as the ringing of the transducer from the pulse emission is superimposed on the first received echo. Depending on the design of the electronics, the receiving part is also oversteered for some time after sending a pulse. In addition, as mentioned by Hoeks *et al.* (1991), measurements inside the near field are affected by an inhomogeneous pressure distribution and a variation in the Doppler angle (Bascom *et al.*, 1986). If the transducer is pulled away from the flow to have the focal point of the pressure field in the region of the pipe wall, a cavity is formed which can accumulate air bubbles or sediments. This method has additional disadvantages if the fluid is highly attenuating, as the available penetration depth is reduced accordingly. Improved set-ups were shown by Lemmin and Rolland (1997) and Wiklund and Stading (2006) involving a film in front of the cavity to minimise influences on the pipe flow streamlines. In this case it is also possible to fill the cavity between the transducer and the film with ultrasound gel or another fluid matched acoustically to the fluid in the pipe to minimise the refraction and Doppler angle change at the interface between the two fluids. It is important to avoid the inclusion of air bubbles in the liquid in front of the transducer, as this would lead to unreproducible artefacts in the measured profile.

It is also possible to measure through the pipe wall, especially for materials such as Plexiglas (Yamanaka *et al.*, 2002). The effects of a layer of Plexiglas or polyethylene on the ultrasound beam as a function of the incidence angle for longitudinal and shear waves were investigated in detail, theoretically and experimentally, by Thompson *et al.* (2000). The influence of the curvature of the pipe on the pressure field was investigated by Thompson and Aldis (1996) and Tortoli *et al.* (1999). Regarding flow adapter material selection, Nowak (2002) and Hung and Goldstein (1983) are of interest as they give sound velocities and densities for various relevant materials (e.g. nylon, PEHD, PET (Mylar), PMMA (Plexiglas), POM (Delrin), PVC and Teflon).

Steel pipes (Kishiro *et al.*, 2004; Wada *et al.*, 2004) are quite difficult to penetrate; many authors used, for example, a wedge transducer (Tezuka *et al.*, 2006) to improve the measurements.

3.3.1 Doppler angle

Two different definitions of the Doppler angle are used in the literature. In the medical field, it is common to use the angle between flow direction and ultrasound direction, as indicated in Fig. 3.3. This is also the

definition used in this text. The fluid mechanics field partly prefers the angle between the normal to the flow and the transducer which corresponds to the incident angle θ_i in Fig. 3.3.

If the transducer is in direct contact with the fluid in the pipe, there is mainly the velocity range which is of interest to determine the Doppler angle. Small angles (e.g. 60°) allow the measurement of low flow velocities, while larger angles are preferred for fast flows. The averaging decreases with the Doppler angle (McArdle and Newhouse, 1996).

When measuring through the pipe wall or some kind of delay line or wedge, the corresponding refraction angles and losses have to be considered (Messer and Aidun, 2009). The angle can be calculated according to Snell's law:

$$c_1 \sin\theta_t = c_2 \sin\theta_i$$

where c_1 and c_2 are the sound velocities in the two media and θ_i and θ_t are the incidence and transmittance angles, respectively. Thus, the closer the sound velocities of the two materials, the smaller the angle change. The ratio of the amplitudes of transmitted and incident waves T_θ also depends on the material densities ρ_1 and ρ_2 and is (Hill *et al.*, 2004) as follows:

$$\begin{aligned} T_\theta &= \frac{\rho_2 c_2 \cos\theta_i - \rho_1 c_1 \cos\theta_t}{\rho_2 c_2 \cos\theta_i + \rho_1 c_1 \cos\theta_t} \\ &= \frac{2\rho_2 c_2 \cos\theta_i}{\rho_2 c_2 \cos\theta_i + \rho_1 \sqrt{c_1^2 - c_2^2 \sin^2\theta_i}} \end{aligned} \tag{3.1}$$

Mounting the transducer either with or against the flow direction should not influence the measured flow profile seen from the sign of the velocity.

3.4 ACOUSTIC PROPERTIES

The measurement of the acoustic properties of particulate suspensions and other food systems has been investigated by many researchers in the past decades. The acoustic properties comprise mainly of ultrasonic velocity, attenuation coefficient and acoustic impedance (McClements, 1997).

3.4.1 Propagation

There are different modes of sound propagation, the three most important being compression, shear and surface waves. The velocity

measurements are made with compression waves; at the pipe–fluid interface shear waves can also be involved (Kishiro *et al.*, 2004).

3.4.2 Attenuation

Ultrasound transducers are phase sensitive; thus, a low measured signal is not certainly due to attenuation but possibly scattering. This is one of the reasons why the measurement of the attenuation is less reliable than the sound velocity measurement. In addition, there are diffraction, losses at interfaces and relaxation effects. The attenuation coefficient can be calculated by fitting the data from a measurement of the amplitude as a function of the distance from the transducer to following equation:

$$\xi = \xi_0 e^{-\alpha z} \tag{3.2}$$

where ξ is the amplitude, z the distance in beam direction and ξ_0 the original amplitude at $z = 0$.

3.4.3 Sound velocity

The velocity of sound is a function of the density and the adiabatic compressibility of the medium. For most materials, with the exception of water, it decreases with increase in temperature. As the pressure waves propagate through the medium, the volume and density fluctuate locally about the normal values. This can be expressed as dilation:

$$D = \frac{\Delta V}{V_0} \tag{3.3}$$

and condensation:

$$s = \frac{\Delta \rho}{\rho_0} \tag{3.4}$$

The adiabatic compressibility κ is then defined as follows:

$$\kappa = -\frac{1}{V}\frac{\partial V}{\partial p} \cong \frac{D}{\Delta p} \tag{3.5}$$

The bulk modulus of elasticity is then:

$$B = -\frac{\Delta p}{D} = \frac{1}{\kappa} \tag{3.6}$$

Wood (1964) showed that the velocity of sound c in *homogeneous* liquids and gases is independent of frequency and is given by the Wood equation:

$$c = \sqrt{\frac{B}{\rho}} = \sqrt{\frac{1}{\kappa\rho}} \tag{3.7}$$

A simple approach to calculate the velocity of sound in a dispersion is the Urick equation (Urick, 1947) in which κ and ρ in the Wood Equation 3.7 are replaced by the following:

$$\kappa = \sum \phi_i \kappa_i, \quad \rho = \sum \phi_i \rho_i \tag{3.8}$$

where i is the ith component of the mixture. This is called a homogeneous description because the properties of each phase contribute independently to the properties of the system (Povey and Mason, 1998, Chapter 3). By adding a second transducer opposite to the one for the velocimetry, this simple relation of concentration and sound velocity can be used to determine approximately the composition, for example solid concentration, in the pipe (Birkhofer *et al.*, 2008; Wiklund and Stading, 2008).

In order to consider scattering effects, Pinfield and Povey (1997) proposed a modified Wood equation. The Urick equation and its extensions were reviewed by McClements and Povey (1987).

3.4.4 Scattering

The scattering of ultrasound in dispersions depends on the size ratio of the wavelength and the particle diameter. Thus, the scattering characteristics can also be used for particle size analysis (Epstein and Carhart, 1953; Allegra and Hawley, 1972; Harker and Temple, 1988; Riebel and Löffler, 1989; Holmes *et al.*, 1993, 1994; Pinfield and Povey, 1997; Storti *et al.*, 2000; Dukhin and Goetz, 2002). Regarding velocity profile measurements, study of Atkinson and Kytömaa (1993) is of interest, as it describes the development of the ultrasonic pressure field, attenuation and sound velocity in suspensions of different concentrations (up to the maximum packing density) and relates it to velocimetry.

3.4.5 Backscattering

The backscattering or the echogenicity of suspensions is investigated mostly in the medical field. For the velocimetry, this property is quite crucial as it decides if and with which penetration depth a measurement

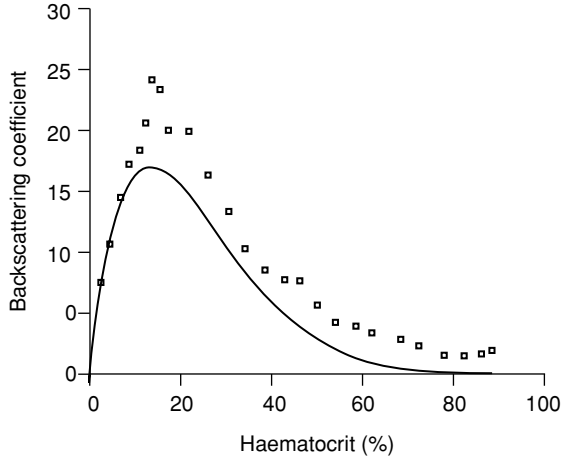

Fig. 3.4 The plot of the backscattering coefficient versus haematocrit for porcine red blood cells suspended in saline (□). The smooth curve represents the Percus–Yevick theory for the packing of hard spheres. (Results from Mo *et al.,* 1994.)

is possible. In blood flow, it is assumed that the red blood cells (erythrocytes) far outnumber the other possible scatterers both in quantity and volume (Shung *et al.*, 1976) and are thereby the main source of scattering in blood. A theoretical analysis of scattering by Angelsen (1980) was based on the assumption that blood is an isotropic continuum and that the scattering arises from fluctuations in the compressibility and mass density of the continuum. This explains the development of the backscattering coefficient as a function of the haematocrit, shown in Fig. 3.4. Until about 20% haematocrit, the backscattering coefficient increases with the concentration of the scatterers. Above this, if the concentration is high enough, the waves scattered by the individual particles will interfere, which leads to phase cancellation. This is why the overall scattering depends on the configuration of the set of scatterers. The more regular is the distribution (higher isotropy), the lower is the backscattering coefficient. So, towards the maximum packing density, the backscattering coefficient reaches its minimum. Also, the flow itself influences the particle fluctuation and therefore the backscattering properties (Sigel *et al.*, 1983; Shung *et al.*, 1984; Cloutier and Shung, 1993; Cloutier and Qin, 1997; Lin and Shung, 1999; Rouffiac *et al.*, 2004).

The models of Angelsen (1980) and Twersky (1988) were further developed independently by Mo *et al.* (1994) and Bascom and Cobbold (1995) by combining them with the voxel model. A voxel refers to an elemental volume that is small enough so that the incident ultrasonic wave may be assumed to arrive with the same phase at every scatterer located within it. Another model for the scattering in tissues was developed by Jensen (1991) in which effects of flow disturbance and haematocrit on

the backscattered Doppler signal were explained by means of a backing dimension and a particle dimension.

Measurement techniques for the backscattering are described by Sigelmann and Reid (1973), Madsen *et al.* (1984), Ueda and Ozawa (1985), Insana *et al.* (1986), Berger *et al.* (1991), Madsen (1993) and Chen and Zagzebski (1996).

3.5 ELECTRONICS, SIGNAL PROCESSING AND SOFTWARE

3.5.1 Electronics

The electronics is responsible for the generation of the electrical signal sent to the transducer and the registration (in most cases digitalisation) of the signal received by the transducer. The working principle is described in several textbooks from the medical field (Jensen, 1996; Evans and McDicken, 2000; Hill *et al.*, 2004; Cobbold, 2007).

The details of the signal processing of the available devices are differing, for example some devices use an analogue demodulation and digitise afterwards, while other recent devices digitise the original signal from the transducer at a high sampling rate and do the demodulation with the digital signal. Parameters such as pulse length, gate (or channel) distance, emission signal amplitude and amplification of the received signal are adjustable for most devices.

3.5.2 Signal processing and profile estimation

There are several different signal processing approaches described in the literature from the medical field to extract the actual flow velocity profile from the echo signal received by the transducer. If and how the signal processing can be customised depends on the hardware. Some devices work rather as a black box and only allow access to the estimated profile. It can be of advantage to have at least access to the complex demodulated signal (I and Q), which allows to obtain the distribution of the Doppler frequency for the individual channels via FFT (fast Fourier transformation). This simplifies the identification of artefacts influencing the profile shape (Jones, 1993). In addition, it is possible to use different velocity estimation approaches such as central or maximum frequency (Tortoli *et al.*, 1995, 1996, 2006).

3.5.3 Software

For the data acquisition (flow profiles and pressure, maybe temperature and flow rate), the rheological calculations and visualisation of the data,

it is probably most efficient to develop custom software to automatise everything. Such a software also allows nearly real-time data analysis and visualisation, which is crucial for industrial applications. Usually, development environments such as MATLAB (Choi *et al.*, 2005) or LabVIEW are used for implementation as they simplify the access to the data acquisition hardware and also provide high-level function, for example for non-linear fitting procedures.

3.6 PIPE FLOW AND FLUID MODELS

As mentioned in the introduction, the UVP-based in-line rheometry makes use of the information contained in the shape of the flow velocity profile. Frequently, the pressure drop over a straight pipe section is measured in parallel to the velocity profile. This allows the direct derivation of the shear stress τ along the radius r, which is given by:

$$\tau = \frac{\Delta P r}{2L} \tag{3.9}$$

where ΔP is the pressure drop measured over a distance L along the axial direction of the pipe (Fig. 3.1).

3.6.1 Gradient method or point-wise rheological characterisation

The shear rate $\dot{\gamma}$ along the pipe radius is given by:

$$\dot{\gamma} = -\frac{\mathrm{d}v}{\mathrm{d}r} \tag{3.10}$$

where v is the flow velocity along the radius r. Thus, using the measured pressure drop and velocity profile, it is possible to derive directly the local viscosity using Equations 3.9 and 3.10:

$$\eta(r) = \frac{\tau(r)}{\dot{\gamma}(r)} \tag{3.11}$$

In the articles from the University Erlangen-Nürnberg (Müller *et al.*, 1997), this is described as 'gradient method', while the same principle is described as 'point-wise rheological characterisation' in the articles from the UC Davis (Arola *et al.*, 1999; Dogan *et al.*, 2005b), where the measured flow profile was first fitted with a fourth-order polynomial whose first derivative was then used to determine the shear rates.

The advantage of the gradient method is that it does not require an a priori flow model. The resulting usable shear rate range is rather limited as the low shear rate region towards the centre of the pipe is given by the velocity resolution of the measurement system, and due to averaging effects it is also difficult to have an accurate measurement towards the pipe wall, which limits the maximum shear rate.

3.6.2 Power law fluid model

The simple power law model

$$\tau = K\dot{\gamma}^n \tag{3.12}$$

respectively

$$\eta = K\dot{\gamma}^{n-1} \tag{3.13}$$

represents Newtonian ($n = 1$), shear-thinning ($n < 1$) or shear-thickening ($n > 1$) non-Newtonian fluids, where K is the consistency index and n is the flow exponent. Combination with Equation 3.9 and integration results in an equation for the radial velocity profile:

$$v = \frac{R}{(1+1/n)}\left(\frac{R\Delta P}{2LK}\right)^{1/n}\left(1-\left(\frac{r}{R}\right)^{1+1/n}\right) \tag{3.14}$$

Having measured the velocity profile and the pressure drop, Equation 3.14 can be used to fit n and K, usually by minimising the sum of the squares of the differences of the measured and the calculated velocity profile.

The local shear rate and viscosity are respectively given by:

$$\dot{\gamma} = \left(\frac{\Delta Pr}{2LK}\right)^{1/n} \tag{3.15}$$

$$\eta = K\left(\frac{\Delta Pr}{2LK}\right)^{1-1/n} \tag{3.16}$$

It would also be possible to derive only n when the volume flow rate is Q, and thus the mean flow velocity $\overline{v}$ is known using (Wilkinson, 1960)

$$v = \overline{v}\left(\frac{3n+1}{n+1}\right)\left(1-\left(\frac{r}{R}\right)^{\frac{n+1}{n}}\right) \tag{3.17}$$

Alternatively, the maximum flow velocity can be used (Kowalewski, 1980):

$$v = v_{\max}\left(1 - \left(\frac{r}{R}\right)n + 1n\right) \tag{3.18}$$

Yet another approach to determine n is to use the wall shear rate $\dot{\gamma}_{\mathrm{w}}$, which can be expressed using the flow rate Q as:

$$\dot{\gamma}_w = \left(\frac{3n+1}{4n}\right)\left(\frac{4Q}{\pi R}\right) \tag{3.19}$$

3.6.3 Herschel–Bulkley fluid model

The analysis in the previous section can be extended to other rheological models such as Herschel–Bulkley with the yield stress τ_0:

$$\tau = \tau_0 + K\dot{\gamma}^n \tag{3.20}$$

The corresponding equation for the velocity is given by:

$$v = \frac{nR}{1+n}\left(\frac{R\Delta P}{2LK}\right)^{\frac{1}{n}}\left(\left(1 - \frac{R_*}{R}\right)^{1+\frac{1}{n}} - \left(\frac{r}{R} - \frac{R_*}{R}\right)^{1+\frac{1}{n}}\right) \tag{3.21}$$

in which $r > R_*$ and $R_* = 2L\tau_0/\Delta P$ is the radius of the plug, which can also be determined directly from the flow profile (Dogan *et al.*, 2003b). The local shear rate and viscosity are respectively given by

$$\dot{\gamma} = \left(\frac{\Delta P}{2LK}\right)^{\frac{1}{n}}(r - R_*)^{\frac{1}{n}} \tag{3.22}$$

$$\eta = \frac{\tau}{\dot{\gamma}} = K\left(\frac{\Delta P}{2LK}\right)^{1-\frac{1}{n}}\frac{r}{(r-R_*)^{\frac{1}{n}}} \tag{3.23}$$

3.6.4 Other models

Power law and Herschel–Bulkley are the two most often applied models, but literature also describes the use of Ellis (Wunderlich and Brunn, 1999), Casson (Dogan *et al.*, 2003b), Eyring (Dogan *et al.*, 2005b) and Sisko (Birkhofer, 2007; Wiklund, 2007) models.

3.7 RHEOMETRY

3.7.1 Averaging effects at the pipe wall

Often, profiles show an unrealistic sigmoidal shape close to the pipe wall, while in theory one would expect the maximum shear rate at the wall. This effect was already explained in the early 1970s (Jorgensen *et al.*, 1973; Jorgensen and Garbini, 1974) by the convolution of flow velocity profile and the sample volume. The sample volume is generated by the ultrasound transducer and has approximately a drop-like shape. The axial length and shape are determined by the pulse length and the dynamic characteristics of the piezoelectric element. The diameter of the sample volume depends on the pressure field. Thus, the echo signal of one measurement channel is, simplified, an intensity-weighted sum of all flow velocities covered by the pulse. In the mentioned articles, Jorgensen and later Hughes and How (1993, 1994) also show a way to make a deconvolution of the two signals involving a transfer to the frequency domain and back to the time domain using (inverse) FFT. An alternative method for the deconvolution would be a single value decomposition. Another approach to obtain a more realistic profile at the pipe wall is shown by Tortoli *et al.* (1995). The method, based on the maximum frequency $f_{\max}$ of the Doppler spectrum, involves a correction factor k for the sample volume shape, which also depends on the transducer characteristics. To calculate the flow velocities v, the following equation (Tortoli *et al.*, 2006) which is a variation of the classical Doppler equation is used (α is a Doppler angle):

$$v = \frac{f_{\max} c}{2 f_0 (\cos(\alpha) + k \sin(\alpha))} \tag{3.24}$$

3.7.2 Fitting

When using the measured data and a model such as power law (Equation 3.14) or Herschel–Bulkley (Equation 3.21), there are a few critical points to be considered. Usually, a non-linear optimisation is used to obtain the parameters n, K and τ_0 (Herschel–Bulkley only). The result of the fitting can be quite sensitive to several parameters such as the section of the start and end point of the profile half used for the fitting (Birkhofer, 2007) or details of the profile shape which can depend on measurement parameters such as the pulse length or even the emission voltage or amplification.

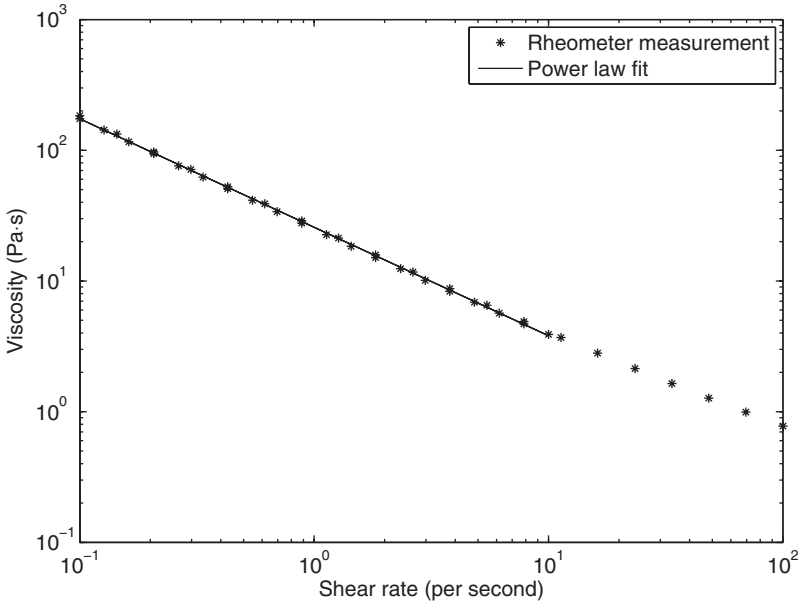

Fig. 3.5 The flow curve of a Carbopol suspension with the points measured with the rheometer and the corresponding power law fit.

3.7.3 Gradient method

For the gradient method, the viscosity is calculated directly using Equations 3.9 to 3.11. The resulting minimum shear rate from the flat part of the profile towards the pipe centre is limited by the resolution of the velocity measurement and possible small distortions. Due to the convolution (Section 3.7.1), the maximum measurable shear rate is shifted away from the wall, therefore lower than the actual wall shear rate $\dot{\gamma}_w$.

3.8 EXAMPLES

The application of the technique is demonstrated with two different model fluids which have the advantage to be reproducible and measurable with a conventional rheometer. The latter allows to verify the in-line (UVP) measurement, which is a recommendable first step.

3.8.1 Carbopol solution

Aqueous Carbopol solution (0.5% wt) is a yield shear-thinning fluid. The flow curve is shown in Fig. 3.5. In the double logarithmic plot, the

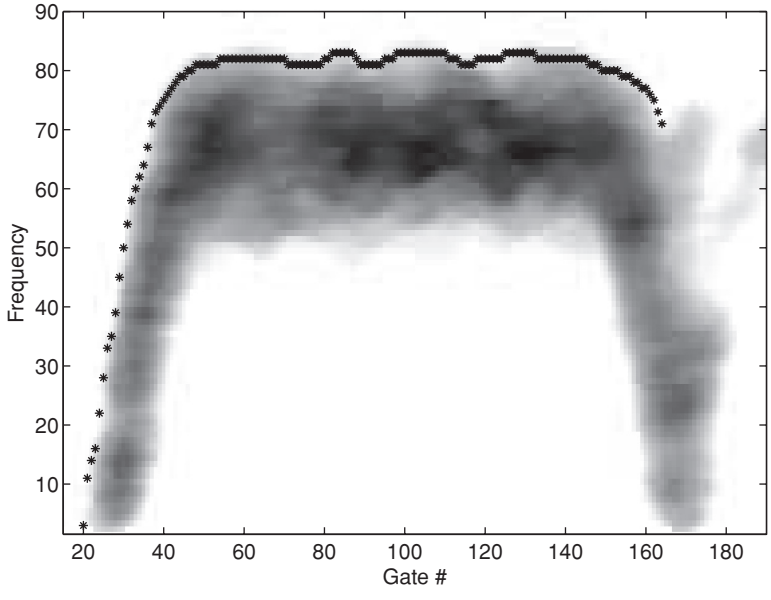

Fig. 3.6 The velocity profile for Carbopol (grayscale, the frequency intensities; $*$, the envelope profile).

relation looks linear, so it can be fitted to the power law (Equation 3.13). With a log transformation and the limitation of the shear rate range to the one expected in the pipe flow (maximum 10/second), the values resulting from the rheometer are $n = 0.170 \pm 0.07$ and $K = 25.7 \pm 0.4$ Pa $\cdot$ s^n. The errors indicate the 95% confidence interval.

The measurement set-up consisted of a pipe with an inner diameter of 25 mm, which was mounted at the exit of a kind of capillary rheometer. The pressure drop was not measured, but the volume flow rate is very well known. The ultrasound transducer was fixed in the pipe wall (rightmost option; Fig. 3.3).

The measured Doppler shift frequency distribution for each gate (or channel) is shown in Fig. 3.6 as surface plot. The darker the level of grey, the higher the corresponding frequency intensity. In the same figure, the envelope (maximum frequency) is indicated by symbols. The second half of the profile shows some artefacts such as the beginning of a ghost profile which is due to multiple reflections.

At the next step, the first half of the velocity profile obtained from Equation 3.24 (Fig. 3.7) and the known volume flow rate Q (or $\overline{v}$) are used to determine n by fitting Equation 3.17. For the Carbopol profile, the result is $n = 0.177 \pm 0.07$ which is quite close to the rheometer result.

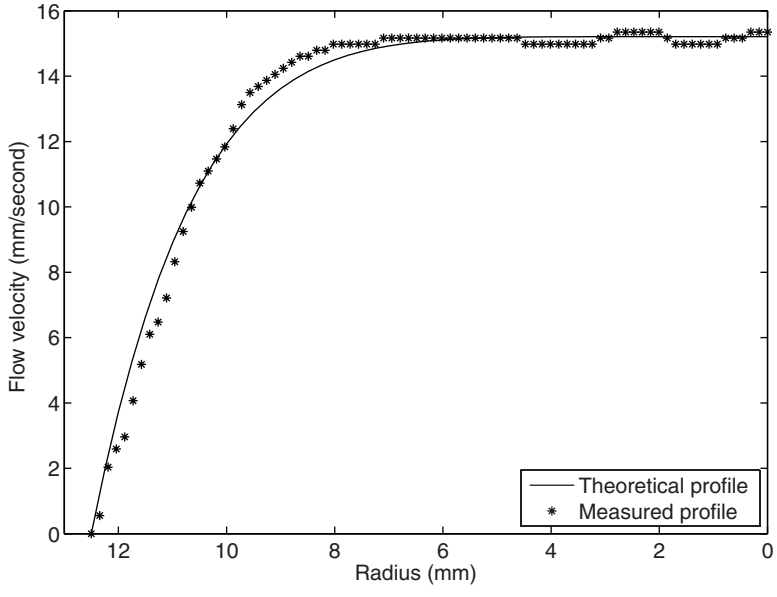

Fig. 3.7 The measured velocity profile and the profile calculated with the rheometer measurement.

3.8.2 Suspension of polyamide in rapeseed oil

The presented data were acquired during a measurement campaign at SIK Gothenburg conducted together with J. Wiklund. The fluid was a suspension of 25% polyamide particles with an average size of 10 μm in rapeseed oil. A flow loop consisting of a vessel, a pump and pipes with an inner diameter of 22.5 mm was used to circulate the fluid. The transducer was mounted 'wetted' but pulled back (the second option from the left in Fig. 3.3). The flow curve (Fig. 3.8) measured with the rheometer shows a shear-thinning behaviour, which can be approximated with the Sisko fluid model ($\eta = K\dot{\gamma}^{n-1} + \eta_\infty$). For this model, there is no analytical solution of the flow profile analogue to Equation 3.14. Therefore, the gradient or point-wise method (Section 3.6.1) is applied.

The measured profile is shown in Fig. 3.9. Although a time-compensated gain was used for this measurement, the intensities clearly decrease with depth which is due to the attenuation in the highly concentrated suspension. It is obvious that for this example the envelope profile would be distorted due to this depth-dependent attenuation; therefore, the central frequency was used for the profile estimation. Towards the pipe walls, the profile shows a sigmoidal shape, and the maximum shear rate is shifted a few gates towards the pipe centre. This is an artefact as the highest shear rate is expected at the pipe wall. In addition to the convolution mentioned in Section 3.7.1, the disturbance of the streamlines

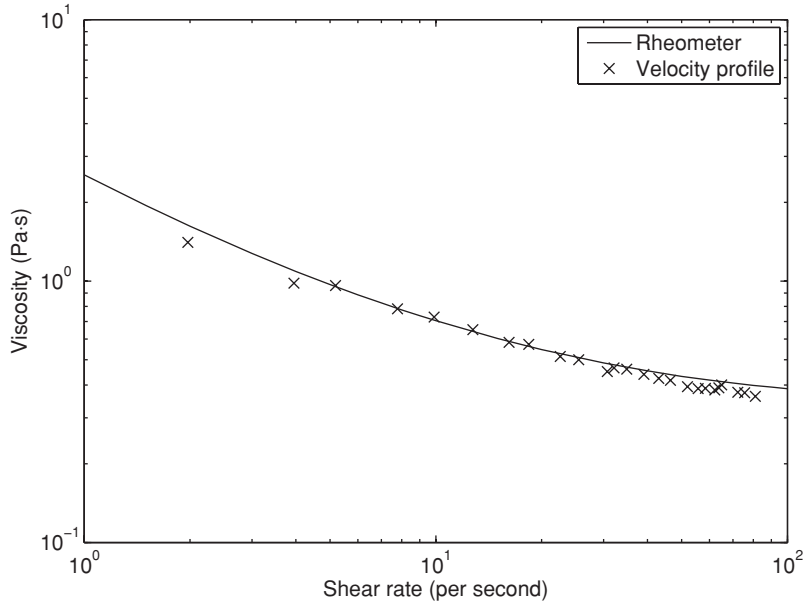

Fig. 3.8 The flow curve for the suspension of polyamide in rapeseed oil (—) and the result of the point-wise (gradient) analysis of the measured flow profile (×).

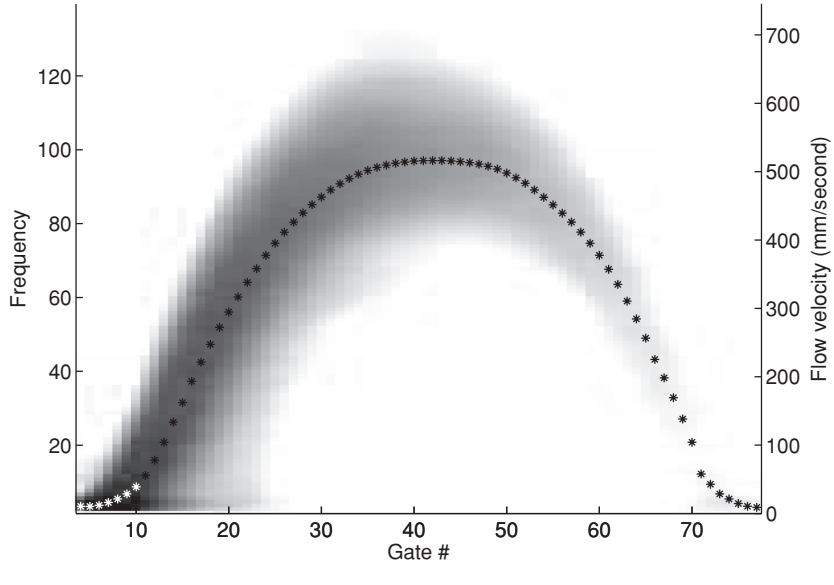

Fig. 3.9 The velocity profile for the suspension of polyamide particles in rapeseed oil with the central frequency indicated (∗).

caused by the cavity in front of the transducer could contribute to this effect.

Fig. 3.8 shows the viscosity calculated with Equation 3.11 versus the shear rate (in this case simply the first derivative of the velocity profile) as symbols. The first few points resulting from the profile data towards the wall below the shear rate maximum were removed. For the leftmost points, the absolute value of the velocity difference is already close to the resolution of the measurement.

3.9 SUMMARY

While the principle of the measurement is rather simple, it is not trivial to obtain quantitative results. The most critical point is the measurement of the velocity profile itself. In many disciplines, a rather qualitative velocity profile measurement is sufficient, while for the UVP-PD method the profile should be as quantitative as possible. But even if the profile is influenced by various artefacts and it is not possible to obtain absolute values characterising the rheological properties, the information on the relative changes of the rheology of the fluid during the measurement can be useful, especially for industrial product quality monitoring.

REFERENCES

Allegra, J.R. and Hawley, S.A. (1972) Attenuation of sound in suspensions and emulsions: theory and experiments. *The Journal of the Acoustical Society of America* **51**(5 (Part 2)), 1545–1564.

Angelsen, B.A.J. (1980) A theoretical study of the scattering of ultrasound from blood. *IEEE Transactions on Biomedical Engineering* **27**(2), 61–67.

Arola, D.F., Powell, R.L., Barrall, G.A. and McCarthy, M.J. (1999) Pointwise observations for rheological characterization using nuclear magnetic resonance imaging. *Journal of Rheology* **43**(1), 9–30.

Atkinson, C.M. and Kytömaa, H.K. (1993) Acoustic properties of solid-liquid mixtures and the limits of ultrasound diagnostics I: experiments. *Journal of Food Engineering* **115**, 665–675.

Baker, D.W. (1970) Pulsed ultrasonic Doppler blood-flow sensing. *IEEE Transactions on Sonics and Ultrasonics* **17**(3), 170–185.

Bascom, P.A.J. and Cobbold, R.S.C. (1995) On a fractal packing approach for understanding ultrasonic backscattering from blood. *The Journal of the Acoustical Society of America* **98**(6), 3040–3049.

Bascom, P.A.J., Cobbold, R.S.C. and Roelofs, B.H.M. (1986) Influence of spectral broadening on continuous wave Doppler ultrasound spectra: a geometric approach. *Ultrasound in Medicine and Biology* **12**(5), 387–395.

Berger, N.E., Lucas, R.J. and Twersky, V. (1991) Polydisperse scattering theory and comparisons with data for red blood cells. *The Journal of the Acoustical Society of America* **89**(3), 1394–1401.

Birkhofer, B.H. (2007) *Ultrasonic In-line Characterization of Suspensions*. PhD thesis, ETH Zurich. URL http://e-collection.ethbib.ethz.ch/view/eth:29828 (accessed 10 September 2010).

Birkhofer, B., Jeelani, S.A.K., Ouriev, B. and Windhab, E.J. (2004) In-line characterization and rheometry of concentrated suspensions using ultrasound. In: Takeda, Y., Murai, Y., Kikura, H. and N. Furuichi, N., editors. Fourth International Symposium on Ultrasonic Doppler Methods for Fluid Mechanics and Fluid Engineering (4th ISUD), Hokkaido University, Sapporo, Japan, September, pp. 65–68.

Birkhofer, B.H., Jeelani, S.A.K., Windhab, E.J., Ouriev, B., Lisner, K.-J., Braun, P. and Zeng, Y. (2008) Monitoring of fat crystallization process using UVP-PD technique. *Flow Measurement and Instrumentation* **19**(3–4), 163–169.

Brandestini, M. (1978) Topoflow – a digital full range Doppler velocity meter. *IEEE Transactions on Sonics and Ultrasonics* **25**(5), 287–292.

Brunn, P., Vorwerk, J. and Steger, R. (1993) Optical and acoustic rheometers: three examples. *Applied Rheology* **3**(1), 20–27.

Brunn, P.O., Wunderlich, T. and Müller, M. (2004) Ultrasonic rheological studies of a body lotion. *Flow Measurement and Instrumentation* **15**(3), 139–144.

Chen, J.-F. and Zagzebski, J.A. (1996) Frequency dependence of backscatter coefficient versus scatterer volume fraction. *IEEE Transactions on Ultrasonics, Ferroelectrics, and Frequency Control* **43**(3), 345–353.

Choi, Y., McCarthy, K. and McCarthy, M. (2002) Tomographic techniques for measuring fluid flow properties. *Journal of Food Science* **67**(7), 2718–2724.

Choi, Y.J., McCarthy, K.L. and McCarthy, M.J. (2005) A MATLAB graphical user interface program for tomographic viscometer data processing. *Computers and Electronics in Agriculture* **47**(1), 59–67.

Choi, Y.J., Milczarek, R.R., Fleck, C.E., Garvey, T.C., McCarthy, K.L. and McCarthy, M.J. (2006) In-line monitoring of tomato concentrate physical properties during evaporation. *Journal of Food Process Engineering* **29**, 615–632.

Cloutier, G. and Qin, Z. (1997) Ultrasound backscattering from non-aggregating and aggregating erythrocytes – a review. *Boirheology* **34**(6), 443–470.

Cloutier, G. and Shung, K.K. (1993) Cyclic variation of the power of ultrasonic Doppler signals backscattered by polystyrene microspheres and porcine erythrocyte suspensions. *IEEE Transactions on Biomedical Engineering* **40**(9), 953–962.

Cobbold, R.S.C. (2007) *Foundations of Biomedical Ultrasound*. New York: Oxford University Press.

Dogan, N., McCarthy, M. and Powell, R. (2002) In-line measurement of rheological parameters and modeling of apparent wall slip in diced tomato suspensions using ultrasonics. *Food Engineering and Physical Properties* **67**(6), 2235–2240.

Dogan, N., McCarthy, M.J. and Powell, R.L. (2003a) In-line flow and rheology measurements of complex, opaque fluids with velocimeter based rheometry using ultrasonics. In: Fischer, P., Marti, I. and Windhab, E.J., editors. *Proceedings of the 3rd International Symposium on Food Rheology and Structure (ISFRS 2003)*, Zurich: ETH Zurich, pp. 453–454.

Dogan, N., McCarthy, M.J. and Powell, R.L. (2003b) Comparison of in-line consistency measurement of tomato concentrates using ultrasonics and capillary methods. *Journal of Food Process Engineering* **25**, 571–587.

Dogan, N., McCarthy, M.J. and Powell, R.L. (2005a) Application of an in-line rheological characterization method to chemically modified and native corn starch. *Journal of Texture Studies* **36**, 237–254.

Dogan, N., McCarthy, M.J. and Powell, R.L. (2005b) Measurement of polymer melt rheology using ultrasonics-based in-line rheometry. *Measurement Science and Technology* **16**, 1684–1690.

Dukhin, A.S. and Goetz, P.J. (2002) *Ultrasound for Characterizing Colloids, Particle Sizing, Zeta Potential, Rheology. Studies in Interface Science*. Amsterdam: Elsevier.

Epstein, P.S. and Carhart, R.R. (1953) The absorption of sound in suspensions and emulsions. I. Water fog in air. *The Journal of the Acoustical Society of America* **25**(3), 553–565.

Evans, D.H. and McDicken, W.N. (2000) *Doppler Ultrasound: Physics, Instrumentation and Signal Processing*, 2nd Edition. Chichester: Wiley.

Fischer, P., Ouriev, B. and Windhab, E.J. (2009) Macroscopic pipe flow of micellar solutions investigated by ultrasound Doppler velocimetry. *Tenside Surfactants Detergents* **46**(3), 140–144.

Fowlis, W.W. (1973) Liquid metal flow measurements using an ultrasonic Doppler velocimeter. *Nature Physical Science* **242**, 12–13.

Garbini, J.L., Forster, F.K. and Jorgensen, J.E. (1982a) Measurement of fluid turbulence based on pulsed ultrasound techniques. Part 1. Analysis. *Journal of Fluid Mechanics* **118**, 445–470.

Garbini, J.L., Forster, F.K. and Jorgensen, J.E. (1982b) Measurement of fluid turbulence based on pulsed ultrasound techniques. Part 2. Experimental investigation. *Journal of Fluid Mechanics* **118**, 471–505.

Haldenwang, R., Kotzé, R., Slatter, P. and Mariette, O. (2006) An investigation in using UVP for assisting in rheological characterisation of mineral suspensions. In: Birkhofer, B.H., Jeelani, S.A.K. and Windhab E.J., editors. Proceedings of the 5th International Symposium on Ultrtasonic Doppler Methods for Fluid Mechanics and Fluid Engineering, pp. 77–80.

Harker, A.H. and Temple, J.A.G. (1988) Velocity and attenuation of ultrasound in suspensions of particles in fluids. *Journal of Physics D: Applied Physics* **21**, 1576–1588.

Hill, C.R., Bamber, J.C. and ter Haar, G.R., editors. (2004) *Physical Principles of Medical Ultrasonics*, 2nd Edition. Hoboken, NJ: Wiley.

Hoeks, A.P.G., Hennerici, M. and Reneman, R.S. (1991) Spectral composition of Doppler signals. *Ultrasound in Medicine and Biology* **17**(8), 751–760.

Holmes, A.K., Challis, R.E. and Wedlock, D.J. (1993) A wide bandwidth study of ultrasound velocity and attenuation in suspensions: comparison of theory with experimental measurements. *Journal of Colloid and Interface Science* **156**, 261–268.

Holmes, A.K., Challis, R.E. and Wedlock, D.J. (1994) A wide bandwidth study of ultrasound velocity and attenuation in suspensions: the variation of velocity and attenuation with particle size. *Journal of Colloid and Interface Science* **168**, 339–348.

Hughes, P.E. and How, T.V. (1993) Quantitative measurement of wall shear rate by pulsed Doppler ultrasound. *Journal of Medical Engineering and Technology* **17**(2), 58–64.

Hughes, P.E. and How, T.V. (1994) Pulsatile velocity distribution and wall shear rate measurement using pulsed Doppler ultrasound. *Journal of Biomechanics* **27**(1), 103–110.

Hung, B.N. and Goldstein, A. (1983) Acoustic parameters of commercial plastics. *IEEE Transactions on Sonics and Ultrasonics* **30**(4), 249–254.

Hunt, J.W., Arditi, M. and Foster, F.S. (1983) Ultrasound transducers for pulse-echo medical imaging. *IEEE Transactions on Biomedical Engineering* **30**(8), 453–481.

Insana, M.F., Madsen, E.L., Hall, T.J. and Zagzebski, J.A. (1986) Tests of the accuracy of a data reduction method for determination of acoustic backscatter coefficients. *The Journal of the Acoustical Society of America* **79**(5), 1230–1236.

Jensen, J.A. (1991) A model for the propagation and scattering of ultrasound in tissue. *The Journal of the Acoustical Society of America* **89**(1), 182–190.

Jensen, J.A. (1996) *Estimation of Blood Velocities Using Ultrasound: A Signal Processing Approach*. Cambridge: Cambridge University Press.

Jones, S.A. (1993) Fundamental sources of error and spectral broadening in Doppler ultrasound signals. *Critical Reviews in Biomedical Engineering* **21**(5), 399–483.

Jorgensen, J.E. and Garbini, J.L. (1974) An analytical procedure of calibration for the pulsed ultrasonic Doppler flow meter. *Transactions of the ASME/Journal of Fluids Engineering* **96**, 158–167.

Jorgensen, J.E., Campau, D.N. and Baker, D.W. (1973) Physical characteristics and mathematical modeling of pulsed ultrasonic flowmeter. *Medical and Biological Engineering* **11**(4), 404–421.

Kishiro, M., Hirayama, N., Yao, H., Yamamoto, T. and Takeda, Y. (2004) Analysis of frequency characteristics on non-invasive ultrasonic-Doppler flow measurement for metal pipes. In: Takeda, Y., Murai, Y., Kikura, H. and N. Furuichi, N., editors. Fourth International Symposium on Ultrasonic Doppler Methods for Fluid Mechanics and Fluid Engineering (4th ISUD), Hokkaido University, Sapporo, Japan, September, pp. 95–100.

Kotzé, R., Haldenwang, R. and Slatter, P. (2008a) Rheological characterisation of highly concentrated mineral suspensions using an ultrasonic velocity profiler. In: Chara, Z. and Bareš, V., editors. Proceedings of the 6th International Symposium on Ultrasonic Doppler Methods for Fluid Mechanics and Fluid Engineering, pp. 99–102.

Kotzé, R., Haldenwang, R. and Slatter, P. (2008b) Rheological characterisation of highly concentrated mineral suspensions using an ultrasonic velocity profiling with combined pressure difference method. *Applied Rheology* **18**(6), 62114-1–62114-10.

Kowalewski, T.A. (1980) Velocity profiles of suspension flowing through a tube. *Archives of Mechanics* **32**(6), 857–865.

Lemmin, U. and Rolland, T. (1997) Acoustic velocity profiler for laboratory and field studies. *Journal of Hydraulic Engineering* **123**(12), 1089–1098.

Lin, Y.-H. and Shung, K.K. (1999) Ultrasonic backscattering from porcine whole blood of varying hematocrit and shear rate under pulsatile flow. *Ultrasound in Medicine & Biology* **25**(7), 1151–1158.

Madsen, E.L. (1993) Method of determination of acoustic backscatter and attenuation coefficients independent of depth and instrumentation. In: Shung, K.K. and Thieme, G.A., editors. *Ultrasonic Scattering in Biological Tissues*. Boca Raton, FL: CRC, pp. 205–250.

Madsen, E.L., Insana, M.F. and Zagzebski, J.A. (1984) Method of data reduction for accurate determination of acoustic backscatter coefficients. *The Journal of the Acoustical Society of America* **76**(3), 913–923.

Manneville, S., Bécu, L. and Colin, A. (2004) High-frequency ultrasonic speckle velocimetry in sheared complex fluids. *European Physical Journal – Applied Physics* **28**(3), 361–373.

Manneville, S., Bécu, L., Grondin, P. and Colin, A. (2005) High-frequency ultrasonic imaging: a spatio-temporal approach of rheology. *Colloid and Surfaces A: Physicochemical and Engineering Aspects* **270–271**, 195–204.

McArdle, A. and Newhouse, V.L. (1996) Doppler bandwidth dependence on beam to flow angle. *The Journal of the Acoustical Society of America* **99**(3), 1767–1778.

McCarthy, K.L., Kauten, R.J., McCarthy, M.J. and Steffe, J.F. (1992) Flow profiles in a tube rheometer using magnetic resonance imaging. *Journal of Food Engineering* **16**, 109–125.

McClements, D.J. (1997) Ultrasonic characterization of foods and drinks: principles, methods, and applications. *Critical Reviews in Food Science and Nutrition* **37**(1), 1–46.

McClements, D.J. and Povey, M.J.W. (1987) Ultrasonic velocity as a probe of emulsions and suspensions. *Advances in Colloid and Interface Science* **27**, 285–316.

Messer, M. and Aidun, C.K. (2009) Main effects on the accuracy of pulsed-ultrasound-Doppler-velocimetry in the presence of rigid impermeable walls. *Flow Measurement and Instrumentation* **20**(2), 85–94.

Mo, L.Y.L., Kuo, Y.-I., Shung, K.K., Ceresne, L. and Cobbold, R.S.C. (1994) Ultrasound scattering from blood with hematocrits up to 100%. *IEEE Transactions on Biomedical Engineering* **41**(1), 91–95.

Müller, M., Brunn, P. and Harder, C. (1997) New rheometric technique: the gradient-ultrasound pulse Doppler method. *Applied Rheology* **7**(5), 204–210.

Nowak, M. (2002) Wall shear stress measurement in a turbulent pipe flow using ultrasound Doppler velocimetry. *Experiments in Fluids* **33**, 249–255.

Nowicki, A. (1979) Simplified automatic measurements of blood flow by the ultrasonic pulse Doppler method. *Archives of Acoustics* **4**(4), 359–366.

Ouriev, B. (2000) *Ultrasound Doppler Based In-line Rheometry of Highly Concentrated Suspensions*. PhD thesis, ETH Zürich.

Ouriev, B. (2002) Investigation of the wall slip effect in highly concentrated disperse systems by means of non-invasive UVP-PD method in the pressure driven shear flow. *Colloid Journal* **64**(6), 740–745.

Ouriev, B. and Windhab, E.J. (2002) Rheological study of concentrated suspensions in pressure-driven shear flow using a novel in-line ultrasound Doppler method. *Experiments in Fluids* **32**, 204–211.

Ouriev, B. and Windhab, E. (2003) Novel ultrasound based time averaged flow mapping method for die entry visualization in flow of highly concentrated shear-thinning and shear-thickening suspensions. *Measurement Science and Technology* **14**(1), 140–147.

Ouriev, B. and Windhab, E. (2004) Transient flow of highly concentrated suspensions investigated using the ultrasound velocity profiler-pressure difference method. *Measurement Science and Technology* **14**(11), 1963–1972.

Ouriev, B., Breitschuh, B. and Windhab, E.J. (2000) Rheological investigation of concentrated suspensions using a novel in-line Doppler ultrasound method. *Colloid Journal* **62**, 234–240.

Ouriev, B., Windhab, E., Braun, P., Zeng, Y. and Birkhofer, B. (2003) Industrial application of ultrasound based in-line rheometry: visualization of steady shear pipe flow of chocolate suspension in pre-crystallization process. *Review of Scientific Instruments* **74**(12), 5255–5259.

Ouriev, B., Windhab, E., Braun, P. and Birkhofer, B. (2004) Industrial application of ultrasound based in-line rheometry: from stationary to pulsating pipe flow of chocolate suspension in precrystallization process. *Review of Scientific Instruments* **75**(10), 3164–3168.

Papadakis, E.P., editor. (1999) *Ultrasonic Instruments & Devices, Reference for Modern Instrumentation, Techniques, and Technology*. San Diego, CA: Academic Press.

Peronneau, P. (1992) Ultrasound pulsed Doppler velocimetry. In: *Engineering in Medicine and Biology Society, Vol. 14. Proceedings of the Annual International Conference of the IEEE*, volume 7, pp. 2863–2866. http://ieeexplore.ieee.org/xpl/mostRecentIssue.jsp?asf_arn=null&asf_iid=null&asf_pun=1028&asf_in=null&asf_rpp=null&asf_iv=null&asf_sp=null&asf_pn=7. Accessed September 10, 2010.

Pfund, D.M., Greenwood, M.S., Bamberger, J.A. and Pappas, R.A. (2006) Inline ultrasonic rheometry by pulsed Doppler. *Ultrasonics* **44**, e477–e482.

Pinfield, V.J. and Povey, M.J.W. (1997) Thermal scattering must be accounted for in the determination of adiabatic compressibility. *Journal of Physical Chemistry. B, Condensed Matter, Materials, Surfaces, Interfaces and Biophysical* **101**(7), 1110–1112.

Pinkel, R. (1979) Observations of strongly nonlinear internal motion in the open sea using a range-gated Doppler sonar. *Journal of Physical Oceanography* **9**(4), 675–686.

Povey, M.J. and Mason, T.J. (1998) *Ultrasound in Food Processing*. London: Blackie Academic & Professional.

Powell, R. and Pfund, D. (2005) Non-invasive diagnostics for measuring physical properties and processes in high level wastes. Technical report, University of California Davis (US). URL http://www.osti.gov/bridge/product.biblio.jsp?query_id=0&page=0&osti_id=841672. Accessed September 10, 2010.

Riebel, U. and Löffler, F. (1989) The fundamentals of particle size analysis by means of ultrasonic spectrometry. *Particle and Particle Systems Characterization* **6**, 135–143.

Rouffiac, V., Guglielmi, J.-P., Barbet, A., Lassau, N. and Peronneau, P. (2004) Application of validated ultrasound indices to investigate erythrocyte aggregation in pigs. Preliminary in vivo results. *Ultrasound in Medicine and Biology* **30**(1), 35–44.

Sandrin, L., Manneville, S. and Fink, M. (2001) Ultrafast two-dimensional ultrasonic speckle velocimetry: a tool in flow imaging. *Applied Physics Letters* **78**(8), 1155–1157.

Satomura, S. (1957) Ultrasonic Doppler method for the inspection of cardiac functions. *The Journal of the Acoustical Society of America* **29**(11), 1181–1185.

Shekarriz, A. and Sheen, D.M. (1998) Slurry pipe flow measurements using tomographic ultrasonic velocimetry and densitometry. In: *Proceedings of FEDMS '98, 1998 ASME Fluids Engineering Division Summer Meeting, 21–25 June 1998*. Washington, D.C., USA: ASME, pp. 1–8.

Shung, K.K., Sigelmann, R.A. and Reid, J.M. (1976) Scattering of ultrasound by blood. *IEEE Transactions on Biomedical Engineering* **23**(6), 460–467.

Shung, K.K., Yuan, Y.W., Fei, D.Y. and Tarbell, J.M. (1984) Effect of flow disturbance on ultrasonic backscatter from blood. *The Journal of the Acoustical Society of America* **75**(4), 1265–1272.

Sigel, B., Machi, J., Beitler, J.C. and Justin, J.R. (1983) Red cell aggregation as a cause of blood-flow echogenicity. *Radiology* **148**, 799–802.

Sigelmann, R.A. and Reid, J.M. (1973) Analysis and measurement of ultrasound backscattering from an ensemble of scatterers excited by sine-wave bursts. *The Journal of the Acoustical Society of America* **53**(5), 1351–1355.

Sinton, S.W. and Chow, A.W. (1991) NMR flow imaging of fluids and solid suspensions in Poiseuille flow. *Journal of Rheology* **35**(5), 735–772.

Storti, G., Hipp, A.K. and Morbidelli, M. (2000) Monitoring latex reactors by ultrasonics. *Polymer Reaction Engineering* **8**(1), 77–94.

Takeda, Y. (1986) Velocity profile measurement by ultrasonic Doppler shift method. *International Journal of Numerical Methods for Heat and Fluid Flow* **7**, 313–318.

Takeda, Y. (1987) Measurement of velocity profile of mercury flow by ultrasound Doppler-shift method. *Nuclear Technology* **79**(1), 120–124.

Tezuka, K., Mori, M., Suzuki, T. and Kanamine, T. (2006) Application of ultrasonic pulse-Doppler flow meter for hydraulic power plant. In: Birkhofer, B.H., Jeelani, S.A.K. and Windhab E.J., editors. Proceedings of the 5th International Symposium on Ultrasonic Doppler Methods for Fluid Mechanics and Fluid Engineering, pp. 105–108.

Thompson, R.S. and Aldis, G.K. (1996) Effect of a cylindrical refracting interface on ultrasound intensity and the CW Doppler spectrum. *IEEE Transactions on Biomedical Engineering* **43**(5), 451–459.

Thompson, R.S., Tortoli, P. and Aldis, G.K. (2000) Selective transmission of a focused Doppler ultrasound beam through a plastic layer. *Ultrasound in Medicine and Biology* **26**(8), 1333–1346.

Tortoli, P., Guidi, G. and Newhouse, V.L. (1995) Improved blood velocity estimation using the maximum Doppler frequency. *Ultrasound in Medicine and Biology* **21**(4), 527–532.

Tortoli, P., Guidi, F., Guidi, G. and Atzeni, C. (1996) Spectral velocity profiles for detailed ultrasound flow analysis. *IEEE Transactions on Ultrasonics, Ferroelectrics, and Frequency Control* **43**(4), 654–659.

Tortoli, P., Thompson, R.S., Berti, P. and Guidi, F. (1999) Flow imaging with pulsed Doppler ultrasound and flow phantoms. *IEEE Transactions on Ultrasonics, Ferroelectrics, and Frequency Control* **46**(6), 1591–1596.

Tortoli, P., Morganti, T., Bambi, G., Palombo, C. and Ramnarine, K.V. (2006) Noninvasive simultaneous assessment of wall shear rate and wall distension in carotid arteries. *Ultrasound in Medicine and Biology* **32**(11), 1661–1670.

Twersky, V. (1988) Low-frequency scattering by mixtures of correlated nonspherical particles. *The Journal of the Acoustical Society of America* **84**(1), 409–415.

Ueda, M. and Ozawa, Y. (1985) Spectral analysis of echoes for backscattering coefficient measurement. *The Journal of the Acoustical Society of America* **77**(1), 38–47.

Urick, R.J. (1947) A sound velocity method for determining the compressibility of finely divided substances. *Journal of Applied Physics* **18**, 983–987.

Wada, S., Kikura, H., Aritomi, M., Mori, M. and Takeda, Y. (2004) Development of pulse ultrasonic Doppler method for flow rate measurement in power plant. Multilines flow rate measurement on metal pipe. *Journal of Nuclear Science and Technology* **41**(3), 339–346.

Wells, P.N.T. (1969) A range-gated ultrasonic Doppler system. *Medical and Biological Engineering* **7**, 641–652.

Wiklund, J. (2007) *Ultrasound Doppler Based In-line Rheometry – Development, Validation and Application*. PhD thesis, Lund University.

Wiklund, J. and Stading, M. (2006) Application of in-line ultrasound Doppler based UVP-PD method to concentrated model and industrial suspensions. In: Birkhofer, B.H., Jeelani, S.A.K. and Windhab E.J., editors. Proceedings of the 5th International Symposium on Ultrasonic Doppler Methods for Fluid Mechanics and Fluid Engineering, pp. 145–148.

Wiklund, J. and Stading, M. (2008) Application of in-line ultrasound Doppler-based UVP-PD rheometry method to concentrated model and industrial suspensions. *Flow Measurement and Instrumentation* **19**(3–4), 171–179.

Wiklund, J., Johansson, M., Shaik, J., Fischer, P., Windhab, E., Stading, M. and Hermansson, A. (2001) In-line rheological measurements of complex model fluids using an ultrasound UVP-PD based method. In: *Annual Transactions – The Nordic Rheology Society, 10th Anniversary Conference*, Trondheim, Norway, pp. 128–130.

Wiklund, J., Johansson, M., Shaik, J., Fischer, P., Windhab, E., Stading, M. and Hermansson, A.-M. (2002) In-line ultrasound based rheometry of industrial and model suspensions flowing through pipes. In: *Papers of the Third International Symposium on Ultrasonic Doppler Methods for Fluid Mechanics and Fluid Engineering*, EPFL Lausanne, Paul Scherrer Institut, pp. 69–76.

Wiklund, J., Stading, M., Pettersson, A.J. and Rasmuson, A. (2006) A comparative study of UVP and LDA techniques for pulp suspensions in pipe flow. *AIChE Journal* **52**(2), 484–495.

Wiklund, J., Shahram, I. and Stading, M. (2007) Methodology for in-line rheology by ultrasound Doppler velocity profiling and pressure difference techniques. *Chemical Engineering Science* **62**, 4277–4293.

Wiklund, J., Fock, H., Rasmuson, A. and Stading, M. (2008) Near wall studies of pulp suspension flow. In: Chara, Z. and Bareš, V., editors. Proceedings of the 6th International Symposium on Ultrasonic Doppler Methods for Fluid Mechanics and Fluid Engineering, pp. 171–174.

Wilkinson, W.L. (1960) *Non-Newtonian Fluids: Fluid Mechanics, Mixing and Heat Transfer*, volume **1**. London: Pergamon Press.

Windhab, E.J. (1994) Sensoren zur On-Line Messung am Beispiel von Struktur- und Fliessparametern in der Schololadentechnologie. In: *Schoko-Technik, Internationale ZDS-Fachtagung SIC-14*, Gürzenich in Köln, Martinstrasse 27–31, D-50667 Köln: Zentralfachschule der Deutschen Süsswarenwirtschaft/Solingen.

Wood, A.B. (1964) *A Textbook of Sound*, 3rd Edition. London: Bell and Sons.

Wunderlich, T. and Brunn, P.O. (1999) Ultrasound pulse Doppler method as a viscometer for process monitoring. *Flow Measurement and Instrumentation* **10**(4), 201–205.

Yamanaka, G., Kikura, H., Takeda, Y. and Aritomi, M. (2002) Flow measurement on an oscillating pipe flow near the entrance using the UVP method. *Experiments in Fluids* **32**(2), 212–220.

Young, N.W.G., Wassell, P., Wiklund, J. and Stading, M. (2008) Monitoring struturants of fat blends with ultrasound based in-line rheometry (ultrasonic velocity profiling with pressure difference). *International Journal of Food Science and Technology* **43**(11), 2083–2089.

4 Hydrocolloid Gums – Their Role and Interactions in Foods

Tim Foster and Bettina Wolf

4.1 INTRODUCTION

Hydrocolloid gums are applied in foods mainly for their thickening and gelling properties. As 'hydrocolloid' implies, these are water-soluble gums and, therefore, tend to be applied in the water-continuous foods. Additionally, low-fat spreads with a dispersed aqueous phase structured and stabilised using hydrocolloids have also been designed. Inclusion of the hydrocolloid is crucial in certain domains of the product microstructure to obtain a stable product with acceptable mouthfeel. Typically, only relatively small amounts of hydrocolloid are required to impart the desired rheological and/or textural properties of the food. This chapter introduces fundamentals of rheology relating to the behaviour of hydrocolloid gums in solution as well as fundamentals of gel rheology to cover the two types of actions of hydrocolloids in an aqueous environment: thickening and gelling. Then, in Table 4.1 a general overview of commonly applied hydrocolloids is provided. The majority of this chapter has been dedicated to presenting the effect of hydrocolloid interactions on the rheological/textural behaviour, followed by a discussion of systems applied in foods.

4.2 BEHAVIOUR OF HYDROCOLLOID GUMS IN SOLUTION

Introducing relatively small amounts of hydrocolloid gums into the aqueous phase of food formulations can lead to a dramatic change in food texture. The nature of the hydrocolloid gum combined with the solvent conditions, for example the presence of salt and the temperature history of the product, will determine whether a 'simple' thickening effect or gelation has been achieved. The focus of this section is on

Practical Food Rheology: An Interpretive Approach
Edited by Ian T. Norton, Fotios Spyropoulos and Philip Cox
 ISBN: 978-1-405-19978-0

Table 4.1 Hydrocolloid gums applied to affect rheology/texture of foods

Hydrocolloid	Molecular structure	Thickening conditions	Gelling conditions
Pectin	Polygalacturonic acid. Varying amounts of methyl-substituted carboxyl groups (Low M or High M).	Lower η with increased ionic strength.	Divalent ions, low pH (LM), high soluble solids and low temperature (HM).
Guar Gum	Mannose backbone with single galactose side chain. Typical M:G = 2:1.	Random coil. η determined by Mw.	Non-gelling. Viscosity enhancement with xanthan.
Locust Bean Gum (LBG)	Mannose backbone with single galactose side chain. Typical M:G = 4:1.	Random coil. η determined by Mw.	Gels when mixed with xanthan.
Carrageenan	Repeating units of galactose and 3,6-anhydrogalactose. Iota carrageenan: 2 sulphates per repeat. Kappa carrageenan: 1 sulphate per repeat.	Viscosify as fluid gel particles at low polymer concentration.	Sodium/potassium/ calcium ions Potassium ions
Gellan gum	Repeat uniting of glucose, glucuronic acid, glucose and rhamnose. The first glucose can have glycerate and acetate groups attached.	Viscosify as fluid gel particles at low polymer concentration.	gel with mono- and divalent ions.
Alginate	Guluronic and mannuronic acid in different content and distribution.	Lower η with increased ionic strength.	Divalent ions, low pH
Xanthan	Glucose backbone with three sugar unit side chain (mannose, glucuronic acid, mannose) every second glucose. Internal mannose may be acetylated external mannose may be pyruvylated.	Weak gel formation providing suspending properties, but flows when sheared.	Gels with the addition of LBG or konjac glucomannan.
Agar	Repeating units of galactose and 3,6-anhydrogalactose.	Viscosify as fluid gel particles at low polymer concentration.	Thermoreversible gels
Cellulosics	Cellulose backbone derivatised to different extents with methyl (MC), hydroxypropyl methyl (HPMC) or carboxymethyl (CMC) substituents.	MC/HPMC: η determined by Mw; CMC degree of substitution determines decrease in η with increased ionic strength.	MC and HPMC gel upon heating and revert to the solution state upon cooling.
Starch	Linear (amylose) or branched (amylopectin) polymer of glucose.	Starch granules swell upon heating and provide space fillings.	Retrogradation produces gels whose textures are determined by the amylose/amylopectin ratio.

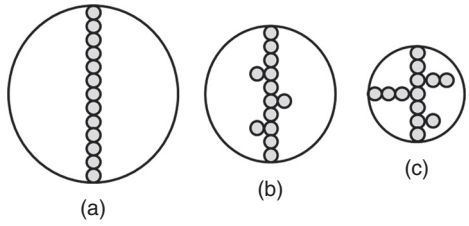

Fig. 4.1 Principle structures for hydrocolloid polymers: (a) linear; (b) linear-branched and (c) branched, with the diameter of gyration decreasing with the increasing degree of branching, for equivalent molecular weights, as indicated by the circles.

the thickening ability of hydrocolloid gums and the fundamentals of hydrocolloid behaviour in solutions. The dissolution medium for hydrocolloids tends to be aqueous based, and future references to hydrocolloid solutions in this chapter refer to their aqueous solutions.

The rheological behaviour of hydrocolloid solutions is affected by the molecular weight and the conformation of the hydrocolloid molecule as well as the solvent conditions. Dextran solutions, for example, can be designed to show Newtonian flow behaviour (constant shear viscosity), whereas guar gum and xanthan gum are classical examples of hydrocolloids forming shear-thinning solutions (shear viscosity decreases with the increasing shear rate or shear stress). The features determining the rheological behaviour of hydrocolloid gums are, in principle, the same as for synthetic polymers. For hydrocolloid polymers, broad structural variety is observed, and specific intra- and intermolecular conformations in solution result in a large spectrum of rheological behaviours. At the individual molecule level, solution behaviour is affected by the structural features of the hydrocolloid backbone and its side chains, as well as the presence of charge, characteristics impacting on the degree of chain stiffness. Fig. 4.1 illustrates three principle structures observed for hydrocolloids and the consequence on the radius of gyration, a measure used to describe the dimensions of the hydrocolloid polymer chain. At equivalent molecular weights, hydrocolloids with a linear non-branched backbone have a bigger radius of gyration than that of branched hydrocolloids. An increase in the degree of branching, at an overall equivalent molecular weight, leads to a decrease in the radius of gyration. The radius of gyration is correlated with the hydrodynamic resistance of the macromolecule to flow, and therefore, it is correlated with the viscosifying capacity of a hydrocolloid gum.

In order to relate the behaviour of individual hydrocolloid chains to solution viscosity, the intrinsic viscosity, $[\eta]$, has to be introduced:

$$[\eta] = \frac{1}{c}\frac{\eta - \eta_s}{\eta_s} \quad \text{for} \quad c \to 0 \tag{4.1}$$

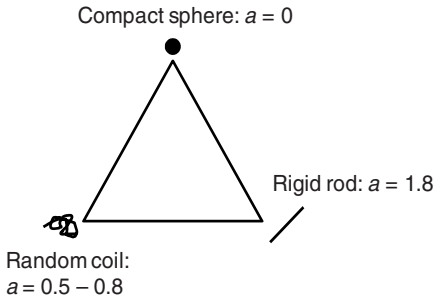

Fig. 4.2 Haug triangle representing extreme forms of macromolecular conformation and associated values for the Mark–Houwink parameter, *a*. The case of a compact sphere is not found for hydrocolloid gums; it is typical for globular proteins. The Mark–Houwink parameter range provided for the random coil corresponds to the equivalent sphere model. The model of the free-draining coil represents an intermediate case along the horizontal hypotenuse with $a = 1.0–1.2$.

where η is the viscosity of the solution and η_s is the viscosity of the solvent. The intrinsic viscosity has the dimension of an inverse concentration, c, and is used to compare the viscosity of dilute solutions of polymers. The value of $[\eta]$ is generally obtained by measuring solution viscosity at a range of concentrations as well as the solvent viscosity, followed by extrapolation to zero concentration ($c \rightarrow 0$). At these very low concentrations, the solution behaviour of hydrocolloid gums is usually Newtonian, and the viscosity values are close to the value of water. Therefore, measurement method and equipment should be selected appropriately. The hydrodynamic behaviour of hydrocolloid chains in solution can be explained by considering each molecule as a flexible chain or a rigid rod. Flexible chain behaviour shows two limiting cases: the free-draining coil model and the equivalent sphere model (Mitchell, 1979). In the free-draining coil model, it is envisaged that the solvent is unperturbed by the presence of the polymer. In the equivalent sphere model, the solvent is entrained in the polymer coil, and the contribution of the coil to solution viscosity is characterised by its radius of gyration. Such models are useful and have led to the relationship between $[\eta]$ and molecular weight, M, given by:

$$[\eta] \propto M^a \tag{4.2}$$

where a is known as the Mark–Houwink parameter. The Haug triangle shown in Fig. 4.2 is often used to represent the three extreme cases of macromolecular conformation.

The solution behaviour of hydrocolloids is interdependent on ionic strength, nature of the counterions, temperature and other solution conditions. Particular attention to solution conditions, with regard to ions,

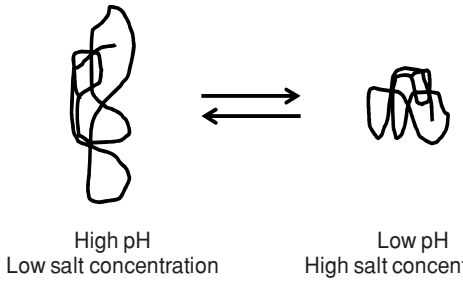

Fig. 4.3 Molecular conformation of charged hydrocolloids in response to pH and salt concentration, which affects rheological response.

should be paid in the application of charged hydrocolloids, since molecular conformation can be drastically altered as indicated in Fig. 4.3.

With increasing concentration, macromolecules begin to interact as sketched in Fig. 4.4; the critical concentration for the onset of interactions is denoted as the coil-overlap concentration, c^*. The nature and extent of interaction is affected by the solvent conditions and the solution behaviour of the individual molecule. At c^*, a change in the slope of the specific viscosity, η_{sp}, defined as:

$$\eta_{sp} = \frac{\eta - \eta_s}{\eta_s} \tag{4.3}$$

where η is the viscosity of the solution and η_s is the viscosity of the solvent, can be observed (note that η_{sp} is dimensionless).

The behaviour is linear with the slope for $c > c^*$ larger than for $c < c^*$ with characteristic values for different hydrocolloids (see Table 4.1). Plotting the dimensionless product $c[\eta]$, also referred to as the coil-overlap parameter, on the abscissa collapses the η_{sp} curves for a large number of hydrocolloids (Morris *et al.*, 1981). Values reported for the slope are ~1.4 and ~3.3 for the dilute regime and the concentrated

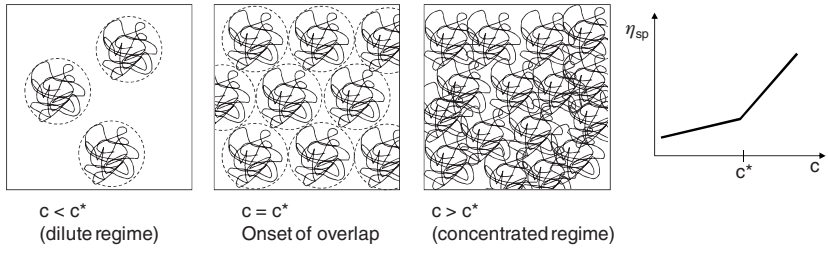

Fig. 4.4 Macromolecular conformation and specific viscosity (η_{sp}) versus concentration (c) relationships for random coil polymers, where c^* is the coil-overlap concentration.

regime, respectively, and $c^*[\eta] \sim 4$ (Morris *et al.*, 1981). Exceptions from this behaviour have been reported for hydrocolloid solutions in which chain–chain interactions have been modified to attain 'extreme' solvent conditions (high/low pH, high ionic strength). Also, acquisition of a large number of η_{sp} data around c^* has, for some hydrocolloids, led to the identification of two critical concentrations, $c^{*\prime}$ and c^{**} (Castelain *et al.*, 1987; Launay *et al.*, 1997), with a slope of ~2.3 in the transition region ($c^{*\prime} < c < c^{**}$).

The discussion so far has considered concentrated solutions as temporary networks in which the physical junctions, the entanglements, are continuously formed, disrupted and reformed among the chains. A further class of molecular theory for hydrocolloids with flexible backbones is based on reptation models (de Gennes, 1971) in which each macromolecule is confined in a tube-like region with contours varying over time and the molecule can only move by diffusion along the tube. Hydrocolloids with rigid backbones can be treated as long rods with the relative orientation of each rod being random as long as the system is not sheared; the whole system appears to be isotropic. Above a critical polymer concentration formation of a liquid, crystalline phase is observed for rigid rod molecules in which a preferred direction of molecular orientation takes place as, for example, for xanthan gum (Lee and Brant, 2002a, 2002b). As a consequence, the viscosity increases drastically.

The shear viscosity of sufficiently dilute hydrocolloid solutions is Newtonian. With increasing concentration, shear-thinning behaviour is often observed, which can be fitted with the model functions. A multitude of these can be found in rheology textbooks (see, for example, Barnes *et al.*, 1989; Macosko, 1994; Larson, 1998; Lapasin and Pricl, 1999; Mezger, 2006), and nowadays the software packages of rheometers tend to have these models programmed in as data-fitting options. The simplest type of shear-thinning behaviour is the power law or Ostwald–de Waele behaviour:

$$\eta = k\dot{\gamma}^{n-1} \tag{4.4}$$

where k is the flow coefficient (or consistency constant) and n is the power law index. For $n = 1$, the flow behaviour is Newtonian, and k equals the viscosity of the solution. For $n < 1$, the hydrocolloid solution is shear thinning, and $n > 1$ denotes shear-thickening behaviour (i.e. an increase in shear viscosity with the increasing shear rate, which is observed for structured liquids of suspension characters rather than for single-phase hydrocolloid solutions).

The Cross model (4.5) considers power law behaviour at intermediate shear rates. At sufficiently low or high shear rates, the shear viscosity is

considered to be shear rate independent, and these regions are referred to as the lower and the upper Newtonian plateaus respectively. The respective viscosities are denoted as zero-shear viscosity, η_0, and high-shear or infinite-shear viscosity, η_∞:

$$\eta = \eta_\infty + \frac{\eta_0 - \eta_\infty}{1 + (k\dot{\gamma})^n} \tag{4.5}$$

where k is the flow coefficient or Cross constant and n is the power law index; η_∞ and η_0 have been introduced above. For η_∞ values considerably lower than η_0 values, application of a simplified version of the Cross model (4.6) often fits experimental data sufficiently well:

$$\eta = \frac{\eta_0}{1 + (k\dot{\gamma})^n} \tag{4.6}$$

Some hydrocolloid solutions show a very pronounced shear-thinning behaviour manifesting itself in a viscosity drop of many decades over a fairly narrow range of low shear rates. Such behaviour is typically interpreted as yield behaviour; there has been a vast debate in the literature over the existence or non-existence of a yield stress (Barnes, 2007), which is defined as the minimum stress required to act on the sample to induce flow. A classical model to consider yield behaviour is the Herschel–Bulkley model:

$$\tau = \tau_{\mathrm{HB}} + k\dot{\gamma}^n \tag{4.7}$$

where τ is the shear stress, τ_{HB} is the yield stress according to the Herschel–Bulkley model, k is the flow coefficient and n is the power law index. Shear viscosity based on a Herschel–Bulkley fit can be calculated by substituting τ in Equation 4.6:

$$\tau = \eta\dot{\gamma} \tag{4.8}$$

Measuring yield stress presents a challenge, and data reported tend to be extrapolated from flow curves (shear stress versus shear rate curves extrapolated to zero-shear rate). It should be noted that flow behaviour in the yield stress region is often thixotropic (time dependent) and, therefore, yield stress values will vary depending on the shear history of the sample.

Hydrocolloid solutions (whether their shear flow characteristics are Newtonian or shear-thinning) may show a certain degree of viscoelasticity which manifests itself in the development of normal stresses in rotational shear and/or a storage modulus far in excess of the values

of loss modulus analysed in dynamic oscillatory shear. Viscoelastic solutions also show extensional viscosity, η_e, behaviour deviating from Trouton's law:

$$\eta_e = 3\eta \tag{4.9}$$

where η is the shear viscosity.

In a dynamic oscillatory shear test, a sample is subjected to periodic sinusoidal shear in the form of a shear stress or a shear strain. In a shear stress controlled experiment, the shear strain is measured, and vice versa. The frequency of oscillation is either kept constant or varied. If the material response is in-phase with the deformation, the material behaviour is fully elastic:

$$\tau = G\gamma \tag{4.10}$$

where τ is the shear stress, G is the elastic modulus and γ is the shear strain. Purely viscous material behaviour manifests itself in a material response out-of-phase with the deformation (corresponding to a phase shift of $\pi/2$ or 90°), and shear stress is proportional to the time derivative of the shear strain. Viscoelastic solutions show a phase shift, δ, between 0 and $\pi/2$ or 90°, and the elastic modulus will show an in-phase component and an out-of-phase component corresponding to the elastic and viscous contributions to the material behaviour. The values of these two components are denoted as the storage modulus, G', and the loss modulus, G'', respectively. It is customary to report the tangent of the phase, tan δ, which is equal to the ratio G''/G'. In order to assess G' and G'' at a range of frequencies, it is important to ensure that the material response is not additionally affected by the deformation amplitude imposed. Therefore, so-called frequency tests are carried out by applying a stress or strain amplitude chosen from the linear viscoelastic domain which is evaluated in an 'amplitude sweep' conducted at a constant frequency. The linear viscoelastic domain is recognised as the region where G' is independent of the deformation amplitude. Hydrocolloid solutions may show a highly extended linear viscoelastic domain such as up to 100% strain, whereas simple emulsion formulations tend to show much smaller critical strains in the order of 1%.

4.3 HYDROCOLLOID GELATION AND GEL RHEOLOGY

Many random coil hydrocolloids possess the ability to form a physically cross-linked gel network, given appropriate solvent conditions or

solution temperature. In the gelled state, the physical entanglements are kinetically trapped. Temperature-induced gelation of polysaccharides tends to be reversible; for example, agar gels form upon cooling of agar solutions from near boiling to below ~40°C, and they will melt upon reheating to near boiling. Temperature hysteresis between gelation and melting is commonly observed for hydrocolloid solutions. Whilst gelatin is a protein, its gel-forming behaviour is akin to that of many polysaccharides with gelation imparted on cooling. A gelatin gel will melt upon heating above ~37°C, and it is this melting temperature in the region of the in-mouth temperature that has led to its wide applications in foods. Globular proteins gel irreversibly upon heating through denaturation. More recently, cellulose derivatives have become more popular since they originate from abundantly available cellulose. Cellulose is not soluble in aqueous solutions; chemical, enzymatic or physical modifications need to be applied to achieve dissolution in aqueous media. Some of the cellulose derivatives available from ingredient suppliers form solutions in cold water and reversible gels upon heating.

Hydrocolloid gel formation can also be ion mediated. An increase in ionic strength tends to increase the temperature of gelation (e.g. for iota and kappa carrageenan, gellan gum) and can induce aggregate formation, which in turn leads to thermal hysteresis. Also, the addition of calcium ions to alginate can form thermo-irreversible gels. The transition between a viscoelastic hydrocolloid solution and a hydrocolloid gel is well defined in terms of their rheology characteristic as, for example, displayed in a dynamic oscillatory shear test. On a more practical note, for example in food product development laboratories, gels are often identified as free-standing samples or samples that remain contained in a beaker after it has been tipped over. Material behaviour is recognised as being gel-like when the storage modulus as acquired in a dynamic oscillatory shear test is larger than the loss modulus and the slope of the storage modulus versus frequency approaches zero.

4.4 HYDROCOLLOID–HYDROCOLLOID INTERACTIONS

In food systems, hydrocolloids are rarely used as single ingredients. Exceptions to this would be products such as table jellies and jams. The properties of such food gels are determined by the fine structure of the polymers (e.g. type A or B gelatins, degree of esterification (DE) of pectin), the polymer concentration and the environment in which the gels were formed (e.g. calcium level, pH, soluble solids, shear during the process). More commonly, hydrocolloids in foods are present in mixtures. Historically, as a function of product development and/or optimisation, mixtures have been devised to confer product-specific attributes. These

are to provide requisite viscosity (e.g. dressings and sauces), gel structures (e.g. milk gels) or stabilisation of particles (e.g. herbs in vinaigrette dressings or cocoa particles in chocolate drinks). In mixed hydrocolloid systems, these attributes are both a function of the individual polymer fine structure and the characteristics of the interactions between them. A classical representation of how hydrocolloids might interact in gelled systems was given by Cairns *et al.* (1987), where two hydrocolloids are depicted in one of four possible mixed ensembles: (i) a single (first) polymer network containing the second polymer within its gel network, (ii) interpenetrating networks, (iii) phase-separated networks and (iv) coupled networks. In the following examples for these different types of mixed ensembles, the rules for their creation as well as those controlling their microstructure will be given. Microstructure control is synonymous with control over properties imparted by microstructure, and the following examples have been taken from an extensive body of research in food material science.

Rheological measurements have been employed, often in combination with other techniques, to provide an understanding of hydrocolloid interactions. Techniques range from viscosity, creep compliance measurements and acquisition of mechanical spectra to others relating to polymer hydrodynamics, such as analytical ultracentrifugation, and large deformation testing in compression or extension.

The study of hydrocolloid mixtures remains a very popular and active research area due to the range of properties that such mixtures can provide. For example, in the field of coupled networks (or more commonly known as synergistic mixtures), two polymer solutions can produce a gel only when mixed together. Similarly, a hydrocolloid might appear to lose its gelling properties once mixed with another non-gelling one if the mixture phase separates and the gelling component becomes the dispersed phase. It is the answers to these observations that have been uncovered over the past three decades of study in the field.

Synergistic interactions have initially been described for mixtures of galactomannans with either xanthan or kappa carrageenan. Locust bean gum (LBG) solutions were found to gel when mixed with xanthan gum, a weak gel-forming hydrocolloid (Dea and Morrison, 1975). Kappa carrageenan gels were shown to be firmer or were able to form at concentrations lower than their critical concentration for gelation when also mixed with LBG. The original models proposed for the gelation of these two types of synergistic gels involved the binding of the galactomannan to the rigid, ordered helices of either xanthan or kappa carrageenan.

Morris (1995) summarised the models for xanthan synergistic interactions as an evolution in the understanding of the requirements of the xanthan molecule in order for it to promote effective interactions with, for example, LBG. Initially, it was believed that the xanthan molecule

should be in the ordered conformation to promote interaction. This was then questioned, indicating that disorder was required. The current understanding is that heterotypic (xanthan–galactomannan) as well as homotypic (xanthan–xanthan) interactions are required for gelation with the heterotypic junction zones being formed with xanthan in the disordered conformation. This model is based on viscosity evidence from low concentration solutions prepared from two stock solutions mixed in different ratios. The technique was developed from the early work of Cuvelier and Launay (1988), but instead of selecting the two stock solutions based on polymer concentration, the technique used was to adjust their zero shear specific viscosity to 1 (twice the viscosity of water). When mixed in different ratios, departure from the zero shear specific viscosities of the two stock solutions provided direct indication of interaction. Polymer-exclusion and phase-separation phenomena are negligible at the low polymer concentrations involved, and therefore, such events are not the origin of the observation, as they would be for systems of higher polymer concentrations. Examples of polymer concentrations of xanthan and LBG required to give such starting stock solutions are 0.007 and 0.06%, respectively, with a 60:40 blend producing a sevenfold increase in the zero shear specific viscosity (Foster, 1992). In the latter study, it was also shown that deacetylation of xanthan (DX) promoted the synergistic interaction with LBG, due to the destabilisation of the ordered helix, which promoted the formation of heterotypic junction zones and resulted in a 100-fold increase in viscosity. On the other hand, for xanthan lacking the terminal mannose unit in its side chain, and therefore the destabilising pyruvate group, the helix was more stable and resisted heterotypic junction zone formation; as a result no interaction was observed across the blending ratios used (Foster and Morris, 1994; Morris and Foster, 1994). A change of the co-synergist to konjac glucomannan (KM) showed a 30-fold and 500-fold increase in the viscosity of xanthan and DX, respectively (Foster, 1992). Thus, comparison of the efficiency of the interaction, relating to the conformation or type of co-synergist, provides not only the fundamental understanding of the nature of the interaction but also the tools for optimising it.

The method was developed further to screen for molecular interactions in mixed hydrocolloid systems, and in addition, it has been applied to measure stoichiometry of interaction (Goycoolea *et al.*, 1995a). Further measurements of stoichiometry of interaction were based on rheological measurements to provide evidence of heterotypic binding. The gel's storage modulus (G') and the enthalpy of transition showed a linear increase with increasing KM:DX to 1:1, with little further change at higher ratios. It was also found that tan δ goes through a sharp minimum at similar compositional ratios, indicating efficiency in the usage of the

polymer chains of the co-synergists in the formation of heterotypic junctions (Goycoolea *et al*., 1995b). Replacing KM by LBG (both having a β-1,4-linked sugar backbone) shows the same trends; however, the sol–gel transition is wider, producing a gel with a modulus thrice that of a KM containing gel. Both these facts indicate that the LBG molecules tend to form a greater number of shorter interactions rather than the longer ones found in heterotypic junction zones containing KM.

The polymeric composition of galactomannans (galactose/mannose with a galactose side-chain distributed on the mannan backbone) was deemed to be a critical factor influencing heterotypic junction zone formation. Guar has a high G:M ratio and it did not seem to interact with xanthan. However, Goycoolea *et al*. (2000, 2001) have shown that the G:M ratio is less important in low salt-containing mixtures of mesquite gum and DX leading to a description of different types of heterotypic junction zones. Mannion *et al*. (1992) also indicated two modes of interaction between xanthan and LBG depending on the G:M ratio. Smaller values for G:M were observed to lead to an increase in the temperature of solubility. As a result of this, G' data measured for the mixtures depended not only on the G:M ratio but also on the temperature of mixing, indicating that the fine structure of both polymers affects the final gel properties. Indeed, Cronin *et al*. (2002) have shown that enzymic debranching of galactomannans (removal of Gs) in the presence of xanthan promotes the formation of strong gels. The influence of temperature of mixing has recently been re-investigated, and while the gels created upon cooling mixtures from high temperature are seen to be stronger and more cohesive than those mixed at a temperature of 20°C (which is below that of the xanthan disorder–order transition), the enthalpy of melting the mixed gels appears to be independent of thermal history (Fitzsimons *et al*., 2008b). Therefore, the lack of cohesiveness of the gel created at low temperature is attributed to a disruption of network formation during mixing. Agoub *et al*. (2007) have furthered the debate, regarding the requirement of the xanthan molecule to be either ordered or disordered, by comparing xanthan with low pyruvate content to a commercial xanthan, which was progressively depyruvylated by low pH treatment. While the overall conclusion is unclear, the findings from the study by Agoub *et al*. (2007) demonstrated an interesting functionality of low pyruvate xanthan when mixed with KM, as the resulting systems produced melt-in-the-mouth gels.

The work on xanthan has recently received new evidence pointing towards an interaction with xyloglucan (Kim *et al*., 2006a, 2006b). The existence of such interactions might not be unexpected, since the xyloglucan molecule has a β-1,4-glucan (cellulose) backbone; nonetheless, the high frequency of di- and tri-saccharide side chains could have been taken as an indication for the absence of any interaction.

Interactions in mixed biopolymers containing other β-1,4 glycans have been discussed by Cui *et al*. (1995, 2006) and Wu *et al*. (2009) and focussed on the interactions between water-soluble yellow mustard mucilage with LBG. These latter studies indicate that there is still scope to improve the understanding of synergistic interaction containing β-1,4-linked backbones, demonstrating a need for an overarching study to look for interactions with new commercial opportunities for renewable biomass resources.

The synergistic interaction between alginate and high methoxy pectin is another one which has recently gained renewed interest. This is at least in part due to their ability to interact as pH is lowered, which is why this system is of particular interest within the context of structuring food in the gastric environment of the digestive tract; for example, to delay gastric emptying and therefore promote an enhanced feeling of satiety (Strom *et al*., 2010). Targeted design of network density also has the potential to affect diffusion of inclusions for controlled delivery. Synergistic liquid mixtures of pectins (high and low methoxy pectin) have been shown to create synergistic gels in which junction zone length, density, and pore size can be controlled depending on the calcium and sugar level of the gelling environment (Lofgren *et al*., 2002). However, the precise mode of interaction between alginate and pectin is still unclear, but there has been phenomenological evidence to show a requirement for alginate to contain high amounts of guluronic acid (high G alginate) and for pectin to have high levels of methoxylation. On the basis of a systematic study for a range of alginates and pectins, Walkenstrom *et al*. (2003) showed that the strongest synergism is between high G alginate and highly esterified pectin, creating the highest gel modulus and showing the fastest kinetics of gelation with maximum values found for a 1:1 mixing ratio. Microscopy revealed an effect on network density and levels of branching.

Cairns *et al*. (1987) introduced the concept of interpenetration networks (IPNs), which have been shown in the work by Clark *et al*. (1999) and Amici *et al*. (2000, 2002) for mixtures containing gellan–maltodextrin, gellan–agarose and agarose–kappa carrageenan, respectively. IPNs offer the opportunity to control pore size as well as network strength and connectivity of gels for controlled release. The rheological properties of these systems are complex, and at present, it does not appear to be a constitutive model. For the agarose–kappa carrageenan system, the first gelling component in the mixture depends on the level of potassium ions present (Brown *et al*., 1995; Amici *et al*., 2002), as this affects the gelation temperature of the kappa carrageenan. Such control varies the ability to describe the modulus of the mixture from simple summation of the pure components, which applies when carrageenan gels before agarose, to a more complex situation when agarose gels

first. Therefore, the physical environment experienced by the separate polysaccharide chains at the point of gelation has to be considered in modelling and when attempting to control the physical properties of such mixtures. When agarose is added to gellan, the resultant gel is reinforced, showing higher gel moduli and stress-to-break without affecting the brittle nature of the gellan gel fracture (Amici *et al*., 2000). In gellan–maltodextrin systems, crystallisation of maltodextrin occurs within the pores of the gellan gels.

Another school of thought is that in mixed systems, the second polymer present has a large impact on the behaviour of the first polymer. However, gel network formation in the presence of a second polymer is far from straightforward, and to date, no conclusive model exists. There has been recent literature to indicate gel formation at lower concentrations than expected for kappa carrageenan (Penroj *et al*., 2005), pectin (Giannouli *et al*., 2004) and whey protein (Fitzsimons *et al*., 2008a) in the presence of a second hydrocolloid in disordered conformation. It appears that the entanglement of the two polymers in a one-phase mixture impacts upon the gel formation. Therefore, consideration for hydrodynamic volume in such mixtures must be given in any explanation of gelation, as it will affect the gelling ability of the polymers and the kinetics of the gelation process. There have been instances reported for mixtures not too dissimilar to those showing evidence for IPN formation, which have been shown to phase separate (segregation into two phases), where the initiator for phase separation is the ordering and gelation of one of the two constituent hydrocolloids. Kasapis *et al*. (1999) and Lundin *et al.* (1999) have shown that this is the case for mixtures of the same polymer type such as for mixtures of high and low acyl gellan and iota- and kappa-carrageenan, respectively. Loren *et al.* (2001) followed quenched mixtures of gelatin and maltodextrin and found that phase separation was initiated when a certain amount of gelatin helices had been formed during ordering. Gelation of gelatin in the presence of a range of hydrocolloids has been shown to drive segregation, leading to flocks or gel particles depending on the type of hydrocolloid (Harrington and Morris, 2009).

The discussion above covers Cairns' description of single hydrocolloid networks containing another hydrocolloid within them, whether the second species can undergo gelation (IPN) or not, and phase-separated networks which depend on the rate of gel structure formation when quenched from a one-phase system. Thermodynamic phase separation can occur when both hydrocolloids are in the solution state and it can be associative or segregative. Associative phase separation can be seen in a similar way to 'coupled' networks, only the structures created are not through space-filling networks but separate into hydrocolloid-rich and hydrocolloid-poor regions. Such associations tend to be induced

when the two hydrocolloids carry opposite charge. Examples include mixtures of gelatin and carrageenan (Michon *et al*., 1995, 2000; Haug *et al*., 2003), gelatin and gum Arabic (Lemetter *et al*., 2009) and β-lactoglobulin and gum Arabic (Schmitt *et al*., 1998). The properties of such complexes change as a function of pH and salt, imparting structural change triggers, which may be of use in their applications. Additionally, gelatin and β-lactoglobulin are surface active, a property which may be exploited for the incorporation of hydrophobic additives into the hydrocolloid-rich complex (van Benthum *et al*., 2004) or for the stabilisation of water and oil emulsion interfaces by the complex itself (Schmitt *et al*., 2005). The formation of such complexes has been proposed to take place by a nucleation and growth mechanism (Sanchez *et al*., 2006).

Haug *et al*. (2003) have shown that upon cooling hydrocolloids which were in equilibrium in the hydrocolloid-poor region, it can undergo segregative phase separation, inducing a highly complex microstructure.

Clark *et al*. (1983) were the first to indicate the effect of phase separation on the rheological properties of phase-separated mixtures. They reported on mixtures of agar and gelatin and showed changes in phase continuity via microscopy, composite gel modulus and melting profiles. A comprehensive study of gelatin:maltodextrin mixtures showed incompatibility in solution (Kasapis *et al.*, 1993a) and in gels (Kasapis *et al.*, 1993b), and the phase sense explained mixed-gel moduli (Kasapis *et al.*, 1993). Morris (1990) built on the work by Clark *et al*. (1983) by using the Takianagi polymer blending laws to describe the composite modulus using the isostress or the isostrain model.

Such analyses can often be used to explain the rheological properties of phase-separated systems. However, the work of Haug *et al*. (2003) demonstrated that complexity of the microstructure might make such simplistic descriptions indicative only. Butler (2002), Butler and Heppenstall-Butler (2003) and Loren *et al*. (1999) have shown that, depending on the quench depth, the initial phase-separation event can be followed by a secondary phase separation induced by hydrocolloid ordering. Normand *et al*. (2002) attempted to explain their rheological results obtained for gelatin:maltodextrin mixtures in this way. Quench depth also determines whether the mechanism of phase separation is that of spinodal decomposition or nucleation and growth. This, in turn, can influence the sharpness of the interface, which may also have an effect on the rheological properties of the mixture. Indeed, Plucknett *et al*. (2001) have shown that debonding at the interface of gelatin:maltodextrin mixed gels occurred when the system was exposed to large deformations in extension tests. Firoozmand *et al*. (2009) have shown that colloidal particles can accumulate at the interface of gelatin:oxidised starch phase-separated mixtures, which results in a viscoelastic interface. This is an

interesting finding and one which will undoubtedly be developed further, as these rheological consequences appear to be attractive in terms of development of new textures and texture control.

Rheological properties of phase-separated mixtures (known as water-in-water (w/w) emulsions) at a temperature where neither hydrocolloid is ordered can be described using an emulsion model (Capron *et al*., 2001; Stokes *et al*., 2001; Simeone *et al*., 2002). This allows for the deduction of the interfacial tension in these systems. Values are in the order of μN/m, which has been confirmed by direct measurement (Ding *et al*., 2002; Simeone *et al*., 2004; Spyropoulos *et al*., 2008). In mixtures with a gelling droplet phase, the shape of the gelled droplets can be controlled by the flow stresses experienced during gelation (Wolf *et al*., 2000; Erni *et al*., 2009). The rheological behaviour of the resulting suspension depends on the particle shape (Wolf *et al*., 2001). The rheological behaviour of particles of different size and shape suspended in a hydrocolloid solution, representative of a number of commercially applicable semi-dilute dispersions, has been described with the Cross model modified to include yield stress behaviour (Rayment *et al*., 2000). Foster *et al*. (1996) showed that high shear during gelation can induce phase inversion of w/w emulsions, with the first gelling hydrocolloid forming the dispersed phase and the starting phase volume being retained. Therefore, high dispersed phase volume systems can be produced. If the particles are able to interact, a string-of-pearls type of structure can be created. Firoozmand *et al*. (2007) described a similar particle gel network for another gelatin:oxidised starch composite formed in the absence of shear.

Recent work on phase-separating materials has produced new insights. Boyd *et al*. (2009) have shown that mixtures of xanthan with other polyelectrolytes possess significantly lower viscosities than those of xanthan solutions of the same concentration alone. This behaviour appears to be less related to a loss of xanthan viscosity as this forms the dispersed phase in the mixture, but more to the low-viscosity liquid crystalline phase that xanthan is driven to form. Upon dilution, the xanthan forms a conventional polymeric solution and the viscosity increases dramatically. Lad *et al*. (2010) have indicated that a similar viscosity reduction can be observed when xanthan is mixed with particulate hydrocolloids such as cold water swelling starch granules.

Foster (2007) and more recently Shrinivas *et al*. (2009) have shown that the spectrum of rheological properties of w/w emulsions can be enhanced further by entrapping oil or fat in the dispersed phase. Such systems can be regarded as (oil-in-water)-in-water emulsions. Air may also be used as the innermost phase, and the opportunity for the creation of a vast range of products with interesting behaviours is obvious. Recent work by Ganzevles *et al*. (2006a, 2006b, 2008) has

shown that the properties of the interface in a protein:polysaccharide phase-separated system is determined by the interaction of the protein with the polysaccharide in the bulk solution, the mixing ratio, the ionic strength and the order of adsorption (simultaneous adsorption of protein/polysaccharide complexes or interaction of the polysaccharide with a protein already adsorbed). Such stabilising effects could be close to providing the viscoelastic interfaces created by hydrophobins (Cox *et al*., 2009; Tchuenbou-Magaia *et al*., 2009).

Current trends in developing an increased understanding of the rheological properties of the respective phases in mixed systems have involved the use of reporters within the phases. Dinsmore *et al*. (2001) and Valentine *et al*. (2001) reported the use of multiple particle tracking, which has also recently been used for food-like microstructures (Moschakis *et al*., 2006). Loren *et al*. (2009) have used NMR to track the diffusion of small molecular weight dendritic polymers through microstructures.

4.5 HYDROCOLLOIDS IN FOODS – ROLE AND INTERACTIONS

The previous section has covered scientific developments in the interactions of hydrocolloids with a view that such types of interactions are experienced when the hydrocolloids are used in food products. The predominance of the hydrophilic nature of hydrocolloids means that they ordinarily reside in the water phase of foods. Foods can contain high amounts of water, for example sauces, emulsions, or low levels, for example baked goods and confectionary. The rheology of hydrocolloids varies, depending on water content, and has been summarised by Kasapis *et al*. (2004), showing a mastercurve, spanning dilute solutions through to the glassy state.

In identifying the role of hydrocolloids in foods, the mantra which should be followed is one of hydrocolloid structure functionality. Therefore, the choice of hydrocolloid should be determined by the position of the hydrocolloid in the food microstructure and the function it has. The functionality of the hydrocolloid is determined by the way it mixes with other ingredients (covered in the previous section) and the properties of the individual polymer itself, as a function of its molecular fine structure, which, as we have shown above, determines the viscosifying or gelling potential of the hydrocolloid. Knowing these parameters may then allow for replacement strategies if a particular hydrocolloid becomes too expensive to use, ethically unacceptable or nutritionally deficient.

Taking a microstructural approach also appreciates the importance of process impact on hydrocolloid location in the product and therefore its functionality. Such process steps might include one or more of the following: temperature changes, pressure changes, different ionic/pH environments, high/low shear and varying points of addition of the hydrocolloid in the process. Developments in microscopy techniques have enabled for the determination of the exact location of hydrocolloids in food microstructures.

Of the synergistic interactions mentioned in the previous section, carrageenan–galactomannan interactions are used in milk-based products for thickening and particle stabilisation and as veggie–gel gelatin replacers. The weak synergistic interaction between xanthan and guar galactomannan is often used in formulations to maintain the required viscosity/weak-gel properties, with a reduction in the amount of xanthan compared to the properties of xanthan at higher usage levels when used as a single ingredient. With guar being a much cheaper ingredient than xanthan, this can often be a cost benefit to the manufacturer, without compromising the consumer perception of the product. The firmer xanthan–LBG gel has recently seen a re-emergence as the gelling agent in the new jelly bouillons.

Associative phase separation has been used for encapsulation and delivery vehicles (van Benthum *et al*., 2004), in which fat/oil has been encapsulated for controlled release/digestion. Schmitt (2010) has shown how coacervate particles can be used as stabilisers in ice cream foams.

Segregative phase separation is the most common occurrence in food microstructures. An example is ice cream, which typically contains polysaccharides LBG and kappa carrageenan, mixed with the milk proteins from either whole milk or cream or solutions made with skimmed milk powder. Schorsch *et al*. (1999) established a phase diagram for skimmed milk protein and galactomannan and also identified that the carrageenan was located in the protein phase. The inclusion of carrageenan in the milk thickens and slows down 'wheying off' (bulk separation into two layers). The LBG phase gels in the ice cream process and the small gel particles aid stabilisation of the ice cream microstructure. An application of the galactomannan–milk protein phase diagram was in the replacement of sahlep in Maras ice cream, enabling novel texture control for frozen desserts. The unusual property of Maras ice cream is its extensibility, which provides stretchy textures at frozen temperatures, at which conventional ice cream would fracture. Daniel *et al*. (2000) measured the differences in texture by cutting dog-bone shaped test samples at -25°C, then loading and tempering the sample before extension at -14°C.

The surface activity of some hydrocolloids has been mentioned in the previous section, due to the hydrophobic patches/stretches on the

primary, secondary, tertiary or quaternary structure of the molecule. Bot *et al*. (2002) have shown that understanding both surface activity and hydrocolloid segregative phase separation can provide texture control in dairy spreads, which are examples of (oil-in-water)-in-water emulsions.

The examples given above have shown that hierarchical microstructure control can be achieved. Burey *et al*. (2009) have indicated that exciting new textures, flavours and appearances will provide scope for innovation in the confectionary market. It appears that Holm *et al.* (2009) have begun to meet such a challenge by creating layered gelatin gels in which the sugar differs in amount in each of the different layers. Controlling the distribution of sugar in the sample produces sweeter gels while the sugar content is maintained at the same level.

REFERENCES

Agoub, A.A., Smith, A.M., Giannouli, P., Richardson, R.K. and Morris, E.R. (2007) 'Melt-in-the-mouth' gels from mixtures of xanthan and konjac glucomannan under acidic conditions: a rheological and calorimetric study of the mechanism of synergistic gelation. *Carbohydrate Polymers* **69**(4), 713–724.

Amici, E., Clark, A.H., Normand, V. and Johnson, N.B. (2000) Interpenetrating network formation in gellan-agarose el composites. *Biomacromolecules* **1**(4), 721–729.

Amici, E., Clark, A.H., Normand, V. and Johnson, N.B. (2002) Interpenetrating network formation in agarose-kappa carrageenan gel composites. *Biomacromolecules* **3**(3), 466–474.

Barnes, H.A. (2007) The 'yield stress myth?' paper – 21 years on. *Applied Rheology* **17**(4), ARTN 43110.

Barnes, H.A., Hutton, J.F. and Walters, K. (1989) *An Introduction to Rheology*. Amsterdam, The Netherlands: Elsevier Science.

Bot, A., Foster, T.J., Lundin, L.O., Pelan, B.M.C. and Reiffers-Magnani, C.K. (2002) Spoonable water-continuous acidified food product, EP1494544A1.

Boyd, M.J., Hampson, F.C., Jolliffe, I.G., Dettmar, P.W., Mitchell, J.R. and Melia, C.D. (2009) Strand-like phase separation in mixtures of xanthan gum with anionic polysaccharides. *Food Hydrocolloids* **23**, 2458–2467.

Brown, C.R.T., Foster, T.J., Norton, I.T. and Underdown, J. (1995) Influence of shear on the microstructure of mixed biopolymer systems. In: Harding, S.E., Hill, S.E. and Mitchell, J.R., editors. *Biopolymer Mixtures*. Nottingham University press, pp. 65–83.

Burey, P., Bhandari, B.R., Rutgers, R.P.G., Halley, P.J. and Torley, P.J. (2009) Confectionary Gels: a review of formulation, rheological and structural aspects. *International Journal of Food Properties* **12**(1), 176–210.

Butler, M.F. (2002) Mechanism and kinetics of phase separation in a gelatin/ maltodextrin mixture studied by small-angle light scattering. *Biomacromolecules* **3**(4), 676–683.

Butler, M.F. and Heppenstall-Butler, M. (2003) 'Delayed' phase separation in a gelatine/ dextran mixture studied by small-angle light scattering, turbidity, confocal laser microscopy and polarimetry. *Biomacromolecules* **4**(4), 928–926.

Cairns, P., Miles, M.J., Morris, V.J. and Brownsey, G.J. (1987) X-ray fibre diffraction studies of synergistic, binary polysaccharide gels. *Carbohydrate Research* **160**, 411–423.

Capron, I., Costeux, S. and Djabourov, M. (2001) Water in water emulsions: phase separation and rheology of biopolymer solutions. *Rheologica Acta* **40**(5), 441–456.

Castelain, C., Doublier, J.L. and Lefebre, J. (1987) A study of the viscosity of cellulose derivatives in aqueous solutions. *Carbohydrate Polymers* **7**(1), 1–16.

Clark, A.H., Eyre, S.C.E., Ferdinando, D.P. and Lagarrigue, S. (1999) Interpenetrating nework formation in gellan-maltodextrin gel composites. *Macromolecules* **32**(23), 7897–7906.

Clark, A.H., Richardson, R.K., Ross-Murphy, S.B. and Stubbs, J.M. (1983) Structural and mechanical properties of agar-gelatin co-gels – small deformation studies. *Macromolecules* **16**(8), 1367–1374.

Cox, A.R., Aldred, D.L. and Russell, A.B. (2009) Exceptional stability of food foams using class II hydrophobin HFBII. *Food Hydrocolloids* **23**(2), 366–376.

Cronin, C.E., Giannouli, P., McCleary, B.V., Brooks, M. and Morris, E.R. (2002) Formation of strong gels by enzymic debranching of guar gum in the presence of ordered xanthan. In: Williams, P.A. and Glyn, O.P., editors. *Gums and Stabilisers for the Food Industry 11*. Cambridge, UK: RSC Publishing, pp. 289–296.

Cui, S.W., Eskin, N.A.M., Biliaderis, C.G. and Mazza, G. (1995) Synergistic interactions between yellow mustard polysaccharide and galactomannans. *Carbohydrate Polymers* **27**(2), 123–127.

Cui, S.W., Eskin, N.A.M., Wu, Y. and Ding, S.D. (2006) Synergisms between yellow mustard mucilage and galactomannans and applications in food products – a mini review. *Advances in Colloid and Interface Science* **128**, 249–256.

Cuvelier, G. and Launay, B. (1988) Xanthan-Carob interactions at very low concentration. *Carbohydrate Polymers* **8**(4), 271–284.

Daniel, A.M., Foster, T.J., Lundin, L.O., Norton, I.T. and Sutton, R. (2000) Maras type ice cream, GB2357954A.

Dea, I.C.M. and Morrison, A. (1975) Chemistry and interactions of seed galactomannans. *Advances in Carbohydrate Chemistry and Biochemistry* **31**, 241–312.

De Gennes, P.G. (1971) Reptation of a polymer chain in presence of fixed obstacles. *Journal of Chemical Physics* **55**, 572–579.

Ding, P., Wolf, B., Frith, W.J., Clark, A.H., Norton, I.T. and Pacek, A.W. (2002) Interfacial tension in phase-separated gelatin/dextran aqueous mixtures. *Journal of Colloid and Interface Science* **253**(2), 367–376.

Dinsmore, A.D., Weeks, E.R., Prasad, V., Levitt, A.C. and Weitz, D.A. (2001) Three-dimensional confocal microscopy of colloids. *Applied Optics* **40**(24), 4152–4159.

Erni, P., Cramer, C., Marti, I., Windhab, E.J. and Fischer, P. (2009) Continuous flow structuring of anisotropic biopolymer particles. *Advances in Colloid and Interface Science* **150**(1), 16–26.

Firoozmand, H., Murray, B.S. and Dickinson, E. (2007) Fractal-type particle gel formed from gelatine plus starch solution. *Langmuir* **23**(8), 4646–4650.

Firoozmand, H., Murray, B.S. and Dickinson, E. (2009) Interfacial structuring in a phase-separating mixed biopolymer solution containing colloidal particles. *Langmuir* **25**(3), 1300–1305.

Fitzsimons, S.M., Mulvihill, D.M. and Morris, E.R. (2008a) Large enhancements in thermogelation of whey protein isolate by incorporation of very low concentrations of guar gum. *Food Hydrocolloids* **22**(4), 576–586.

Fitzsimons, S.M., Tobin, J.T. and Morris, E.R. (2008b) Synergistic binding of konjac glucomannan to xanthan on mixing at room temperature. *Food Hydrocolloids* **22**(1), 36–46.

Foster (1992) *Conformation and Properties of Xanthan Variants*, PhD Thesis. Silsoe College, Bedfordshire, UK: Cranfield Institute of Technology.

Foster, T. (2007) Structure design in the food industry. In: Brockel, U., Meier, W. and Wagner, G., editors. *Product Design and Engineering Volume 2: Raw Materials, Additives and Applications*. Weinheim, Germany: Wiley-VCH, pp. 617–629.

Foster, T.J., Brown, C.R.T. and Norton, I.T. (1996) Phase inversion of water-in-water emulsions. In: Phillips, G.O., Williams, P.A. and Wedlock, D.J., editors. *Gums and Stabilisers for the Food Industry*, Volume **8**. Oxford: Oxford University Press, UK, pp. 297–306.

Foster, T.J. and Morris, E.R. (1994) Xanthan polytetramer – conformational stability as a barrier to synergistic interaction. In: Phillips, G.O., Williams, P.A. and Wedlock, D.J., editors. *Gums and Stabilisers for the Food Industry*, Volume **7**. Oxford: Oxford University Press, UK, pp. 281–289.

Ganzevles, R.A., Fokkink, R., van Vliet, T., Stuart, M.A.C. and de Jongh, H.H.J. (2008) Structure of mixed beta-lactoglobulin/pectin adsorbed layers at air/water interfaces: a spectroscopy study. *Journal of Colloid and Interface Science* **317**(1), 137–147.

Ganzevles, R.A., Stuart, M.A.C., van Vliet, T. and de Jongh, H.H.J. (2006b) Use of polysaccharides to control protein adsorption to the air/water interface. *Food Hydrocolloids* **20**(6), 873–878.

Ganzevles, R.A., Zinoviadou, K., van Vliet, T., Stuart, M.A.C. and de Jongh, H.H.J. (2006a) Modulating surface rheology by electrostatic protein/polysaccharide interactions. *Langmuir* **22**(24), 100089–10096.

Giannouli, P., Richardson, R.K. and Morris, E.R. (2004) Effect of polymeric cosolutes on calcium pectinate gelation. Part 1. Galactomannans in comparison with partially depolymerised starches. *Carbohydrate Polymers* **55**(4), 343–355.

Goycoolea, F.M., Milas, M. and Rinaudo, M. (2000) Heterotypic interactions of deactylated xanthan with a galactomannan of high galactose substitution during synergistic gelation. *Gums and Stabilisers for the Food Industry* **10**, RSC, 229–240.

Goycoolea, F.M., Milas, M. and Rinaudo, M. (2001) Associative phenomena in galactomannan-deacetylated xanthan systems. *International Journal of Biological Macromolecules* **29**(3), 181–192.

Goycoolea, F.M., Morris, E.R. and Gidley, M.J. (1995a) Screening for synergistic interactions in dilute polysaccharide solutions. *Carbohydrate Polymers* **28**(4), 351–358.

Goycoolea, F.M., Richardson, R.K., Morris, E.R. and Gidley, M.J. (1995b) Stoichiometry and conformation of xanthan in synergistic gelation with locust bean gum or konjac glucomannan – Evidence for heterotypic binding. *Macromolecules* **28**(24), 8308–8320.

Harrington, J.C. and Morris, E.R. (2009) Conformational ordering and gelation of gelatin in mixtures with soluble polysaccharides. *Food Hydrocolloids* **23**(2), 327–336.

Haug, I., Williams, M.A.K., Lundin, L., Smidrød, O. and Draget, K.I. (2003) Molecular interactions in, and rheological properties of, a mixed biopolymer system undergoing order/disorder transitions. *Food Hydrocolloids* **17**, 439–444.

Holm, K., Wendin, K. and Hermansson (2009) Sweetness and texture perceptions in structured gelatine gels with embedded sugar rich domains. *Food Hydrocolloids* **23**(8), 2388–2393.

Kasapis, S., Morris, E.R., Norton, I.T. and Clark, A.H. (1993) Phase-equilibria and gelaion in gelatin/maltodextrin systems. 4. Composition dependence of mixed gel moduli. *Carbohydrate Polymers* **21**(4), 269–276.

Kasapis, S., Giannouli, P., Hember, M.W.N., Evageliou, V., Poulard, C., Tort-Bourgeois, B. and Sworn, G. (1999) Structural aspects and phase behaviour in deacylated and high acyl gellan systems. *Carbohydrate Polymers* **38**(2), 145–154.

Kasapis, S., Mitchell, J., Abeysekera, R. and MacNaughton, W. (2004) Rubber-to-glass transitions in high sugar/biopolymer mixtures. *Trends in Food Science & Technology* **15**, 298–304.

Kasapis, S., Morris, E.R., Norton, I.T. and Brown, C.R.T. (1993b) Phase-equilibria and gelation in gelatin/maltodextrin systems. 3. Phase separation in mixed gels. *Carbohydrate Polymers* **21**(4), 261–268.

Kasapis, S., Morris, E.R., Norton, I.T. and Gidley, M.J. (1993a) Phase-equilibria and gelaion in gelatin/maltodextrin systems. 2. Incompatibility in solution. *Carbohydrate Polymers* **21**(4), 249–259.

Kim, B.S., Takemasa, M. and Nishinari, K. (2006a) Effect of pH and added salt on the synergistic interaction between xyloglucan and xanthan. *Transactions of the Materials Research Society of Japan* **31**(3), 719–722.

Kim, B.S., Takemasa, M. and Nishinari, K. (2006b) Synergistic interaction of xyloglucan and xanthan investigated by rheology, differential scanning calorimetry and NMR. *Biomacromolecules* **7**(4), 1223–1230.

Lad, M.D., Samanci, S., Mitchell, J.R. and Foster, T.J. (2010) Viscosity development during competitive hydration of starch and hydrocolloids. In: Phillips, G.O. and Williams, P.A., editors. *Gums and Stabilisers for the Food Industry*, Volume **15**. Cambridge, UK: Royal Society of Chemistry Publishing, pp. 126–136.

Lapasin, R. and Pricl, S. (1999) *Rheology of Industrial Polysaccharides: Theory and Applications*. US: Aspen Publishers Inc.

Larson, R.G. (1998) *The Structure and Rheology of Complex Fluids*. Oxford University Press.

Launay, B., Cuvelier, G. and Martinez-Reyes, S. (1997) Viscosity of locust bean, guar and xanthan gum solutions in the Newtonian domain: a critical examination of the log(eta(sp))(O)-logC[eta](o) master curves. *Carbohydrate Polymers* **34**(4), 385–395.

Lee, H.-C. and Brant, D.A. (2002a) Rheology of concentrated isotropic and anisotropic xanthan solutions. 1. A rodlike low molecular weight sample. *Macromolecules* **35**, 2212–2222.

Lee, H.-C. and Brant, D.A. (2002b) Rheology of concentrated isotropic and anisotropic xanthan solutions. 2. A semiflexible wormlike intermediate molecular weight sample. *Macromolecules* **35**, 2223–2234.

Lemetter, C.Y.G., Meeuse, F.M. and Zuidam, N.J. (2009) Control of the morphology and size of complex coacervate microcapsules during scale-up. *AIChE Journal* **55**(6), 1487–1496.

Lofgren, C., Walkenstrom, P. and Hermansson, A.M. (2002) Microstructure and rheological behaviour of pure and mixed pectin gels. *Biomacromolecules* **3**(6), 1144–1153.

Loren, N., Hermansson, A.M., Williams, M.A.K., Lundin, L., Foster, T.J., Hubbard, C.D., Clark, A.H., Norton, I.T., Bergstrom, E.T. and Goodall, D.M. (2001) Phase separation induced by conformational ordering of gelatine in gelatin/maltodextrin mixtures. *Macromolecules* **34**(2), 289–297.

Loren, N., Langton, M. and Hermansson, A.M. (1999) Confocal laser scanning microscopy and image analysis of kinetically trapped phase-separated gelatin/maltodextrin gels. *Food Hydrocolloids* **13**(2), 185–198.

Loren, N., Shtykova, L., Kidman, S., Jarvoll, P., Nyden, M. and Hermansson, A.M. (2009) Dendrimer diffusion in kappa-carrageenan gel structures. *Biomacromolecules* **10**(2), 275–284.

Lundin, L.O., Odic, K. and Foster, T.J. (1999) Phase separation in mixed carrageenan systems. *Proceedings to Supermolecular and Colloidal Structures in Biomaterials and Biosubstrates*, Mysore, India.

Macosko, C. (1994) *Rheology: Principles, Measurements and Applications*. Poughkeepsie, NY: Wiley/VCH.

Mannion, R.O., Melia, C.D., Launay, B., Cuvelier, G., Hill, S.E., Harding, S.E. and Mitchell, J.R. (1992) Xanthan-Locust bean gum interactions at room temperature. *Carbohydrate Polymers* **19**(2), 91–97.

Mezger, T.G. (2006) *The Rheology Handbook*. Hannover: Vincentz Network.

Michon, C., Cuvelier, G., Launay, B., Parker, A. and Takerkart, G. (1995) Study of the compatibility/incompatibility of gelatin/iota-carrageenan/water mixtures. *Carbohydrate Polymers* **28**(4), 333–363.

Michon, C., Vogouroux, F., Boulenguer, P., Cuvelier, G. and Launay, B. (2000) Gelatin/iota-carrageenan interactions in non-gelling conditions. *Food Hydrocolloids* **14**(3), 203–208.

Mitchell, J.R. (1979) Rheology of polysaccharide solutions and gels. In: Blanshard, J.M.V. and Mitchell, J.R., editors. *Polysaccharides in Food*. London: Butterworths, pp. 51–72.

Morris, E.R. (1990) 'Mixed polymer gels'. In: Harris, P., editor. *Food Gels*. London: Elsevier, pp. 291–359.

Morris, E.R. (1995) Polysaccharide synergism – more questions than answers. In: Harding, S.E., Hill, S.E. and Mitchell, J.R., editors. *Biopolymer Mixtures*. Nottingham University Press, pp. 247–288.

Morris, E.R., Cutler, A.N., Ross-Murphy, S.B., Rees, D.A. and Price, J. (1981) Concentration and shear rate dependence of viscosity in random coil polysaccharide solutions. *Carbohydrate Polymers* **1**(1), 5–21.

Morris, E.R. and Foster, T.J. (1994) Role of conformation in synergistic interactions of xanthan. *Carbohydrate Polymers* **23**(2), 133–135.

Moschakis, T., Murray, B.S. and Dickinson, E. (2006) Particle tracking using confocal microscopy to probe the microrheology in a phase-separating emulsion containing nonadsorbing polysaccharide. *Langmuir* **22**(10), 4710–4719.

Normand, V., Pudney, P.D.A., Aymard, P. and Norton, I.T. (2002) Weighted-average isostrain and isostress model to describe the kinetic evolution of the mechanical properties of a composite gel: application to the system gelatin : maltodextrin. *Journal of Applied Polymer Science* **77**(7), 1465–1477.

Penroj, P., Mitchell, J.R., Hill, S.E. and Ganjanagunchorn, W. (2005) Effect of konjac glucomannan deacetylation on the properties of gels formed from mixtures of kappa carrageenan and konjac glucomannan. *Carbohydrate Polymers* **59**, 367–376.

Plucknett, K.P., Pomfret, S.J., Normand, V., Ferdinando, D.P., Veerman, C., Frith, W.J. and Norton, I.T. (2001) Dynamic experimentation on the confocal laser scanning microscope: application to soft-solid food materials. *Journal of Microscopy* **201**, 279–290.

Rayment, P., Ross-Murphy, S.B. and Ellis, P.R. (2000) Effect of size and shape of particulate inclusions on the rheology of guar galactomannan solutions. *Carbohydrate Polymers* **43**(1), 1–9.

Sanchez, C., Mekhloufi, G. and Renard, D. (2006) Complex coacervation between beta-lactoglobulin and Acacia gum: a nucleation and growth mechanism. *Journal of Colloid and Interface Science* **299**(2), 867–873.

Schmitt, C. (2010) Protein-polysaccharide complexes: from basics to food applications. In: *Gums and Stabilisers for the Food Industry*, Volume **15**, RSC, pp. 211–222.

Schmitt, C., da Silva, T.P., Bovay, C., Rami-Shojaei, S., Frossard, P., Kolodziejczyk, E., Leser, M.E., Schmitt, C., da Silva, T.P., Bovay, C., Rami-Shojaei, S., Frossard, P., Kolodziejczyk, E. and Leser, M.E. (2005) Effect of time on the interfacial and foaming properties of beta-lactoglobulin/acacia gum electrostatic complexes and coacervates at pH 4.2. *Langmuir* **21**(17), 7785–7795.

Schmitt, C., Sanchez, C., Desobry-Banon, S. and Hardy, J. (1998) Structure and technofunctional properties of protein-polysaccharide complexes: a review. *Critical Reviews in Food Science and Nutrition* **38**(8), 689–753.

Schorsch, C., Jones, M.G. and Norton, I.T. (1999) Thermodynamic incompatibility and microstructure of milk protein locust bean gum sucrose systems. *Food Hydrocolloids* **13**(2), 89–99.

Shrinivas, P., Kasapis, S. and Tongdang, T. (2009) Morphology and mechanical properties of bicontinuous gels of agarose and gelatin and the effect of added lipid phase. *Langmuir* **25**(15), 8763–8773.

Simeone, M., Alfani, A. and Guido, S. (2004) Phase diagram, rheology and interfacial tension of separated phases in gelatin/pullulan mixtures. *Food Hydrocolloids* **19**(3) 567–574.

Simeone, M., Molè, F. and Guido, S. (2002) Measurement of average droplet size in aqueous mixtures of Na-alginate and Na-caseinate by linear oscillatory tests. *Food Hydrocolloids* **16**(5), 449–459.

Spyropoulos, F., Ding, P., Frith, W.J., Norton, I.T., Wolf, B. and Pacek, A.W. (2008) Interfacial tension in aqueous biopolymer-surfactant mixtures. *Journal of Colloid and Interface Science* **317**(2), 604–610.

Stokes, J.R., Wolf, B. and Frith, W.J. (2001) Phase-separated biopolymer mixture rheology: prediction using a viscoelastic emulsion model. *Journal of Rheology* **45**(5), 1173–1191.

Strom, A., Boers, H.M., Koppert, R., Melnikov, S.M., Wiseman, S. and Peters, H.P.F. (2010) Physico-chemical properties of hydrocolloids determines its appetite effects. In: *Gums and Stabilisers for the Food Industry*, Volume **15**, RSC, pp. 341–355.

Tchuenbou-Magaia, F.L., Norton, I.T. and Cox, P.W. (2009) Hydrophobin stabilised air-filled emulsions for the food industry. *Food Hydrocolloids* **23**(7), 1877–1885.

Valentine, M.T., Kaplan, P.D., Thota, D., Crocker, J.C., Gisler, T., Prud'homme, R.K., Beck, M. and Weitz, D.A. (2001) Investigating the microenvironments of inhomogeneous soft materials with multiple particle tracking. *Physical Review E* **64**(6), 061506.

van Benthum, W.A.J., Duchateau, S.M.J.E. and Peters, H.P.F. (2004) Food product e.g. for controlling body weight comprises a satiety agent encapsulated by cross-linked encapsulation material with a specified degree of cross-linking, WO2004105505-A1.

Walkenstrom, P., Kidman, S., Hermansson, A.M., Rasmussen, P.B. and Hoegh, L. (2003) Microstructure and rheological behaviour of alginate/pectin mixed gels. *Food Hydrocolloids* **17**(5), 593–603.

Wolf, B., Frith, W.J., Singleton, S, Tassieri, M. and Norton, I.T. (2001) Shear behaviour of biopolymer suspensions with spheridal and cylindrical particles. *Rheologica Acta* **40**(3), 238–247.

Wolf, B., Scirocco, R., Frith, W.J. and Norton, I.T. (2000) Shear-induced anisotropic microstructure in phase-separated biopolymer mixtures. *Food Hydrocolloids* **14**(3), 217–225.
Wu, Y., Cui, S.W., Eskin, N.A.M. and Goff, H.D. (2009) Rheological investigation of synergistic interactions between galactomannans and non-pectic polysaccharide fraction from water soluble yellow mustard mucilage. *Carbohydrate Polymers* **78**(1), 112–116.

5 Xanthan Gum – Functionality and Application

Graham Sworn

5.1 INTRODUCTION

The polysaccharide xanthan gum is produced by the microorganism *Xanthomonas campestris*. *Xanthomonas* species are pathogenic organisms which are responsible for blight diseases of a number of important crop plants, including, beans, peas, cabbage and cotton. Xanthan gum is soluble in cold water and forms highly viscous solutions. It is used in a very wide variety of food products, including dressings, sauces, baked goods, dairy desserts, beverages and frozen products. To understand how to use xanthan gum in these many applications, one must first understand the functionality of the gum and how the molecular structure can influence this. This can then be supported by knowledge of how the main components of the food influence the functionality. These are primarily water, salts, acids (pH), sugars and proteins. The processes used to prepare the food, such as mixing, heating and freezing, must also be considered. Finally, how the xanthan interacts with the structures created in the food products will contribute to the final stability, texture and, ultimately, consumer satisfaction.

5.2 XANTHAN MOLECULAR STRUCTURE AND ITS INFLUENCE ON FUNCTIONALITY

Two of the key properties of xanthan gum that set it apart from other hydrocolloid thickeners are its unique rheology and its ability to interact synergistically with galactomannans. The rheology can be characterised by the development of very high viscosity at low shear rates and pseudoplastic flow. As illustrated in Fig. 5.1, xanthan solutions are more pseudoplastic than must other thickeners and develop a higher

Practical Food Rheology: An Interpretive Approach
Edited by Ian T. Norton, Fotios Spyropoulos and Philip Cox
 ISBN: 978-1-405-19978-0

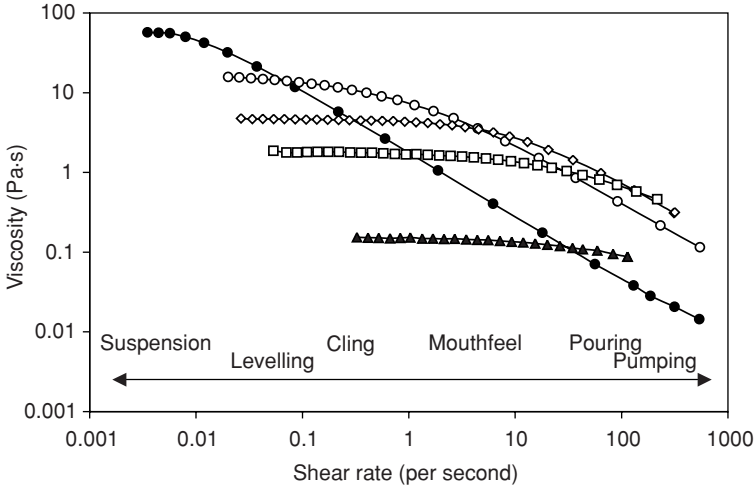

Fig. 5.1 Comparison of the flow behaviour of thickening agents: 0.3% xanthan gum (•), 1% guar gum (○), 1% LBG (◊), 1% alginate (■), and 1% cellulose gum (▲).

viscosity at low shear rates at much lower concentrations. Behaviour at low shear rates is important for suspension stability, whereas behaviour at medium rates can provide information about cling and mouthfeel. Viscosity at high shear rates can determine the behaviour in processes such as filling, pouring, pumping and spraying.

The flow behaviour of xanthan gum is a result of intermolecular association among xanthan polymer chains which results in the formation of a complex network of entangled rod-like molecules. These associations are driven by the charges that are carried on the pyruvate group of the terminal mannose and the glucuronic acid unit sandwiched between the two mannose units of the trisaccharide side chain. This highly ordered network of entangled stiff molecules gives rise to xanthan solutions having the viscoelastic characteristics of a weak gel. This is illustrated in Fig. 5.2, which shows that the xanthan solution has a dominant elastic response to frequency in contrast to other polysaccharide thickeners, such as guar, which have a dominant viscous response. These rheological characteristics provide suspension stability to finished products, combined with the ease of filling, pouring and pumping.

Xanthan gum also has the ability to interact with galactomannans such as guar gum, cassia gum, tara gum and locust bean gum (LBG) and with structurally similar polysaccharides such as the glucomannan konjac (Kovacs, 1973; Pettitt, 1982; Dalbe, 1992; Urlacher and Noble, 1999; Sworn, 2000). The specific binding between the extracellular polysaccharide and typical components of plant cell walls, such as galactomannans and other polysaccharides having a β-1,4-linked

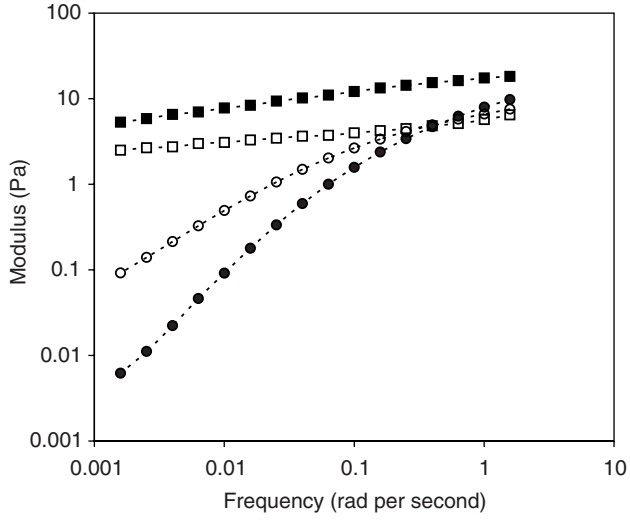

Fig. 5.2 Viscoelastic profile of 0.6% xanthan gum (■G', □G'') and 0.6% guar gum (G'●, G''○).

backbone, may suggest a part in the host–pathogen relationship. It has been suggested that the extracellular polysaccharide could represent a 'molecular holdfast' to recognise the site at which the bacteria are finally to attach themselves. The simplest of such functions would be to locate the bacteria at the plant cell surface in a single layer. A more elaborate possible function of this type, suggested by the selectivity of binding, *in vitro*, could be to identify a particular area of the surface of a particular type of plant cell by means of the characteristic polysaccharide composition of its wall (Morris *et al.*, 1977).

The interaction with galactomannans results in either a synergistic increase in viscosity in the case of guar gum, or the formation of strong self-supporting gels as seen with LBG. With LBG, xanthan is able to form a very elastic gel with optimum strength at a ratio of 60:40 Xanthan:LBG. At low gum concentration, this synergy can be used to increase the thickening impact of xanthan or LBG and create fluid systems with gel-like viscoelastic properties.

With guar gum, an increase in viscosity can be seen beyond the value predicted for a simple mixture. The optimum synergy occurs at a ratio of 80:20 guar:xanthan. The addition of xanthan gum to guar gum significantly increases the viscoelasticity of the solutions. This is illustrated in Fig. 5.3: as the xanthan content in the mixture is increased, the elastic modulus is increased and becomes less dependent on frequency, indicating a more gel-like rheology. This is particularly relevant to suspension stability in finished products.

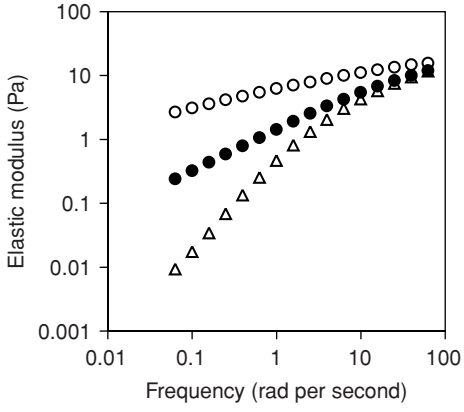

Fig. 5.3 Elastic modulus for 0.6% solutions of 100% guar (△), 80:20 guar:xanthan (•) and 50:50 guar:xanthan (○).

The primary structure of xanthan gum is shown in Fig. 5.4. It consists of a cellulosic backbone of β-1,4-linked D-glucose units substituted on alternate glucose residues with a trisaccharide side chain.

The trisaccharide side chain is composed of two mannose units separated by a glucuronic acid (Jansson *et al.*, 1975; Melton, 1976). Approximately half the terminal mannose units are linked to a pyruvate group, and the non-terminal residue usually carries an acetyl group. The carboxyl groups on the side chains render the gum molecules anionic. Xanthan gum has a molecular weight of about 2×10^6 Da.

X-ray diffraction studies on xanthan gum fibres have identified a right-handed fivefold helix conformation (Moorhouse *et al.*, 1977). In this conformation, the side chains are aligned with the backbone and stabilise the overall conformation. In the solution, the side chains wrap around the cellulose-like backbone, thereby protecting it. For example, although the xanthan gum has a cellulosic backbone, it is very resistant to enzymatic degradation by cellulases because, due to the presence of the side chain, they are unable to access the main β-1,4-linked chain.

The role of the acetate and pyruvate groups in the molecular structure of xanthan gum and their impact on functionality are probably the most widely studied aspect of the structure–function relationship. Particular emphasis has been given to their role in controlling the rheology of the xanthan gum and their influence on interactions with the galactomannans. Assuming only one acyl group per side chain, the stoichiometric amounts of acetyl and pyruvate are 5.0 and 8.1%, respectively (Shatwell *et al.*, 1990). However, the levels in commercial xanthan gum are typically lower than this.

It has been shown in several studies that increasing the pyruvate content of xanthan increases the viscosity (Sanford *et al.*, 1977; Smith

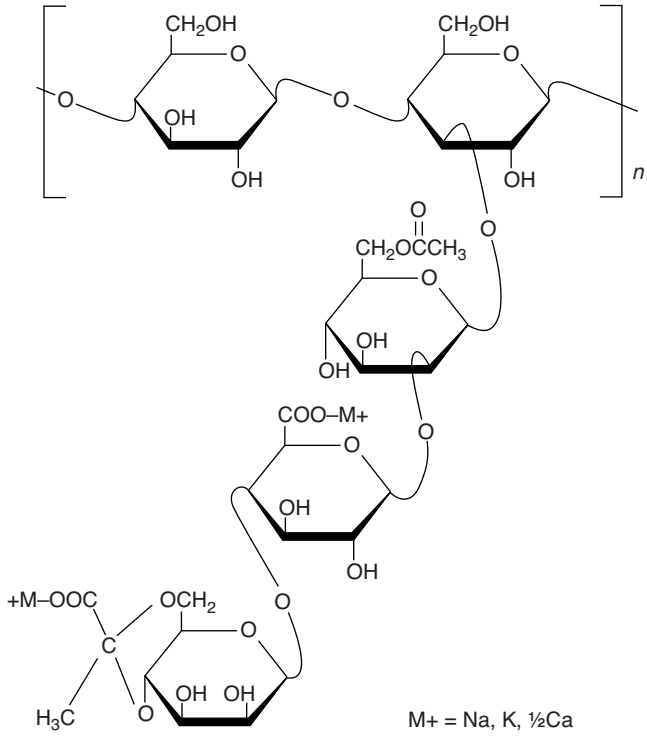

Fig. 5.4 The primary structure of xanthan gum.

et al., 1981; Cheetham and Norma, 1989; Hassler and Doherty, 1990). It has been suggested that there is no continuous relationship between pyruvate content and viscosity, but rather, that there is a steep increase when going from below 2% to above 3% pyruvate (Flores Candia and Deckwer, 1999). It has also been demonstrated that the viscosity of low pyruvate xanthan is less sensitive to the addition of salts (Cheetham and Norma, 1989).

There is one published paper that contradicts this and claims that pyruvate content has no significant effect on solution viscosity, and the authors attributed the differences observed in other studies to possible differences in molecular weight (Bradshaw *et al.*, 1983). However, in this study, viscosity was measured at shear rates between 8.8 and 88.8 per second. These relatively high shear rates may account for the lack of difference in measured viscosity. Generally, the viscosity differences are far more marked at shear rates below 0.1 per second. Christensen *et al.* have shown that the terminal β-mannose is relatively susceptible to acid hydrolysis. Thus, low pyruvate samples prepared in this way may also have reduced molecular weight due to removal of this sugar (Christensen *et al.*, 1993). The presence of acetate, on the other hand,

tends to reduce xanthan gum viscosity (Hassler and Doherty, 1990). It has been shown that an acetate-free xanthan has higher viscosity than native xanthan.

Initial studies on the mechanism of xanthan gum synergy with galactomannans proposed a model in which the unsubstituted, galactose-free (smooth) regions of the galactomannans bind to xanthan in its ordered state (Morris *et al.*, 1977). This model has been used to explain the difference in the degree of interaction between galactomannans of differing degrees of substitution. Subsequent studies, which showed that interactions were enhanced after heating the mixture to temperatures above the coil–helix transition of the xanthan, were interpreted as evidence that the binding occurred with the cellulosic backbone of the xanthan gum in the ordered state (Cairns *et al.*, 1986, 1987). An alternative explanation was that when the hydrocolloids are mixed at temperatures below the setting point of the gel, they form an inferior, disrupted network with melting and resetting giving a stronger, coherent gel (Morris, 1990). More recent studies tend to support this interpretation and favour the original model of Morris *et al.* (Morris and Foster, 1994; Cronin *et al.*, 2002; Fitzsimons *et al.*, 2008; Sworn and Kerdavid, 2009).

The strength of gels of xanthan and LBG or konjac mannan have been shown to be very dependent upon the degree of acetyl substitution and have generally concluded that the interactions increase with decreasing acetylation (Shatwell *et al.*, 1991a, 1991b; Wang *et al.*, 2002; Morrison *et al.*, 2004). The result of which is stronger gels with LBG and konjac mannan. It has also been suggested that low-acetate xanthan has stronger interactions with guar gum compared with that of standard xanthan (Lopes *et al.*, 1992; Morris and Foster, 1994; Milas *et al.*, 1996; Morrison *et al.*, 2004). For example, evidence for this was demonstrated in the form of increased viscosity at 1 per second in low-acetate xanthan/guar mixtures compared with standard xanthan/guar mixtures (Morrison *et al.*, 2004). There is very little published evidence to suggest that the pyruvate content of xanthan has an influence on interactions with galactomannans. Gel strength with LBG has been shown to be reduced slightly with the reduction of pyruvate level, but results were not conclusive because the molecular weight of the low-pyruvate samples was lower than standard xanthan (Shatwell *et al.*, 1991a). They also showed that a xanthan sample from a mutant strain of *Xanthomonas campestris*, believed to lack the terminal mannose residue from the trisaccharide side chains, formed very weak gels, suggesting that the side chain may play an important role in the interaction with LBG. However, recent work has identified a xanthan gum with high pyruvate content that has exceptionally high synergy with galactomannans (Sworn *et al.*, 2009). This work also showed that the synergy was not increased by selective removal of

the acetate group by alkali hydrolysis. These results appear to question the conventional thinking on xanthan gum structure and synergy and suggest that the pyruvate group, and perhaps the acetate/pyruvate ratio, plays a more important role than previously thought.

The structure of the galactomannan also has an influence on the synergy with xanthan gum. The degree/strength of associations is increased as galactose substitution is decreased. For example, LBG, which has a galactose content of 17–26%, forms self-supporting gels with xanthan gum, whereas guar gum, which has a galactose content of 33–40%, forms weak gel networks, resulting in a synergistic increase in viscosity. The molecular weight of the galactomannans is also known to influence their interactions with xanthan gum. The lower the molecular weight, the weaker the interactions seen with xanthan gum (Schorsch *et al.*, 1997; Sworn, 2009).

5.3 THE CONFORMATIONAL STATES OF XANTHAN GUM

Solutions of xanthan gum undergo a conformational transition during heating, which is associated with the change from a rigid, ordered state at low temperature to a more flexible, disordered state at high temperatures. This conformational change was first observed as a sigmoidal change in viscosity (Jeanes *et al.*, 1961). This is illustrated in Fig. 5.5 using a 0.5% solution of xanthan gum in 0.1% NaCl. The temperature of the conformational transition increases with increasing ionic strength of the solution as shown for NaCl concentration in Fig. 5.6.

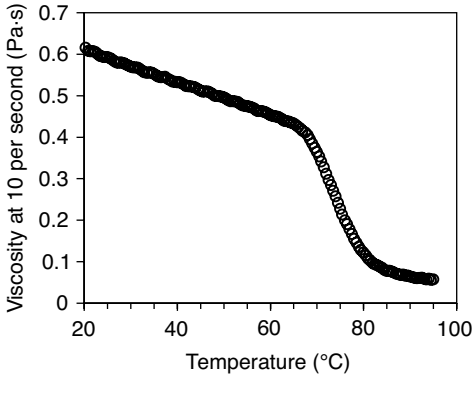

Fig. 5.5 The conformational transition of 0.5% xanthan gum solution in 0.10% NaCl measured by viscosity.

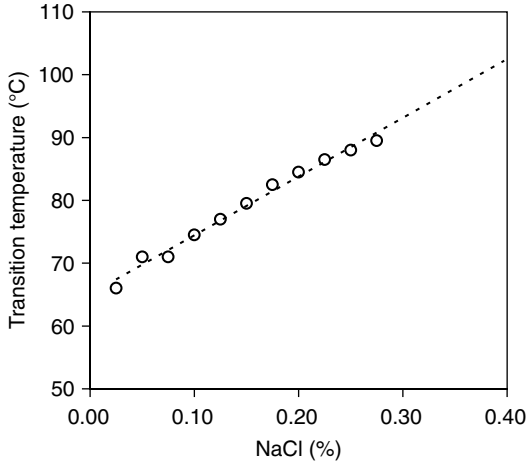

Fig. 5.6 The midpoint temperature of the thermal transition of 0.5% xanthan gum as a function of NaCl concentration as measured in Fig. 7.5.

Xanthan gum has been described as having three conformational states (Holzwarth and Prestridge, 1977; Milas and Rinaudo, 1984):

(i) Native, ordered form
  – Never heated
(ii) Denatured, ordered form
  – Heated to transition temperature or above, then cooled
(iii) Disorderd form
  – Present at high temperature or low salt concentrations, or both

The native, ordered form (i) is the typical form of the xanthan gum in the broth at the end of fermentation which has not been subjected to a heat treatment. It has been shown to have lower relative viscosity and intrinsic viscosity compared with that of the denatured, ordered form (ii), but the same molecular weight, suggesting a more compact conformation. During the production of commercial xanthan gum, the fermentation broth undergoes a thermal treatment to kill the bacteria prior to the precipitation of the gum. This means that solutions prepared with commercial xanthan gum can be considered to be predominantly in the denatured, ordered form (ii). The impact of the conformational transition on the rheological properties of xanthan gum in relation to food ingredients and processes will be discussed in detail in the subsequent sections.

5.4 FOOD INGREDIENTS AND THEIR EFFECTS ON XANTHAN GUM FUNCTIONALITY

Xanthan gum is an anionic polysaccharide. Food components such as salts and acids will influence the ionic strength of the environment, which will, in turn, influence the functionality of the xanthan gum through changes in the balance of the charges. Other charged molecules such as proteins also have the potential to influence the functionality of the xanthan gum.

5.4.1 Salts

The hydration rate of xanthan is decreased in the presence of salts. Fig. 5.7 shows that after 30 minutes of mixing at 650 rpm with a propeller-type mixer, full viscosity is not developed above approximately 2% NaCl. It is recommended that, when possible, xanthan is hydrated in the water before the addition of salt. However, continued mixing will eventually lead to full development of the viscosity at higher salt levels. Once hydrated, xanthan has very good salt tolerance and up to 20–30% salt can be added without adversely affecting the viscosity.

The effect of salts on the viscosity is dependent upon the concentration of the xanthan gum. At low concentrations of xanthan, below approximately 0.3%, addition of salts results in a slight decrease in the viscosity. At concentrations above 0.3%, addition of salts results in an increase in viscosity (see Table 5.1). The viscosity of the xanthan gum solution is equivalent in deionised water and 1% KCl at 0.3% gum.

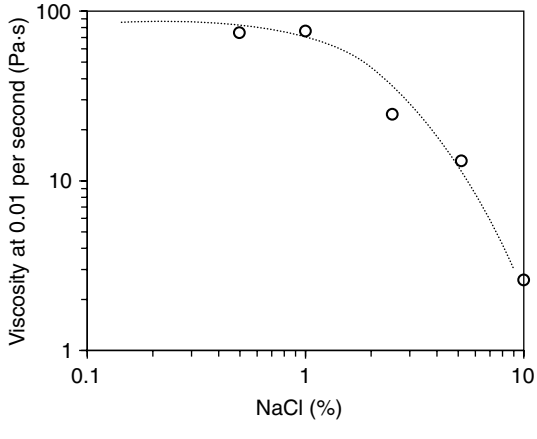

Fig. 5.7 Viscosity of 0.3% xanthan gum after 30 minutes mixing at medium shear (650 rpm propeller mixer).

Table 5.1 Xanthan gum concentration and the effect of salt on solution viscosity

	Brookfield viscosity (12 rpm)	
Xanthan conccentration (%)	**Deinised water**	**1% KCl**
0.1	130	60
0.3	712	750
0.5	1550	1 830
1	3920	7 040
2	9050	31 000

Below this concentration, xanthan has a higher viscosity in deionised water. Above this concentration, the xanthan has a higher viscosity in the salt solution. The viscosity of xanthan gum is stabilised with the addition of approximately 0.1% sodium chloride. Additional salt will have little or no further effect on the viscosity (see Table 5.2).

Addition of salt to hot xanthan gum solutions can have an impact on the final rheology. For example, addition of 0.5% NaCl to a hot solution in which the xanthan is in the disordered form (iii), at sufficient levels to induce the disorder–order transition to occur immediately, results in lower viscosity upon cooling compared with that of a solution which is heated and cooled in the presence of the same level of NaCl (see Fig. 5.8). It has been suggested that the salt addition at high temperatures drives the xanthan molecule partially into the native, ordered state (i), which results in a viscosity intermediate between the form (i) and (ii) (Milas and Rinaudo, 1986).

As with viscosity, the addition of salts to hot solutions of xanthan–LBG can have a negative impact on the strength of the gels. For example, addition of 1% NaCl when the xanthan–LBG mix is hot and the xanthan is in the disordered form results in weaker gels compared to that when the salt is added before heating (see Fig. 5.8). The quality of mixed xanthan–LBG gels is greatest when the xanthan is maintained in the ordered form throughout the preparation process (Sworn and Kerdavid, 2009). Hydrating the gums in the presence of at least 0.4% NaCl

Table 5.2 Effect of salt concentration on the viscosity of xanthan gum solutions

	Brookfield viscosity, 12 rpm (mPa · s)		
NaCl concentration (%)	**0.1% xanthan**	**0.5% xanthan**	**1.0% xanthan**
0.001	130	1560	3 920
0.01	115	1820	9 800
0.1	100	2010	10 600
0.5	85	—	—
1	90	1900	10 600

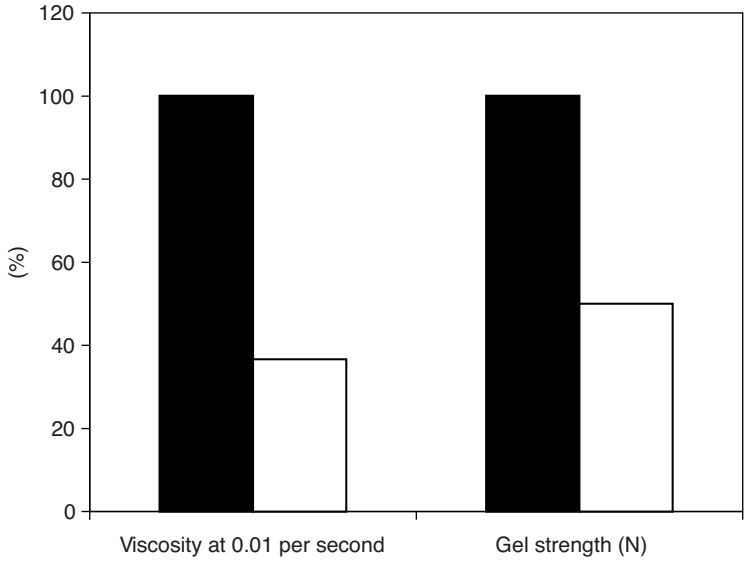

Fig. 5.8 Effect of preparation procedure on the viscosity of 0.5% xanthan gum in 0.5% NaCl and the gel strength of 1% 60:40 xanthan:LBG gels in 1% NaCl, (■ NaCl added prior to heating and □ NaCl added at 87°C).

or other salts of equivalent ionic strength will raise the transition temperature to greater than 90°C, which is the temperature required to fully hydrate the LBG and will maximise the gel strength.

When mixed xanthan–LBG gels are made under optimum conditions (salt addition prior to heating), the gel strength increases with increasing salt concentration up to ~100 mM for the monovalent ions. This is equivalent to ~0.58% as sodium chloride and 0.75% as potassium chloride (see Fig. 5.9). Gels prepared with potassium ions are slightly stronger than those with sodium. Gels prepared with calcium are significantly weaker.

5.4.2 Acids (pH)

There are two questions that need to be answered when considering the effect of pH on a gum solution:

(i) How does the viscosity change as a function of pH?
(ii) How stable is the viscosity as a function of time at any given pH?

The first can be considered to be a question of sensitivity, and the second can be considered to be a question of stability.

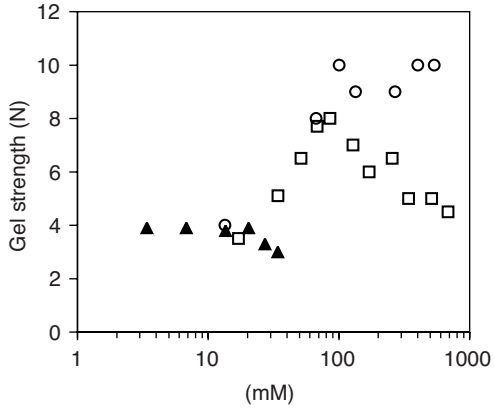

Fig. 5.9 The effect of sodium (□), potassium (○) and calcium (▲) on the gel strength of 1% 60:40 xanthan:LBG gels.

5.4.2.1 *The pH sensitivity of xanthan gum solution viscosity*

Early product literature for xanthan gum reported that solution viscosity was insensitive over a very broad range of pH (Pettitt, 1979, 1982). The measurements were made at high gum concentrations (1%) and relatively high shear rates (Brookfield viscometer at 30 rpm). On the basis of this data, it is often assumed, wrongly, that this insensitivity can be applied to all xanthan gum concentrations and across the complete rheological profile of the solution. This has been revised in more recent texts to show that some reduction of viscosity occurs at pHs below 2.5 (Urlacher and Noble, 1999; Sworn, 2000). In fact, Fig. 5.10 illustrates that the viscosity at low shear rates is particularly sensitive to changes in

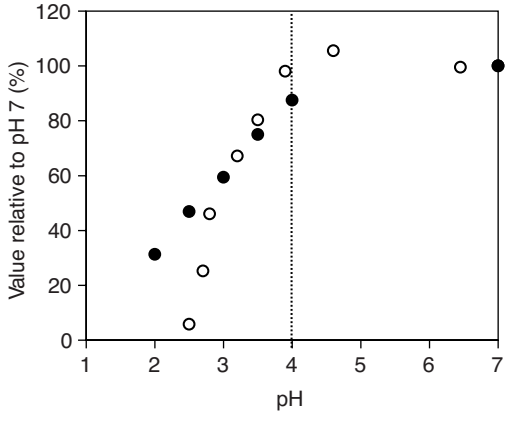

Fig. 5.10 Effect of pH on gel strength of 1% 60:40 xanthan:LBG gels in 0.5% NaCl (○) and viscosity at 0.01 per second of 0.3% xanthan gum in 1% NaCl (●).

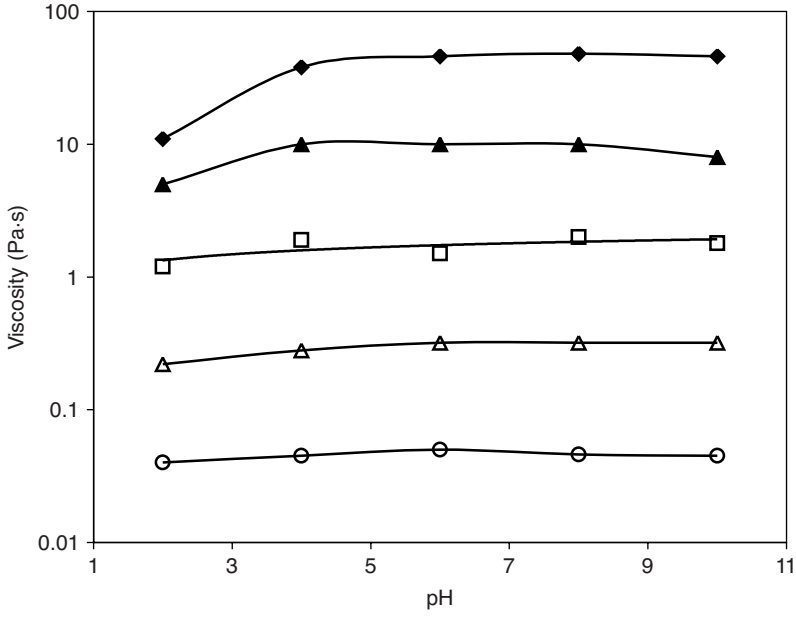

Fig. 5.11 The pH sensitivity of 0.3% xanthan in 1% NaCl measured at 0.01 per second (◇), 0.1 per second (▲), 1 per second (□), 10 per second (△) and 100 per second (○) different shear rates (pH adjusted with a solution of citric acid or NaOH).

pH below 4. This effect, however, is completely reversible upon neutralisation, indicating that it is due to changes in molecular conformation rather than degradation. The effect of pH on the viscosity is much less marked at higher shear rates, which would indicate that mouthfeel would be affected less than suspension stability (see Fig. 5.11).

The effect of pH on the synergy of xanthan gum with galactomannans shows a similar trend to the viscosity of the xanthan at low shear rates (Sworn and Kerdavid, 2009). The gel strength of the xanthan–LBG mixed system remains relatively unchanged between pH 7 and 4, but as the pH is decreased below 4, a progressive drop in the gel strength is observed (see Fig. 5.10).

Xanthan is a charged polymer and so the pH sensitivity of the low shear viscosity and synergy is to be expected, since changes in the pH will result in changes to the charge density of the xanthan, which will, in turn, influence the molecular associations between the xanthan molecules themselves and between xanthan and other food ingredients. Reducing the pH of xanthan gum solutions progressively converts the carboxylate groups from the ionised to the un-ionised form ($COO^- + H^+ = COOH$), with consequent suppression of electrostatic repulsion between xanthan side chains (Agoub *et al.*, 2007; Rinaudo and Moroni, 2009). This could reduce the stiffness of the molecule, allowing adoption

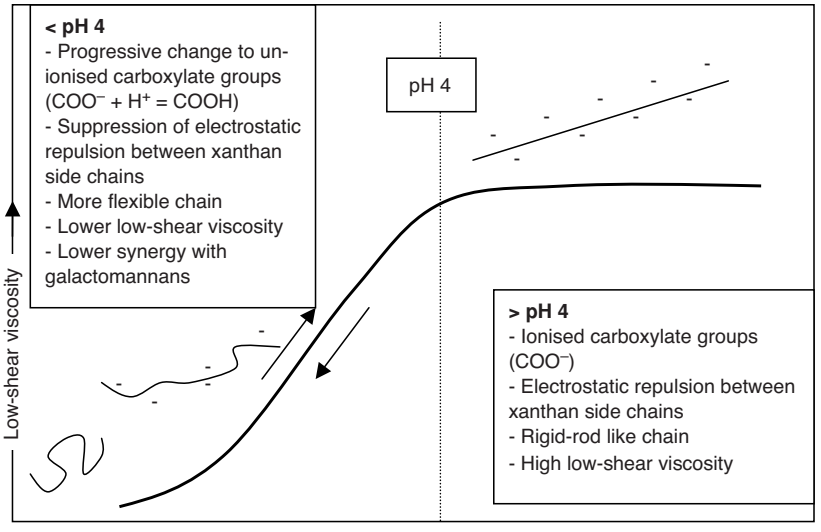

Fig. 5.12 Schematic representation of the reversible change in xanthan viscosity below pH 4.

of a more compact molecular shape, resulting in the observed reduction in viscosity. Neutralisation would re-ionise the carboxylate groups and allow the xanthan to return to the original conformation at neutral pH with the associated recovery of the original viscosity. This is illustrated schematically in Fig. 5.12.

It is important to understand that between pH 4 and 2, the low shear viscosity of xanthan and the synergistic interactions with galactomannans will decrease with decreasing pH. The practical implications of this are that small changes in pH in this range could result in changes in the suspension power, and hence stability, in some acidic food products such as dressings and vinaigrettes. However, since the viscosity at higher shear rates is less sensitive to the pH, it is likely that the mouthfeel of the products will remain relatively unaffected.

5.4.2.2 *The stability of xanthan at low pH*

Although it has been shown that the viscosity of xanthan gum is sensitive to pH below 4, the stability with time in acidic conditions is still excellent. Xanthan is widely used in acidic food products such as salad dressings and vinaigrettes, where it shows exceptional long-term stability. This is illustrated in Fig. 5.13 in a model vinaigrette solution at pH 2.5, which has a virtually constant viscosity at low shear rate during

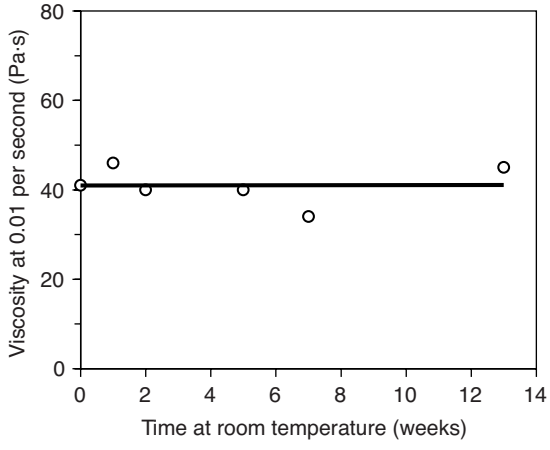

Fig. 5.13 Variation with time of the low shear viscosity of xanthan gum in a model vinaigrette (0.3% xanthan, pH 2.5, 1% NaCl).

the 13 weeks storage at room temperature. This translates into good stability throughout the shelf life of the product.

5.4.3 Xanthan and proteins

The incompatibility of polysaccharides with milk proteins is well known. It is the result of depletion flocculation, is dependent on the concentration of polysaccharide and milk protein and often results in phase separation. Xanthan gum is no exception (Hemar *et al.*, 2001).

For example, when low concentrations of xanthan gum (0.01%–0.1%) are added to milk and stored at 5°C for 3 days, phase separation occurs (see Fig. 5.14). Using rheological measurements, it can be shown that the upper phase is enriched with the polysaccharide evidenced by the typical pseudoplastic flow characteristics of xanthan gum, whereas the Newtonian flow of the lower phase indicates that it is enriched with the protein (see Fig. 5.15). A simple phase diagram of milk content (protein) and xanthan concentration identifies two principal regions (see Fig. 5.16). The continuous line separating the two regions is called the binodal curve. In the monophasic (stable) region, below the binodal curve, the two polymers coexist in one single phase. There is thermodynamic compatibility. In the biphasic (unstable) region, above the binodal, the system separates spontaneously into two phases. There is thermodynamic incompatibility. At high levels of xanthan, a single phase is seen. Flocculation may occur in this region, but the phase separation is not visible due to the stabilising effects of the viscosity from the xanthan gum.

Fig. 5.14 Phase separation after addition of xanthan gum to semi-skimmed milk. For a colour version of this figure, please see the colour plate section.

In practice, many dairy products such as desserts are manufactured very successfully with xanthan gum. These are typically formulated with xanthan gum concentrations between 0.1% and 0.3% and often contain other gelling and thickening agents such as starch and carrageenan, which, together with the viscosity of the xanthan gum, provide product stability. This enables the formulation of smooth, creamy-textured dairy desserts.

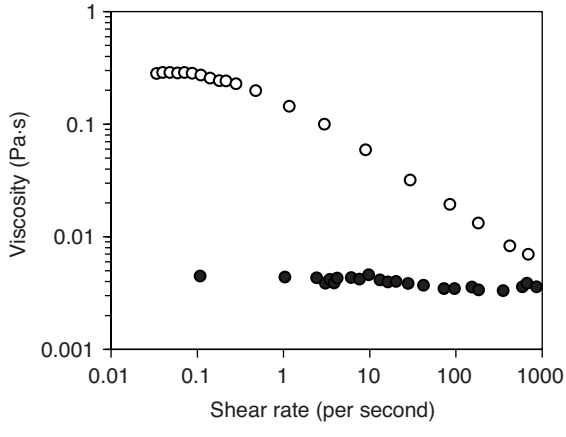

Fig. 5.15 The flow curves of the upper (○) and lower (●) phase 3 days after addition of 0.05% xanthan gum to semi-skimmed milk.

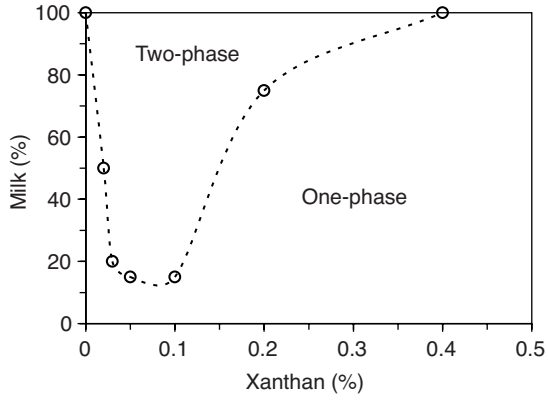

Fig. 5.16 Phase diagram for xanthan compatibility with milk.

5.4.4 Xanthan and starch

Starches are very widely used in food, and addition of low levels of xanthan gum to starch-based products can improve their properties. Xanthan gum does not significantly affect the gelatinisation of the starch but can inhibit retrogradation, making the starch solutions more stable. Xanthan gum is also effective at improving the freeze–thaw stability of starches by controlling syneresis (Arocus *et al.*, 2009). Xanthan is widely used in baked goods where its benefits are seen as better water retention and lower crumb firming during storage. The high viscosity of the xanthan gum also helps with suspension of particulates such as fruit and chocolate pieces during the baking process. This gives an even distribution throughout the product. The viscoelastic properties of the xanthan gum help to increase the volume through better crumb structure. Xanthan gum can also reduce liquid separation (syruping) in refrigerated doughs (Simsek, 2009).

5.5 FOOD PROCESSING AND ITS IMPACT ON XANTHAN GUM FUNCTIONALITY

5.5.1 Thermal treatment

Heating of food products during their manufacture and/or prior to consumption is common practice. Its purpose is to preserve the product through destruction of the microorganisms and enzymes responsible for spoilage and to improve the texture and palatability of the product. The heat treatment can vary from cooking to sterilisation according to the type of product and the shelf life required. Sterilisation refers to the complete destruction of microorganisms, including spores, and typically

requires that the whole food is heated to at least 121°C for 15 minutes. For solid and canned foods, this is often performed in static or agitating retorts. Rapid heating of liquids can be performed in a plate heat exchanger. Often referred to as Ultra High Temperature (UHT) sterilisation processes, they involve heating the liquid to as high as 150°C, in some cases for 1–2 seconds, and then rapidly cooling. Pasteurisation is a much less severe heat treatment typically carried out at temperatures below the boiling point of water. For example, batch pasteurisation of milk requires heating to 62.8°C (145°F) for 30 minutes. High temperature-short time pasteurisation (HTST) is also commonly used in which the milk is heated to 71.7°C (161°F) for at least 15 seconds.

It is essential to understand the effect of thermal treatments in terms of the conformational transition of the xanthan gum, as this can have an effect on the final solution rheology. In general when there is:

- no conformational transition during heat treatment:
  - low shear viscosity is maintained (see Fig. 5.17a);
  - degradation at low pH is minimised during heating;
  - synergy with galactomannans is maximised (see Fig. 5.8).
- a conformational transition during heat treatment:
  - low shear viscosity is reduced (see Fig. 5.17b);
  - degredation at low pH is a greater risk during heating;
  - synergy with galactomannans is reduced (see Fig. 5.8).

To maximise the stability of the xanthan gum and minimise any effects of thermal treatment on its rheology, it is recommended that any salts present in the formulation are added to the xanthan gum solution prior to the thermal treatment. As discussed earlier, the conformational transition of xanthan gum is dependent upon the concentration of salts, so whether or not the xanthan solution will pass through the conformational transition will be dependent on the ionic strength of the system and the temperature of the treatment. Fig. 5.6 can be used as a guide. It is to be noted that in the vast majority of applications, there are sufficient salts present, in the form of sodium, potassium and/or calcium, to raise the transition temperature of the xanthan gum above that of the typical processing temperatures. This means that the xanthan gum solution viscosity is very stable during heat treatments and can provide suspension at high temperatures.

5.5.2 Homogenisation

Xanthan gum solutions are very stable during high shear mixing. Xanthan gum solution viscosity is unchanged after homogenisation in equipments such as colloid mills.

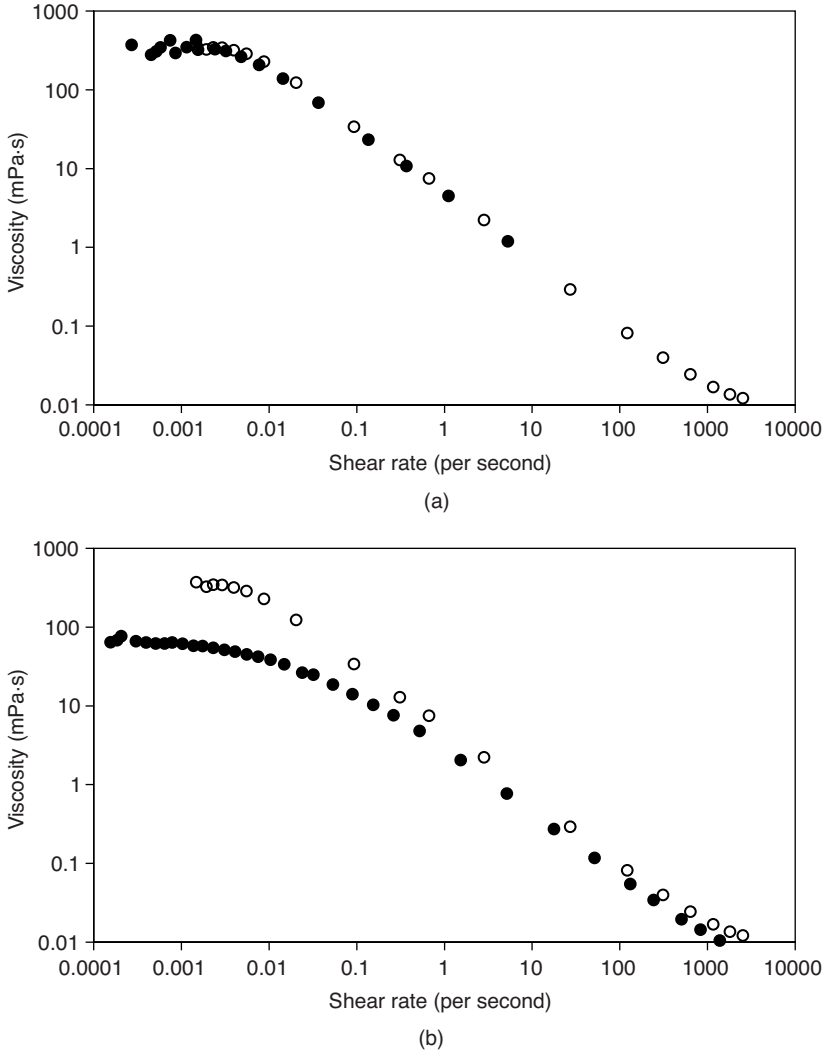

Fig. 5.17 (a) The flow curve of 0.5% xanthan solution in 1% NaCl measured at 20°C before (○) and after (●) heating to 85°C. (b) The flow curve of 0.5% xanthan solution in 0.1% NaCl measured at 20°C before (○) and after (●) heating to 85°C.

5.5.3 Freezing

Xanthan gum has no effect on the freezing point of a given system, but is able to help stabilise the systems to freeze/thaw cycles because its solutions are stable to freezing and thawing. It also helps to limit the growth of ice crystals, which are one of the principal causes for the loss of quality in frozen foods. Addition of xanthan can also minimise syneresis when products are thawed by increasing the viscosity of the liquid phase.

5.6 FOOD STRUCTURES

5.6.1 Emulsions

One of the main food applications of xanthan gum is in salad dressings. These are oil in water emulsions that vary considerably in their composition and texture. Oil content may vary from 75 to 84% in mayonnaise, 35 to 50% in spoonable dressings and 30 to 40% in pourable dressings. Low fat dressings and vinaigrettes may contain between 0 and 3%. A large part of the texture in these products is brought by the emulsion itself. Table 5.3 summarises the factors that influence the rheology of dessings. A more detailed discussion of the rheology of emulsions can be found in Chapter 3.

It is often argued that the xanthan stabilises the emulsions due to the yield stress imparted to the product by the xanthan gum. This has been shown to be incorrect as xanthan solutions, at concentrations used in dressings, do not exhibit a yield stress (Parker *et al.*, 1995). The flow curves of xanthan gum solutions in Figs. 5.1 and 5.17a and b all tend towards a lower Newtonian plateau at low shear rates. The presence of a yield stress would be indicated by a tendency of viscosity to infinity at low shear rates. It is believed that the yield stress is developed with the help of the xanthan gum through flocculation of the oil droplets. This, together with the thickening effect on the aqueous phase, stabilises the system in terms of creaming and coalescence over the shelf life of the product. The flow curve of a typical 30% oil dressing formulated with 0.3% xanthan (see Table 5.4) compared with that of 0.3% xanthan solution in 1% NaCl shows that the dressing has a much higher

Table 5.3 A summary of the factors that influence the rheology of dessings

Factor	Action	Influence on the rheology of the dressing
Oil content	Influence on the phase volume	Viscosity increases with the phase volume fraction of the dispersed phase
Oil droplet size	Contribution to interfacial rheology	Viscosity increases with decreasing droplet size
	Increased flocculation/aggregation in finer emulsions	
Xanthan gum	Increases viscosity of aqueous phase	Imparts non-Newtonian rheology to emulsion
	Induces flocculation/aggregation	Increases viscosity/structure, creates yield stress
	Stabilises against coalescence and creaming	

Table 5.4 Formulation for a 30% oil dressing

Ingredient	**(%)**
Water	59.10
Oil	30.00
Salt	1.50
Sugar	2.00
Starch	1.00
Xanthan gum	0.30
Egg yolk	4.00
Vinegar 12%	2.00
Potassium sorbate	0.10
Antimicrobials	0.02
Total	*100.00*

viscosity than that of the xanthan solution but a very similar profile (see Fig. 5.18).

5.6.2 Gels

Addition of xanthan gum to gels made with other hydrocolloids such as carrageenan or gellan gum tends to reduce the break strength, but does not affect the brittleness. This can in some cases improve the mouthfeel by imparting a smoother texture to the gel. The xanthan gum can also help to reduce syneresis. For these reasons, xanthan is widely used in water jellies and dairy desserts.

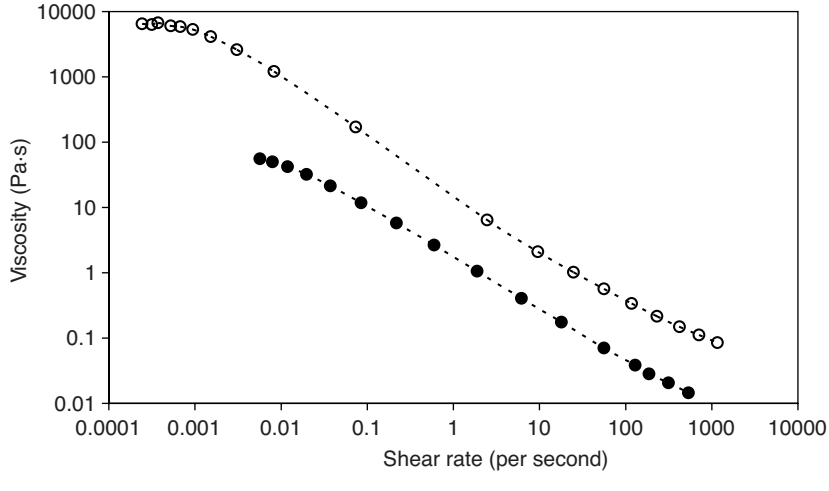

Fig. 5.18 Flow curve of a 30% oil dressing formulated with 0.3% xanthan (○) compared to a 0.3% xanthan gum solution in 1% NaCl (●).

5.7 APPLICATIONS

A particularly interesting application for xanthan gum, which takes advantage of many of the properties described here, is its use in the management of the rheology of liquids for patients suffering from swallowing disorders known generally as dysphagia (Sworn *et al.*, 2008). Swallowing is a very complex neuromuscular process, and there are many disorders that can cause dysphagia. These include neurological disorders, stroke, traumatic brain injury, Huntingdon's disease, multiple sclerosis, Parkinson's disease and cerebral palsy. Approximately 10 million Americans are evaluated with swallowing difficulties every year and figures suggest that ~14% of those aged over 60 are affected by dyspahgia. Dysphagia is not directly associated with aging but is a symptom of the degenerative diseases common in old age. Apart from the obvious problems of potential dehydration and malnutrition due to reduced food and fluid intake, other problems such as aspiration can occur. Aspiration, which is the entry of food or fluids into the airway, can lead to complications with the respiratory system, such as chronic obstructive pulmonary disease or aspiration pneumonia.

The rheological properties of the bolus significantly influence the swallowing process, and the use of hydrocolloids to control the rheology can greatly help in the management of the condition. Hydrocolloid thickeners are ideal for controlling the consistency of liquids and foods and are an obvious choice for use in the management of dysphagia. To be an effective thickener for this application, the following properties are important:

- Easy dispersion at low mixing speeds.
- Fast hydration (cold and hot).
- Stable viscosity as a function of:
  - time;
  - temperature.

In addition to this, the thickener must perform in a variety of media such as water, fruit juice, milk, tea and coffee.

The most widely used thickeners are modified starch (E1442), xanthan and guar gum. Although all three are very effective thickeners, they have very different rheological profiles. Products for this application are often described in terms of consistency and some standards have been proposed by the National Dysphagia Diet project based on viscosity at 50 per second. These are thin (1–50 mPa · s), nectar-like (51–350 mPa · s), honey-like (351–1750 mPa · s) and spoon-thick (>1750 mPa · s). Using these criteria, the xanthan-based products are able to cover the

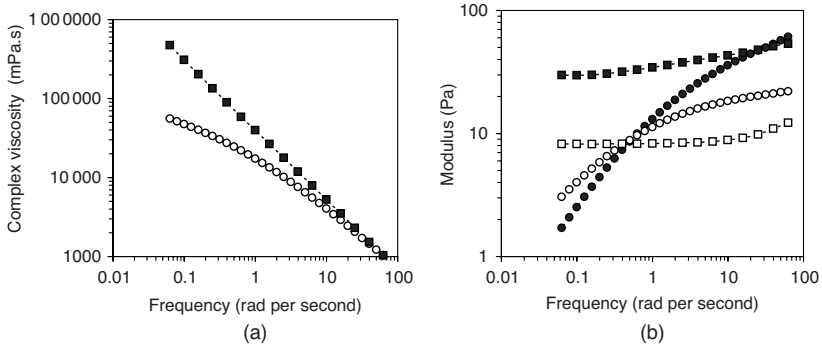

Fig. 5.19 (a) Complex viscosity as a function of frequency for 1.2% xanthan (■) and 2% modified starch (○) in tap water. (b) Mechanical spectrum of 1.2% xanthan (■ G', □ G'') and 2% modified starch (● G', ○ G'') in tap water.

nectar-like and honey-like consistencies, but because of the highly pseudoplastic nature of the viscosity, very high concentrations are needed to reach the spoon-thick consistency. The starch products must be used at higher concentration than the xanthan and, based on this measurement criterion, are more able to create the spoon-thick consistency.

The consistency categories are based on a single point viscosity measurement and do not reflect the overall texture of the products. The viscoelastic properties of xanthan and modified starch at concentrations that give approximately equivalent viscosity at a shear rate of 50 per second are shown in Fig. 5.19a and b. The dynamic viscosity of the products is very similar at 50 rad per second, but the xanthan has a constant slope approaching −1, which is typical of a gel, whereas the starch tends towards a Newtonian plateau at low frequencies, which is more typical of an entanglement network. Similarly for the moduli, the xanthan response is typical of a weak gel with the elastic modulus (G') dominating across the measured frequency range and both moduli showing very limited frequency dependence. The starch has a profile typical of an entanglement network: both moduli show frequency dependence with the viscous modulus (G'') dominating at lower frequencies and the elastic modulus (G') dominating at higher frequencies. The ideal rheology for swallowing has yet to be established, but perhaps the most important factor in the choice of the thickener will be the palatability of the product, after all, if the product is not acceptable from a sensory standpoint, then patients will not eat the products.

Recent work on the miscibility of solutions thickened with different hydrocolloids has revealed some interesting differences that could be of relevance to this application. It has been shown that solutions prepared with particulate thickeners such as starch mix more easily with water than do those thickened by polymer solutions such as guar gum and

xanthan gum (Mitchell *et al.*, 2008). The implications of this and food perception are discussed in chapter 8, but in this application, the effects on viscosity are of interest. In the case of starch, easy mixing with the saliva could lead to dilution and loss of viscosity in the mouth prior to swallowing, whereas with xanthan, the poorer mixing may mean that the gel-like rheology would be more likely to remain intact during swallowing. This could potentially offer better protection against aspiration. Starch systems are also susceptible to amylase degradation upon contact with saliva. This can result in a loss of viscosity and a risk to the patient. Amylase-resistant systems have been developed by adding gums such as xanthan to the starch, and it has been demonstrated that this reduces viscosity loss (Sliwinski *et al.*, 2009). Although the mechanism is not clear, it is likely that the reduction in the miscibility due to the gums offers some protection to the starch from the amylase attack by limiting the contact time before swallowing.

5.8 FUTURE TRENDS

The differentiation of commercial xanthan grades has been based primarily on their physical characteristics such as solution clarity, dispersion and hydration. Differentiation in dispersion and hydration has been achieved through control of the particle size distribution of the powder by milling, sieving or agglomeration. As discussed previously, the functionalities of xanthan gum that set it apart from other hydrocolloid thickeners are its unique rheology and its ability to interact synergistically with galactomannans. Effective suspension and stabilisation of many food products requires a high viscosity at low shear rates, and this can vary according to the type of thickener used (see Fig. 5.1) and can also vary from batch to batch and supplier to supplier for the different thickeners. Xanthan gum is well known as the most effective thickener for creating, at low concentrations, high viscosity at low shear rates, and this is recognised as being critical for the functionality of xanthan gum in many applications. Xanthan gum has for many years been sold on a viscosity value specified at high concentrations (1% gum in 1% KCl) and high shear rates (Brookfield viscometer, spindle 3 at 60 rpm) as described in the Food Chemical Codex (FCC). According to the FCC, this value must be a minimum of 600 mPa · s, and virtually all xanthan sold for food applications today are specified between 1200 and 1800 mPa · s using this test method.

It can be shown that, for typical in-use concentrations of xanthan gum, there is no correlation between their FCC viscosity value and their viscosity at low shear rates (see Fig. 5.20). The lack of correlation means the FCC viscosity offers no guideline to the end user in terms of

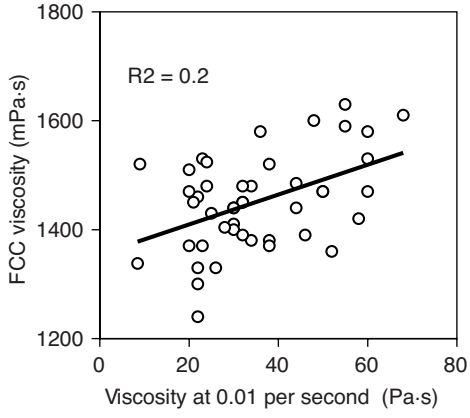

Fig. 5.20 Correlation between Xanthan FCC viscosity (1% gum in 1% KCl) and low shear viscosity of 0.3% xanthan gum in 1% NaCl.

performance in the application and no opportunity for the manufacturers to differentiate on one of the main functional properties of xanthan gum.

Recently, a new approach to the specification of xanthan gum has been taken by Danisco with the introduction of a xanthan gum range with application-related specifications linked to key functionalities such as low shear viscosity and synergistic interaction with galactomannans. This approach provides for the first time a range differentiated on these properties (see Fig. 5.21a and b) and specifications that provide the end user with a guarantee of consistent performance. In addition, focus on

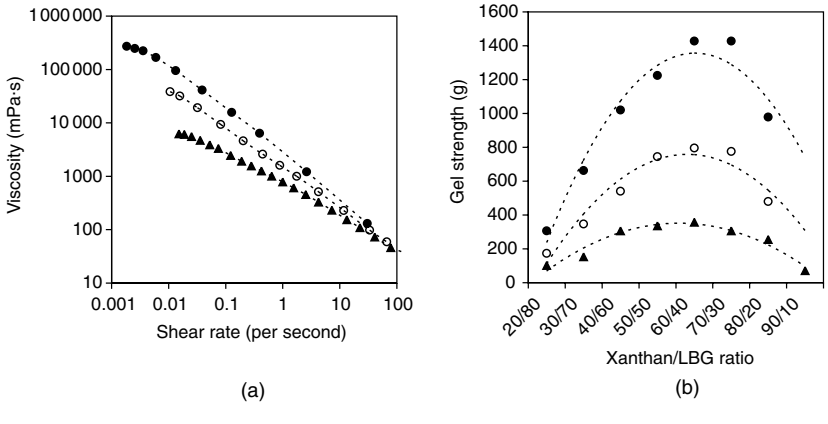

Fig. 5.21 (a) Differentiation of xanthan gum based on the rheological profile at 0.3% gum in 1% NaCl. GRINDSTED® Xanthan SAV-SH (●), GRINDSTED® Xanthan 80 (○) and GRINDSTED® Xanthan SAV-SH SOFT (▲). (b) Differentiation of xanthan gum based on the synergistic interaction with lbg at 1% 60:40 xanthan:LBG in 1% NaCl. GRINDSTED® Xanthan SAV-SH (●), GRINDSTED® Xanthan 80 (○) and GRINDSTED® Xanthan SAV-SH SOFT (▲).

the functionality has enabled the development of higher performance products which offer the possibility of optimising dosage.

ACKNOWLEDGEMENTS

The author would like to acknowledge the technical assistance of E Kerdavid and J Fayos in the production of the rheological data.

REFERENCES

Agoub, A.A., Smith, A.M., Giannouli, P., Richardson, R.K. and Morris, E.R. (2007) "Melt-in –the-mouth" gels from mixtures of xanthan and konjac glucomannan under acidic conditions: a rheological and calorimetric study of the mechanism of synergistic gelation. *Carbohydrate Polymers* **69**, 713–724.

Arocus, A., Sanz, T. and Fiszman, S.M. (2009) Improving effect of xanthan and locust bean gums on the freeze-thaw stability of white sauces made with different native starches. *Food Hydrocolloids* **23**, 2478–2484.

Bradshaw, I.J. Nisbet, B.A., Kerr, M.H. and Sutherland, I.W. (1983) Modified xanthan – its preparation and viscosity. *Carbohydrate Polymers* **3**, 23–38.

Cairns, P., Miles, M.J. and Morris, V.J. (1986) Intermolecular binding of xanthan gum and carob gum. *Nature* **322**, 89–90.

Cairns, P., Miles, M.J., Morris, V.J. and Brownsey, G.J. (1987) X-Ray fibre-diffraction studies of synergistic binary polysaccharide gels. *Carbohydrate Research* **160**, 411–423.

Cheetham, N.W.H. and Norma, N.M.N. (1989) The effect of pyruvate on viscosity properties of xanthan. *Carbohydrate Polymers* **10**, 55–60.

Christensen, B.E., Smidsrod, O. and Stoke, O. (1993) Xanthans with partially hydrolysed side chains: conformation and transitions. In: Yalpini, M., editor. *Carbohydrates and Carbohydrate Polymers. Analysis, Biotechnology, Modification, Antiviral, Biomedical and Other Applications*. Shrewsbury: ATL Press, pp. 166–173.

Cronin, E.E., Giannouli, P., McCleary, B.V., Brooks, M. and Morris, E.R. (2002) Formation of strong gels by enzymic debranching of guar gum in the presence of ordered xanthan. In: Williams, P.A. and Phillips, G.O., editors. *Gums and Stabilisers for the Food Industry 11*. Cambridge: RSC, pp. 289–296.

Dalbe, B. (1992) Interactions between xanthan and konjac mannan. In: Phillips, G.O., Williams, P.A. and Wedlock, D.J., editors. *Gums and Stabilisers for the Food Industry 6*. Oxford University Press, Oxford, pp. 201–208.

Fitzsimons, S.M., Tobin, J.T. and Morris, E.R. (2008) Synergistic binding of konjac glucomannan to xanthan on mixing at room temperature. *Food Hydrocolloids* **22**, 36–46.

Flores Candia, J.-L. and Deckwer, W.-H. (1999) Effect of the nitrogen source on pyruvate content and rheological properties of xanthan. *Biotechnology Progress* **15**, 446–452.

Hassler, R.A. and Doherty, D.H. (1990) Genetic engineering of polysaccharide structure: Production of variants of xanthan gum in *Xanthomonas campestris*. *Biotechnology Progress* **6**, 182–187.

Hemar, Y., Tamehana, M., Munro, P.A. and Singh, H. (2001) Viscosity, microstructure and phase behaviour of aqueous mixtures of commercial milk protein products and xanthan gum. *Food Hydrocolloids* **15**, 565–574.

Holzwarth, G. and Prestridge, E.B. (1977) Multistranded helix in xanthan polysaccharide. *Science* **197**, 757–759.

Jansson, P.E., Kenne, L. and Lindberg, B. (1975) Structure of the exocellular polysaccharide from *Xanthomonas campestris*. *Carbohydrate Research* **45**, 275–282.

Jeanes, A., Pittsley, J.E. and Senti, F.R. (1961) Polysaccharide B-1459: a new hydrocolloid polyelectrolyte produced from glucose from bacterial fermentation. *Journal of Applied Polymer Science* **5**, 519–526.

Kovacs, P. (1973) Useful incompatibility of xanthan gum with galactomannans. *Food Technology* **27**(3), 26–30.

Lopes, L., Andrade, C.T., Milas, M. and Rinaudo, M. (1992) Role of conformation and acetylation of xanthan on xanthan – guar interaction. *Carbohydrate Polymers* **17**, 121–126.

Melton, L.D., Mindt, L., Rees, D.A. and Sanderson G.R. (1976) Covalent structure of the polysaccharide from *Xanthomonas campestris*: evidence from partial hydrolysis studies. *Carbohydrate Research* **46**, 245–257.

Milas, M., Reed, W.F. and Printz, S. (1996) Conformations and flexibility of native and renatured xanthan in aqueous solutions. *International Journal of Biological Macromolecules* **18**, 211–221.

Milas, M. and Rinaudo, M. (1984) On the existence of two different secondary structures for the xanthan in aqueous solutions. *Polymer Bulletin* **12**, 507–514.

Milas, M. and Rinaudo, M. (1986) Properties of xanthan gum in aqueous solutions: role of the conformational transition. *Carbohydrate Research* **158**, 191–204.

Mitchell, J.R., Ferry, A.L., Desse, M., Hill, S.E., Hort, J., Marciani, L. and Wolf, B. (2008) Mixing hydrocolloids and water: polymers versus particulates. In: Williams, P.A. and Phillips, G.O., editors. *Gums and Stabilisers for the Food Industry 14*. Cambridge: RSC, pp. 29–39.

Moorhouse, R., Walkinshaw, M.D. and Arnott, S. (1977) Xanthan gum-molecular conformation and interactions. In: Sandford, P.A. and Laskin, A., editors. *Extracellular Microbial Polysaccharides, ACS Symposium Series no. 45*. American Chemical Society, Washington, DC, pp. 90–102.

Morris, E.R. (1990) Mixed polymer gels. In: Harris, P., editor. *Food Gels*. London, UK: Elsevier, pp. 291–359.

Morris, E.R. and Foster, T.J. (1994) Role of conformation in the synergistic interactions of xanthan. *Carbohydrate Polymers* **23**, 133–135.

Morris E.R., Rees D.A., Young G., Walkinshaw, M.M. and Darke A. (1977) Order-disorder transition for a bacterial polysaccharide in solution. A role for polysaccharide conformation in recognition between *Xanthomonas* pathogen and its plant host. *Jouranl of Molecular Biology* **110**, 1–16.

Morrison, N.A., Clark, R., Talashek, T. and Yuan, C.R. (2004) New forms of xanthan gum with enhanced properties. In: Williams, P.A. and Phillips, G.O., editors. *Gums and Stabilisers for the Food Industry 12*. Cambridge: RSC, pp. 124–130.

Parker, A., Gunning P.A., Ng, K. and Robins, M.M. (1995) How does xanthan stabilise salad dressing? *Food Hydrocolloids* **9**, 333–342.

Pettitt, D.J. (1982) Xanthan gum. In: Glicksman, M., editor. *Food Hydrocolloids*, Volume **I**. Boca Raton, Florida: CRC Press, pp. 127–149.

Pettitt, D.J. (1979) Xanthan gum. In: Blanshard, J.M.V. and Mitchell, J.R., editors. *Polysaccharides in Foods*. London: Butterworth & Co Ltd., pp. 51–72.

Rinaudo, M. and Moroni, A. (2009) Rheological behaviour of binary and ternary mixtures of polysaccharides in aqueous medium. *Food Hydrocolloids* **23**, 1720–1728.

Sandford, P.A., Pittsley, J.E., Knutson, C.A., Watson, P.R., Cadmus, M.C. and Jeanes, A. (1977) Variation in *Xanthomonas campestris* NRRL B-1459: Characterisation of xanthan products of differing pyruvic acid contents. In: Sandford, P.A. and Laskin, A., editors. *Extracellular Microbial Polysaccharides*. Washington: ACS, pp. 192–210.

Schorsch, C., Garnier, C. and Doublier, J.-L. (1997) Viscoelastic properties of xanthan/galactomannans mixtures: comparison of guar gum with locust bean gum. *Carbohydrate Polymers* **34**, 165–175.

Shatwell, K.P., Sutherland, I.W. and Ross-Murphy, S.B. (1990) Influence of acetyl and pyruvate substituents on the solution properties of xanthan polysaccharide. *International Journal of Biological Macromolecules* **12**, 71–78.

Shatwell, K.P., Sutherland, I.W., Ross-Murphy, S.B. and Dea, I.C.M. (1991a) Influence of the acetyl substituent on the interaction of xanthan with plant polysaccharides – I. Xanthan – locust bean gum systems. *Carbohydrate Polymers* **14**, 29–51.

Shatwell, K.P., Sutherland, I.W., Ross-Murphy, S.B. and Dea, I.C.M. (1991b) Influence of the acetyl substituent on the interaction of xanthan with plant polysaccharides – III. Xanthan – konjac mannan systems. *Carbohydrate Polymers* **14**, 131–147.

Simsek, S. (2009) Application of xanthan gum for reducing syruping in refrigerated doughs. *Food Hydrocolloids* **23**, 2354–2358.

Sliwinski, E.L., La Faille, S. and Oudhuis, L.A.C.M. (2009) Effect of human siliva on the consistency of thickened foods for patients with dysphagia. *Clinical Nutrition Supplements* **4**, 135.

Smith, I.H., Symes, K.C., Lawson, C.J. and Morris E.R. (1981) Influence of the pyruvate content of xanthan on macromolecular association in solution. *International Journal of Biological Macromolecules* **3**, 129–134.

Sworn, G. (2000) Xanthan gum. In: Phillips, G.O. and Williams, P.A., editors. *Handbook of Hydrocolloids*. Cambridge: Woodhead Publishing Ltd., pp. 103–116.

Sworn, G. (2009) Xanthan gum. In: Imeson, A., editor. *Food Stabilisers, Thickeners and Gelling Agents*. Oxford: Blackwell Publishing Ltd., pp. 325–342.

Sworn, G. and Kerdavid E. (2009) Influence of preparation method on the quality of xanthan-locust bean gum mixed gels. In: Williams, P.A. and Phillips, G.O., editors. *Gums and Stabilisers for the Food Industry 15*. Cambridge: RSC, pp. 247–253.

Sworn, G., Kerdavid, E., Chevallereau, P. and Fayos, J. (2009) High synergy xanthan gum. European patent application N° EP 09157217.2.

Sworn, G., Kerdavid, E. and Fayos, J. (2008) The role of hydrocolloids in the management of dysphagia. In: Williams, P.A. and Phillips, G.O., editors. *Gums and Stabilisers for the Food Industry 14*. Cambridge: RSC, pp. 392–401.

Urlacher, B. and Noble, O. (1999) Xanthan gum. In: Imeson, A., editor. *Thickening and Gelling Agents for Food*, 2nd Edition. Maryland: Aspen Publishers Inc., pp. 284–311.

Wang, F., Wang, Y.-J. and Sun, Z. (2002) Conformational role of xanthan in its interaction with locust bean gum. *Journal of Food Science* **67**, 2609–2614.

6 Alginates in Foods

Alan M. Smith and Taghi Miri

Alginate has been widely investigated since it was first isolated and described in 1881 by Stanford (E.C.C Stanford, 1881) and has since become a vastly utilised polymer with a variety of applications. Alginate is exploited not only in the food industry, but also in the paper and textile industries, and for pharmaceutical and, more recently, biomedical applications. The versatility of alginate has led to it being a fairly well-understood material and has been subject to a great number of systematic rheological investigations, information from which has been subsequently utilised in food applications. More recently, their 'high value' pharmaceutical and biomedical applications have driven the development and understanding of alginate further. This chapter intends to provide a brief overview of the chemical properties of alginates and to review the influence of molecular structure on the physical, functional and, more specifically, rheological properties which are exploited in food systems. Specific applications in foods are also covered, which highlight the multi-functional nature of alginate and its future potential.

6.1 ALGINATE SOURCE AND MOLECULAR STRUCTURE

Alginate is the major structural component of brown seaweed (Phaeophyceae), providing both mechanical strength and plasticity to seaweed that is analogous to pectins in plants. There are different species of brown seaweed that contain alginates; however, the species that are most commercially exploited for alginate production are *Laminaria hyperborea, Macrocystis pyrifera, Saccharina japonica* and *Ascophyllum nodosum* (Gomeza *et al.*, 2009), with an estimated annual industrial production of 30,000 metric tonnes (Draget *et al.*, 2006b). Alginate composition and hence physical properties vary depending on the area of the plant the alginate is extracted from (Jothisaraswathi *et al.*, 2006). This can also vary

Practical Food Rheology: An Interpretive Approach
Edited by Ian T. Norton, Fotios Spyropoulos and Philip Cox
 ISBN: 978-1-405-19978-0

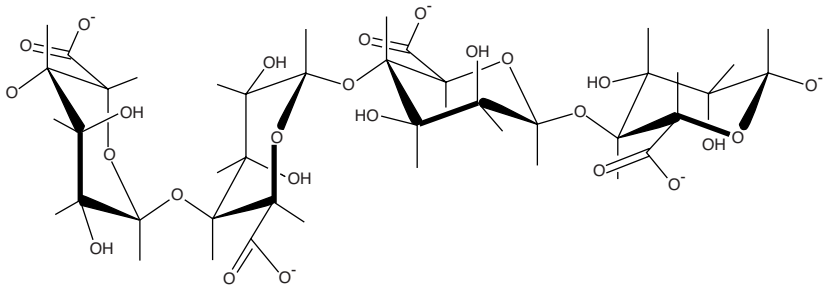

Fig. 6.1 Molecular structure of alginate.

with respect to different growth conditions and seasons (Andresen *et al.*, 1977; Indergaard and SkjakBraek, 1987). Several publications have described the process of alginate extraction in detail (Nussinovitch, 1997; Owusu-Apenten, 2005). As a basic guide, however, extraction of alginate from seaweed can be achieved using the following procedure: Seaweed is milled (either wet or dry) and washed with acid before extraction with hot alkali. The alginate is then filtered, precipitated with calcium and acidified to produce alginic acid. The insoluble alginic acid can afterwards be treated with metallic carbonate, hydroxide or oxide to produce the desired salt form of alginate.

In addition to seaweed, it should also be mentioned that bacterial exopolysaccharides similar to alginate can be produced by fermentation of several species of bacteria, which include *Azobacter vinelandii* (Gorin and Spencer, 1966) and *Pseudomonas aeruginosa* (Carlson and Matthews, 1966; Linker and Jones, 1964). Indeed, these species have helped scientists elucidate the mechanisms of alginate biosynthesis.

On a molecular level, alginate is described as a linear polysaccharide consisting of two uronic acid residues 1,4-linked β-D-mannuronic (M) acid and 1,4-linked α-L-guluronic acid (G), which occur along the polymer chain as blocks of mannuronate, blocks of guluronate and heteropolymeric blocks of both monomers (Fig. 6.1).

During the biosynthesis of alginate, polymer chains consisting solely of mannuronate are initially produced, some of which are then converted to α-L-guluronate by enzymatic epimerisation at C(5). With regard to molecular conformation, this epimerisation results in converting the inter-residue linkages from 1,4 equatorial to 1,4 axial, having the effect of altering the geometry throughout the polymer chain. Polymannuronate blocks have what is described as flat, extended ribbon geometry due to the 1,4 equatorial bond, with polyguluronate blocks having 'buckled ribbon' geometry due to the 1,4 axial configuration

and heteropolymeric regions having an irregular geometry, which cannot pack together uniformly. The overall molecular conformation of the alginate molecule is described as a ridged rod (Tombs and Harding, 1998), with the relative stiffness of the polymer chain reported to increase in the order MG < MM < GG (Smidsrød *et al.*, 1973). This, however, has been challenged recently by Vold and co-workers (Vold *et al.*, 2007), who argued that individual block types in natural and *in vitro* epimerised polymannuronans showed no significant difference in chain stiffness.

Several alginate derivatives have been developed, although only propylene glycol alginate (PGA) is licensed for food use. First prepared by Steiner (Steiner, 1947), it is produced by partial esterification of the carboxyl group on the uronic acid residues in a reaction with propylene oxide (Moe *et al.*, 1995). The main benefit of PGA is witnessed in low pH solutions, where native alginate would precipitate.

6.2 ALGINATE HYDROGELS

The most interesting feature of alginate with regard to academic interest and industrial applications is the formation of ionotropic hydrogels, consequently the process of which is well understood. First described by Grant (Grant *et al.*, 1973), the 'egg box model' is widely accepted as the gelation mechanism of alginate (and pectin), whereby intermolecular junction zones are formed by direct binding of divalent cations to carboxylate groups on the guluronate residues of adjacent polymer chains. This binding has been shown to be highly selective towards differing divalent cations generally in the order $Pb^{2+} > Cu^{2+} > Ba^{2+} > Sr^{2+} > Ca^{2+} > Mn^{2+} > Mg^{2+}$ (Haug and Smidsrod, 1965). The affinity of binding and strength of alginate gels produced are directly related to the polymer composition. Taking this into account, a major consideration prior to using alginate is the sequential structure, in particular, the total content of guluronate residues and the average length of G blocks along the polymer chain (Kohn and Larsen, 1972). This is because alginates rich in G blocks generally produce stronger gels than those rich in M blocks. More recently, it was reported that mixed junctions occurred between G and MG blocks, highlighting the importance of MG repeating units in alginate gelation (Donati *et al.*, 2005).

Generally, calcium ions are the favoured cross-linking species used in alginate gelation due to the acceptability and relative safety in food and pharmaceutical products. The commercial availability of alginates consisting of almost 100% polymannuronate to 70% guluronate can provide physical properties that are flexible and diverse, ideal for applications in the food industry.

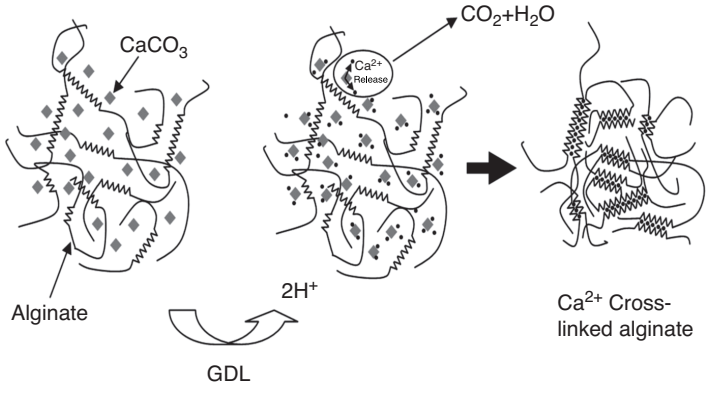

Fig. 6.2 Schematic diagram of internal gelation method.

Calcium can be introduced to the polymer in a variety of ways and forms. Indeed, the method used for introducing the calcium ions can produce different types of gels described as homogeneous and inhomogeneous gels. When calcium chloride is added to a solution of alginate, localised instantaneous gelation or precipitation occurs, which makes it extremely difficult to attain homogeneous gels.

To overcome this problem, an internal gelation mechanism developed by Draget *et al.* (1990) can be used. This method utilises calcium in an insoluble form (such as calcium carbonate) that can be mixed throughout the alginate solution. The calcium carbonate is then dissociated by slowly reducing the pH by the addition of glucono-δ-lactone (GDL), which hydrolyses over a period of 40–60 minutes. This controlled release of the Ca^{2+} is known as internal gelation (Fig. 6.2).

The acidity, gelation time and strength of the resulting gels can be regulated by carefully adjusting the ratio of $CaCO_3$ to GDL. Rheologically, an example of the typical mechanical spectra exhibited by a 2% (w/v) alginate sample prior to and following cross-linking by internal gelation is shown in Fig. 6.3a and b, respectively. These examples show spectra as expected for a typical entangled polymer solution and a cross-linked gel network. Gelation rate and final gel strength, however, are also affected by alginate concentration, molecular weight and MG sequence (Draget *et al.*, 1990). Particle size of the insoluble calcium salt can also be used to control gelation rate without affecting the final gel strength, with smaller particle size favouring a more rapid gelation (Fig. 6.4) (Draget *et al.*, 2000, 2006b).

When calcium is introduced to the alginate in the soluble form (e.g. $CaCl_2$), the gels produced are usually inhomogeneous. The junctions formed when gelling alginate in this manner are more concentrated at the surface of the gel and require diffusion of calcium ions through the gel, resulting in a structure that is stronger at the exterior than at the interior

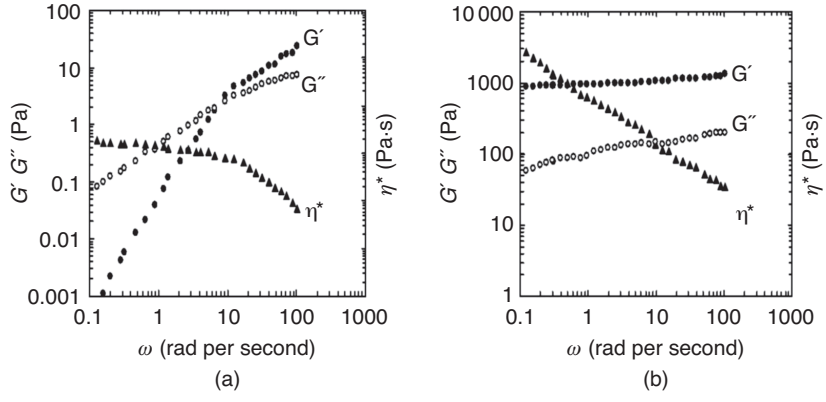

Fig. 6.3 Typical mechanical spectra showing the frequency dependence of the storage modulus (G'), loss modulus (G'') and complex dynamic viscosity η^* for (a) 2% alginate solution and (b) after cross-linking using 22.5/45 mM $CaCO_3$/GDL.

(Fig. 6.5). When cross-linking alginates using this technique, the gelation kinetics are extremely rapid, witnessed by an instantaneous sol–gel transition at the surface of the alginate. This instantaneous gelation has been exploited most notably in the pharmaceutical and biotechnology sectors to encapsulate drug molecules or cells.

As with internal gelation, the physical properties of the gels produced can be manipulated by variations in molecular weight of the alginate, M:G ratio and concentration of the calcium ions. These factors have also been shown to create variations in the extent of inhomogeneity, thus allowing scope for tailored mechanical properties and textures throughout the gels.

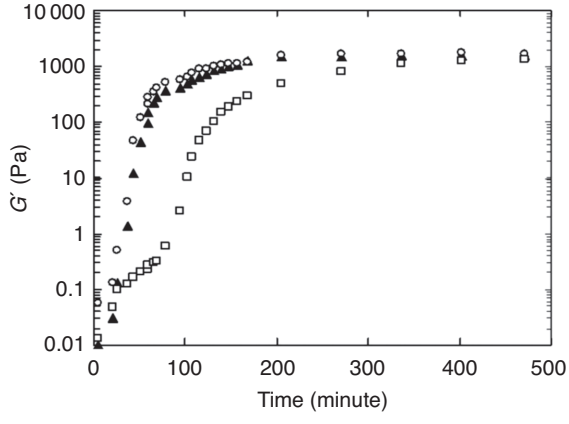

Fig. 6.4 Time dependence of G' highlighting the effect of particle size of $CaCO_3$ on gelation time. Open circles 1.5 μm, filled triangles 4 μm and open squares 20 μm (Data from Draget *et al.*, 2006b)

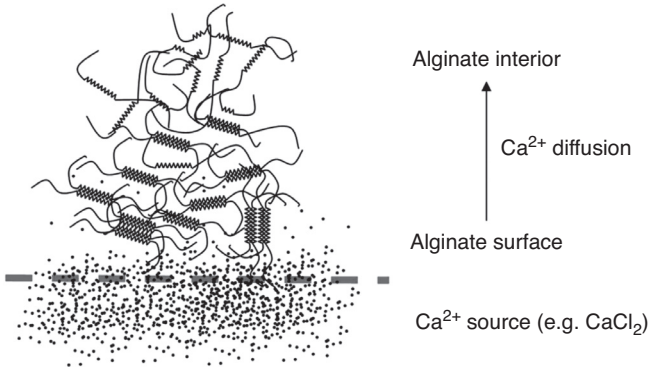

Fig. 6.5 Schematic diagram of external gelation.

The simplest route to immobilisation is to drop an alginate solution containing the encapsulant through a syringe into a bath of calcium chloride, a method first developed by Kierstan and Bucke (1977). A disadvantage of this technique is that bead size is restricted by the aperture of the syringe and the viscosity of the alginate, although this can be overcome by techniques such as applying electrostatic pulses (Hommel *et al.*, 1988), vibrating needles (Hulst *et al.*, 1985), atomisation (Matsumoto *et al.*, 1986) or more recently novel microfluidics (Sugiura *et al.*, 2005). The main drawback, however, is that this technique is not easily scaled up (Poncelet *et al.*, 1992). To achieve a smaller bead size with a more practical scale up procedure, an emulsion templating technique was developed (Wan *et al.*, 1992), whereby a water in oil emulsion is formed using alginate and the encapsulant in the water phase. Once a stable emulsion is formed, $CaCl_2$ can be added, which cross-links the alginate droplets, giving a narrow particle size distribution. The particle size, as with most emulsions, is controlled by the selection of material for the oil phase and shear rate used in forming the emulsion, in addition to the rate of addition of cross-linker.

If a larger bulk gel is required, the alginate solution can be added to a dialysis membrane, which is then submerged into a solution of $CaCl_2$. The gelation time using this method can be several hours. The concentration of the $CaCl_2$ and the time the alginate is exposed regulate the gel strength and homogeneity.

Because of the complex nature of food systems, it is important to understand interactions of alginate gels with other molecules in the system. In particular, phosphates and citrates which are regularly used in food can complex calcium, causing the dissolution of alginate gels. In addition, as alginate is a polyanion, there is potential for electrostatic interactions with other macromolecules, for example proteins (Zhao *et al.*, 2009) or other polysaccharides (Toft *et al.*, 1986) within food,

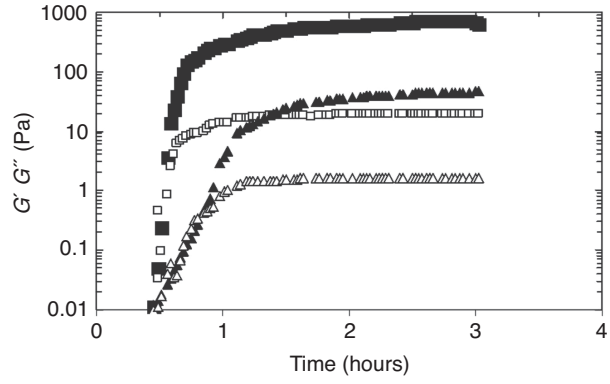

Fig. 6.6 Time dependence of *G′* (filled symbols) and *G″* (open symbols) for the formation of alginic acid gels made from 1% high *G* alginate (Squares) and 1% intermediate *G* alginate (Triangles) of similar molecular weights. (Data from Draget *et al.*, 2003).

which may cause instability in the system or, conversely, have a favourable interaction. With respect to processing, alginate is an attractive gelling agent to use. The gel-forming mechanism is generally considered as independent of temperature, which is unlike most other polysaccharides, and once formed, the gels cannot be melted by heating. The gelation temperature, however, and indeed the pH and ionic strength used during gelation do affect the mechanical properties.

6.3 ALGINIC ACID

Alginic acid is the water-insoluble protonated form of alginate (Draget *et al.*, 1994). The pKa of guluronic acid and mannuronic acid in 0.1 M NaCl are known to be 3.65 and 3.38, respectively (Haug, 1961). A sudden decrease in pH of an alginate solution to below the pKa of the monomers causes the precipitation of alginic acid (Haug and Larsen, 1963). It is also well known that if the reduction in pH is performed in a controlled manner, it is possible to form alginic acid gels (Draget *et al.*, 1994, 1996, 2003). An excellent example of a product that utilises these properties is the anti-heartburn medication Gaviscon®. This orally administered liquid contains sodium alginate as the active ingredient. When the medicine reaches the stomach, the acidic gastric fluid causes the alginate solution to form an alginic acid gel raft on the surface, subsequently preventing gastric reflux. This *in situ* gelation has also been explored in food systems as an appetite suppressor, which will be discussed later in this chapter.

The rheological properties of alginic acid, similar to alginate salts, vary with molecular weight and G:M ratio. This is illustrated in Fig. 6.6,

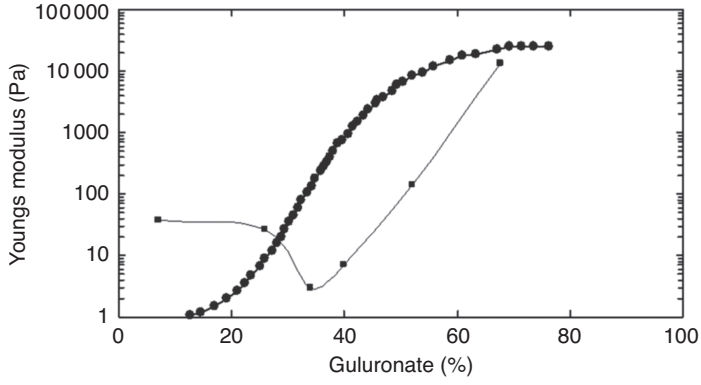

Fig. 6.7 Effect of guluronic acid content on the Young's Modulus of alginic acid gels at apparent equilibrium (squares) in comparison to predicted results for ionically cross-linked alginate gels (circles). (Adapted from Draget *et al.*, 2006b).

where measurements of dynamic moduli show acid gels prepared from a high G alginate have values that are about 2 orders of magnitude greater than those of intermediate G alginate (Draget *et al*., 2003). Acid gels, however, do show some variations from ionic alginate gels in the nature of gel network formation and subsequently in rheology. These differences are summarised in detail by Draget *et al*. (2006a), where it is explained that M blocks provide stable intermolecular bonds which are not apparent in ionically cross-linked alginate (Fig. 6.7). Furthermore, alginic acid gels seem to be of an equilibrium nature, and the largest junction zones are of higher multiplicity than the largest junction zones in the ionically cross-linked gels (Draget *et al.*, 2006a).

6.4 ALGINATE SOLUTIONS

Generally, solutions of alginate tend to be highly viscous. Concentrated, entangled solutions of alginate, however, exhibit shear-thinning behaviour. This effect is shown by Rezende *et al.* (2009), where apparent viscosity is reduced in various alginate concentrations on increasing rate of deformation. Like most polysaccharides, the viscosity of concentrated alginate solutions is highly dependent upon the molecular weight, with viscosity increasing with increased molecular weight. In alginates, other factors such as G:M ratio, pH, ionic strength and, in particular, presence of divalent cations can all cause variations in viscosity (Onsøyen, 2001). Solutions of alginate also obey the cox-merz rule, where steady-state viscosity as a function of shear rate is highly comparable to the complex viscosity as a function of frequency. Therefore, when measuring rheological properties by oscillatory deformation,

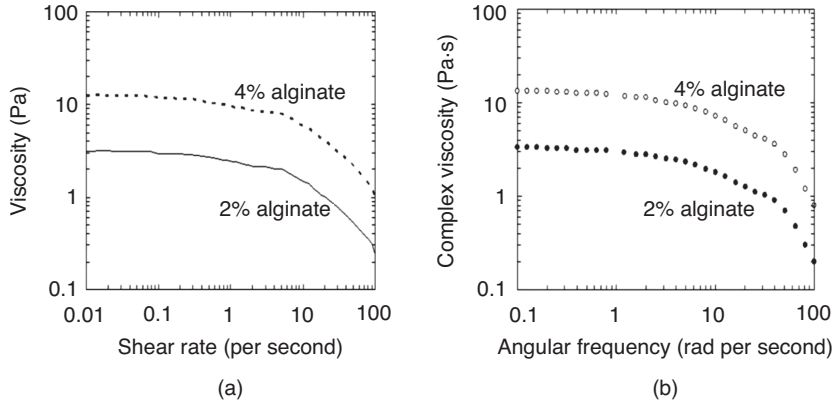

Fig. 6.8 Shear-thinning behaviour of alginate, highlighting Cox-Merz superimposition of steady-state viscosity and complex viscosity in 2 and 4% alginate solutions using (a) rotational measurements and (b) dynamic oscillatory measurements.

complex dynamic viscosity can be considered analogous to steady-state viscosity. This is highlighted by comparing Fig. 6.8a with b.

6.5 ENZYMATICALLY TAILORED ALGINATE

In order to fully exploit the potential of alginates, several research groups have managed to engineer specific MG sequences and subsequently tailor physical properties. As mentioned above, alginate is biosynthesised initially as poly-β-D-mannuronate, from which some of the residues are converted to α-L-guluronate by enzymatic epimerisation at C(5) by mannuronan C(5) epimerases, producing polymers with various sequences. Recent genome elucidation of the alginate-producing bacterium *Azobacter vinelandii* has shown that the bacteria produce seven different mannuronan epimerases to facilitate alginate biosynthesis. These enzymes have subsequently been produced in *E. coli* using recombinant enzyme technology and are termed AlgE1-AlgE7. Although these enzymes perform the same function (i.e. C(5) epimerisation of mannuronan), their collective action can produce alginates with vastly different sequences. For example, both AlgE1 and AlgE6 produce polyguluronate blocks. However, AlgE1 initially forms only long homopolymeric G-blocks >50 residues, while AlgE6 gives shorter blocks with a broader block size distribution (Holtan *et al.*, 2006). Alg4, on the other hand, converts mannuronate to guluronate in an alternating manner (Hartmann *et al.*, 2006).

In a recent study by Hartmann (Hartmann *et al.*, 2006), alginate samples from different sources were modified using recombinant AlgE4,

which converted the M blocks into MGM blocks with no effect on G blocks. The solubility and gelling kinetics at low pH were then analysed in the epimerised polymers produced. It was found that the gelling of the MG-rich alginate with acid is kinetically slower compared with native alginates. This is thought to occur due to the alternating axial–equatorial/equatorial–axial glycosidic linkages, which generates a delay in the sol/gel transition compared to the di-equatorial (poly-M) and di-axial (poly-G) sequences (Draget *et al.*, 2006a). These findings highlight the potential of using epimerases to regulate alginate gelling kinetics by simply controlling the fraction of MG sequences in the polymer chain. The ability to produce tailor-made alginate provides a platform for the development of intelligently designed high-value applications of alginate in food, pharma and biotechnology sectors.

The remainder of this chapter will focus on summarising the various applications of alginates in food systems and how the structural aspects discussed above are used to develop and produce improved products.

6.6 ALGINATES AS FOOD ADDITIVE

Alginates are safe and approved as food additives by the European Community and by the U.S. Food and Drug Administration and listed in the United Nations (FAO/WHO) Codex Alimentarius (Draget *et al.*, 2006b). As a food additive, alginates are commonly referred to within the European Union by the following E numbers (Brownlee *et al.*, 2009):

- *E400:* alginic acid;
- *E401–E404:* sodium, potassium, ammonium and calcium salts, respectively;
- *E405:* esters of alginic acids, PGAs.

Alginates are routinely used in foods to improve, change, and stabilise texture by exploiting properties such as gelation, viscosity enhancement and stabilisation of aqueous mixtures, dispersions and emulsions (Draget, 2000, 2006b). Some of these enhancements originate from the native physical properties of alginates themselves, as summarised above, but some of these properties result from interactions with other components of the food product, for example, proteins, fat, or fibre. In addition to these routine applications, alginates have more recently been utilised as encapsulating vehicles for controlled release, edible films and as a functional food ingredient. Key functions of alginate in various foods are listed in Table 6.1.

Table 6.1 Key functions of alginate in food products (Walter, 1998; Draget *et al.*, 2006b)

Product	Thickening agent	Stabiliser	Gelling agent
Ketchup	*		
Mayonnaise	*		
Margarine	*		
Milkshakes	*		
Fruit juices	*		
Liquors	*		
Ready-made soups	*		
Ice cream	*	*	
Sauces	*	*	
Dressings	*	*	
Frozen foods		*	
Syrups		*	
Dry mixed		*	
Pastry fillings		*	
Bakery icings		*	
Salad dressings		*	
Beer		*	
Fruit drinks		*	
Desserts		*	*
Icing			*
Topping			*
Jams			*
Puddings			*
Bakery whipped cream			*
Pie fillings			*
Restructured foods			*
Simulated fruit			*
Mashed potatoes			*

6.6.1 Gelling agent

A major advantage of alginates as gel formers over other gelling agents lies in their ability to form gels at low (room) temperature, which are thermo-irreversible, i.e. alginate gels are heat stable as described above (Onsøyen, 2001). This thermal stability enables alginate to be used in baking products. However, it should be noted that alginates are prone to thermal and chemical degradation processes. Therefore, prolonged heating may weaken the gel (Draget, 2000).

The room temperature gelling function is particularly valuable in the restructuring of foods that may become damaged or oxidised under high temperatures (e.g. meat products, fruits and vegetables). Reconstituted onion rings and pimento sections for use in olives are common restructured foods produced using alginates (Brownlee *et al.*, 2009), in which alginates enable the production of products of regular size and consistency. This consistency in restructured material significantly facilitates mass production of these products. Alginates also have a number

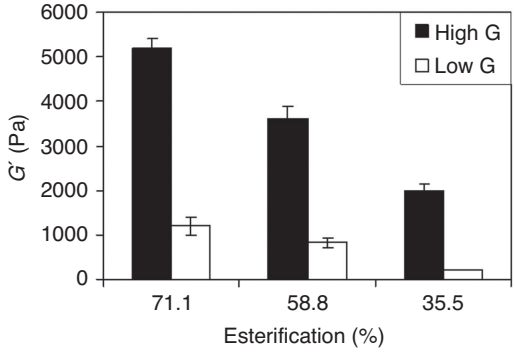

Fig. 6.9 Elastic modulus, G', of alginate/pectin 60:40 mixed gels (1.5% total polymer concentration) at 20°C. Illustrating the differences between high and low G alginate and different degrees of esterification (data from Walkenström *et al.*, 2003).

of similar applications in meat, seafood, fruit, vegetable and some extruded food products (e.g. pastas and noodles).

The ability of alginate to form synergistic gels with other polysaccharides such as pectin or chitosan provides further scope for its use in food. Alginate–pectin synergistic gels, in particular, is a well-studied mechanism, which is utilised for applications in jams, jellies and fruit fillings. The alginate–pectin gel, in contrast to the purely ionically cross-linked alginate, is thermo-reversible (Draget *et al.*, 2006b) and gives a higher viscosity than does either individual component. The pH value is also an important parameter for gel formation like that of acid gels of both alginate and pectin. Generally, a pH value less than 4 encourages gel formation with increasing gel strength as the pH decreases from 3.5 to 3.0) then remaining reasonably constant below pH 3 (Walkenström *et al.*, 2003). The gel structure is also independent of sugar content, unlike the pectin gels, and may, therefore, be used in low-calorie products (Rehm, 2009). Generally, alginates rich in guluronate residues combined with highly esterified pectins give the strongest gels, with weaker gels with lower melting points formed with low G alginates (Thom *et al.*, 1982; Walkenström *et al.*, 2003). This is illustrated in Fig. 6.9, where measurements of G' were taken in mixed alginate–pectin gels at a ratio of 60:40, using both high and low G alginate in combination with pectins of varying degrees of esterification.

6.6.2 Thickening agent

The viscosity of alginate solution has a direct relation to the length of the alginate polymer chain. The addition of alginate to water hydrates the alginate, causing the solution to gain viscosity. The dissolved molecule chains are not completely flexible, and it is well known that solutions

of stiff macromolecules are highly viscous, which is generally true for alginates. The thickening effect and rheology of alginate solutions, however, can be controlled through the choice of grade and formulation as well as concentration of alginate (Onsøyen, 2001).

Alginates are commonly used as thickening agents in ice creams, desserts and savoury sauces, including mayonnaise as well as in jams, marmalades and fruit sauces (Brownlee *et al.*, 2009).

Use of alginates on their own or in conjunction with other thickening agents has been shown to improve the acceptability of a number of low-fat processed foods (Rehm, 2009).

6.6.3 Film-forming agent

A film or coating can be achieved by applying a thin layer of alginate gel or alginate solution and, consequently, drying it (Onsøyen, 2001). Edible films and coatings for foodstuffs are developing technologies that have a high potential, owing to the current call for reduction or replacement of non-biodegradable or non-recyclable food packaging (Brownlee *et al.*, 2009).

Sodium alginate food films show good tensile strength, flexibility and resistance to tearing, and are impermeable to oils. Antimicrobial agents can be incorporated in the alginate gel to provide an effective barrier to microbial surface spoilage of vegetables, meat and fish products. The low temperature formation of the alginate gel coating minimises damage to the antimicrobial agents as well as to the foodstuff itself. This property makes the alginate coating suitable for fresh fruit and vegetable products, such as lettuce and freshly cut apple and melon sections, where the coating increases the shelf life, reduces browning, maintains crispness and texture and reduces vitamin C loss (Brownlee *et al.*, 2009).

Alginates films also can be used to protect frozen fish from oxidation and loss of water by stabilising the ice layer and making it more impermeable to oxygen and moisture. Meat carcasses and meat pieces can be protected by a calcium alginate film, which both reduces water loss and improves the food safety (Onsøyen, 2001).

6.6.4 Encapsulation and immobilisation

Encapsulation in food processing is a specialised form of edible packaging. If encapsulation is utilised in a food process, usually the approach is to apply the encapsulation only to those ingredients which are unstable, volatile or particularly reactive. Therefore, encapsulation renders a cover around these ingredients, which provides stability and protection for the whole product (Nussinovitch, 2003).

Alginate immobilisation technologies in food processing can enhance productivity in continuous operations by entrapping cells or enzymes used in the production and reusing them. Immobilisation technology is used to produce a wide range of bacterial metabolites, including enzymes, amino acids, organic acids (e.g. acetic acid) and alcohols (Brownlee *et al.*, 2009). For example, alginate immobilisation technology can be used in the production of fermented beverages to entrap and reuse various cell yeast cultures (Navratil *et al.*, 2002) or in the dairy industry, where various lactic acid producing bacteria are used as a starter culture (Champagne *et al.*, 1994).

The addition of bioactive ingredients to foods is a challenging process which is on the forefront of food research and development. Difficulties particularly arise with respect to the stability of the bioactive compounds during processing, storage and preventing interactions with other ingredients. Alginate encapsulation may have use in the development of such functional foods. The mild encapsulation process and acid insolubility of alginate gels offer protection to the encapsulated contents from the physiological extremes of pH once ingested, thus presenting the potential to deliver fully functional enzymes or live probiotic bacteria to the intestine. The enteric properties of alginate, in particular, provide a great advantage when attempting to deliver live bacteria (Lee and Heo, 2000; Hansen *et al.*, 2002; Krasaekoopt *et al.*, 2003; Clark *et al.*, 2008) or fully functioning bioactive proteins and peptides (George and Abraham, 2006) to the intestine.

6.6.5 Texturisation of vegetative materials

Many processed foods contain hydrocolloids, including alginates, which govern the product's functionality and acceptability (Aguilera, 2005). Novel structured fruit products are made from pulp and alginate, in which particulates are embedded in the alginate gel matrix. Sodium alginate is also used in the production of artificial fruits from sodium alginate solutions (Nussinovitch, 2003).

Restructured food based on Ca-alginate gels seems to be a steadily growing application of alginates. The restructuring process is based on binding together a flaked, sectioned, chunked or milled foodstuff to make it resemble the original, such as onion rings, pimento olive fillings, crabsticks and cocktail berries (Draget *et al.*, 2006b).

6.6.6 Stabiliser

Alginates produce stable gels both at high or low temperatures and at low pH (Draget, 2000). Therefore, they can be used for a number of food processing applications as food stabilisers. Ice cream was the first

application of alginate as a stabiliser in the food industry (Onsøyen, 2001). While alginate allows control of the ice cream's viscosity, it also increases heat-shock resistance, reduces shrinkage and ice crystal formation and enables ice cream to have a prolonged meltdown, which is a desired characteristic (Onsøyen, 2001; Brownlee *et al.*, 2009). If calcium ions are present in the food matrix, then alginate is usually mixed with sodium phosphate, which binds excess calcium and prevents the precipitation of calcium alginate. Routine use of alginates in bakery creams provides the cream with freeze/thaw stability and reduces separation of the solid and liquid components (Brownlee *et al.*, 2009).

The esterified alginate derivative, PGA, is commonly used in acid-based salad dressings, acidic fruit drinks and to maintain foam stability, including applications in mousse and other desserts. This is due to its higher solubility at low pH (Moe *et al.*, 1995). Another major use of PGA is in the brewing industry, where it is added to different beers and lagers to stabilise the froth head when poured, which also protects it from foam-negative contaminants (Brownlee *et al.*, 2009).

6.6.7 Appetite control

The microstructure and bulk properties of food products are known to influence the uptake of nutrients or other components of food and can also influence satiety (Di Lorrenzo *et al.*, 1988; Bergmann *et al.*, 1992). Of particular interest is research by several groups that suggests that daily ingestion of a strong-gelling alginate reduces energy intake by slowing gastric clearance and attenuating uptake from the small intestine. This, in turn, modulates the human appetite (Pelkman *et al.*, 2007; Paxman *et al.*, 2008). High viscosity or gel strength in the mouth is associated with poor acceptability of foods. At the same time, however, high viscosity in the stomach is linked to increased gastric distension and thereby increased satiety (Pelkman *et al.*, 2007). Also, alginates appear to have some inhibitory effects on a range of digestive enzymes *in vitro*. This is likely to be due to their high viscosity, which in turn reduces the availability of substrate for enzyme action (Rehm, 2009).

This has opened up an interesting and potentially lucrative application of alginate as an appetite suppressor to control obesity. Unlike other viscous polysaccharides which need to be administered in gel form to exist as a gel in the stomach, alginates have the unique ability to spontaneously form gels at low temperature in the presence of acid or calcium ions. The nature of alginate gelation in the stomach and the effect on satiety in human subjects has been investigated by Norton *et al.* (2006), using NMR/MRI techniques. Alginate solutions were consumed before MRIs of the stomach were taken at regular intervals over a two-hour period. These images of the gels within the stomach were analysed

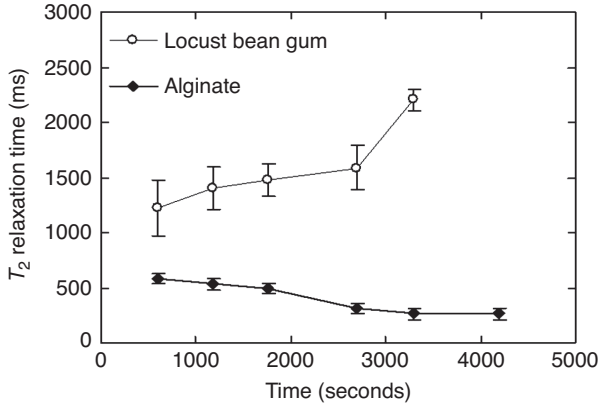

Fig. 6.10 NMR studies comparing the change in the T_2 relaxation time of alginate and locust bean gum meals in the stomach as a function of time. (Adapted from Norton *et al.*, 2006).

in terms of their respective spin–spin (T_2) relaxation time, which is related to the viscosity (Marciani *et al.*, 1999), allowing real time *in vivo* viscosity measurements. The change in T_2 relaxation time of the alginate was compared with that of the non-acid gelling locust bean gum as a function of time after consumption. It was found that T_2 relaxation time of the locust bean gum solution increased with time due to the dilution of the viscous solution within the stomach. The T_2 relaxation time of the alginate, on the other hand, decreased with time due to the gradual gelation in the acidic gastric fluid (Fig. 6.10). The mechanical forces that exist in the stomach cause the alginate, when ingested, to be subject to shear forces during the gelation process. Consequently, the gels formed are likely to be inhomogeneous. Indeed, the MR imaging techniques used by Norton *et al.* (2006), recorded immediately after a solution of alginate had been ingested, revealed 'string-like' gel structures, which were considered to be inhomogeneous alginate gels.

6.6.8 Summary

A brief description of the chemistry and the physical properties of alginates are presented in this chapter alongside some current applications in food. Alginates are being used, or have the potential to be used, in an increasing variety of applications in the food industry. However, for successful food formulations, a complete understanding of the structure–function relationships in alginates is necessary.

The versatility of alginates is due to the availability of a wide range of structural conformations and, subsequently, diverse physical properties. Their unique gelling abilities at low temperature alongside good heat

stability make them ideal for use as thickeners, stabilisers or restructuring agents, as well as for encapsulating active enzymes and live bacteria, and for protective coating of fruits and vegetables.

Furthermore, alginate intake in the diet has a number of physiological effects. Alginates can be given in low viscosity formulations, which can increase palatability. Because of the presence of acid in the stomach, alginate formulations can gel *in situ*, which can increase satiety and reduce absorption and digestion rates of other macronutrients in the diet.

The constant advancement and interest in 'high value' applications of alginate in drug delivery, biomedicine and functional foods will develop the knowledge base, the application of specific design and the novel functionality of alginates. Large steps are already being taken to achieve this with the pioneering work performed at several institutions on the design of alginate sequence using mannuronan epimerases and the development of chemically modified alginates, both of which can ultimately be prepared 'application specific'.

REFERENCES

Aguilera, J.M. (2005) Why food microstructure? *Journal of Food Engineering* **67**, 3–11.

Andresen, I., Skipnes, O., Smidsrod, O., Ostgaard, K. and Hemmer, P. (1977) Some biological functions of matrix components in benthic algae in relation to their chemistry and the composition of seawater. In: Arthur, J.C., Jr, editor. *Cellulose Chemistry and Technology*. Washington, D. C.: American Chemical Society, pp. 361–381.

Bergmann, J.F., Chassany, O., Petit, A., Triki, R., Caulin, C. and Segrestaa, J.M. (1992) Correlation between echographic gastric emptying and appetite: influence of psyllium. *Gut* **33**, 1042–1043.

Brownlee, I.A., Seal, C.J., Wilcox, M., Dettmar, P.W. and Pearson, J.P. (2009) Applications of alginates in food. In: Rehm, B.H.A., editor. *Alginates: Biology and Applications*. London: Springer, pp. 211–228.

Carlson, D.M. and Matthews, L.W. (1966) Polyuronic acids produced by pseudomonas aeruginosa. *Biochemistry* **5**, 2817–2822.

Champagne, C.P., Lacroix, C. and Sodinigallot, I. (1994) Immobilized cell technologies for the dairy-industry. *Critical Reviews in Biotechnology* **14**, 109–134.

Clark, S., Cross, M.L., Smith, A., Court, P., Vipond, J., Nadian, A., Hewinson, R.G., Batchelor, H.K., Perrie, Y., Williams, A., Aldwell, F.E. and Chambers, M.A. (2008) Assessment of different formulations of oral mycobacterium bovis Bacille Calmette-Guerin (BCG) vaccine in rodent models for immunogenicity and protection against aerosol challenge with M-bovis. *Vaccine* **26**, 5791–5797.

Di Lorrenzo, C., Williams, C.M., Hajnal, F. and Valenzuela, J.E. (1988) Pectin delays gastric emptying and increases satiety in obese subjects. *Gastroenterology* **95**, 1211–1215.

Donati, I., Holtan, S., Morch, Y.A., Borgogna, M. and Dentini, M. (2005) New hypothesis on the role of alternating sequences in calcium−alginate gels. *Biomacromolecules* **6**, 1031–1040.

Draget, K.I. (2000) Alginates. In: Phillips, G.O. and Williams, P.A., editors. *Handbook of Hydrocolloids*. Cambridge: Woodhead Publishing Limited, pp. 379–396.

Draget, K.I., Moe, S.T., Skjåk-Bræk, G. and Smidsrød, O. (2006b) Alginates. In: Stephen, A.M., Phillips, G.O. and Williams, P.A., editors. *Food Polysaccharides and Their Applications*. Boca Raton, FL: CRC Press, pp. 289–334.

Draget, K.I., Ostgaard, K. and Smidsrød, O. (1990) Homogeneous alginate gels – a technical approach. *Carbohydrate Polymers* **14**, 159–178.

Draget, K.I., Skjåk Bræka, G., Christensen, B.E., Gaserod, O. and Smidsrød, O. (1996) Swelling and partial solubilization of alginic acid gel beads in acidic buffer. *Carbohydrate Polymers* **29**, 209–215.

Draget, K.I., Skjåk Bræka, G. and Smidsrød, O. (1994) Alginic acid gels: the effect of alginate chemical composition and molecular weight. *Carbohydrate Polymers* **25**, 31–38.

Draget, K.I., Skjåk Bræka, G. and Stokke, B.T. (2006a) Similarities and differences between alginic acid gels and ionically crosslinked alginate gels. *Food Hydrocolloids* **20**, 170–175.

Draget, K.I., Stokke, B.T., Yuguchi, Y., Urakawa, H. and Kajiwara, K. (2003) Small-angle x-ray scattering and rheological characterization of alginate gels. 3. Alginic acid gels. *Biomacromolecules* **4**, 1661–1668.

Draget, K.I., Strand, B., Hartmann, M., Valla, S., Smidsrød, O. and Skjåk Bræka, G. (2000) Ionic and acid gel formation of epimerised alginates; the effect of AlgE4. *International Journal of Biological Macromolecules* **27**, 117–122.

George, M. and Abraham, T.E. (2006) Polyionic hydrocolloids for the intestinal delivery of protein drugs: Alginate and chitosan – a review. *Journal of Controlled Release* **114**, 1–14.

Gomeza, C.G., Lambrechta, M.V.P., Lozanoa, J.E., Rinaudob, M. and Villara, M.A. (2009) Influence of the extraction-purification conditions on final properties of alginates obtained from brown algae (Macrocystis pyrifera). *International Journal of Biological Macromolecules* **44**, 365–371.

Gorin, P.A.J. and Spencer, J.F.T. (1966) Exocellular alginic acid from azotobacter vinelandii. *Canadian Journal of Chemistry* **44**, 993–998.

Grant, G.T., Morris, E.R., Rees, D.A., Smith, P.J.C. and Thom, D. (1973) Biological interactions between polysaccharides and divalent cations: the egg-box model. *FEBS Letters* **32**, 195–198.

Hansen, L.T., lan-Wojtas, P.M., Jin, Y.L. and Paulson, A.T. (2002) Survival of Ca-alginate microencapsulated Bifidobacterium spp. in milk and simulated gastrointestinal conditions. *Food Microbiology* **19**, 35–45.

Hartmann, M., Dentini, M., Draget, K.I. and Skjak-Braek, G. (2006) Enzymatic modification of alginates with the mannuronan C-5 epimerase AlgE4 enhances their solubility at low pH. *Carbohydrate Polymers* **63**, 257–262.

Haug, A. (1961) Dissociation of alginic acid. *Acta Chemica Scandinavica* **15**(4), 950–952.

Haug, A. and Larsen, B. (1963) Solubility of alginate at low pH. *Acta Chemica Scandinavica* **17**, 1653–1662.

Haug, A. and Smidsrod, O. (1965) Effect of divalent metals on properties of alginate solutions. 2. Comparison of different metal ions. *Acta Chemica Scandinavica* **19**, 341–351.

Holtan, S., Bruheim, P. and Skjak-Braek, G. (2006) Mode of action and subsite studies of the guluronan block-forming mannuronan C-5 epimerases AlgE1 and AlgE6. *Biochemical Journal* **395**, 319–329.

Hommel, M., Mein-Fang Sun, A. and Goosen, M.F.A. (1988) Microcapsule composition suitable for cardiovascular injection. United States Patent 4789550.

Hulst, A.C., Tramper, J., Vantriet, K. and Westerbeek, J.M.M. (1985) A new technique for the production of immobilized biocatalyst in large quantities. *Biotechnology and Bioengineering* **27**, 870–876.

Indergaard, M. and SkjakBraek, G. (1987) Characteristics of alginate from Laminaria digitata cultivated in a high-phosphate environment. *Hydrobiologia* **151/152**, 541–549.

Jothisaraswathi, S., Babu, B. and Rengasamy, R. (2006) Seasonal studies on alginate and its composition II: turbinaria conoides (J. Ag.) Kütz. (Fucales, Phaeophyceae). *Journal of Applied Phycology* **18**, 161–166.

Kierstan, M. and Bucke, C. (1977) Immobilization of microbial-cells, subcellular organelles, and enzymes in calcium alginate gels. *Biotechnology and Bioengineering* **19**, 387–397.

Kohn, R. and Larsen, B. (1972) Preparation of water-soluble polyuronic acids and their calcium salts, and the determination of calcium ion activity in relation to the degree of polymerization. *Acta Chemica Scandinavica* **26**, 2455–2468.

Krasaekoopt, W., Bhandari, B. and Deeth, H. (2003) Evaluation of encapsulation techniques of probiotics for yoghurt. *International Dairy Journal* **13**, 3–13.

Lee, K.Y. and Heo, T.R. (2000) Survival of Bifidobacterium longum immobilized in calcium alginate beads in simulated gastric juices and bile salt solution. *Applied and Environmental Microbiology* **66**, 869–873.

Linker A.L.F.R. and Jones, R.S. (1964) A Polysaccharide resembling alginic acid from a pseudomonas micro-organism. *Nature* **204**, 187–188.

Marciani, L., Spiller, R.C., Gowland, P.A., Manoj, P., Moore, R.J., Young, P., Al-Sahab, S. and Fillery-Travis, A. (1999) Influence of meal viscosity and nutrient content on gastric emptying, meal dilution and satiety assessed non-invasively by echo-planar imaging. *Gastroenterology* **116**, A1036.

Matsumoto, S., Kobayashi, H. and Takashima, Y. (1986) Production of monodispersed capsules. *Journal of Microencapsulation* **3**(1), 25–31.

Moe, S.T., Skjåk Bræka, G., Draget, K.I. and Smidsrød, O. (1995) Alginates. In: Stephen, A.M., editor. *Food Polysaccharides and Their Applications*. New York: Marcel Dekker.

Navratil, M., Gemeiner, P., Klein, J., Sturdik, E., Malovikova, A., Nahalka, J., Vikartovska, A., Domeny, Z. and Smogrovicova, D. (2002) Properties of hydrogel materials used for entrapment of microbial cells in production of fermented beverages. *Artificial Cells Blood Substitutes and Immobilization Biotechnology* **30**, 199–218.

Norton, I.T., Frith, W.J. and Ablett, S. (2006) Fluid gels, mixed fluid gels and satiety. *Food Hydrocolloids* **20**, 229–239.

Nussinovitch, A. (1997) Hydrocolloid Applications: Gum Technology in the Food and Other Industries. London: Blackie Academic and Professional.

Nussinovitch, A. (2003) *Water-Soluble Polymer Applications in Foods*. Oxford: Blackwell Publishing Ltd.

Onsøyen, E. (2001) Alginate: production, composition, physicochemical properties, physiological effects, safety, and food applications. In: Sungsoo Cho, S. and Dreher, M.L., editors. *Handbook of Dietary Fibers*. New York: Marcel Dekker, Inc.

Owusu-Apenten, R. (2005) *Introduction to Food Chemistry*. Boca Raton, FL: CRC Press.

Paxman, J.R., Richardson, J.C., Dettmar, P.W. and Corfe, B.M. (2008) Daily ingestion of alginate reduces energy intake in free-living subjects. *Appetite* **51**, 713–719.

Pelkman, C.L., Navia, J.L., Miller, A.E. and Pohle, R.J. (2007) Novel calcium-gelled, alginate-pectin beverage reduced energy intake in nondieting overweight and obese women: interactions with dietary restraint status. *American Journal of Clinical Nutrition* **86**, 1595–1602.

Poncelet, D., Lencki, R., Beaulieu, C., Halle, J.P., Neufeld, R.J. and Fournier, A. (1992) Production of alginate beads by emulsification internal gelation.1. methodology. *Applied Microbiology and Biotechnology* **38**, 39–45.

Rehm, B.H.A. (2009) *Alginates: Biology and Applications*. London: Springer.

Rezende, R.A., Bartolo, P.J., Mendes, A. and Maciel, R. (2009) Rheological behavior of alginate solutions for biomanufacturing. *Journal of Applied Polymer Science* **113**, 3866–3871.

Smidsrød, O., Glover, R.M. and Whittington, S.G. (1973) The relative extension of alginates having different chemical composition. *Carbohydrate Research* **27**, 107–118.

Stanford, E.C.C. (1881) British Patent 142.

Steiner, A.B. (1947) Manufacture of glycol alginates. US Patent 2,426,215.

Sugiura, S., Oda, T., Izumida, Y., Aoyagi, Y., Satake, M., Ochiai, A., Ohkohchi, N. and Nakajima, M. (2005) Size control of calcium alginate beads containing living cells using micro-nozzle array. *Biomaterials* **26**, 3327–3331.

Thom, D., Dea, I.C.M., Morris, E.R. and Powell, D.A. (1982) Interchain associations of alginate and pectins. *Progress in Food and Nutrition Science* **6**, 97–108.

Toft, K., Grasdalen, H. and Smidsrod, O. (1986) Synergistic gelation of alginates and pectins. In: Fishman, M.L., editor. *Chemistry and Function of Pectins*. Washington, DC: American Chemical Society, pp. 117–132.

Tombs, M. and Harding, S.E. (1998) *An Introduction to Polysaccharide Biotechnology*. London: Taylor and Francis.

Vold, I.M.N., Kristiansen, K.A. and Christensen, B.E. (2007) A study of the chain stiffness and extension of alginates, in vitro epimerized alginates, and periodate-oxidized alginates using size-exclusion chromatography combined with light scattering and viscosity detectors (vol 7, pg 2136, 2006). *Biomacromolecules* **8**, 2627.

Walkenström, P., Kidman, S., Hermansson, A.-M., Rasmussen, P.B. and Hoegh, L. (2003) Microstructure and rheological behaviour of alginate/pectin mixed gels. *Food Hydrocolloids* **17**, 593–603.

Walter, R.H. (1998) *Polysaccharide Dispersions: Chemistry and Technology in Food*. Academic Press: San Diego.

Wan, L.S.C., Heng, P.W.S. and Chan, L.W. (1992) Drug encapsulation in alginate microspheres by emulsification. *Journal of Microencapsulation* **9**, 309–316.

Zhao, Y., Li, F., Carvajal, M.T. and Harris, M.T. (2009) Interactions between bovine serum albumin and alginate: An evaluation of alginate as protein carrier. *Journal of Colloid and Interface Science* **332**, 345–353.

7 Dairy Systems

E. Allen Foegeding, Bongkosh Vardhanabhuti and Xin Yang

7.1 INTRODUCTION

Rheological measurements have become essential tools in food companies for characterising ingredients and final products, as well as for predicting product performance and consumer acceptance. The rheological properties of dairy products can range from liquids such as milk to semi-solids or soft gels such as yoghurt and sour cream to hard solids such as cheddar and Parmesan cheeses. Understanding the rheological and mechanical properties of various dairy products is important in the design of flow processes for quality control, in predicting storage and stability measurements and in understanding and designing texture. With the latter, quality attributes such as viscosity, spreadability and creaminess, or hardness and breakdown properties are extremely important to the acceptance of liquid, semi-solid, and solid dairy products; therefore, one use of rheological measurements is in determining which physical properties are associated with the sensory perception of texture. In rheological tests, a fixed stress or strain (similar to those occuring during processing and consumption) is applied to a sample and the relationship among stress, strain, and time scales of foods is investigated. Selection of an instrumental technique for the determination of the rheological properties of a dairy product depends on its properties (i.e. whether the product is liquid, semi-solid or solid) and more importantly on the purpose of the measurement. This chapter will focus on the rheological properties of liquid milk, some semi-solid dairy products and solid cheese to show how rheological techniques have been and can be used to characterise the mechanical properties of these materials.

Practical Food Rheology: An Interpretive Approach
Edited by Ian T. Norton, Fotios Spyropoulos and Philip Cox
 ISBN: 978-1-405-19978-0

7.2 FLUID MILK

Milk is a colloidal suspension in which the solid components dissolve or disperse in a continuous water phase. From a rheological perspective, milk can be categorised as a typical fluid because it deforms and flows immediately when subjected to a stress. Knowledge of the flow behaviour of milk is important to the design and operation of dairy processing equipments involved in mixing, storage and pumping. Rheological properties of milk closely correlate with sensory perception of texture.

7.2.1 Rheological properties of milk

The rheological characterisation of a fluid can be described using the relationship between shear stress (σ) and shear rate ($\dot{\gamma}$) in a steady laminar flow. A Newtonian fluid displays a linear relationship between shear stress and shear rate, independently of time, and has no yield stress. Because the major component of milk is water, normal milk shows similar rheological properties as water – a Newtonian flow behaviour (Equation 7.1):

$$\text{Newtonian model} \quad \sigma = \mu\dot{\gamma} \tag{7.1}$$

where μ is the Newtonian viscosity, which is a measurement of the resistance of fluid to flow due to the 'internal friction'. Newtonian viscosity can be affected by temperature and composition of the fluid. The Newtonian viscosity of water is 1.0 mPa · s at 20°C, while representative values for milk and milk fractions at 20°C are 2.0 mPa · s (whole milk), 1.5 mPa · s (non-fat milk), and 1.2 mPa · s (cheese whey) (Sherbon, 1999). From these values, it is evident that the casein micelles and the fat globules in milk can contribute to its viscosity. The Newtonian viscosities of milks and creams of different fat contents increase with decreasing temperature (Bakshi and Smith, 1984). van Vliet and Walstra (1980) indicated that milk fat globules can undergo a crystallisation transition and cold agglutination at temperatures below 40°C, corresponding to a deviation from the Newtonian behaviour of milk. When milk is concentrated, the particle-to-particle interactions can contribute significantly to viscosity. A transition from Newtonian to non-Newtonian flow occurs when the solid concentration of milk reaches a certain level (Walstra and Jenness, 1984; Prentice, 1992), which is attributed to a decrease of free volume of the solid particles with removal of water. Power law model (Equation 7.2) is frequently used to describe a non-Newtonian fluid when the flow behaviour is time-independent and shows no yield stress:

$$\text{Power law model} \quad \sigma = K\dot{\gamma}^n \tag{7.2}$$

where K is the consistency coefficient (unit of Pa $\cdot$ s^n) and n is the dimensionless flow behaviour index. Milk products usually show shear-thinning (pseudoplastic) behaviour with flow behaviour indexes of $0 < n < 1$. Apparent viscosity (η) can be calculated (Equation 7.3) for a shear-thinning fluid as:

$$\text{Apparent viscosity} \quad \eta = \frac{\sigma}{\dot{\gamma}} = K\dot{\gamma}^{n-1} \tag{7.3}$$

The flow behaviour index indicates the deviation from Newtonian behaviour ($n = 1$), which reflects the changing rate of fluid viscosity with shear rate. For a shear-thinning fluid ($n < 1$), a lower value of the flow behaviour index suggests a faster decrease of the apparent viscosity with increasing shearing rate. A higher consistency coefficient does not necessarily guarantee a higher viscosity, which is also dependent on the flow behaviour index and shear rate for shear-thinning fluids. Vélez-Ruiz and Barbosa-Cánovas (1998, 2000) found Newtonian behaviours for milks with <22.3% solid contents and shear-thinning behaviours for concentrated milks with solid contents between 22.3 and 30.5%. The flow behaviour index of concentrated milk decreased with increasing solid content, showing a larger magnitude of shear-thinning behaviour (Vélez-Ruiz and Barbosa-Cánovas, 1998, 2000). Shear-thinning behaviour was explained based on asymmetric molecules aligning with the shear planes and thereby reducing frictional resistance (Tung, 1978). The consistency coefficient of concentrated milk increased markedly with solid content (Vélez-Ruiz and Barbosa-Cánovas, 1998, 2000). The transition of milk flow behaviour from Newtonian to non-Newtonian with increasing solid content has been reported by other groups but with different critical solid concentrations, such as 25% by Chang and Hartel (1997) and 15% by Solanki and Rizvi (2001). This most probably reflects differences in milk composition combined with processing effects.

An increase in milk viscosity as a function of storage time has been reported as the so-called 'age-thickening' process (Snoeren *et al*., 1984; Vélez-Ruiz *et al*., 1998; Bienvenue *et al*., 2003). This is proposed to be due to changes such as structural transformations in casein micelles and whey proteins (Snoeren *et al*., 1984); however, the precise physicochemical changes involved in age thickening are unknown.

Yield stress is observed for concentrated milks and is associated with the high amounts of solids, allowing for weak gel formation. In these cases, the Bingham (Equation 7.4) or Herschel–Bulkley models (Equation 7.5) describe the rheological characteristics of milks (Vélez-Ruiz and Barbosa-Cánovas, 1998; Bienvenue *et al*., 2003):

$$\text{Bingham model} \quad \sigma = \sigma_0 + \eta_{\text{pl}}\dot{\gamma} \tag{7.4}$$

$$\text{Herschel-Bulkley model} \quad \sigma = \sigma_0 + K\dot{\gamma}^n \tag{7.5}$$

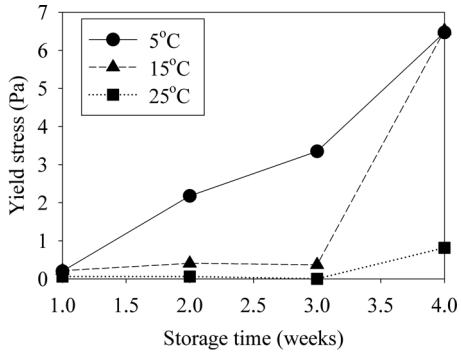

Fig. 7.1 The Herschel–Bulkley yield stresses, extrapolated from flow curves, for concentrated skim milks (48.6% total solids) as a function of storage time. The flow behaviour was measured at the temperatures indicated in the figure. The concentrated skim milks were stored at 2–4°C. Data are from Vélez-Ruiz and Barbosa-Cánovas (1998).

where σ_0 is the yield stress value at $\dot{\gamma} = 0$ per second and η_{pl} is the plastic viscosity. The transition from low shear stress ($\sigma < \sigma_0$) to high shear stress ($\sigma > \sigma_0$) corresponds to the transition from solid-like to liquid-like behaviour. Bienvenue *et al.* (2003) used the Bingham model to describe the rheological properties of concentrated skim milk with a total solids content of 45%. The yield stress for freshly concentrated milk was close to zero but increased to ~44 Pa after being stored at 50°C for 11 hours. The storage-induced increase of yield stress suggests flocculation due to weak attraction among casein micelles and rearrangement of the three-dimensional structure during storage. Vélez-Ruiz and Barbosa-Cánovas (1998) observed yield stresses for concentrated milks with >42.4% solid contents at 5–25°C after storing them for 1–4 weeks at 2–4°C and the flow behaviour conformed to Herschel–Bulkley model (Fig. 7.1).

Chang and Hartel (1997) found that the Herschel–Bulkley model better described the flow behaviour of freshly freeze-concentrated skim milk (25–40% total solids) than power law model, suggesting the need to account for yield stress. However, they also indicated that the predicted yield stresses were not significantly different from zero. This is not surprising since the yield stresses for concentrated milks are close to zero for the fresh samples and increase to more significant values during storage (Vélez-Ruiz and Barbosa-Cánovas, 1998; Bienvenue *et al.*, 2003). Yield stress is an important parameter for engineering calculations, product quality and sensory assessment (Steffe, 1996) and a major characteristic for the semi-solid dairy products.

The apparent viscosity of fluids cannot be predicted as a finite value by using power law model for a shear-thinning fluid when shear rate (or shear stress) is close to zero (Equation 7.3). There are two characteristic types of flow behaviours of a shear-thinning material at low shear

stresses – curves with an initial (zero-shear-rate) Newtonian viscosity limit and curves with a yield stress limit (Malkin and Isayev, 2006). With more sophisticated instrumentation, a low stress range is observed for shear-thinning fluids in which the apparent viscosity is constant (range of zero-shear-rate or initial Newtonian viscosity). The Carreau model (Equation 7.6) describes not only the power law behaviour but also regimens of Newtonian flow at very low and very high shear rates, which are often referred to as the Brownian and the hydrodynamic regimes, respectively (Bird *et al*., 1987).

$$\text{Carreau model} \quad \eta = [1 + (\dot{\gamma}\lambda)^2]^{(n-1)/2}[\eta_0 - \eta_\infty] + \eta_\infty \tag{7.6}$$

where η_0 is the limit viscosity at low shear rate (zero-shear viscosity) and η_∞ is the limit viscosity at high shear rate (infinite-shear-rate viscosity). The λ is the characteristic viscous relaxation time. The slope of $\log(\eta)$ versus $\log((\dot{\gamma}))$ in the shear-thinning region is related to n ($0 < n < 1$), where $n = 1$ represents a Newtonian liquid ($\eta = \eta_0$) (Bird *et al*., 1987). This model describes the shear-thinning behaviour in intermediate shear rate range as well as the Newtonian regimens at very low ($\dot{\gamma} \to 0$, $\eta = \eta_0$) and very high ($\dot{\gamma} \to \infty$, $\eta = \eta_\infty$) shear rates. Yasuda modified the Carreau model by adding one more parameter (Equation 7.7) (Bird *et al*., 1987):

$$\text{Carreau-Yasuda model} \quad \eta(\dot{\gamma}) = [1 + (\dot{\gamma}\lambda)^a]^{(n-1)/a}[\eta_0 - \eta_\infty] + \eta_\infty \tag{7.7}$$

where a is a dimensionless parameter called the 'Yasuda-constant'. The Carreau–Yasuda model was shown to describe the rheological behaviour of skim milk concentrates (Karlsson *et al*., 2005). The η_∞, which is determined only by the hydrodynamic interactions between particles, was used to estimate the voluminosity of casein micelles, which is the volume occupied by one gram of micellar material (Karlsson *et al*., 2005). The voluminosity of casein micelles was shown to be altered by addition of salts and changing the pH.

Viscoelastic properties – elastic modulus (G'), loss modulus (G'') and phase angle – can be measured for milk although they are not used as frequently as the flow properties. A dilute solution (close to Newtonian behaviour) is expected to show pure fluid properties, corresponding to a phase angle close to 90° and $G'' \gg G'$ (Steffe, 1996). The phase angle decreased to ~50° for a concentrated solution (viscoelastic behaviour), ~4° for a gel (elastic behaviour), and 0° for a Hooke solid (pure elastic behaviour), corresponding to an increase of the elastic modulus (Steffe, 1996). Karlsson *et al*. (2005) measured the viscoelastic properties of concentrated milks at a frequency of 1 Hz and strain of 0.01. The

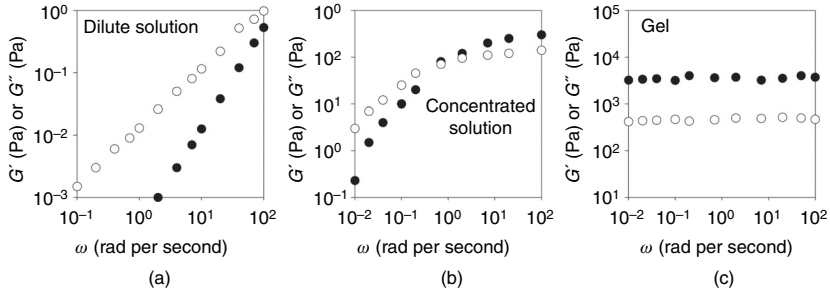

Fig. 7.2 Typical dynamic frequency sweep data for a dilute solution (a), a concentrated solution (b) and a gel (c). •, G' ○, G''. Reproduced from Steffe (1996).

phase angle of milk concentrates decreased from ~55° at pH 5.4 to ~10° at pH 4.8, corresponding to an increase of the elastic modulus (Karlsson *et al*., 2005). Since the pI value of casein is ~pH 4.6, the interactions among caseins become more intensive as the net charge decreases with pH decreasing from 5.4 to 4.8. The pH-induced gelation of milk concentrates leads to the formation of a fine network which exhibits both elastic and viscous properties. High pressure treatment on milk concentrates also showed an enhancing effect on elastic modulus, suggesting the formation of a more solid-like structure (Vélez-Ruiz *et al*., 1998).

Frequency dependence of rheological properties are used to generate mechanical spectra that provide characteristic patterns for dilute solutions, concentrated solutions and gels (Fig. 7.2) (Steffe, 1996). With dilute solutions, G'' is larger than G' over the entire frequency range but approach each other at higher frequencies (Fig. 7.2a). For a concentrated solution, G'' is larger than G' in the lower frequency range, showing more liquid-like properties, and the G'' becomes lower than G' in the higher frequency range, exhibiting more solid-like properties (Fig. 7.2b). G' is always greater than G'' throughout the whole frequency range for a gel (Fig. 7.2c). Concentrated solution behaviour was observed for milk beverages with the addition of Salep glycomannan or locust bean gum; while gel-like behaviour was found for milk beverages with addition of guar gum (Yaşar *et al*., 2009).

A complex viscosity (η^*) can be calculated using complex modulus (G^*) and frequency (ω) (Equation 7.8). Cox-Merz rule states that the complex viscosity is nearly equal to the steady shear viscosity when the angular velocity is equal to the shear rate (Equation 7.9) (Steffe, 1996):

$$\text{Complex viscosity} \quad \eta^* = \frac{G^*}{\omega} \tag{7.8}$$

$$\text{Cox-Merz rule} \quad \eta^* = \eta_a|_{\dot{\gamma}=\omega} \tag{7.9}$$

Comparison of the dynamic rheological properties (η^*) and the steady shear rheological properties (η) can provide insight on the structure of the sample. For example, milk beverages with locust bean gum conform to the Cox-Merz rule but those with guar gum added required a shift factor (α) of 0.18, (i.e. the complex viscosity was calculated at a frequency of $\alpha\omega$ instead of ω) (Yaşar *et al*., 2009). The departures from the Cox-Merz rule with the magnitudes of η^* greater than η_a was explained by the structure decay due to the effect of the stress applied to the system, which is low in oscillatory shear and high in steady shear (Yaşar *et al*., 2009). Milk beverages with addition of guar gum, which showed more solid-like properties than the samples containing locust bean gum, would be more sensitive to the effect of stress deformation as it may be disrupting a network structure.

7.2.2 Measurements of the rheological properties of milk

Three types of viscometers are frequently used to measure milk viscosity: falling sphere method (an empirical method), U-tube capillary viscometers and rotational viscometers. For foods that exhibit Newtonian behaviour, viscometers that operate at a single shear rate (e.g. falling sphere method and U-tube capillary viscometers) are acceptable. However, for foods that exhibit non-Newtonian behaviour, data should be obtained at several shear rates, and this is most typically done using rotational viscometers.

7.2.2.1 *Falling sphere method*

Falling sphere method involves a vertical tube where a sphere of known size and density is allowed to fall under a given force (e.g. gravity) through a Newtonian fluid. The falling time of the sphere over a certain distance or the falling velocity is determined by two forces – the sphere gravity and the drag force (viscosity) of the fluid – and is used to calculate the fluid viscosity according to Stokes' law. The fluid viscosity is assumed to be independent of the shear rate (Newtonian behaviour) when measured by this device. The flow behaviours of milks with $<30\%$ solid content and at $T > 40^{\circ}$C are very close to Newtonian behaviour with $n > 0.9$ flow behaviour index observed in many studies. The falling sphere method is considered acceptable to determine the apparent viscosity of milks in these cases (Fernández-Martín, 1972).

A general discussion of falling sphere viscometers that presents conditions for and limitations of their use is found in Weber (1956). The falling sphere method has been frequently used in earlier studies but rarely used recently. A more frequently used method to determine the Newtonian viscosity is U-tube capillary viscometer.

7.2.2.2 *U-tube capillary viscometers*

U-tube capillary viscometer is a simple and widely used method for qualitative estimation of liquid viscosity. The essence of this method is to measure the resistance of liquid to flow through a 'U'-shaped capillary channel. The flow time of a liquid through a certain length of the channel is recorded as the efflux time and is used to calculate apparent viscosity. Several types of U-tube capillary viscometers, such as Ostwald, Canon-Fenske, Ubbelohde, and Kimax®, have been used to measure the apparent viscosity of milks. These instruments differ in geometry of the glass tube and are all designed as gravity-operated devices. U-tube capillary viscometers are only suitable for Newtonian fluids because shear rate varies during discharge of the fluid. Griffin *et al*. (1989) found that concentrated skimmed milk showed Newtonian behaviour at stresses below 16 $mN \cdot m^{-2}$ and measured viscosity using an Ostwald U-tube viscometer. The flow behaviour of milk can be assumed as Newtonian during discharge in a U-tube capillary viscometer because the shear rate range of this process is very low.

U-tube capillary viscometers are mostly used to measure relative viscosity (Equation 7.10) of milk samples:

$$\text{Relative viscosity } \eta_{rel} = \frac{\eta_{solution}}{\eta_{solvent}} \tag{7.10}$$

where $\eta_{solution}$ and $\eta_{solvent}$ correspond to the apparent viscosities of solution (milk) and solvent (water). The apparent viscosity of skimmed milk was also used as $\eta_{solvent}$ when studying the effect of fat content to viscosity (Kyazze and Starov, 2004). The apparent viscosity is proportional to the efflux time of fluid flowing through the capillary tube. Therefore, the time required for the solution to flow through a capillary viscometer is measured, divided by the time required for the solvent to flow through the same viscometer, and reported as relative viscosity. Relative viscosity is positively associated with total solids or specific components, such as fat, representing the contributions of dispersed or dissolved components to viscosity.

Relative viscosity has been used not only to determine the effects of milk composition on viscosity but also the effects of other factors such as heat treatment. Jeurnink and de Kruif (1993) studied the effect of heat treatment on skim milk viscosity using an Ubbelohde capillary viscometer. The U-tube viscometer is a convenient and inexpensive method to measure and compare the apparent viscosity of milk products. However, the data collected is only at a certain range of shear rates, which depends on the physical properties of fluid and the tube geometry and cannot be controlled. The fluid is assumed to be Newtonian within this

shear rate range. Rotational viscometers can be used to obtain the flow behaviour of milk products at a controlled shear rate.

7.2.2.3 *Rotational viscometers*

Rotational viscometers are useful to evaluate the rheological properties of liquids, as they allow measurements over a range of shear rates. The basic theory of rotational instruments is covered by many reviews (e.g. Steffe, 1996; Malkin and Isayev, 2006). The rheological parameters – Newtonian viscosity, consistency coefficient, flow behaviour index and yield stress – can be calculated from the curve of shear stress vs. shear rate and used for further analysis. Often a pre-shear step, usually at a shear rate of ~100 per second, is conducted before measurement to equilibrate the sample. Shear rate ranged from 0.132 to 13.2 per second (Chang and Hartel, 1997) to 0 to 2700 per second (Solanki and Rizvi, 2001) in studies on milk rheology. An advantage of rotational viscometers is that flow behaviour of a fluid can be characterised at a selected range of shear rates to coincide with a particular application. Shear rates of oral processing and typical industrial operations of dairy products are summarised by Steffe (1996).

Many rheometers are capable of operating in oscillatory mode as well as rotational. Vélez-Ruiz *et al*. (1998) determined the viscoelastic properties of concentrated milks using a frequency sweep from 1 to 100 Hz at a strain of 0.2. They found that the effect of solid content on the elastic modulus is more apparent at the lower frequency range (1–10 Hz). The elastic moduli of all samples increased and became similar at a higher frequency range (10–100 Hz).

7.2.3 Factors influencing milk rheological properties

The flow properties (bulk properties) of milk – a colloidal sol/emulsion – are related to its microstructure, which is dependent on a number of factors: colloidal (i.e. particle-particle interactions), Brownian (the random movement of particles), hydrodynamic (i.e. particle to fluid interactions) and more complex interactions (Kyazze and Starov, 2004). The major factors influencing milk rheological properties are its composition, especially the volume fraction of colloidal particles, and the measurement or processing conditions, such as temperature and shear rate.

7.2.3.1 *Milk composition*

The bulk viscosity of milk is associated with the volume fraction of dispersed particles – fat globules, casein micelles, whey protein aggregates

(heat-treated milks) or total solids. Although dissolved carbohydrates and salts can influence viscosity, the major factors determining milk viscosity are the two dispersed particles – fat globules and colloidal proteins (McCarthy and Singh, 2009).

In fluid milk, the milk fat is almost entirely in the form of globules, ranging from 0.1 to 15 μm in diameter (Jenness, 1999). van Vliet and Walstra (1980) indicated that the volume fraction and physical state, e.g. crystallisation at $T < 35°C$, of fat globules can influence the flow behaviour of milks and creams. At higher temperatures ($T > 40°C$), the flow behaviour of milks and creams approached Newtonian flow (Phipps, 1969). More non–Newtonian flow behaviour can be expected as temperature decreases. This is partially explained by crystals interacting with each other and/or with other milk constituents in a different way during shearing, leading to shear-thinning behaviours (van Vliet and Walstra, 1980). The viscosities (Newtonian or apparent) of milks and creams increase with increasing volume fraction of fat globules, due to more interactions among the solid constitutes (van Vliet and Walstra, 1980). Kyazze and Starov (2004) indicated that fat globules can form clusters with increasing volume fraction, changing the milk microstructure. In this case, fat globules cannot be simply assumed as discrete particles when evaluating their effects on milk viscosity; instead, the cluster size distribution and the packing density of droplets inside clusters become the major parameters (Kyazze and Starov, 2004). Vélez-Ruiz and Barbosa-Cánovas (2000) observed the microstructure of concentrated milks and found fat globules surrounded by a membrane of proteins, which was thicker in concentrated milk than in fresh milk. This is attributed to a variety of changes to proteins and fat globules under the effects of heat and water removal during concentration steps. Note that different concentration steps – evaporation, freeze concentration, or microfiltration – result in variations in the compositions of concentrated milks, corresponding to slightly dissimilar flow behaviours (Chang and Hartel, 1997; Vélez-Ruiz and Barbosa-Cánovas, 1998; Solanki and Rizvi, 2001).

The viscosity of skim milks can be described as a function of the volume fraction occupied by macromolecular materials (proteins: casein, native whey protein, denatured whey protein) (Snoeren *et al.*, 1982). This volume fraction depends on weight concentrations and voluminosities of the macromolecular materials. Increasing solid content in skim milk corresponds to an increase of the volume fraction occupied by macromolecules, assuming unchanged voluminosities, leading to a higher apparent viscosity. Factors influencing the voluminosities of macromolecules, such as heat treatment, solvent modification (pH adjustment, salt addition) and storage, will alter the viscosity of milk.

Changes in viscosity of skim milk after heat treatment can be attributed to denaturation of whey proteins. The viscosity of skim milk does not change much after heat treatment at 60°C, which is lower than the denaturation temperature of whey protein (70°C), but increases significantly after heat treatment at 90°C (Jeurnink and de Kruif, 1993). The effect of heat treatment on skim milk viscosity becomes less significant after removal of whey proteins, suggesting the enhancing effects are attributed to heat-denatured whey proteins, especially β-lactoglobulin aggregates (Jeurnink and de Kruif, 1993). When milk is heated, denatured whey proteins can form whey protein aggregates as well as associate with casein micelles. Interactions between whey proteins and casein produce two different changes in casein micelles: (i) The micelle grows in size, and (ii) the interaction between micelles is altered (Jeurnink and de Kruif, 1993). Anema *et al*. (2004) indicated that viscosity changes in reconstituted skim milk after heat treatment were related to a change in volume fraction of the casein micelles, which was correlated with the amount of denatured whey protein associated with casein micelles.

Karlsson *et al*. (2005) indicated that the voluminosity of casein micelles was affected by addition of salts and changes in pH, corresponding to variations in the apparent viscosity of skim milk concentrates. Addition of NaCl increased the voluminosity of casein micelles due to the exchange of Ca^{2+} bound to casein micelles with Na^{+} altering micelle structure. The reduction in the voluminosity of casein micelles upon lowering its pH from 6.5 to 6.0 (Solanki and Rizvi, 2001) corresponds to a less significant enhancing effect of the solid content to the apparent viscosity for microfiltrated skim milk retentates. Griffin *et al*. (1989) found that addition of ethanol at concentrations below that required for coagulation caused a reduction in the voluminosity of casein micelles, corresponding to a reduction in the hydrodynamic radius of micelles and a decrease of the apparent viscosity of concentrated skimmed milk.

The effect of storage on milk viscosity is attributed to the loosening of casein micelles, and thereby an increase of the voluminosity (Snoeren *et al*., 1984). A higher storage temperature corresponds to a faster loosening rate of casein micelles and a faster increase of the apparent viscosity with storage time (Snoeren *et al*., 1984).

7.2.3.2 *Mathematical models*

Various models, including polynomial, logarithmic, exponential and power law, have been used to fit the relationship between viscosity and solid concentrations for milks (Fernández-Martín, 1972; Buckingham, 1978; Bloore and Boag, 1981; Langley and Temple, 1985). These models can provide empirical predictions but rarely are explained based on milk microstructure and how it influences viscosity. The volume fraction

of the suspended particles is more meaningful than concentration when considering the effects of particles to the microstructure and viscosity of milk. Einstein equation describes a relationship between the viscosity of a dilute dispersion (milk) and the volume fraction of hard spheres (fat globules and macromolecules) in a continuous phase of known viscosity (water) (Dewan *et al*., 1973):

$$\text{Einstein equation} \quad \eta = \eta_c(1 + 2.5\phi) \tag{7.11}$$

where η and η_c are the viscosities of the dispersion (milk) and continuous (water) phase and ϕ is the volume fraction of the hard spheres. However, the Einstein equation fails in more concentrated systems; in these cases, the viscosity can be better described by Eilers equation (Dewan *et al*., 1973):

$$\text{Eilers equation} \quad \eta_{\text{rel}} = \frac{\eta}{\eta_c} = \left(1 + \left(\frac{1.25\phi}{1 - \phi/\phi_{\max}}\right)\right)^2 \tag{7.12}$$

where $\phi_{\max}$ is the hypothetical maximum volume fraction that could be occupied by the close packing of the representative particles and accounts for the interactions among particles. The $\phi_{\max}$ depends on the shape of the particles and their size distribution. van Vliet and Walstra (1980) described the relationship between the viscosity of milk and cream and the fat content using Eilers equation. They used the total volume fraction of fat, proteins, and lactose instead of that for fat alone in their model, and the volume fractions of proteins and lactose were assumed to be constants. Snoeren *et al*. (1982) showed that the Eilers equation described concentrated skim milk viscosity as a function of volume fraction occupied by the macromolecular materials. The effects of the voluminosities of constitutes (casein micelles, whey proteins, fat globules, fat-protein complexes) on milk viscosity are accounted for in Eilers model by using the volume fraction instead of weight concentration (Griffin *et al*., 1989; Solanki and Rizvi, 2001; Anema *et al*., 2004).

More complicated models involving viscosity of the particles have been applied to describe the relationship between milk viscosity and the volume fraction of fat globules (Kyazze and Starov, 2004). This approach demonstrated the importance of cluster formation of fat globules on the viscosity of concentrated milk.

7.2.3.3 *Temperature*

The effect of temperature on Newtonian viscosity, apparent viscosity or the consistency coefficient (if the flow behaviour index is not

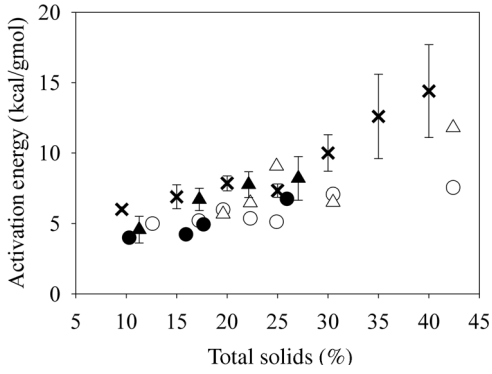

Fig. 7.3 Activation energy as a function of % total solids concentration from different studies. From Vélez-Ruiz and Barbosa-Cánovas (1998): ○, concentrated milk (week 1); △, concentrated milk (week 4). From Chang and Hartel (1997): ×, freeze-concentrated skim milk. From Solanki and Rizvi (2001): •, microfiltrated concentrated skim milk (pH 6.0); ▲, microfiltrated concentrated skim milk (pH 6.5).

temperature dependent) can be modeled with the Arrhenius equation:

$$\text{Arrhenius equation} \quad \eta \cdot \eta_a \cdot K = A_0 \exp\left(\frac{E_a}{RT}\right) \tag{7.13}$$

where η is the Newtonian viscosity, η_a is the apparent viscosity, K is the consistency coefficient, A_0 is a constant, E_a is the activation energy for flow, R is the universal gas constant and T is the absolute temperature. Activation energy values estimated from different studies are in a similar range and increase with the total solids concentrations (Fig. 7.3).

The activation energy increases in a faster rate in freeze-concentrated skim milk than in the others (Fig. 7.3), possibly due to different structures of the constituents, such as casein micelles, from various concentration techniques. The activation energy slightly increases with the storage time, which is interpreted as being due to changes occurring during storage such as structural transformations in casein micelles and whey proteins (Fig. 7.3; Vélez-Ruiz and Barbosa-Cánovas, 1998). The activation energy is greater for concentrated skim milks as pH increases (Fig. 7.3; Solanki and Rizvi, 2001). This, again, can be attributed to different structures and voluminosities of the constitutes at various pHs (Solanki and Rizvi, 2001).

7.2.4 Correlating rheological properties of milk to sensory perceptions

Viscosity as measured in rheometers reflects the resistance of a fluid to the flow. This physical viscosity is a component of the perceived

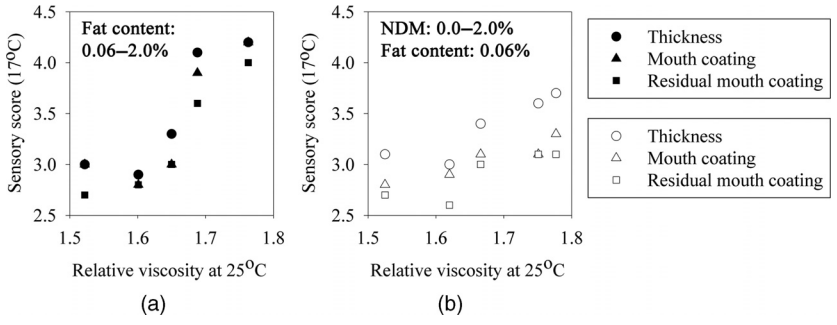

Fig. 7.4 The relationship between the sensory scores and the relative viscosity for milks. (a): milks with fat contents of 0.06, 0.5, 1.0, 1.5 and 2.0%. (b): milks of 0.06% fat with addition of non-fat dry milk (NDM) powder of 0.0, 0.5, 1.0, 1.5 and 2.0%. Samples were evaluated under red light to mask color. Data is from Phillips *et al*. (1995a, 1995b).

viscosity – 'thickness' – of a fluid, which can be evaluated by oral or non-oral (vision and touch) methods (Christensen and Casper, 1987). The perception of solution viscosity has been discussed by Christensen (1987).

Phillips *et al*. (1995a, 1995b) found that the textural sensation (thickness, mouth coating and residual mouth coating) of milk increased as the relative viscosity was increased by addition of fat or nonfat dry milk (NDM) powder (Fig. 7.4).

It should be remembered that drawing conclusions between mechanical and sensory viscosity is complicated by a number of factors, including testing conditions. For example, the addition of nonfat dry milk (NDM) powder into milk containing 0.06% fat can achieve similar relative viscosity as milks containing higher fat amounts; however, the sensory textural scores of the NDM-containing milks are still lower (Fig. 7.4) (Phillips *et al*., 1995a, 1995b). It is likely that complex conditions experienced in the mouth (various shear rates and increasing temperature) could explain differences when milk is filled with fat as compared to protein (i.e. NDM powder).

7.2.5 Process engineering calculation

The rheological properties of fluids are important for controlling the flow during various manufacturing operations, such as pumping, spray drying, mixing, homogenising, and thermal processing (Steffe, 1996; Steffe and Daubert, 2006). Fluid viscosity is included in many equations used for process engineering calculations. Some such equations and examples are presented in food engineering books (Steffe, 1996; Steffe and Daubert, 2006). Examples of pumping milk and spray drying dairy concentrates will be given in the following text.

Pump selection requires an evaluation of the power requirements to move fluid through a pipeline, which is calculated using the overall mechanical energy balance equation (the modified Bernoulli equation). The energy changes in a pipeline include (i) the pressure energy loss, (ii) the kinetic energy loss, (iii) the potential energy loss and (iv) the friction energy losses (Steffe and Daubert, 2006). The friction energy loss in a straight pipe can be determined using a Fanning friction factor, in which the viscosity of fluid is required. Bakshi and Smith (1984) developed a regression equation to estimate the Newtonian viscosity of milk with varying fat content (0.1–30%) and temperature (0–30°C), which can be used to calculate the friction energy losses in a pipeline and the power requirement during pumping.

The viscosity of fluids can also influence the droplet size and thereby the powder particle size during spray drying. Keogh *et al*. (2003) used ultrafiltrated milk samples from different sources to standardise their fat contents prior to evaporation and drying. Concentrated milk samples containing a variety of total solid contents were obtained after ultrafiltration, corresponding to dissimilar apparent viscosities. A positive linear relationship was established between the powder particle size and the apparent viscosity (Keogh *et al*., 2003).

7.3 SOLID CHEESE

Cheese rheology is a function of its composition, microstructure, the physical chemical properties of its components, and the macrostructure (the presence of heterogeneities such as cracks and fissures) (Fox *et al*., 2000). Factors that influenced the physical properties of cheese include initial cheese–milk composition, processing procedures, and the extent of proteolysis during ripening. These are influenced by environmental conditions such as pH, temperature, and ionic strength. In the first ripening phase (7–14 days), the degradation of casein structure over time due to proteases is the primary contributor to textural changes. This proteolysis leads to the reduction in firmness and an increase in deformability as cheese ages (Tunick *et al*., 1990). More gradual changes occur in the second phase where the rest of α_{s1} casein and other caseins are broken down. Understanding the aggregation of caseins is vital in understanding the physical and chemical properties of cheese (Lucey *et al*., 2003). The number, strength, and types of bonds among casein molecules as well as the spatial arrangements of these bonds constitute the basis of cheese rheology.

As with fluid milk, rheological measurements are used in a variety of applications such as evaluating structure development and understanding the physical basis for sensory texture. When the goal of rheological

tests is to understand how the structure and interactions of the cheese network determine sensory texture, it becomes more complex because a solid requires structural breakdown and lubrication to prepare for swallowing. In order to use rheological tests to characterise the physical properties of cheese, the tests must measure the physical properties associated with a human psychophysical interpretation of the tactile and visual perceptions that occur when consuming cheese. Descriptive sensory analysis is the tool for qualitatively and quantitatively differentiating cheeses and for defining the relationship between sensory and instrumental perception of cheese texture. Cheese texture terms have been developed to define texture attributes of several different types of cheeses (Drake *et al*., 1999; Lawlor and Delahunty, 2000; Gwartney *et al*., 2002; Adhikari *et al*., 2003). By using these attributes, the effects of cheese making parameters as well as the differentiation between cheese types can be determined.

7.3.1 Small amplitude oscillatory tests

The viscoelastic properties of cheese can be determined under small amplitude oscillatory shear conditions by applying small sinusoidal stresses (force per unit area) or strains (deformation per unit length) at levels that do not cause significant irreversible changes in the cheese, and the responding strain or stress is measured. Small amplitude oscillatory tests are implemented in the linear viscoelastic (LVE) region and are suitable for probing material structure and structure development during different processes. The measurements allow the determination of (i) storage modulus (or elastic modulus, G') and (ii) loss modulus (or viscous modulus, G'') as a function of test frequency (ω) in the LVE region of the test material (Gunasekaran and Ak, 2003). Another important parameter is phase angle (δ) or the phase shift between the deformation and response. Phase angle is often expressed as loss tangent ($\tan \delta =$ the ratio of energy lost to energy stored or G''/G'), which describes the relative degree of viscoelasticity. Phase angles of 0° and 90° indicate purely elastic and viscous materials, respectively. A decrease in phase angle indicates that the material is reacting to an external stress in a relatively more elastic manner. When $G' = G''$ ($\delta = 45^\circ$ and $\tan \delta = 1$), the modulus value at this point is called the 'crossover modulus' and the state of the material is crossing over from predominately solid to liquid or vice versa (Gunasekaran and Ak, 2003). Different types of small strain oscillatory tests can be set up by changing strain (or stress), frequency, temperature, and time. Common tests are strain (or stress) sweep, frequency sweep, temperature sweep and time sweep.

Frequency sweep is used to investigate time-dependent shear behaviour of cheese, since frequency is the inverse value of time. High

frequency represents short-term behaviour such as biting into a piece of cheese, while an example of long-term behaviour includes eye formation in Swiss-type cheese. For short-time response, the elastic behaviour dominates, whereas the viscous component is prominent in long-term response. In frequency sweep tests, a sinusoidal strain (or stress) of fixed amplitude (from strain or stress sweep test) is applied on the material, and the dynamic moduli are determined over a wide range of frequencies. This produces the mechanical spectra of the sample within the LVE region (Foegeding *et al*., 2003).

A time sweep measurement is performed at constant strain (or stress) amplitude and frequency. It may be conducted along with a temperature sweep program to examine the changes in rheological behaviour due to the combined effect of time and temperature. Oscillation frequency is commonly set at 1 Hz (Gunasekaran and Ak, 2003). Time sweep tests can be used to monitor the formation or breakdown of structure during curing. Temperature sweeps are useful to investigate phase transitions, such as melting of cheese or the molecular interactions in the protein network that take place during heating (Udyarajan *et al*., 2007).

Before starting a small amplitude oscillatory measurement, the limit of a LVE region of the test materials must be determined by performing a strain sweep (for controlled strain rheometer), while the frequency is held constant. The common frequency used is 1 Hz ($\omega = 6.28$ rad/s) or 10 rad/s ($f = 1.6$ Hz) (Mezger, 2006). A strain level in the linear region is then selected and a frequency sweep is performed. By performing the test in the LVE region of the materials, the elastic and loss moduli become only a function of time and not a function of the magnitude of the stress or strain applied (Rao and Skinner, 1986). For a controlled stress rheometer, a stress sweep is performed to carry out the same purpose of identifying the strain limit of the LVE region. It should be noted that the limiting amplitude value of the LVE region is valid for the used frequency only. At higher frequency, many materials often exhibit less flexibility and thus higher rigidity (G' dominates), leading to lower limiting amplitude (Mezger, 2006).

Small amplitude oscillatory tests are commonly used to measure LVE properties of cheeses during gelation and ripening as well as the change as affected by ingredients (i.e. fat or calcium phosphate) and processing parameters. The viscoelastic property of cheese is mostly influenced by protein network as well as fat and moisture, which modify the network properties. Other factors include proteolysis, temperature, pH and salt content (Walstra *et al*., 1987). Protein–protein bonds are primarily responsible for the elastic response, whereas the viscous response can be due to flow of the matrix material, flow of liquid through the matrix and movement of other structural elements relative to each other (Luyten *et al*., 1991). Together with microscopy techniques, the change in

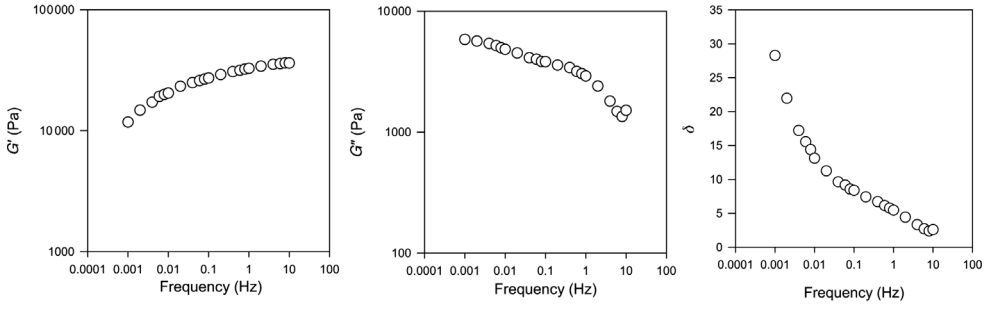

Fig. 7.5 Storage modulus (G'), loss modulus (G'') and phase angle (δ) over changing frequencies for process cheeses at 4 days of age (from Brown, 2002, to Brown *et al.*, 2003).

texture can be explained by using small strain rheology and correlating the rheological properties to microstructure. As previously stated, the limit of LVE region must be determined before any measurement. Typical viscoelastic characterisation of cheese is shown in Fig. 7.5. The magnitude of G' was higher for all samples than the magnitude of G'', and G' increased with increasing frequency. These trends are generally observed with weak gels (Kavanagh and Ross-Murphy, 1998) and cheeses (Nolan *et al.*, 1989; Ma *et al.*, 1996; Tunick, 2000). At very low frequencies (0.001 Hz), δ is relatively high, indicating the dominant effect of the viscous component; the cheeses behave more fluid-like when deformed at slower speeds. When the frequency is increased from 0.01 to 1.0 Hz, δ levels, showing that the speed has less of an influence on the relative effects of the viscoelastic properties. At very high frequencies, δ is low, showing the dominant effect of the elastic component; the cheeses behave more 'solid-like' at such higher speeds (Brown, 2002).

The most important factor affecting rheological and physical properties of cheese during ripening is proteolysis, which contributes to the final texture of cheese. Decreasing G' during ripening has been observed in mozzarella (Tunick *et al.*, 1993a, 1993b). The casein matrix becomes softer and less elastic due to the breakdown of α_{S1} casein, which provides the major contribution to the structure of caseins in curd. Similarly, Subramanian and Gunasekaran (1997) found that the strain limit of the LVE region of mozzarella cheese decreased with age and increasing temperature and hypothesised that this was due to proteolysis and thermal softening over time. Change in G' and loss tangent during ripening has been reported for cheddar cheese (Lucey *et al.*, 2003; Lucey *et al.*, 2005). G' values determined at 40 and 80°C decreased during ripening especially during the first 60 days. At low temperature (5–35°C), there was no significant difference in loss tangent among cheddar cheeses. Loss tangent increased during ripening when measured at 40–60°C.

Change in formulation also affects viscoelastic characterisation of cheese. Reducing the amount of fat in cheese has been known to cause an increase in elastic component (G') of cheese. Low fat mozzarella cheese has a higher G', G'', and η^* compared to full-fat cheese at the same age (Tunick *et al*., 1993a). Hennelly *et al*. (2006) investigated the effect of inulin (fat substitute) on rheological properties of imitation cheese. At 22°C, there was no significant difference between G' and G'' of cheeses containing different amounts of inulin. However, when cheeses without inulin were heated from 22 to 90°C, G' decreased and tan δ increased with heating temperature, indicating the weakening of the protein–protein interaction within the casein network. For imitation cheeses with high inulin concentration (>13.1% w/w), G' started to increase at >55°C and tan δ values gradually increased with increasing temperature to about 55°C and then decreased at higher temperature, reflecting a strengthening of the cheese matrix at these temperatures.

Small amplitude test can be used to study the effect of cheese processing parameters. Homogenising milk or processing at higher temperature causes an increase in G' of mozzarella cheese (Tunick *et al*., 1993a). The effect of pH on rheological properties and the microstructure of process cheese was investigated by Marchesseau *et al*. (1997). The dependence of firmness on pH was shown by a decrease in G' as pH increased from 5.7 to 6.7 and when pH decreased from 5.7 to 5.2. In agreement with the rheological results, the microstructure of process cheese at pH 5.2 (lowest G') had a highly distorted structure that included large spherical particles. As pH was increased to 5.7, the cheese microstructure consisted of more homogeneous and dense network with a clear separation between fat globules and the protein network. At pH 6.7, small condensed aggregates were formed and appeared to disrupt the protein matrix. A very logical application of small strain oscillatory tests is the characterisation of melting properties. Mounsey and O'Riordan (1999) studied the melting properties of imitation cheeses by comparing tan δ of different cheeses as a function of temperature. When temperature was increased from 22 to 90°C, the tan δ values for the cheese with 0–9% pregelatinised maize starch increased, indicating that the elastic component decreased to a greater extent than the viscous component. The observed maximum tan δ values decreased with increasing starch content, reflecting the tendency of starch to hinder meltability. Imitation cheeses containing starch maintained their elastic properties on heating to a higher degree than control samples. A high correlation was found between maximum tan δ values and meltability determined by an empirical melt test. Another investigation (Ustunol *et al*., 1994) suggested that complex modulus (G^*) could be a useful predictor of meltability of full-fat and reduced-fat cheddar cheeses as measured by the Arnott test.

7.3.2 Large strain rheological analysis

When deformed to a large extent, cheeses fracture: the phenomenon that resembles what happens during biting and mastication of foods. Large-strain and fracture methods are commonly used when the desire is to correlate with sensory properties. By deforming a cheese sample to the point of abrupt mechanical yield, fracture properties such as fracture stress, fracture strain, and fracture modulus can be determined. The measurements are performed in the non-linear regime and deformation of the sample is permanent. One of the challenges of any rheological testing, that is emphasised in large-strain tests, is that they are based on the assumption that samples are homogeneous, isotropic and incompressible, which may not strictly be the case with cheese. These factors should be considered when evaluating results.

7.3.2.1 *Uniaxial compression*

Uniaxial compression is the most popular test for determining the rheological properties of foods at fracture due to the simple sample preparation and execution. In a typical compression test, a specimen of known shape (typically cylindrical shape) and size is placed between two parallel rigid plates of a Universal Testing Machine, and often the upper plate is moved downward at a constant crosshead speed while the force is recorded as a function of time. The responding force–time data can be converted into stress and strain values. When the test is executed correctly (i.e. cylindrical sample with flat and parallel ends and no significant contribution of plate-cheese friction), the Young modulus (slope from stress and strain plot) may be calculated from the initial slope. If the goal is to only compare various cheeses, the maximum force can be used. It must be realised, however, that only results expressed as true stresses and true strains can be compared with those of other tests (van Vliet, 1991). Attention must be given to assure that the test is performed under conditions where there is no friction so that the deformation is homogeneous and the sample retains its cylindrical shape. Friction between the sample and the loading plate will lead to an inhomogeneous stress – strain state in the sample, which can be seen as bulging or a barrel shape of the specimen during compression. The resulting strain calculation becomes inaccurate or invalid (Gunasekaran and Ak, 2003) and the sample appears stiffer (Charalambides *et al*., 2001). The effect of friction can be reduced by lubricating the sample–plate interfaces or increasing the sample height (Charalambides *et al*., 2001). Since cheese is viscoelastic and therefore time-sensitive, another test parameter to consider is strain rate or crosshead speed. Shama and Sherman (1973) found that firmness of Gouda cheese depended on the compression speed

and the degree of compression. The tendency for stress at fracture to increase with compression speed has been found for cheddar, Cheshire and Leicester (Dickinson and Goulding, 1980; Ak and Gunasekaran, 1992; Brown *et al*., 2003). At higher deformation rates, the viscoelastic cheese has less time to relax during compression, giving higher values of the measured stress. Crosshead speed may be selected to mimic chewing speeds, which will vary from person to person and depend on type of foods, etc. Reported rates of jaw movement during chewing range from 15 mm/s to 30 mm/s (Langley and Marshall, 1993). The average bite velocities from chewing 15.9 mm^3 cheese sample ranged from 19.8 to 35.1 mm/s (Meullenet *et al*., 2002). More information on sample preparation for uniaxial compression test can be found in van Vliet and Peleg (1991).

With feta cheese, Wium *et al*. (1997) found the high correlation between instrumental results (stress at fracture, work at fracture as calculated by the area under the stress–strain curve until fracture and deformability modulus as calculated by the maximum slope of the stress–strain curve) and hand and oral firmness. The main component in cheese that builds the structure and gives the solid character is casein. Decreasing firmness, as shown by a decrease in fracture stress during ripening, corresponds to an increase in proteolysis and a decrease in intact casein (Rynne *et al*., 2004). Increasing pasteurisation temperature significantly reduced fracture stress, fracture strain and firmness of cheeses due to increased moisture content and thereby reduction in protein concentration (Rynne *et al*., 2004). Another possibility is that the level of denatured whey proteins (which complex with casein micelles during heating) increases and thus reduces the connectivity among the casein network.

Besides casein, fat also plays an important role in the texture of cheese. The structure and texture of cheeses are affected by the interactions between the surface of milk fat globules and the casein matrix. Native milk fat globules do not interact with the protein network in cheeses and act mainly as inert fillers or structure breakers, depending on their size and number (van Vliet, 1988; Michalski *et al*., 2002). Fat has been replaced with other ingredients in making low fat cheeses. Mozzarella cheese containing soy protein produced strong gel networks as indicated by highest compressive stress, showing that soy protein functioned like an increase in casein rather than a decrease in fat (Hsieh *et al*., 1993). Though egg, whey and caseinate significantly influenced the magnitude of G' and G'', they showed no effect on compressive stress. Everett and Olson (2003) studied the effect of the surface coating on fat globules on rheological properties during ripening of cheddar cheese. Stress at fracture (firmness) decreased during ripening as expected from proteolysis. Cheeses containing α_{s2}-casein-coated globules fractured at a lower stress and a smaller strain than those containing

globules coated with α_{s1}-casein, β-casein, κ-casein, α-lactalbumin or β-lactoglobulin. Images from confocal microscopy revealed that larger and more irregular fat globules existed in cheese where globules were coated with α_{s2}-casein or natural milk fat control. It was concluded that coating fat globules with highly charged α_{s2}-casein prevents the development of a strong protein network.

7.3.2.2 *Uniaxial tension*

Uniaxial tension can be performed on the same machine capable of doing uniaxial compression except that the stress is applied in the opposite direction. In general, tension testing is not suitable for routine measurements due to complications associated with gripping and lengthy sample preparation. Another important consideration is the geometric coupling of fracture stress and fracture strain. When the gel fracture criteria is a stress level, fracture strain is a function of elongation needed to reduce the specimen cross section to an area producing the critical fracture stress (Hamann *et al*., 2006). This results in similar increase or decrease of fracture stress and fracture strain with varying variables such as concentration. It has been found that fracture strain from tension is lower than compression and torsion (Tang *et al*., 1994; Hamann *et al*., 2006). Stress increases more rapidly in tension, causing the material to fail at small strain. Another reason is that defects are more exaggerated in tension due to the volume-increasing nature of the test. The advantage of the tension test is the absence of the friction problem as that which occurs in a compression test. Sample slipping and gripping problem can be eliminated with special grip design (Gunasekaran and Ak, 2003). A test piece that is thin in the middle and gluing the specimen to the grip can help avoiding the problem (Rosenthal, 1999). Lelievre *et al*. (1992) and Stading and Hermansson (1991) used molds to form specimen and were able to work with fragile gels.

Tensile testing is of practical importance for mozzarella cheese, which is one of the major ingredients in pizza. Consumer acceptability of mozzarella cheese is mostly determined by its functional and textural properties such as shreddability, stretchability, meltability, hardness and springiness. Fracture strain in tensile testing has been related to stretchability (Ak *et al*., 1993). Mozzarella processing involves kneading and stretching the curd in hot water, resulting in materials with oriented structure which exhibits anisotropy. This anisotropic property is one factor to consider in tensile testing. Studying the effect of sampling direction (parallel or perpendicular to protein fiber orientation) on fracture properties of mozzarella cheese, Ak and Gunasekaran (1997) found that fracture stress and strain were greater when cheeses were pulled in the parallel direction than in the perpendicular direction. They

proposed that the individual protein strands (controlling the fracture in parallel direction) were much stronger than interface bonds between constituents (responsible for bond breaking when pulled in perpendicular direction). Reduced fat mozzarella had higher fracture stress and strain compared to low moisture, part-skim mozzarella. Other important testing parameters include deformation rate and testing temperature. Increasing deformation rate increases fracture strain but decreases fracture stress and deformability modulus (Ak *et al*., 1993). Raising the testing temperature from 10 to 40°C increases fracture strain but decreases fracture stress and deformability modulus.

Tensile testing has been used to study the effects of aging on rheological properties of cheeses. During the first 2 weeks of refrigerated storage, mozzarella showed an increase in fracture strain due to fusion of the curd strands, which enhanced cohesiveness and strain (Ak *et al*., 1993). At 28 days, fracture strain remained unchanged but fracture stress significantly decreased, corresponding to an increase in proteolysis of casein. The effectiveness of different large strain tests in determining the cohesion of Gruyere-type cheese was compared (Pesenti and Luginbühl, 1999). Cheeses with either strong or weak cohesion were prepared by two different processes. Rheological tests performed on the cheeses included uniaxial compression, uniaxial tension, 3-point bending, cutting, stress relaxation and creep tests. Fracture parameters are especially suitable to quantify cohesion, since they reflect the macroscopic effect of breaking bonds. Tensile testing proved to be the most powerful test, allowing rapid differentiation of the cohesion of the two cheeses as shown by the values of all parameters (fracture stress, fracture strain, work to fracture and modulus of deformability).

7.3.2.3 *Torsion test*

In torsion testing, the material is twisted about its longitudinal axis to fracture. The specimen is formed to a capstan shape so that the fracture takes place at the narrow centre of the specimen. The disk-shaped ends allow the specimen to be gripped by the testing apparatus or glued to plastic disks for attachment to the testing devices. During sample twisting, torque and degree of rotation required to break the sample are monitored and stress and strain at fracture can be calculated. Torsion produces a condition of pure shear on the material, generating equal distribution of stress and shear through the sample. The specimen shape is maintained during the test, avoiding geometric considerations. The material can fracture in shear, tension, compression or a combination mode. The test is ideal for the materials that may exude water or fat under applied stress. The disadvantages of torsion are the sample preparation and that it is not suitable for soft materials.

Similar to uniaxial compression and tension, strain rate is an important test parameter in torsion testing. Fracture modulus (the ratio between true shear stress and true shear strain) increases as strain rate increases, indicating the viscoelastic, time-dependent nature of cheeses (Brown *et al*., 2003). Comparing full-fat and low-fat commercial cheeses (Monterey Jack, mild Cheddar, sharp Cheddar, and American cheeses), Gwartney *et al*. (2002) found that fracture stress is correlated with sensory firmness and springiness (first bite terms). Low-fat cheeses have higher fracture stress and thus increased sensory firmness, springiness and chewiness. Torsion testing has been used to study the effect of aging on rheological properties of Monterey Jack cheeses from goat milk (Van Hekken *et al*., 2004). Fracture stress and fracture modulus decreased during the first 8 weeks of storage, while fracture strain significantly increased over the first 4 weeks. A decrease in fracture stress correlated with a decrease in native casein and an increase in peptides.

7.3.2.4 *Vane method*

The vane method is an effective means to measure the yield stress using the rotational viscometer without slipping effects (Barnes and Nguyen, 2001). The vane geometry is similar to the concentric cylinder system, except that the inner cylinder is a spindle with 4–8 thin blades. The vane is immersed in a sample and rotated slowly at a constant rate, while the torque exerted on the vane blades is measured as a function of time. Stress and strain at fracture can be calculated and used to describe textural properties of foods. Key assumptions in vane test are that the shearing stress is uniform over the cylindrical surface, the material trapped between the blades is rotating as a rigid body and there are no secondary flows between the blades (Barnes and Nguyen, 2001). These assumptions are valid if the vane has at least four blades and rotates at low speed. The advantages of the vane method are the following: sample preparation is simple, weak samples can be tested, and the wall-slip problem is avoided. Using vane method in testing cheddar cheese, Truong *et al*. (2002) found good correlation between vane stress and apparent strain with sensory firmness and cohesiveness, respectively. When compared with torsion method in characterisation of cheeses (process, cheddar and mozzarella), Truong and Daubert (2001) showed similar texture maps of cheeses were generated by plotting stress and strain or angular deformation values from the two testing methods.

7.3.2.5 *Cutting with wire*

Wire cutting is a popular process used in the food industry during the manufacture and testing of products. The process comprises fracture,

large strain deformation and surface friction. Wire cutting test involves pushing wires of known diameters through specimens. It is assumed that the material flows only in a small area around the crack tip and only the material in the vicinity of the wire undergoes plastic deformation. The relationship between force and displacement depends on a combination of fracture, plastic/viscous deformation and surface friction. The cutting energy is calculated by dividing the cutting force (F) by the specimen width (B). The cutting energy (F/B) is then plotted against wire diameters (d). Conventionally, by extrapolating the cutting energy to zero, the value of fracture toughness is determined according to Equation 7.14 (Kamyab *et al*., 1998):

$$\frac{F}{B} = G_c + (1 + \mu)\sigma_\gamma d \tag{7.14}$$

where G_C is the fracture toughness, μ is the coefficient of friction and σ_γ is the characteristic stress.

Goh *et al*. (2005) investigated the effect of cutting speed and found that fracture toughness increased with increasing speed. They developed a modified model which enables fracture toughness to be determined as a function of strain rate. Details on the modified model can be found in Goh *et al*. (2005) and Gamonpilas *et al*. (2009).

7.3.3 Creep and stress relaxation

The goal of creep test is to predict the viscoelastic properties of materials over the long term. For example, creep occurs when cheese is gradually compressed under its own weight during retailing. A common approach to determine the LVE properties of solid cheese as a function of time is to apply a constant load or deformation, and the responding behaviour is monitored with the lapsing time. It should be noted that these tests are used within LVE region and beyond. Creep and stress relaxation tests can be performed in different configurations (i.e. compression, tension, shear, torsion, etc.); however, the most common mode in cheese studies is compression (Gunasekaran and Ak, 2003). In a creep test, an instantaneous and constant stress is placed on the material, while the strain or compliance (J) is measured as a function of time. Data from creep tests can be used to determine the retardation time, which is a characteristic time descriptor of the material (Foegeding *et al*., 2003). This constant provides an insight into how a material can adapt to an applied load, and the larger the constant, the slower the material relaxation. Another component of a creep test is recovery upon removal of load. Cheeses with little or no recovery have a significant viscous component.

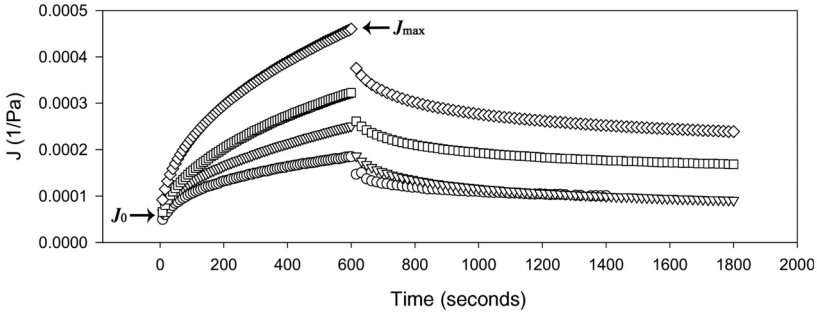

Fig. 7.6 Creep recovery curves for mozzarella cheeses at 4 days (○), 10 days (▽), 17 days (□), and 38 days (◇) of age (from Brown, 2002 to Brown *et al.*, 2003).

A creep test is more appropriate for longer time relaxation compared to the frequency sweep test; however, one has to determine whether the maximum level of strain is still within the LVE region (Foegeding and Drake, 2007). Creep test has been used to study the viscoelastic properties of cheeses during aging (Fig. 7.6). The instantaneous compliance (J_0) is the compliance at time zero as determined by extrapolating the compliance to zero time. The compliance at the end of creep test (at 600 seconds in this test) is called the maximum compliance (J_{max}). As cheese ages, J_{max} increases, indicating an increase in the level of deformation and the cheese becomes less elastic. This observation corresponds to the decrease in G' during ripening. A strong negative correlation between J_{max} values and sensory firmness was found with higher J_{max}, indicating a less firm structure (Brown *et al.*, 2003). Another creep testing parameter, creep recovery, can be determined by removal of stress at a time during creep test and measuring the height of sample after allowing sufficient time to recovery. Percent creep recovery indicates the degree of elasticity. Firmer cheeses such as cheddar are more elastic and have higher percent creep recovery. Investigating cheddar cheese having different fat levels, Rogers *et al.* (2009) found that, within the linear region, low-fat cheeses had higher J_{max} overtime, reflecting that these cheeses deformed more at a constant stress than full-fat cheeses. There was no difference in percent recovery (an indication of elastic recovery) and the retardation time between the full-fat and low-fat cheeses, indicating a similar viscoelasticity.

In a stress relaxation test, a material is subjected to an instantaneous strain and the stress is measured over time. The resultant stress–time curve is used to determine the relaxation time (λ), defined as the time required for stress to decay to about 37% of the initial level (Gunasekaran and Ak, 2003). Ideal elastic solids show a perfect memory of the initial state (stress is maintained), whereas the stress of ideal viscous liquids

decays to zero immediately when strain is applied. Viscoelastic materials including cheeses exhibit an intermediate response where stress relaxes at a finite rate characterised by the relaxation time (Peleg, 1987). Testing parameters to be considered in stress relaxation measurements include the effects of surface friction and lubrication. Goh and Sherman (1987) found that at higher percent compression (>20%), cracks developed in Gouda cheese, and the true stress relaxation behaviour could be studied only when the upper and lower surfaces of the samples were lubricated prior to the initial compression. The apparent relaxation time (i.e. the time required for the stress to relax to ~37% of its initial value) was useful in comparing among cheeses.

7.4 RHEOLOGICAL PROPERTIES OF SEMI-SOLID DAIRY FOODS

The category of semi-solid dairy foods includes yoghurt, sour cream, custards, and other dairy desserts (mixed carbohydrate and milk gel systems). Semi-solid dairy foods show the intermediate behaviour of both liquid and solid. Benezech and Maingonnat (1993) reviewed two aspects (viscoelastic properties and flow behaviour) of the rheological properties of three types of yoghurt (set-type, stirred and drinking), which represent semi-solid dairy products with a variety of rheological properties. More recent reviews on the rheological characterisations of semi-solid foods have been published by Kealy (2006) and Mortazavian *et al*. (2009).

7.4.1 Flow properties

The flow behaviours of semi-solid dairy products can be measured by different types of viscometers, among which rotational viscometers are most frequently used. Since the semi-solid products show some solid-like properties due to the formation of a weak gel structure, they exhibit a variety of non-Newtonian characteristics, such as time-dependency and yield stress.

7.4.1.1 *Time-dependent flow behaviour characterisation*

Many semi-solid dairy products show thixotropic behaviour, in which the apparent viscosity decreases with time of shearing at a constant shear rate (Abu-Jdayil, 2003). Two methods have been used to determine this characteristic – hysteresis loop and shear stress decay (Tárrega *et al*., 2004).

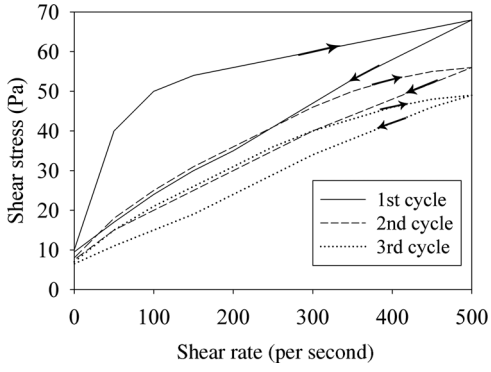

Fig. 7.7 The typical hysteresis loops in the flow curves (shear stress vs. shear rate) of a stirred yoghurt during three consecutive shear cycles. Adapted from Ramaswamy and Basak (1991).

7.4.1.2 *Hysteresis loop*

The time-dependency of the flow behaviours of semi-solid dairy products can be tested under a shear rate cycle. A hysteresis in the flow curve (shear stress vs. shear rate) suggests that shearing at high-shear rate modifies the material structure (Doublier and Durand, 2008). The area of the hysteresis loop corresponds to the extent of structural breakdown during the shearing cycle (Halmos and Tiu, 1981). Ramaswamy and Basak (1991) measured the flow behaviour of stirred yoghurts under three consecutive shear rate cycles (Fig. 7.7).

The hysteresis loop area associated with the first cycle is larger than those associated with the following cycles, suggesting that the first shearing cycle caused the major degradation of sample structure (Fig. 7.7). The hysteresis loop areas associated with the second and third shearing cycles are comparable to each other, indicating similar structure changes. The shear stress of the second or third shearing cycle is lower than its preceding cycle, indicating a continual breakdown of structure. The overlapping of the ascending shear curve of the second or third cycle with its preceding descending shear curves suggested that the structural loss in the ascending shearing process might be partially recovering during the descending shearing process (Ramaswamy and Basak, 1991). To determine the recovery of the thixotropic structural breakdown, Ramaswamy and Basak (1991) rested the yoghurt samples for an hour after three consecutive shearing cycles and repeated the test. They found that the shear stress of yoghurt in the repeating test cannot reach the same level as in the first test and suggested that the thixotropic structural breakdown during shearing was irreversible within one hour.

Tárrega *et al*. (2004) compared the hysteresis area for seven samples of a semi-solid Spanish dairy dessert and observed a larger 'absolute' hysteresis area (the area within the hysteresis cycle) for a more viscous

sample. They indicated that comparison of the 'absolute' hysteresis loop areas among samples of different viscosity might not provide valid conclusions on the time-dependent structural breakdown. Therefore, the percentage of the relative hysteresis area was calculated as the ratio of the 'absolute' hysteresis area to the area under the ascending shear curve and used for thixotropic characterisation (Tárrega *et al*., 2004). Both the 'absolute' and relative hysteresis areas were greater at lower temperatures, suggesting a more significant destructive effect of shearing on the structure; while the temperature-induced differences in the relative hysteresis areas were not as significant as those in the 'absolute' hysteresis areas (Tárrega *et al*., 2004).

Flow behaviour models have been used to fit the flow curves of hysteresis loop. The upward shear-rate flow behaviour of yoghurt samples could be described by the Herschel–Bulkley model, while the downward shear-rate curves were essentially linear (Ramaswamy and Basak, 1991). Similarly, the power law model has been used to fit the rheological data of stirred yoghurt during increasing shear rate (Keogh and O'Kennedy, 1998). Analysis of the parameters in these models for semi-solids is the same as for fluids.

The viscosity of semi-solid dairy products increases with the total solid concentration (Sodini *et al*., 2004). In this case, the contributors to texture are not only fat globules and proteins, as in concentrated milks, but also other ingredients such as polysaccharides, which are added into the systems and modify the texture (Sodini *et al*., 2004). Ramaswamy and Basak (1991) described the relationship between apparent viscosity and temperature for both the up and down curves in three consecutive shear rate cycles for a stirred yoghurt using the Arrhenius equation (Equation 7.13). The activation energy E_a (kcal/mole) for the up curve in the first cycle gradually decreased as shear rate increased, suggesting a less significant temperature effect on the flow behaviour; while the E_a values for the up curves in the second and third cycles and the three down curves varied only slightly with shear rate.

7.4.1.3 *Shear stress decay*

In a shear stress decay test, a constant shear rate is applied to the semi-solid samples over a period of time and the shear stress is measured. The stress (σ, Pa) decay behaviour of semi-solid dairy products can be expressed as a function of time (t, second), such as in the Weltmann (1943) model (Equation 7.15) or the modified one (Equation 7.16):

$$\text{Weltmann model } \sigma = A - B[\ln t] \tag{7.15}$$

$$\text{Modified Weltmann model } \sigma = A - B\left[\ln\left(\frac{t}{t_m}\right)\right] \tag{7.16}$$

where A is the initial shear stress (where $t = 1$ second in Equation 7.15 and $t = t_m$ in Equation 7.16) and B is the time coefficient of thixotropic breakdown. The parameter B corresponds to the rate of the breakdown of thixotropic structure during agitation at a constant rate of shear (Weltmann, 1943). Note that a zero-time stress is nonexistent in the Weltmann model (σ reaches infinity as time approaches zero). The t_m in Equation 7.16 is the time at maximum observed shear stress, corresponding to the starting point of the stress decay or structural breakdown process. The modified Weltmann model assumes the semi-solid structure starts to breakdown after shear stress reaches a certain value of A. The parameters A and B are dependent on the applied shear rate and temperature. Ramaswamy and Basak (1992) applied the modified Weltmann model to fit the shear stress decay data and compared the parameters A and B for two yoghurt samples. The A (or B) values for the two samples were similar at low shear rates but showed dissimilarity at high shear rates. At a certain shear rate, these parameters decreased with increasing temperature in a linear pattern, suggesting less time dependency of the flow behaviour. Ramaswamy and Basak (1992) described the relationship between $A/\dot{\gamma}$ (viscosity, Pa · s), where $\dot{\gamma}$ is the applied shear rate, and temperature using the Arrhenius equation (Equation 7.13), which shows that the E_a values gradually decreased as the shear rate increased. This is similar to their observations in the hysteresis loop test and suggests that the temperature effect on the flow behaviour is less significant at a higher shear rate (Ramaswamy and Basak, 1991). Tárrega *et al*. (2004) fitted the shear stress decay data to the Weltmann model for the Spanish dairy dessert samples and compared the results with those from the hysteresis loop test. The parameters A and B showed lower values at higher temperature and corresponded to less hysteresis areas, suggesting a slower rate of structure breakdown (Tárrega *et al*., 2004).

Other models have also been used to describe the time dependency of semi-solid dairy products (O'Donnell and Butler, 2002; Camacho *et al*., 2005). A common one is the structural kinetic model (Equation 7.17) proposed by Dzuy Nguyen *et al*. (1998). The structural kinetic model postulates that the change in time-dependent flow properties is due to shear-induced breakdown of the internal structure. This is represented by the kinetics of the process of going from the structured state (apparent viscosity of η_0) to the non-structured state (apparent viscosity of η_∞) (Abu-Jdayil, 2003):

$$\text{The structural kinetic model is } \left[\frac{(\eta - \eta_\infty)}{\eta_0 - \eta_\infty}\right]^{1-n} - 1 = (n-1)^{kt} \tag{7.17}$$

where t is time (second), n is the kinetic order and k is the model parameter, representing the rate of the structural breakdown during shearing (Abu-Jdayil, 2003). Tárrega *et al*. (2004) applied this model to fit the experimental data of a shear stress decay test, assuming a kinetic order of $n = 2$. The viscosity of semi-solid dairy dessert samples decreased rapidly with time within the first 300 seconds of shearing and approached a constant value, which was used as η_∞ (Tárrega *et al*., 2004). The η_0/η_∞ ratio was lower at a higher temperature for all samples, suggesting a lower extent of the structure breakdown; however, the temperature effect on the k values was not the same for different samples, possibly due to the differences of the structure responsible for the effect of temperature on the rate of thixotropic breakdown (Tárrega *et al*., 2004).

7.4.2 Yield stress

Yield stress is frequently detected for semi-solid dairy products. It can be measured as the initial stress value for the upward shear-rate flow curve in a hysteresis loop, which is the minimum stress required to make the sample flow (Fig. 7.8a). In this case, Herschel–Bulkley and Casson models are usually used to fit the rheological data (Ramaswamy and Basak, 1991; Tárrega *et al*., 2004). Yield stress was assigned to the maximum value of the flow curve for some semi-solid samples, such as cream cheese in Sanchez *et al*. (1994) (Fig. 7.8b). Kealy (2006) determined yield stress of cream cheese samples using a controlled stress rheometer. Shear stress was gradually increased and the deformation (shear strain) was measured. The yield stress was determined at the intersection of two linear regions in the displacement profile (Fig. 7.8c), at which the reversible deformation has ended and the material has begun to flow (Kealy, 2006). Measurements with the 'vane' device in low shear conditions also provided a way to estimate yield stress, at rest and after shearing (Breidinger and Steffe, 2001; Doublier and Durand, 2008). The maximum stress value in shear stress–time curve is taken as yield stress (Fig. 7.8d). Note that a pre-shear process can destroy the weak gel structure of a semi-solid product and significantly decrease the stress (Fig. 7.8d).

Barnes and Walters (1985) suggested that yield stress does not exist except in a few limited circumstances. The creep behaviour for solids, soft solids and structured liquids at low stresses can be described by a Newtonian-plateau viscosity (Barnes, 1999). Tárrega *et al*. (2005) obtained the zero-shear viscosity by fitting the experimental data to Carreau model (Equation 7.6). Their results suggest that semi-solid sample can flow even under a very small stress (close to zero), since no yield stress exists; however, it may take an extremely long time for the

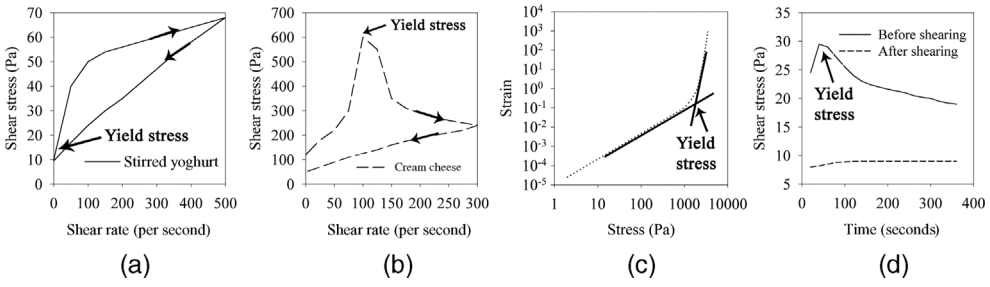

Fig. 7.8 The typical hysteresis loops in the flow curves (shear stress vs. shear rate) of a stirred yoghurt (a) and a cream cheese (b). The displacement profile (dotted line) of strain (deformation) vs. applied stress for a cream cheese sample (c). The shear stress as a function of time measured using the vane geometry at a certain rotation rate for a custard model (d). The assigned yield stresses are marked in figures. Adapted from Ramaswamy and Ak (1991), Sanchez *et al*. (1994), Kealy (2006) and Doublier and Durand (2008).

sample to flow a short distance because of a large zero-shear viscosity ($>10\,000$ Pa $\cdot$ s) or a high resistance to deformation. Therefore, the applied stress on the semi-solid samples needs to reach a certain level – a 'yield stress' – to make the sample flow with a measurable viscosity.

Yield stress is an important parameter for the sensory quality and the engineering calculations of semi-solid products. Kealy (2006) indicated that cream cheeses with a larger yield stress corresponded to higher sensory panel scores for hardness and adhesiveness. Breidinger and Steffe (2001) established a texture map of yield stress vs. yield strain for various cream cheese samples. This approach showed that a decrease in yield stress corresponded to an increase in yield strain. Fat-free cream cheese showed the highest yield stress (the lowest yield strain), while whipped cream cheese exhibited the lowest yield stress (the highest yield strain), corresponding to differences in spreadability (Breidinger and Steffe, 2001). In the same study, it was suggested that a texture map could be used for determining acceptable levels of spreadability in quality control and product development applications. Yield stress is involved in engineering calculation for semi-solid products, which has been covered by several engineering books and reviews (Steffe, 1996; Steffe and Daubert, 2006).

7.4.3 Viscoelastic properties of semi-solid dairy products

Dynamic oscillatory testing can provide very useful information on the gel formation process of semi-solid dairy products such as yoghurt. The effects of processing variables, especially preheating of milks, on the formation and properties of gels prepared by acidification with glucono-δ-lactone (GDL) have been extensively studied (van Vliet and Keetels, 1995; Lucey *et al*., 1997a, 1997b, 1999). Preheating milk resulted in a

reduction in gelation time and a significant increase in firmness (G') of the gels. According to van Vliet and Keetels (1995), the deformation of gels is proportional to the number of contact points per cross section of the network. Cross-linking by heat-denatured whey proteins within gels from heated milk could be responsible for increased G' of the network (Lucey *et al*., 1997a, 1998). Using confocal scanning laser microscopy, Lucey *et al*. (1998) found that heating milks at ~80°C resulted in a microstructure of GDL-induced acid gels that appeared 'branched' and had a higher 'apparent interconnectivity' of aggregates compared to unheated or less severely heated milks, which had irregular clusters and strands making up the network and less 'apparent interconnectivity'.

The effect of composition on acid milk gels was studied using small strain rheology. When the native fat globule membrane is intact, fat globules act as inert fillers, since they do not interact with casein (van Vliet, 1988). Increasing the volume fraction of fat having intact native membrane resulted in a decrease in G' of acid milk gels (van Vliet and Dentener-Kikkert, 1982). On the contrary, gels made with homogenised milk had an increase in G' since the native fat globule membrane was replaced by casein and whey protein, allowing for interactions between fat globule membrane and the protein matrix. Native whey proteins have been found to act as fillers in yoghurt. Lucey *et al*. (1999) showed that addition of whey protein concentrates to yoghurt milk, after milk had been heated, resulted in the reduction of G' and shear stress at yielding. The influence of stabilisers on yoghurt has been studied (Everett and McLeod, 2005). With increasing concentration of adsorbing polymer (pectin and carrageenan), the stabilisation–destabilisation mechanisms undergo transitions from (i) bridging flocculation (decrease in G'), to (ii) steric stabilisation (increased G' and phase angle), to (iii) depletion flocculation by unadsorbed polysaccharide in the serum phase (increased phase angle). For non-adsorbing polysaccharides (guar, locust bean and xanthan gums), increasing concentration led to a transition from depletion flocculation to colloidal particles trapped in a viscous polymer network as shown by a decrease and then increase in G' (Syrbe *et al*., 1998).

7.5 EFFECT OF ORAL PROCESSING ON INTERPRETATION OF RHEOLOGICAL MEASUREMENT

Texture is an essential part of the whole spectrum of sensory properties of foods. Consumers find texture more important in solid foods than liquids (Matsumoto and Matsumoto, 1977). The breaking down of solid foods and the mixing with saliva during chewing lead to changes in texture perception of solid foods far more than the change in viscosity

of liquid foods. As previously stated, one major goal of instrumental tests, including rheological measurements, is to relate the results with sensory perception. It is challenging to find a good correlation between instrumental test and oral perception because humans simultaneously detect many aspects of material properties including flavor, aroma, texture, appearance, color, and sound (Nishinari, 2004). The processing occurring in the mouth during eating can have a big impact on sensory perception. Therefore, the effect of oral processing should be considered in interpreting the rheological results.

Factors contributing to the final texture perception are initial product characteristics, oral processing, the stimuli from the receptors and their integration in the brain to a conscious perception (van Vliet *et al*., 2009). Recently, the role of oral processing in sensory perception has been the subject of much interest. Important processes in the mouth during chewing solid foods such as cheese include fracturing during biting and chewing, water uptake, dissolving, lubrication, bolus formation, swallowing and clearing (van Vliet *et al*., 2009). Hutchings and Lillford (1988) proposed that food will be swallowed only after its structure has been broken down far enough to obtain particles below a certain size and the food has been moistened sufficiently by saliva, allowing the formation of the bolus. The size of the bolus that is swallowed depends on foods and the ability of individuals to grind foods. The swallowing threshold is affected by product characteristics and oral physiology such as the saliva flow rate. Using computer simulations to study the chewing of Brazil nuts and raw carrots, Prinz and Lucas (1997) found that the masticatory system of humans is highly responsive to changes in food texture. During mastication of solid foods, the particles mix with saliva and form more or less a coherent bolus. Food particles could also stick to the oral mucosa. Factors determining whether particles aggregate or stick to the mucosa are the work of adhesion between food–food and food–mucosal interfaces, the surface tension of fluid in the mouth, its viscosity and the frictional resistance needed to displace food particles from the mucosa by the tongue (Prinz and Lucas, 1997; Lucas *et al*., 2004). For semi-solid dairy products, sensory attributes that are important to consumer perception are firmness, crumbliness, creaminess, stickiness, spreadability, and consistency (van Vliet *et al*., 2009). Oral processing between the tongue and palate becomes more important with adhesion and creaminess. Important textural attributes of liquid foods include thickness, sliminess, creaminess, roughness, fattiness, and the after-feel texture of the coating formed on the mucosa (van Vliet *et al*., 2009). Oral processing mainly involves the tongue, which pushes down the throat followed by swallowing.

In order to get a clear understanding of the texture perception of solid foods, a thorough background in fracture mechanics and the

interaction between foods and saliva, oral physiology and sensory sciences is needed. Yielding behaviour and adhesion between food particles and oral mucosa are also important for semi-solid foods. For liquid foods, rheological properties of the products, their adhesion to oral surfaces, the interaction between the products and saliva and their effect on lubrication, as well as the formation of coatings, are important in the perception during oral processing.

REFERENCES

Abu-Jdayil, B. (2003) Modelling the time-dependent rheological behavior of semi-solid foodstuffs. *Journal of Food Engineering* **57**(1), 97–102.

Adhikari, K., Heymann, H. and Huff, H.E. (2003) Textural characteristics of lowfat, fullfat and smoked cheeses: sensory and instrumental approaches. *Food Quality and Preference* **14**(3), 211–218.

Ak, M.M. and Gunasekaran, S. (1992) Stress-strain curve analysis of cheddar cheese under uniaxial compression. *Journal of Food Science* **57**(5), 1078–1081.

Ak, M.M. and Gunasekaran, S. (1997) Anisotropy in tensile properties of Mozzarella cheese. *Journal of Food Science* **62**(5), 1031–1033.

Ak, M.M., Bogenrief, M.D., Gunasekaran, S. and Olson, N.F. (1993) Rheological evaluation of mozzarella cheese by uniaxial horizontal extension. *Journal of Texture Studies* **24**(4), 437–453.

Anema, S.G., Lowe, E.K. and Li, K. (2004) Effect of pH on the viscosity of heated reconstituted skim milk. *International Dairy Journal* **14**(6), 541–548.

Bakshi, A.S. and Smith, D.E. (1984) Effect of fat content and temperature on viscosity in relation to pumping requirements of fluid milk products. *Journal of Dairy Science* **67**(6), 1157–1160.

Barnes, H.A. (1999) The yield stress – a review or '$\pi\alpha\nu\tau\alpha\ \rho\varepsilon\iota$' – everything flows? *Journal of Non-Newtonian Fluid Mechanics* **81**(1–2), 133–178.

Barnes, H.A. and Nguyen, Q.D. (2001) Rotating vane rheometry – a review. *Journal of Non-Newtonian Fluid Mechanics* **98**(1), 1–14.

Barnes, H.A. and Walters, K. (1985) The yield stress myth? *Rheologica Acta* **24**(4), 323–326.

Benezech, T. and Maingonnat, J.F. (1993) Flow properties of stirred yoghurt: structural parameter approach in describing time-dependency. *Journal of Texture Studies* **24**(4), 455–473.

Bienvenue, A., Jimenez-Flores, R. and Singh, H. (2003) Rheological properties of concentrated skim milk: influence of heat treatment and genetic variants on the changes in viscosity during storage. *Journal of Agricultural and Food Chemistry* **51**(22), 6488–6494.

Bird, R.B., Armstrong, R.C. and Hassager, O. (1987) *Dynamics of polymeric liquids Vol 1 Fluid Mechanics*, 2nd Edition. NewYork: Wiley, pp. 99–162.

Bloore, C.G. and Boag, I.F. (1981) Some factors affecting the viscosity of concentrated skim milk. *New Zealand Journal of Dairy Science & Technology* **16**, 143–154.

Breidinger, S.L. and Steffe, J.F. (2001) Texture map of cream cheese. *Journal of Food Science* **66**(3), 453–456.

Brown, J.A. (2002) Cheese Texture. M.S. Thesis, Raleigh, NC: North Carolina State University.

Brown, J.A., Foegeding, E.A., Daubert, C.R., Drake, M.A. and Gumpertz, M. (2003) Relationships among rheological and sensorial properties of young cheeses. *Journal of Dairy Science* **86**(10), 3054–3067.

Buckingham, J.H. (1978) Kinematic viscosities of New Zealand skim-milk. *Journal of Dairy Research* **45**(1), 25–35.

Camacho, M.M., Martinez-Navarrete, N. and Chiralt, A. (2005) Rheological characterization of experimental dairy creams formulated with locust bean gum (LBG) and λ-carrageenan combinations. *International Dairy Journal* **15**(3), 243–248.

Chang, Y.H. and Hartel, R.W. (1997) Flow properties of freeze-concentrated skim milk. *Journal of Food Engineering* **31**(3), 375–386.

Charalambides, M.N., Goh, S.M., Lim, S.L. and Williams, J.G. (2001) The analysis of the frictional effect on stress – strain data from uniaxial compression of cheese. *Journal of Materials Science* **36**(9), 2313–2321.

Christensen, C.M. (1987) Perception of solution viscosity. In: Moskowitz, H.R., editor. *Food Texture: Instrumental and Sensory Measurement*. New York: Marcel Dekker Inc., pp. 129–143.

Christensen, C.M. and Casper, L.M. (1987) Oral and nonoral perception of solution viscosity. *Journal of Food Science* **52**(2), 445–447.

Dewan, R.K., Bloomfield, V.A., Chudgar, A. and Morr, C.V. (1973) Viscosity and voluminosity of bovine milk casein micelles. *Journal of Dairy Science* **56**(6), 699–705.

Dickinson, E. and Goulding, I.C. (1980) Yield behavior of crumbly English cheeses in compression. *Journal of Texture Studies* **11**(1), 51–62.

Doublier, J.L. and Durand, S. (2008) A rheological characterization of semi-solid dairy systems. *Food Chemistry* **108**(4), 1169–1175.

Drake, M.A., Gerard, P.D., Truong, V.D. and Daubert, C.R. (1999) Relationship between instrumental and sensory measurements of cheese texture. *Journal of Texture Studies* **30**(4), 451–476.

Dzuy Nguyen, Q.C., Jensen, T.B. and Kristensen, P.G. (1998) Experimental and modelling studies of the flow properties of maize and waxy maize starch pastes. *Chemical Engineering Journal* **70**(2), 165–171.

Everett, D.W. and Olson, N.F. (2003) Free Oil and rheology of cheddar cheese containing fat globules stabilized with different proteins. *Journal of Dairy Science* **86**(3), 755–763.

Everett, D.W. and McLeod, R.E. (2005) Interactions of polysaccharide stabilisers with casein aggregates in stirred skim-milk yoghurt. *International Dairy Journal* **15**(11), 1175–1183.

Fernández-Martín, F. (1972) Influence of temperature and composition on some physical properties of milk and milk concentrates. II. Viscosity. *Journal of Dairy Research* **39**(65), 75–82.

Foegeding, E.A. and Drake, M.A. (2007) Invited review: sensory and mechanical properties of cheese texture. *Journal of Dairy Science* **90**(4), 1611–1624.

Foegeding, E.A., Brown, J., Drake, M.A. and Daubert, C.R. (2003) Sensory and mechanical aspects of cheese texture. *International Dairy Journal* **13**(8), 585–591.

Fox, P.F., Guinee, T.O., Cogan, T.M. and McSweeney, P.L.H. (2000) Cheese rheology and texture. In: Fox, P.F., Guinee, T.O., Cogan, T.M. and McSweeney, P.L.H., editors. *Fundamentals of Cheese Science (305–340)*. Gaithersburg, Maryland: Aspen Publishers, Inc., pp. 305–340.

Gamonpilas, C., Charalambides, M. and Williams, J. (2009) Determination of large deformation and fracture behaviour of starch gels from conventional and wire cutting experiments. *Journal of Materials Science* **44**(18), 4976–4986.

Goh, H.C. and Sherman, P. (1987) Influence of surface friction on the stress relaxation of Gouda cheese. *Journal of Texture Studies* **18**(4), 389–404.

Goh, S.M., Charalambides, M.N. and Williams, J.G. (2005) On the mechanics of wire cutting of cheese. *Engineering Fracture Mechanics* **72**(6), 931–946.

Griffin, M.C.A., Price, J.C. and Griffin, W.G. (1989) Variation of the viscosity of a concentrated, sterically stabilized, colloid: effect of ethanol on casein micelles of bovine milk. *Journal of Colloid and Interface Science* **128**(1), 223–229.

Gunasekaran, S. and Ak, M.M. (2003) *Cheese Rheology and Texture*. Boca Raton, FL: CRC Press.

Gwartney, E.A., Foegeding, E.A. and Larick, D.K. (2002) The texture of commercial full-fat and reduced-fat cheese. *Journal of Food Science* **67**(2), 812–816.

Halmos, A.L. and Tiu, C. (1981) Liquid foodstuffs exhibiting yield stress and shear degradability. *Journal of Texture Studies* **12**, 39–46.

Hamann, D.D., Zhang, J., Daubert, C.R., Foegeding, E.A. and Diehl, K.C. (2006) Analysis of compression, tension and torsion for testing food gel fracture properties. *Journal of Texture Studies* **37**(6), 620–639.

Hennelly, P.J., Dunne, P.G., O'Sullivan, M. and O'Riordan, E.D. (2006) Textural, rheological and microstructural properties of imitation cheese containing inulin. *Journal of Food Engineering* **75**(3), 388–395.

Hsieh, Y.L., Yun, J.J. and Rao, M.A. (1993) Rheological properties of Mozzarella cheese filled with dairy, egg, soy proteins, and gelatin. *Journal of Food Science* **58**(5), 1001–1004.

Hutchings, J.B. and Lillford, P.J. (1988) The perception of food texture – the philosophy of the breakdown path. *Journal of Texture Studies* **19**(2), 103–115.

Jenness, R. (1999) Composition of milk. In: Wong, N.P., Jenness, R., Keeney, M. and Marth, E.H., editors. *Fundamentals of Dairy Chemistry*, 3rd Edition. Maryland: Aspen Publishers, Inc., pp. 424–428.

Jeurnink, T.J.M. and de Kruif, K.G. (1993) Changes in milk on heating: Viscosity measurements. *Journal of Dairy Research* **60**(2), 139–150.

Kamyab, I., Chakrabarti, S. and Williams, J.G. (1998) Cutting cheese with wire. *Journal of Materials Science* **33**(11), 2763–2770.

Karlsson, A.O., Ipsen, R., Schrader, K. and Ardö, Y. (2005) Relationship between physical properties of casein micelles and rheology of skim milk concentrate. *Journal of Dairy Science* **88**(11), 3784–3797.

Kavanagh, G.M. and Ross-Murphy, S.B. (1998) Rheological characterization of polymer gels. *Progress in Polymer Science* **23**, 533–562.

Kealy, T. (2006) Application of liquid and solid rheological technologies to the textural characterisation of semi-solid foods. *Food Research International* **39**(3), 265–276.

Keogh, M.K. and O'Kennedy, B.T. (1998) Rheology of stirred yogurt as affected by added milk fat, protein and hydrocolloids. *Journal of Food Science* **63**(1), 108–112.

Keogh, M.K., Murray, C.A. and O'Kennedy, B.T. (2003) Effects of ultrafiltration of whole milk on some properties of spray-dried milk powders. *International Dairy Journal* **13**(12), 995–1002.

Kyazze, G. and Starov, V. (2004) Viscosity of milk: Influence of cluster formation. *Colloid Journal* **66**(3), 316–321.

Langley, K.R. and Marshall, R.J. (1993) Jaw movement during mastication of fibrous and nonfibrous composite foods by adult subjects. *Journal of Texture Studies* **24**(1), 11–25.

Langley, K.R. and Temple, D.M. (1985) Viscosity of heated skim milk. *Journal of Dairy Research* **52**, 223–227.

Lawlor, J.B. and Delahunty, C.M. (2000) The sensory profile and consumer preference for ten speciality cheeses. *International Journal of Dairy Technology* **53**(1), 28–36.

Lelievre, J., Mirza, I.A. and Tung, M.A. (1992) Failure testing of gellan gels. *Journal of Food Engineering* **16**(1–2), 25–37.

Lucas, P.W., Prinz, J.F., Agrawal, K.R. and Bruce, I.C. (2004) Food texture and its effect on ingestion, mastication and swallowing. *Journal of Texture Studies* **35**(2), 159–170.

Lucey, J.A., Johnson, M.E. and Horne, D.S. (2003) Invited review: perspectives on the basis of the rheology and texture properties of cheese. *Journal of Dairy Science* **86**(9), 2725–2743.

Lucey, J.A., Munro, P.A. and Singh, H. (1999) Efects of heat treatment and whey protein addition on the rheological properties and structure of acid skim milk gels. *International Dairy Journal* **9**, 275–279.

Lucey, J.A., Cheng, T.T., Munro, P.A. and Singh, H. (1997a) Rheological properties at small (dynamic) and large (yield) deformations of acid gels made from heated milk. *Journal of Dairy Research* **64**, 591–600.

Lucey, J.A., Mishra, R., Hassan, A. and Johnson, M.E. (2005) Rheological and calcium equilibrium changes during the ripening of Cheddar cheese. *International Dairy Journal* **15**(6–9), 645–653.

Lucey, J.A., Teo, C.T., Munro, P.A. and Singh, H. (1998) Microstructure, permeability and appearance of acid gels made from heated skim milk. *Food Hydrocolloids* **12**(2), 159–165.

Lucey, J.A., van Vliet, T., Grolle, K., Geurts, T. and Walstra, P. (1997b) Properties of acid casein gels made by acidification with glucono-δ-lactone. 1. Rheological properties. *International Dairy Journal* **7**, 381–388.

Luyten, H., van Vliet, T. and Walstra, P. (1991) Characterization of the consistency of Gouda cheese: rheological properties. *Netherland Milk Dairy Journal* **45**, 33–53.

Ma, L., Drake, M.A., Barbosa-CÁnovas, G.V. and Swanson, B.G. (1996) Viscoelastic properties of reduced-fat and full-fat Cheddar cheeses. *Journal of Food Science* **61**(4), 821–823.

Malkin, A.Y. and Isayev, A.I. (2006) *Rheology – Concepts, Methods, & Applications*. Toronto, Canada: ChemTec Publishing.

Marchesseau, S., Gastaldi, E., Lagaude, A. and Cuq, J.L. (1997) Influence of pH on protein interactions and microstructure of process cheese. *Journal of Dairy Science* **80**(8), 1483–1489.

Matsumoto, N. and Matsumoto, F. (1977) Taste of food. Factors related to the evaluation. *Japan Journal of Cookery Science* **10**, 97–101.

McCarthy, O.J. and Singh, H. (2009) Physico-chemical properties of milk. In: Fox, P.F. and McSweeney, P., editors. *Advanced Dairy Chemistry. Volume 3: Lactose, Water, Salts and Minor Constituents*. New York: Springer.

Meullenet, J.F., Finney, M.L. and Gaud, M. (2002) Measurement of biting velocities, and predetermined and individual crosshead speed instrumental imitative tests for predicting cheese hardness. *Journal of Texture Studies* **33**(1), 45–58.

Mezger, T. (2006) *The Rheology Handbook: For Users of Rotational and Oscillatory Rheometers*. Hannover, Germany: Vincentz Network.

Michalski, M.C., Cariou, R., Michel, F. and Garnier, C. (2002) Native vs. Damaged milk fat globules: membrane properties affect the viscoelasticity of milk gels. *Journal of Dairy Science* **85**(10), 2451–2461.

Mortazavian, A., Rezaei, K. and Sohrabvandi, S. (2009) Application of advanced instrumental methods for yogurt analysis. *Critical Reviews in Food Science and Nutrition* **49**(2), 153–163.

Mounsey, J.S. and O'Riordan, E.D. (1999) Empirical and dynamic rheological data correlation to characterize melt characteristics of imitation cheese. *Journal of Food Science* **64**(4), 701–703.

Nishinari, K. (2004) Rheology, food texture, and mastication. *Journal of Texture Studies* **35**, 113–124.

Nolan, E.J., Holsinger, V.H. and Shieh, J.J. (1989) Dynamic rheological properties of natural and imitation Mozzarella cheese. *Journal of Texture Studies* **20**(2), 179–189.

O'Donnell, H.J. and Butler, F. (2002) Time-dependent viscosity of stirred yogurt. Part I: Couette flow. *Journal of Food Engineering* **51**(3), 249–254.

Peleg, M. (1987) The basics of solid foods rheology. In: Moskowitz, H.R., editor. *Food Texture: Instrumental and Sensory Measurement*. New York, NY: Marcel Dekker, pp. 3–33.

Pesenti, V. and Luginbühl, W. (1999) Assessment of cohesion in Gruyere-type cheese by rheological methods. *Journal of Texture Studies* **30**(1), 1–16.

Phillips, L.G., Mcgiff, M.L., Barbano, D.M. and Lawless, H.T. (1995a) The influence of fat on the sensory properties, viscosity, and color of lowfat milk. *Journal of Dairy Science* **78**(6), 1258–1266.

Phillips, L.G., Mcgiff, M.L., Barbano, D.M. and Lawless, H.T. (1995b) The influence of nonfat dry milk on the sensory properties, viscosity, and color of lowfat milks. *Journal of Dairy Science* **78**(10), 2113–2118.

Phipps, L.W. (1969) The interrelationship of the viscosity, fat content and temperature of cream between 40° and 80°C. *Journal of Dairy Research* **36**, 417–426.

Prentice, J.H. (1992) *Dairy Rheology. A Concise Guide*. New York, NY: VCH.

Prinz, J.F. and Lucas, P.W. (1997) An optimization model for mastication and swallowing in mammals. *Proceedings of the Royal Society B. Biological Sciences* **264**(1389), 1715–1721.

Ramaswamy, H.S. and Basak, S. (1991) Rheology of stirred yogurts. *Journal Texture Studies* **22**(2), 231–241.

Ramaswamy, H.S. and Basak, S. (1992) Time dependent stress decay rheology of stirred yogurt. *International Dairy Journal* **2**(1), 17–31.

Rao, V.N.M. and Skinner, G.E. (1986) Rheological properties of solid foods. In: Rao, M.A. and Rizvi, S.S.H., editors. *Engineering Properties of Foods*. New York, NY: Marcel Dekker, pp. 215–254.

Rogers, N.R., Drake, M.A., Daubert, C.R., McMahon, D.J., Bletsch, T.K. and Foegeding, E.A. (2009) The effect of aging on low-fat, reduced-fat, and full-fat Cheddar cheese texture. *Journal of Dairy Science* **92**(10), 4756–4772.

Rosenthal, A.J. (1999) *Food Texture – Measurement and Perception*. Gaithersburg, Maryland: Aspen Publishers, Inc.

Rynne, N.M., Beresford, T.P., Kelly, A.L. and Guinee, T.P. (2004) Effect of milk pasteurization temperature and in situ whey protein denaturation on the composition, texture and heat-induced functionality of half-fat Cheddar cheese. *International Dairy Journal* **14**(11), 989–1001.

Sanchez, C., Beauregard, J.L., Chassagne, M.H., Duquenoy, A. and Hardy, J. (1994) Rheological and textural behaviour of double cream cheese. II: Effect of curd cooling rate. *Journal of Food Engineering* **23**(4), 595–608.

Shama, F. and Sherman, P. (1973) Evaluation of some textural properties of foods with the instron universal testing machine. *Journal of Texture Studies* **4**(3), 344–352.

Sherbon, J.W. (1999) Physical properties of milk. In: Wong, N.P., Jenness, R., Keeney, M. and Marth, E.H., editors. *Fundamentals of Dairy Chemistry*, 3rd Edition. Maryland: Aspen Publishers, Inc.; pp. 424–428.

Snoeren, T.H.M., Damman, A.J. and Klok, H.J. (1982) The viscosity of skim milk concentrate. *Netherland Milk and Dairy Journal* **36**, 305–316.

Snoeren, T.H.M., Brinkhuis, J.A., Damman, A.J. and Klok, H.J. (1984) Viscosity and age-thickening of skim-milk concentrate. *Netherlands Milk and Dairy Journal* **38**, 43–53.

Sodini, I., Remeuf, F., Haddad, S. and Corrieu, G. (2004) The relative effect of milk base, starter, and process on yogurt texture: a review. *Critical Reviews in Food Science and Nutrition* **44**(2), 113–137.

Solanki, G. and Rizvi, S.S.H. (2001) Physico-chemical properties of skim milk retentates from microfiltration. *Journal of Dairy Science* **84**(11), 2381–2391.

Stading, M. and Hermansson, A.M. (1991) Large deformation properties of P-lactoglobulin gel structures. *Food Hydrocolloids* **5**, 339–352.

Steffe, J.F. (1996) *Rheological Methods in Food Process Engineering*, 2nd Edition. Michigan: Freeman Press.

Steffe, J.F. and Daubert, C.R. (2006) *Bioprocessing Pipelines: Rheology and Analysis*. Michigan: Freeman Press.

Subramanian, R. and Gunasekaran, S. (1997) Small amplitude oscillatory shear studies on Mozzarella cheese part I. Region of linear viscoelasticity. *Journal of Texture Studies* **28**(6), 633–642.

Syrbe, A., Bauer, W.J. and Klostermeyer, H. (1998) Polymer science concepts in dairy systems – an overview of milk protein and food hydrocolloid interaction. *International Dairy Journal* **8**(3), 179–193.

Tang, J., Lelievre, J., Tung, M.A. and Zeng, Y. (1994) Polymer and ion concentration effects on gellan gel strength and strain. *Journal of Food Science* **59**(1), 216–220.

Tárrega, A., Durán, L. and Costell, E. (2004) Flow behaviour of semi-solid dairy desserts. Effect of temperature. *International Dairy Journal* **14**(4), 345–353.

Tárrega, A., Durán, L. and Costell, E. (2005) Rheological characterization of semisolid dairy desserts. Effect of temperature. *Food Hydrocolloids* **19**(1), 133–139.

Truong, V.D. and Daubert, C.R. (2001) Textural characterization of cheeses using vane rheometry and torsion analysis. *Journal of Food Science* **66**(5), 716–721.

Truong, V.D., Daubert, C.R., Drake, M.A. and Baxter, S.R. (2002) Vane rheometry for textural characterization of cheddar cheeses: correlation with other instrumental and sensory measurements. *Lebensmittel-Wissenschaft Und-Technologie* **35**(4), 305–314.

Tunick, M.H. (2000) Rheology of dairy foods that gel, stretch, and fracture. *Journal of Dairy Science* **83**(8), 1892–1898.

Tunick, M.H., Mackey, K.L., Shieh, J.J., Smith, P.W., Cooke, P. and Malin, E.L. (1993a) Rheology and microstructure of low-fat Mozzarella cheese. *International Dairy Journal* **3**(7), 649–662.

Tunick, M.H., Malin, E.L., Smith, P.W., Shieh, J.J., Sullivan, B.C., Mackey, K.L. and Holsinger, V.H. (1993b) Proteolysis and rheology of low fat and full fat Mozzarella cheeses prepared from homogenized milk. *Journal of Dairy Science* **76**(12), 3621–3628.

Tunick, M.H., Nolan, E.J., Shieh, J.J., Basch, J.J., Thompson, M.P., Maleeff, B.E. and Holsinger, V.H. (1990) Cheddar and cheshire cheese rheology. *Journal of Dairy Science* **73**(7), 1671–1675.

Tung, M.A. (1978) Rheology of protein dispersions. *Journal of Texture Studies* **9**(1), 3–13.

Udyarajan, C.T., Horne, D.S. and Lucey, J.A. (2007) Use of time–temperature superposition to study the rheological properties of cheese during heating and cooling. *International Journal of Food Science and Technology* **42**(6), 686–698.

Ustunol, Z., Kawachi, K. and Steffe, J. (1994) Arnott test correlates with dynamic rheological properties for determining Cheddar cheese meltability. *Journal of Food Science* **59**(5), 970–971.

Van Hekken, D.L., Tunick, M.H. and Park, Y.W. (2004) Rheological and proteolytic properties of Monterey Jack goat's milk cheese during aging. *Journal of Agricultural and Food Chemistry* **52**(17), 5372–5377.

van Vliet, T. (1988) Rheological properties of filled gels. Influence of filler matrix interaction. *Colloid & Polymer Science* **266**(6), 518–524.

van Vliet, T. (1991) Inventory of test methods. In: *Anonymous. Rheological and fracture properties of cheese. Bulletin of the International Dairy Federation*, Vol. **268**. Brussels, Belgium: I.D.F., pp. 16–25.

van Vliet, T. and Dentener-Kikkert, A. (1982) Influence of the composition of the milk fat globule membrane on the rheological properties of acid milk gels. *Netherlands Milk and Dairy Journal* **36**, 261–265.

van Vliet, T. and Keetels, C.J.A.M. (1995) Effect of preheating of milk on the structure of acidified milk gels. *Netherlands Milk and Dairy Journal* **49**, 27–35.

van Vliet, T. and Peleg, M. (1991) Effects of sample size and preparation. *Rheological and Fracture Properties of Cheese. Bulletin of the International Dairy Federation*, Vol. **268**. Brussels, Belgium: I.D.F., pp. 26–29.

van Vliet, T. and Walstra, P. (1980) Relationship between viscosity and fat content of milk and cream. *Journal of Texture Studies* **11**, 65–68.

van Vliet, T., van Aken, G.A., de Jongh, H.H.J. and Hamer, R.J. (2009) Colloidal aspects of texture perception. *Advances in Colloid and Interface Science* **150**(1), 27–40.

Vélez-Ruiz, J.F. and Barbosa-Cánovas, G.V. (1998) Rheological properties of concentrated milk as a function of concentration, temperature and storage time. *Journal of Food Engineering* **35**(2), 177–190.

Vélez-Ruiz, J.F. and Barbosa-Cánovas, G.V. (2000) Flow and structural characteristics of concentrated milk. *Journal of Texture Studies* **31**(3), 315–334.

Vélez-Ruiz, J.F., Swanson, B.G. and Barbosa-Canovas, G.V. (1998) Flow and viscoelastic properties of concentrated milk treated by high hydrostatic pressure. *LWT-Food Science and Technology* **31**(2), 182–195.

Walstra, P. and Jenness, R. (1984) *Dairy Chemistry and Physics*. New York: Wiley.

Walstra, P., Luyten, H. and van Vliet, T. (1987) Consistency of cheese. Milk the vital force. *Proceedings of the XXII International Dairy Congress*, Netherlands: D Reidel Publishing Company, pp. 159–168.

Weber, W. (1956) Systematic investigation of falling ball viscometers with inclined tubes. *Kolloid Z.* **147**, 14–28.

Weltmann, R.N. (1943) Breakdown of thixotropic structure as function of time. *Journal of Applied Physics* **14**, 343–350.

Wium, H., Qvist, K.B. and Gross, M. (1997) Uniaxial compression of UF-Feta cheese related to sensory texture analysis. *Journal of Texture Studies* **28**(4), 455–476.

Yaşar, K., Kahyaoglu, T. and Şahan, N. (2009) Dynamic rheological characterization of salep glucomannan/galactomannan-based milk beverages. *Food Hydrocolloids* **23**(5), 1305–1311.

8 Relationship between Food Rheology and Perception

John R. Mitchell and Bettina Wolf

8.1 INTRODUCTION

The study of the relationship between rheology and perception has a long history. Studies in this area have two related objectives:

(i) Prediction of perception from instrumental rheological measurements. There are clearly considerable practical advantages in using instruments instead of sensory panels.
(ii) The development of an understanding of the relationship between food structure and perception. Rheology is not the only tool that can be used to help achieve this understanding, but it is an important one.

Although not completely incompatible, food science and rheology often make less than satisfactory bedfellows (Mitchell, 1984). The reason for this is that foods are generally inhomogeneous on quite large distance scales and many natural products, for example meat and fruits are anisotropic. This makes the application and interpretation of fundamental rheological tests difficult. There is a long history of development and use of empirical test methods particularly for quality control purposes. In this context, readers might be interested in the short and slightly sad paper written by Scott Blair (Blair, 1978), one of the founders of food rheology.

A significant advance in the context of the aforementioned objective (i) was the development of the Texture Profile by scientists working for General Foods (Friedman *et al*., 1963; Szczesniak, 1963). This recognised that food texture was multidimensional and aimed at building a direct relationship between sensory and instrumental measurements of these different dimensions. The instrumental approach was almost entirely empirical. It involved the two bite test. The food was compressed

Practical Food Rheology: An Interpretive Approach
Edited by Ian T. Norton, Fotios Spyropoulos and Philip Cox
 ISBN: 978-1-405-19978-0

twice and the texture dimensions, for example hardness, cohesiveness and adhesiveness, could be calculated from the force response. This approach is still extensively used. For example, it is one of the standard software packages on commercial instruments for the measurement of food texture. There have been early attempts to consider this approach in more fundamental rheological terms, but in the authors' opinion, there is little point in doing so. Texture profiling can be useful, but it is some way from what most people would regard as rheology. A good discussion of empirical measurements of food texture is given in the book by Bourne (2002), and elements of this are addressed in other chapters in the current volume.

This contribution focuses on the relationship between perception and fundamental rheological parameters. The work considered will be on liquids or gels, since these are isotropic and homogenous and therefore more amenable to a fundamental rheological approach. Of course, the word homogenous needs to be associated with a distance scale, but in this context, emulsions such as milk are considered homogenous, whereas a meat chunk in gravy product is not.

The topics covered are as follows:

(i) Rheology and thickness perception.
(ii) Rheology and flavour perception.
(iii) Mixing, microstructure, mouthfeel and gels.
(iv) Beyond shear rheology.

Following guidance from the editors, this chapter will focus more on (ii), (iii) and (iv), since there has been a considerable recent interest in this area by the lead author and colleagues at the University of Nottingham.

8.2 RHEOLOGY AND THICKNESS PERCEPTION

The relationship between the rheology of liquids and thickness perception should be the simplest to address experimentally. This is because at first sight, the only relevant rheological parameter is an instrumentally measured shear viscosity. Since most foods are non-Newtonian, i.e. viscosity depends on shear rate/shear stress, it is necessary to decide what the measurement conditions for the best correlation with sensory perception are. The first study that was done to determine the appropriate shear rate for the measurements of a viscosity which would correlate to thickness perception was carried out by Wood (1968). This approach involved using a sensory panel to compare the perceived thickness of non-Newtonian liquid foods (cream soups) with Newtonian glucose

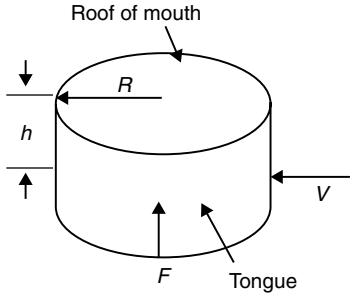

V = velocity of tongue (2 cm per second)
F = normal force (1 N)
R = radius of plug (2.5 cm)
t = time (per second)
h_0 = initial plug height (0.2 cm)
m = consistency index
n = power law index

(values in brackets are those assumed in the calculation of oral shear stress)

$$\tau = mV^n \left(\frac{1}{h_0^{(n+1)/n}} + \left(\frac{F}{R^{n+3}} \cdot \frac{n+3}{2\pi m} \right)^{1/n} \cdot \frac{(n+1)t}{2n+1} \right)^{n^2/(n+1)} \qquad (8.1)$$

Fig. 8.1 A model mouth geometry and the Kokini oral shear stress. Reproduced from Cook *et al*. (2003), with permission from Oxford University Press.

syrups. The viscosity curves (viscosity as a function of shear rate) of a soup and a glucose syrup of similar perceived viscosity will cross, and the shear rate where this occurs was considered to be the shear rate pertinent to thickness perception. The value for this shear rate that Wood found from his work was 50 per second. In recent work, this value is often still considered to be the appropriate shear rate for viscosity measurement if sensory perception studies are to be carried out subsequently.

Since Woods original work, there were many other studies. Shama and Sherman (Shama and Sherman, 1973) used a similar approach with a much wider range of foods. They reported a range of shear rates and shear stresses relevant to perception of viscosity, suggesting that the mechanism of perception was different for high-viscosity foods when compared to low-viscosity foods. At high viscosities, perception is driven by the stress required to shear the food at a shear rate of 10 per second, whereas for low-viscosity foods, the shear rate in response to a shear stress of 10 Pa drives perception. The shear stress and shear rate conditions for thickness perception from the Shama and Shermans' experimental work agree quite well with the results of a modelling approach developed by Kokini and co-workers (Dickie and Kokini, 1983; Kokini and Cussler, 1983; Kokini, 1985). This considered the liquid food as sheared between the tongue and the roof of the mouth (Fig. 8.1). One output from this approach is an oral shear stress defined by Equation 8.1 (see Fig. 8.1), which it can be argued is an appropriate parameter to relate to thickness perception. As discussed in the following text, the Kokini oral shear stress has often been used as a parameter for sensory studies of taste perception.

There are two limitations to predicting an oral perceived viscosity simply from the viscosity curve (viscosity–shear rate relationship). These are as follows:

(i) There will be other rheological parameters which must be important. For example, it has been shown (Cutler *et al*., 1983; Richardson *et al*., 1989) that weak gels such as xanthan gum solutions were perceived as being thicker than the measured steady shear viscosity shows. It was found that if a complex viscosity measured at a frequency of about 50 rad/s was used, then the perceived thickness could be predicted correctly (Richardson *et al*., 1989). This could be taken as showing that a dynamic viscosity is more appropriate for predicting perceived thickness than a steady shear viscosity, but there is no obvious direct mechanistic reason why this should be the case. A possible reason for under-predicting the perceived thickness of xanthan gum solution from shear viscosity measurements is that there is a stress overshoot when the elastic xanthan solution is sheared, and this peak stress rather than the equilibrium value is the relevant one for thickness perception.

(ii) Time effects will be important. Many non-Newtonian liquid foods are thixotropic, that is to say, the viscosity decreases not only with increasing shear rate but also with the time of shearing. This clearly complicates the measured liquid viscosity required to predict perceived thickness. As will be discussed in more detail below, dilution with saliva may also be important. To obtain the best correlation between perceived thickness and instrumental measurements, it is advisable to ask the panel to make the judgement immediately after the product enters the mouth.

8.3 RHEOLOGY AND FLAVOUR PERCEPTION

There is a long history of studies showing that if the viscosity of a solution is increased, for example by adding a hydrocolloid, there is a reduction in perceived flavour or taste (Stone *et al*., 1974). The mechanism for this is a matter of debate. Perception of flavour comes initially from a combination of taste which is perceived in the mouth and volatiles which are perceived in the nose. The reduction in perception with viscosity is found for a wide variety of thickeners though, as demonstrated below, starch may be an important exception. This generality of the effect argues against a specific binding between the volatile and the thickener being the ubiquitous mechanism, though there have been several studies where this has been suggested for specific cases. In a series of particularly valuable studies, Baines and Morris (1987, 1988,

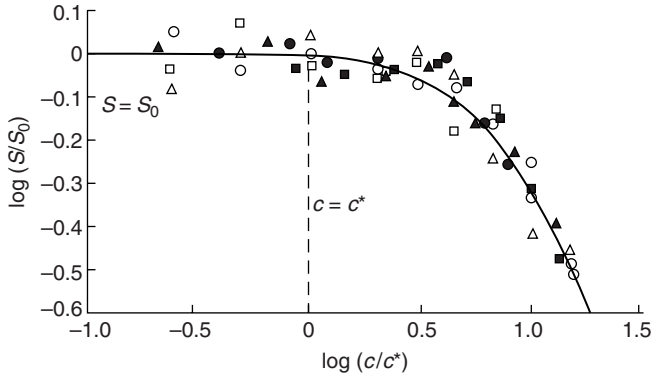

Fig. 8.2 Flavour/taste suppression by random coil polysaccharides. Results (mean values of panel scores for sweetness and flavour intensity) are shown for alginate (▲), carboxymethylcellulose of high (■) and medium (●) molecular weight, and guar gum of high (□), medium (○) and low (△) molecular weight. Reproduced from Baines and Morris (1988), with permission from Oxford University Press.

1989) compared the relationship between the perceived flavour and the concentration of a hydrocolloid. The results showed that perception decreased when the concentration of the hydrocolloid c exceeded the c^* concentration. The latter is the concentration where the hydrodynamic domains of the polymer coils start to overlap. Above this concentration, non-Newtonian behaviour becomes much more pronounced because of disruption of entanglements between coils with increasing shear rate and the concentration dependence of the zero shear rate viscosity changes from an approximately linear dependence to a dependence on $c^{3–4}$.

In these studies, magnitude estimation was used by the panel to estimate the degree of inhibition of taste and flavour perception. This involved the panel being told to rate the product relative to a value of 100 for the control containing no thickener. Thus, if a thickened product was perceived as being half as sweet as the control, then it would be given a score of 50. Fig. 8.2 displays the relationship between the S/S_O, where S and S_O is the score for the thickened product and the unthickened control, respectively, and c/c^*.

The obvious question is what is the mechanism responsible for this decrease in perception? One hypothesis is that the release of volatiles from the solution is decreased once the concentration exceeds c^*. Following the development of a direct interface between air exhaled from the nose and a Mass Spectrometer developed by Taylor and Linforth (Taylor *et al.*, 2000), it was possible to test this. For solutions thickened by hydroxypropylmethyl cellulose (HPMC), the flavour perception measured by a sensory panel was in agreement with the Baines and Morris results shown in Fig. 8.2. There was however no significant difference in the concentration of the volatile detected in the nose as the HPMC

concentration exceeded c^* (Hollowood *et al*., 2002). Therefore, the hypothesis that binding of the volatile to the thickener or inhibition of volatile release in some other way causes the decrease in perception can be rejected. As stated earlier, this does not mean that there are not specific cases of binding of volatiles or indeed tastants which can be important, such as in the entrapment of flavour molecules in the amylose helix.

A second hypothesis is that there is a direct relationship between the rheology of the solution and perception. In a comprehensive study, Cook *et al*. (2003) investigated the relationship between various viscosity-related parameters and taste perception and found the strongest dependence on the Kokini oral shear stress defined by Equation 8.1. Of course, a viscosity dependence of perception must result from the relationship shown in Fig. 8.2, but it is of interest that a parameter which may be a somewhat better indication of thickness perception than, for example, the viscosity at a shear rate of 50 per second gives the best prediction of perception. Since the hypothesis of a decrease in volatile release with increasing viscosity can be rejected as discussed above, then there are two further hypotheses that should considered:

(i) Viscosity reduces the extent and/or rate at which the tastant reaches the taste receptors on the tongue and palate.
(ii) The signal reaching the brain related to the oral shear stress, when processed in combination with the signals from the taste and volatile receptors, influences the total perception.

The second hypothesis was suggested by Cook *et al.* (2002, 2003) to explain the oral shear stress dependence. This multimodal idea where the response of the brain to changes in apparently unrelated signals results in perturbation of the 'perception' of the particular response of interest is very general. It is a very important and exciting aspect of food science which is developing rapidly, partly because the increasing ease with which brain activity can be monitored during food consumption. Partly because it is less directly related to rheology, this will not be discussed further in the remainder of this chapter.

In addressing hypothesis 1, it is helpful to have exceptions to the general relationship between viscosity and perception as found by Baines and Morris (1988) and Cook *et al*. (2003). One of these is solutions thickened by gelatinised starch. In view of the importance of starch as a thickener, it is surprising that not more work has been carried out on flavour perception from starch-thickened systems. Hill *et al.* (1995) related the sensory parameters of a lemon pie filling thickened with cornflour with a range of dynamic rheological parameters. Although dynamic rheological data were used, it was clear that when these results

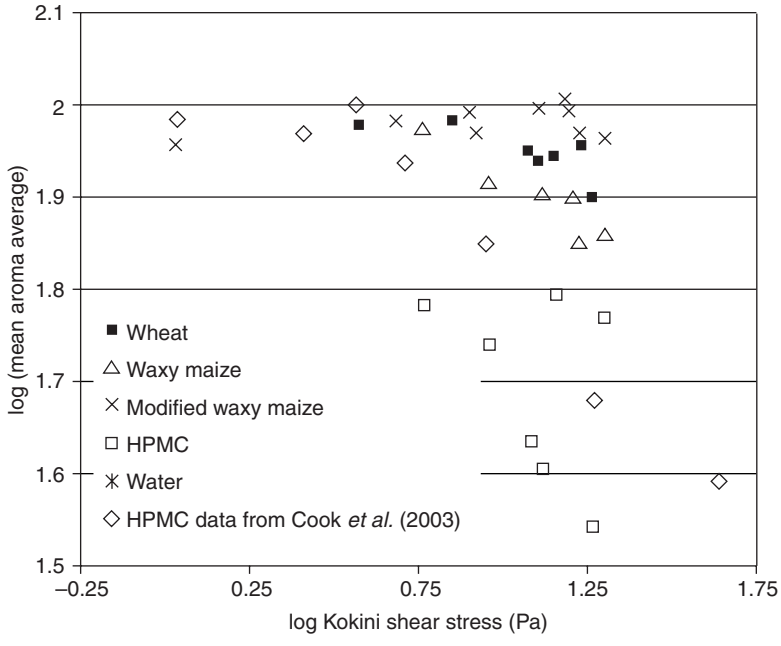

Fig. 8.3 Comparison of perceived flavour from Cook *et al*. (2003) data on banana-flavoured sweet HPMC samples and data from a study on basil-flavoured savoury systems. (Reproduced from Ferry *et al*., 2006a. Copyright 2006, with permission from Elsevier.)

were considered in the light of the Baines and Morris' studies and the later work of Cook *et al.*, these starch-thickened products gave a much better taste and flavour perception than would be expected based on the ideas developed for the much more extensively studied 'linear' hydrocolloids. A possible mechanism which would support hypothesis (i) above, first proposed by Baines and Morris for hydrocolloid-thickened systems used for the results in Fig. 8.2, was that above the c^* concentration, mixing of the viscous solution (in the mouth with saliva) was restricted. In the next section, the hypothesis that the difference between the perception of high-viscosity starch-thickened and hydrocolloid-thickened products is due to differences in mixing is explored.

8.4 MIXING, MICROSTRUCTURE, GELS AND MOUTHFEEL

8.4.1 Mixing

The better flavour perception from starch-thickened foods when compared to those thickened by linear polysaccharides was confirmed in the study by Ferry *et al*. (2006a), who compared hydroxypropylmethyl cellulose and starch-thickened systems directly. Fig. 8.3 shows the

perception results plotted against the oral shear stress parameter which Cook *et al*. (2003) suggested was the driver for taste perception.

There is more data scatter from an ideal curve compared to some of the previous study of Cook *et al.* on HPMC-thickened systems, which is also included in the Figure. This may be due to the high temperature used by the sensory panel, since the study by Ferry and colleagues was required to be relevant to soup products. Nevertheless, it is clear that perception from the starch-thickened systems at high values of the oral shear stress is much better than that from the HPMC-thickened solution. Indeed, when wheat starch and modified waxy maize starch are used as thickeners, it could be argued that there is no inhibition of taste even at the highest value of oral shear stress measured. If the mixing hypothesis is to survive, it would therefore be expected that a starch-thickened solution would mix better with water than a hydrocolloid (linear polysaccharide) solution. To investigate this, Ferry *et al*. (2006a) used the simple approach of hand mixing a coloured high-viscosity 'solution' (380 mPa · s at 50 per second and 25°C) with water. The differences between the starch and the hydrocolloid-thickened solution were quite dramatic. The results in Figs. 8.2 and 8.3 would suggest that for the linear polysaccharide, there should be a change in mixing ability in the vicinity of the $c*$ concentration. Subsequent work by Koliandris *et al*. (2008) with locust bean gum showed that this is indeed the case. The photographs reproduced in Fig. 8.4 illustrate these two related ideas showing the difference in mixing between the appearance of the HPMC- and starch-thickened systems mixed at comparable viscosity and the change in locust bean gum-thickened systems as the concentration is increased from 0.5 to 0.6%.

The reason why decreasing mixing efficiency should reduce flavour perception is clear. For a tastant to be perceived, it has to reach the taste receptor. This receptor will be coated by a static boundary layer of fluid, and diffusion will be the only mechanism through which the tastant can be finally transported to the receptor. Diffusion processes however are extremely slow. For example, for small molecules or ions such as Na^+, the diffusion coefficient in water or in the gel is $\sim 10^{-9}$ m^2/s. It is easy to show that even after 100 seconds, almost none of the molecular species will have moved a distance of 1 mm from the surface of a gel sphere with a diameter of 1 mm if diffusion is the only transport mechanism (Crank *et al*., 1981). Thus if mixing is poor, there will be regions which retain the original high viscosity/weak gel consistency of the ingested product. Between these regions, there will be other regions with a low concentration of tastant. If some of these low-concentration regions are at the surface of the fluid boundary layer coating, the taste receptor there will be a reduction in the driving force for diffusion across this boundary layer. The simple mixing experiment is of course not directly relevant to the distance scale of mixing or concentrations of tastants in the

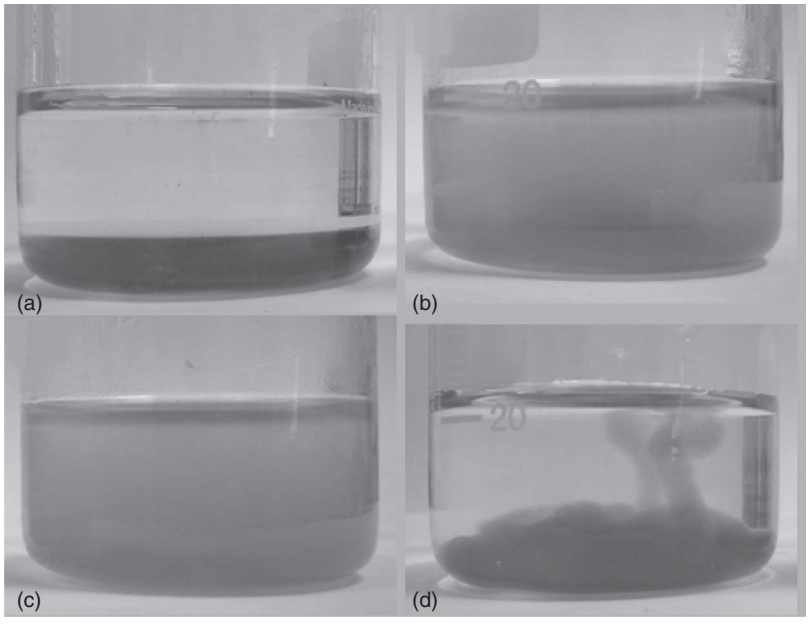

Fig. 8.4 Mixing behaviour of (a) a polymeric thickener (HPMC) and (b) a particulate thickener (swollen suspension of granular starch) with a viscosity of 380 mPa · s measured at 50 per second and 25°C and locust bean gum at a concentration of (c) 0.5% and (d) 0.6%. Adapted from Ferry *et al.*, 2006a. Copyright 2006, with permission from Elsevier; and Koliandris *et al.* (2008). Copyright 2008, with permission from Elsevier.

mouth. Nevertheless, the authors consider it as a valuable experiment in predicting differences in perception between high-viscosity liquid foods.

8.4.2 Microstructure

Clearly, if it is accepted that good mixing is desirable for good perception, then it will be important to understand the microstructure that is required to promote this. The hypothesis is that solutions which are thickened by swollen particles, most obviously starch granules but probably also plant fibres (there is increasing interest in the latter as an alternative to hydrocolloids), will mix well, whereas polymers in solution will mix poorly when the c^* concentration is exceeded. Evidence in support for this comes from a study on the mixing of gelatinised starches from different sources and the effect of amylase activity on starch-thickened systems. It is easy to show that amylase activity reduces starch viscosity on time scales relevant to oral consumption (Ferry *et al.*, 2004). A consequence of the enzymes' attack on a swollen starch granule is a disruption of the structure, resulting in a partial change in solution microstructure from a suspension of swollen particles to a polysaccharide solution. Waxy maize starch that contains no amylose

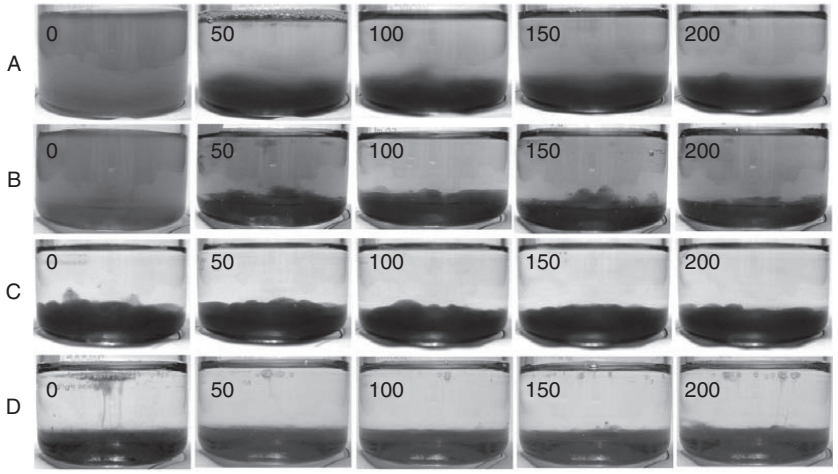

Fig. 8.5 Mixing efficiency of viscous systems with solutions containing an increasing amount of R-amylase. Viscous samples (480 mPa · s at 50 per second) of different starches (wheat, A; modified waxy maize, B; waxy maize, C; HPMC, D) were stirred into distilled water or solutions containing 50, 100, 150, and 200 U · mL^{-1} of amylase and photographed after 1 minute. Reproduced from Ferry *et al.* (2006b), copyright 2006, with permission from American Chemical Society.

has a weak granule structure which is easily disrupted during processes involving heating and shearing. For this reason, waxy maize starches are often chemically cross-linked or physically treated to maintain granule integrity. For amylose-containing starches, such as wheat or maize, following gelatinisation, there will be a release of some amylose into solution following gelatinisation, but the swollen granule will be much 'stronger' than unmodified waxy maize starch.

If viscosity was the dominant factor, an increase in perception with amylase activity would be expected, since it has been shown that flavour perception normally increases with decreasing viscosity. If for these systems microstructure through its influence on mixing 'overrides' viscosity as the dominating effect, then perception should decrease with increasing amylase activity. The latter view is supported by the second study by Ferry *et al*. (2006b).

For systems thickened with wheat starch, native waxy maize starch, a waxy maize starch modified to maintain granule integrity following gelatinisation and HPMC, Figs. 8.5 and 8.6 illustrate the change of mixing efficiency with amylase concentration in the water to which the stained viscous 'solution' was added. Figure 8.5 shows observed mixing efficiency. The quantitative data plotted in Fig. 8.6 are based on monitoring the concentration of K^+ with a specific ion electrode inserted into the top surface shortly after mixing (KCl and not NaCl was used since the amylase preparation added to the water contained Na^+).

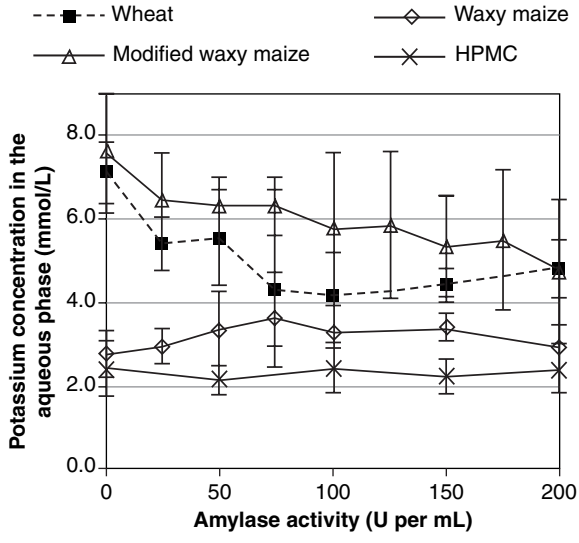

Fig. 8.6 Effect of amylase activity on potassium concentration in the aqueous phase after mixing of the four different viscous systems (480 mPa · s at 50 per second). Reproduced from Ferry *et al.* (2006b), copyright 2006, with permission from the American Chemical Society.

A sensory study was carried out on soups thickened with these four systems using panellists whose in-mouth amylase activity had been measured. The correlation coefficients between the panellists' amylase activity and saltiness score are shown in Table 8.1.

It is noteworthy that for the starch suspensions that have an initial microstructure consisting predominantly of swollen granules (wheat, modified waxy maize), there is a highly significant negative correlation between amylase activity and perceived saltiness. When this is considered in conjunction with

- the initial drop in K^+ detected at the liquid surface after mixing when amylase is added to the starches that have a granular microstructure, i.e. modified waxy maize and wheat,
- the poorer salt release from and mixing ability of the HPMC and native waxy maize starch-thickened systems,

this supports the hypothesis that, at high viscosities, a particulate microstructure is better than a polymeric one to impart enhanced salt perception. In the absence of amylase, the difference between 'solutions' of native waxy maize starch with its poor granular integrity and 'solutions' of wheat and modified waxy maize starch which have a more particulate microstructure is clear.

Table 8.1 Pearson's correlation coefficients between salivary amylase activity and sensory scores for salt perception by a sensory panel

Thickener type	Saltiness
HPMC	0.11[a]
Waxy maize starch	−0.20[b]
Modified waxy maize starch	−0.43[c]
Wheat starch	−0.25[c]

Reproduced from Ferry *et al.* (2006b), copyright 2006, with permission from the American Chemical Society.
[a]Not significant at a level of 5%, $p > 0.05$.
[b]Significant at a level of 5%.
[c]Significant at a level of 1%.

8.4.3 Mouthfeel

More than 40 years ago, Szczesniak and Farkas (1962) attempted to relate the mouthfeel of hydrocolloid solutions to solution rheology. They matched the viscosity of a wide range of hydrocolloid and starch 'solutions' where this viscosity was measured semi-empirically at a shear rate which would be lower than the value of 50 per second, which as discussed above is often considered to be the shear rate prevalent in the mouth. The sensory panel was asked to evaluate these solutions in terms of sliminess, where a slimy solution was considered to be one difficult to swallow. The hydrocolloid solutions were split into three classes on the basis of their degree of shear thinning. At higher levels of shear thinning, the solutions were perceived as increasingly less slimy, i.e. easier to swallow. It has been argued that these differences simply reflect difference in dynamic viscosity or shear viscosity at the appropriate values for perception in the mouth (Richardson *et al.*, 1989). However, it is interesting that this class of least slimy solutions contains the starch systems, which would be expected to maintain a granular microstructure after gelatinisation (maize starch and high-amylose starch were used in this study), and xanthan gum, whereas waxy maize starch was in the slimy category. Returning to the mixing argument, it seems a useful and testable hypothesis that mouthfeel improves with the ease of mixing. Swallowing will be easier for a viscous solution which mixes more readily with saliva compared to something that maintains a semi-gel-like consistency in the mouth. As so often happens, xanthan gum does not seem to fit the hypotheses. This polysaccharide would be expected to mix in a polymeric fashion, i.e. poorly; however, observations on its in-mouth behaviour reveal a behaviour more akin to that of a particulate system. It is possible that this is because of its dramatic shear thinning behaviour causing the concentration required to match the viscosity at in-mouth shear rate of the other hydrocolloids to be below the entanglement

threshold. In this very dilute region, non-Newtonian behaviour would result from orientation of rod-shaped molecules rather than disruption of entanglements.

8.4.4 Gels

Flavour perception from gels has been extensively investigated. The majority of investigations have focused on individual or at most on pairs of gelling systems. There is some analogy to work that has been carried out on hydrocolloid-thickened solutions. Undoubtedly, there are situations where binding of volatiles to the matrix will be significant in reducing the levels of perception; however, it is particularly valuable to develop a hypothesis that is applicable to as wide a range of textures and gelling agents as possible. Many of the gel rheology studies have been concerned with the small deformations required to remain within the linear viscoelastic region. These parameters are less central to perception than large deformation measurements which fracture gels. For example, in a very early work, Wood (1979) showed that the perceived hardness of a gel correlated better to the force required to facture the gel than to the Bloom Strength which correlates with the small deformation modulus. The study of Morris (1994) including a wide range of hydrocolloid gelling systems showed stronger correlations between the strain at break and perceived flavour as well as sweetness than that was seen for the elastic modulus or the rupture stress. As with thickened solutions, one question to be asked is whether this relationship can be understood in terms of a change in the concentration of volatiles reaching the nose, the concentration of tastants reaching the receptors in the mouth or whether it is the result of a multimodal effect? It is reasonable that gels with a lower strain at break (brittle gels) will release tastants and volatiles more efficiently because of the more rapid increase in surface area on consumption. In support of this, Morris demonstrated a strong negative correlation between the strain at break and flavour perception for a range of gels (Morris, 1994). A more recent study by Koliandris *et al*. (2008) demonstrates that the increase in tastant release is a more significant consequence of in-mouth processing of gellan and carrageenan gels than the increase in volatile release.

It is generally accepted that gelatin is one of the best if not the best gelling agent for taste perception and mouthfeel. In the authors' view, there are two reasons for this:

(i) A gel melting temperature $\sim$30°C which results in a gelatin gel melting in the mouth.
(ii) The efficient mixing of molten gelatin with water or saliva.

Fig. 8.7 Mixing behaviour of molten gelatin solutions at 10% (a) and 30% (b) concentration. Adapted from Ferry *et al.* (2006a). Copyright 2006, with permission from Elsevier; and Koliandris *et al*. (2008). Copyright 2008, with permission from Elsevier.

Fig. 8.7 shows the results of mixing molten gelatin solutions at a temperature of 50°C at concentrations of 10 and 30% with water also at 50°C. Even at a concentration of 30%, which is well above the c^* concentration (Wulansari *et al*., 1998), gelatin solutions mix very efficiently with water in the same way as granular starch does. The possible consequences of this for tastant release compared to that of other hydrocolloid solutions can be appreciated from Fig. 8.8.

Fig. 8.8 shows the result of a salt release experiment from coloured gelatin and locust bean gum solutions which were spiked with NaCl followed by measuring the salt concentration at the top of the beaker.

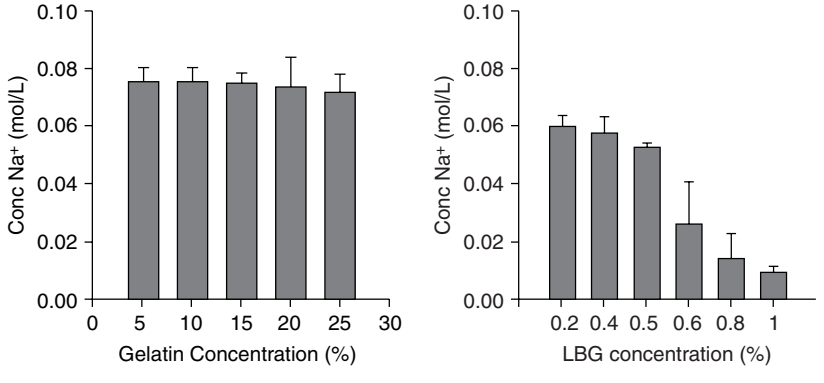

Fig. 8.8 Na^+ release for different concentrations of gelatin and LBG solutions. Reproduced from Koliandris *et al*. (2008). Copyright 2008, with permission from Elsevier.

For locust bean gum, there is a decrease in salt release when the concentration exceeds 0.5%, which, not surprisingly, is consistent with the change in mixing efficiency shown in Fig. 8.4 and the change in flavour perception for hydrocolloids once c^* is exceeded as shown in Fig. 8.2.

An additional factor which may be important is the low viscosity of gelatin solutions as evidenced by the low value of intrinsic viscosity compared to that of polysaccharide gelling agents (Wulansari *et al*., 1998). This may result in more effective distribution of biopolymer molecules from the gel surface into the bulk solution on melting. This is a slightly different idea from the mixing of high-viscosity solutions which the main part of this discussion has addressed.

8.5 BEYOND SHEAR RHEOLOGY

For liquid foods, the shear viscosity is not sufficient to predict flavour perception in viscous solutions as is shown by the result in Fig. 8.3. It also does not provide a complete basis for the prediction of mouthfeel. In this chapter, it has been argued that the ease with which a liquid mixes with saliva is an important driver for both taste perception and mouthfeel. It seems, therefore, reasonable to postulate that the resistance to break up a viscous fluid droplet when in contact with water or saliva prevents rapid mixing. The hypothesis here is that a liquid-thickened food comprised of swollen granules suspended basically in water posses a comparatively lower resistance to break up and therefore mix more readily in the mouth.

Droplet break-up has been extensively investigated both experimentally and theoretically for immiscible fluids, although data on suspensions are scarce. For homogeneous polymer solutions, the rheological properties of both immiscible fluids and the interfacial characteristics control droplet deformation and break up at given flow stresses. The rheological properties of the polymer solutions are of course imparted by the molecular conformation and the state of entanglement. Similar rules should also apply to suspension droplets; however, the boundary layer inside the droplet adjacent to immiscible continuous fluid phase is depleted of particles. Hence, the flow stresses act on the suspension medium, and the behaviour of the total system is not akin to the behaviour classically observed for a pair of homogeneous immiscible fluids. This was investigated by following the behaviour of microscopically small HPMC and physically cross-linked waxy maize starch suspension droplets using a flow shear cell described by Vervoort and Budtova (2003).

As can be seen in Fig. 8.9, the pattern of droplet break-up is very different for these two thickener systems. Under these conditions, the

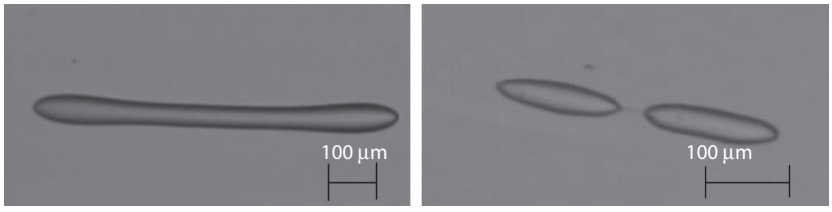

Fig. 8.9 Left-hand side micrograph shows a HPMC droplet immersed in 200 Pa · s viscosity silicone oil submitted after shear rate step up to 6 per second. The right-hand side micrograph shows the equivalent experiment for a physically cross-linked waxy maize starch suspension droplet. The shear viscosity of both droplet fluids was 15 Pa · s at 6 per second. Note that the micrographs represent a snapshot from a time-dependent experiment.

HPMC droplet does not break up even though it becomes highly elongated. On the contrary, the starch droplet disrupts under these conditions. The ease of break-up for droplets of the granular starch system is evident from Fig. 8.10. It shows the well-known Grace curve for shear-induced droplet break-up of Newtonian droplets immersed in second immiscible Newtonian fluid as well as experimental data obtained for the starch droplets (Desse *et al*., 2009). The situation for the starch droplets is quite complex, for example variation of the viscosity ratio p, see caption of Fig. 8.10 for definition, in these experiments was achieved by changing

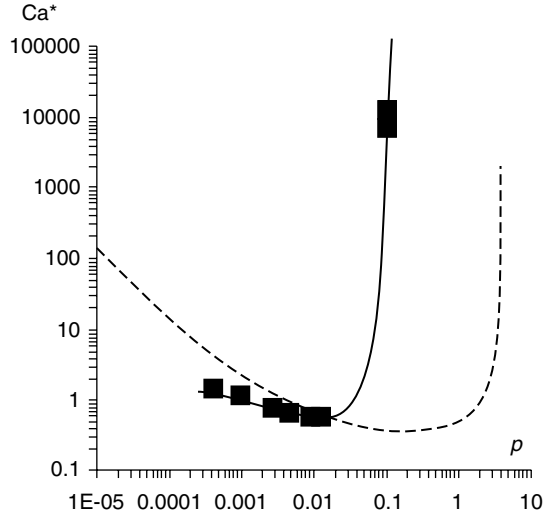

Fig. 8.10 Critical Capillary number as a function of viscosity ratio (defined as the viscosity of the droplet fluid over the viscosity of the second immiscible fluid) for starch suspension droplets (points, solid line added for guidance only) and for a Newtonian fluid. For p larger than roughly 0.1, droplet break-up was not observed for the starch droplet system investigated here. Error bars are smaller than the size of the points. (Desse *et al*., 2009). Reproduced with permission.

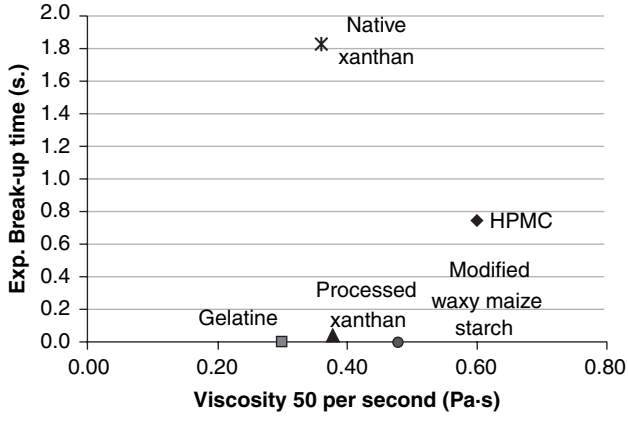

Fig. 8.11 Comparison between shear viscosity at 50 per second and filament break-up time using the Haake CaBER extensional rheometer (at 20°C) (reference).

shear rate and taking the shear viscosity measured for the starch suspension at the shear rate applied to calculate p. Hence, since the viscosity of the second immiscible fluid was kept constant, larger p values coincide with lower applied shear rates and therefore flow stresses. As soon as these were below the yield stress, droplet break-up was no longer observed; the reader should consult the original publication for detail.

Another approach to evaluate the differences in break-up behaviour between microstructurally and fundamentally different fluids is to produce filaments of these fluids, for example in the Haake CaBER extensional rheometer. This instrument allows filaments to be stretched rapidly to a given height. Following stretching, the filament thickness at half the stretching height is monitored with a laser micrometer. The filament may not always be the thinnest at half height, which, however, is not crucial for this application as the interest lies in the break-up time as a parameter, which can be obtained from the instrument's software. Fig. 8.11 contrasts the difference in droplet break-up time for five systems discussed in the chapter (molten gelatin, modified waxy maize starch, native xanthan, xanthan processed to give a particulate structure (Sereno *et al*., 2007) and HPMC). It can be seen that the good mixing systems cross-linking starch, gelatin and particulate xanthan have much shorter droplet break-up times than that of the poor mixers HPMC and native xanthan.

To predict perception, the authors believe that a combination of shear and extensional parameters are required. This book is entitled *Practical Food Rheology*. Most food laboratories are not well equipped to measure extensional viscosity, which provides considerable experimental and theoretical challenges. From a practical point of view, it may be possible to develop a semi-empirical quantitative parameter related to droplet

break-up and ease of mixing, which when combined with shear viscosity will provide a better prediction of mouthfeel and taste perception than that has been achieved so far. A very wide range of native and modified starches are available, which when gelatinised provide a wide range of liquid 'textures'. A study of these systems rather than hydrocolloid solutions may be more appropriate for taking this area forward.

8.6 CONCLUSIONS

The generic conclusion that emerges from the above is that for good taste perception and mouthfeel, the solution or gel should be easy to swallow.

For solutions this is favoured by a low viscosity and the ability to mix well with water or saliva and to disrupt easily whilst undergoing in-mouth processing. The ease of disruption can be judged in droplet or filament break-up experiments, and it is easy to imagine that a less stretchy liquid food is easier to swallow. For gels, ease of swallowing is favoured by low strains at break so the gel will disrupt into small elements. Gelatin is an exception because, although the gel has a high strain at break, it melts in the mouth, converting to a liquid which mixes very efficiently with water or saliva even at high viscosities.

The concept which unifies gels and high-viscosity solutions which have good perception is the easy of structure break-up in the mouth. For solutions, this is favoured by a particulate microstructure, for example a suspension of swollen starch granules.

ACKNOWLEDGEMENTS

The views expressed are the authors' own, but discussions with Tatiana Budtova, David Cook, Sandra Hill, Joanne Hort, Edwin Morris and Andy Taylor are gratefully acknowledged.

REFERENCES

Baines, Z.V. and Morris, E.R. (1987) Flavour/taste percption in thickenend systems. The effect of guar above and below c^*. *Food Hydrocolloids* **1**, 197–205.

Baines, Z.V. and Morris, E.R. (1988) Effects of polysaccharide thickeners on organoleptic attributes. In: Phillips, G.O., Williams, P.A. and Wedlock, D.J., editors. *Gums and Stabilisers for the Food Industry 4*. Oxford: IRL Press, pp. 192–201.

Baines, Z.V. and Morris, E.R. (1989) Suppression of perceived flavour and taste by food hydrocolloids. In: Bee, R.D., Richmond, P. and Mingens, J., editors. *Food Colloids*, Vol. **75**. Cambridge: Royal Society of Chemistry, pp. 184–192.

Blair, G.W.S. (1978) Ripening time. *Journal of Texture Studies* **9**(3), 353–361.
Bourne, M. (2002) *Food Texture and Viscosity: Concept and Measurement*, 2nd Edition. San Diego: Academic Press.
Cook, D.J., Hollowood, T.A., Pettelot, E. and Taylor, A.J. (2002) Effects of viscosity on flavor perception: Multi-modal approach. *Abstracts of Papers of the American Chemical Society* **224**, 076-AGFD.
Cook, D.J., Hollowood, T.A., Linforth, R.S.T. and Taylor, A.J. (2003) Oral shear stress predicts flavour perception in viscous solutions. *Chemical Senses* **28**(1), 11–23.
Crank, J., McFarlane, N.R., Newby, J.C., Paterson, G.D. and Pedley, J.B. (1981) *Diffusion Processes in Environmental Systems*. London: MacMilllan, pp. 45–52.
Cutler, A.N., Morris, E.R. and Morris L.J. (1983) Oral perception of viscosity in fluid foods and model systems. *Journal of Texture Studies* **14**(4), 377–395.
Desse, M., Wolf, B., Mitchell, J. and Budtova, T. (2009) Experimental study of the break-up of starch suspension droplets in step-up shear flow. *Journal of Rheology* **53**(4), 943–955.
Dickie, A.M. and Kokini, J.L. (1983) An improved model for food thickness from non-Newtonian fluid-mechanics in the mouth. *Journal of Food Science* **48**(1), 57–65.
Ferry, A.L., Hort, J., Mitchell, J.R., Lagarrigue, S. and Valles-Pamies, B. (2004) Effect of amylase activity on starch paste viscosity and its implications for flavor perception. *Journal of Texture Studies* **35**(5), 511–524.
Ferry, A.L., Hort, J., Mitchell, J.R., Lagarrigue, S. and Valles-Pamies, B. (2006a). Viscosity and flavour perception: Why is starch different from hydrocolloids? *Food Hydrocolloids* **20**(6), 855–862.
Ferry, A.L.S., Mitchell, J.R., Hort, J., Hill, S.E., Taylor, A.J., Lagarrigue, S. and Valles-Pamies B. (2006b). In-mouth amylase activity can reduce perception of saltiness in starch-thickened foods. *Journal of Agricultural and Food Chemistry* **54**(23), 8869–8873.
Friedman, H.H., Whitney, J.E. and Szczesniak A.S. (1963) The texturometer–a new instrument for objective texture measurement. *Journal of Food Science* **28**, 390.
Hill, M.A., Mitchell, J.R. and Sherman P.A. (1995) The relationship between the rheological and sensory properties of a lemon pie filling. *Journal of Texture Studies* **26**(4), 457–470.
Hollowood, T.A., Linforth, R.S.T. and Taylor A.J. (2002) The effect of viscosity on the perception of flavour. *Chemical Senses* **27**(7), 583–591.
Kokini, J.L. (1985) Fluid and semi-solid food texture and texture taste interactions. *Food Technology* **39**(11), 86–95.
Kokini, J.L. and Cussler, E.L. (1983) Predicting the texture of liquid and melting semi-solid foods. *Journal of Food Science* **48**(4), 1221–1225.
Koliandris, A., Lee, A., Ferry, A.L., Hill, S. and Mitchell J. (2008) Relationship between structure of hydrocolloid gels and solutions and flavour release. *Food Hydrocolloids* **22**(4), 623–630.
Mitchell, J.R. (1984) Rheological techniques. In: Gruenwedel, D. and Whitaker, J. editors. *Food Analysis: Principles and Techniques. Volume 1. Physical Characterization*. New York: Dekker, pp. 151.
Morris, E.R. (1994) Rheological and organoleptic properties of food hydrocolloids. In: Nishinari, K. and Doi, E., editors. *Food Hydrocolloids, Structure Properties and Functions*. New York, Plenum Press, pp. 201–210.
Richardson, R.K., Morris, E.R., Ross-Murphy, S.B., Taylor, L.J. and Dea I.C.M. (1989) Characterization of the perceived texture of thickened systems by dynamic viscosity measurements. *Food Hydrocolloids* **3**(3), 175–191.
Sereno, N.M., Hill, S.E., Sereno, N.M., Hill, S.E. and Mitchell, J.R. (2007) Impact of the extrusion process on xanthan gum behaviour. *Carbohydrate Research* **342**(10), 1333–1342.
Shama, F. and Sherman, P. (1973) Identification of stimuli controlling the sensory evaluation of viscosity-II Oral methods. *Journal of Texture Studies* **4**, 111–118.
Stone, H., Sidel, J., Oliver S., Woolsey A. and Singleto R.C. (1974) Sensory evaluation by quantitative descriptive analysis. *Food Technology* **28**(11), 24–34.
Szczesniak, A.S. (1963) Classification of textural characteristics. *Journal of Food Science* **28**(4), 385–389.
Szczesniak, A.S. and Farkas, E. (1962) Objective characterization of moutfeel of gum solutions. *Journal of Food Science* **27**(4), 281–285.

Taylor, A.J., Linforth, R.S.T., Harvey, B.A. and Blake, A. (2000) Atmospheric pressure chemical ionisation mass spectrometry for in vivo analysis of volatile flavour release. *Food Chemistry* **71**(3), 327–338.

Vervoort, S. and Budtova, T. (2003) Evidence of shear-induced polymer release from a swollen gel particle. *Polymer International* **52**(4), 553–558.

Wood, F. (1979) Psychophysical studies on liquid foods and gels. In: Sherman, P., editor. *Food Texture and Rheology*. London: Academic Press, pp. 21–31.

Wood, F.W. (1968) Psychophysical studies on the consistency of liquid foods. *Rheology and Texture of Foodstuffs*, S.C.I. Monograph. **27**, 40–49.

Wulansari, R., Mitchell, J.R., Blanshard, J.M.V. and Paterson, J.L. (1998) Why are gelatin solutions Newtonian. *Food Hydrocolloids* **12**(2), 245–249.

9 Protein-Stabilised Emulsions and Rheological Aspects of Structure and Mouthfeel

Fotios Spyropoulos, Ernest Alexander K. Heuer, Tom B. Mills and Serafim Bakalis

9.1 INTRODUCTION

Emulsions are an integral part of many food products. In the past, research in emulsion-based systems focused mainly on understanding the mechanisms of formation and stabilisation of these systems. More recently, efforts have been devoted towards obtaining an understanding of the behaviour of emulsion-based foods during oral processing ('eating'), aimed at designing novel functional products that deliver advanced health benefits.

There is evidence that such health benefits can indeed be achieved from food formulations, especially in order to tackle issues such as the obesity crisis (Norton, Fryer, *et al*., 2006). As obesity has reached epidemic levels in the Western world, it is clear that calorifically dense foods, such as (high-fat) emulsions, have to be redesigned. In order to achieve this, an understanding of the phenomena occurring in-mouth as well as their link to consumer perception would have to be obtained. In the past, research in this area was mainly driven by medical sciences and focused on understanding some of the fundamental mechanisms of transport within the body; for example, movement of the bolus and identification of some relevant forces in the mouth. Work on physical characterisation and *in vitro* measurements of the physical and structural changes that food emulsions (and food in general) experience during oral processing is now becoming more widespread. If perception and sensory properties of a product can be related to these instrumental measurements, improvements can be made much faster and without the need for human subjects. Current work in the field of emulsions has been promising, especially when relating important key attributes such as creaminess or slipperiness to on-board friction measurements carried out on instruments (tribology).

Practical Food Rheology: An Interpretive Approach
Edited by Ian T. Norton, Fotios Spyropoulos and Philip Cox
 ISBN: 978-1-405-19978-0

This chapter will provide a description of the structure of emulsions stabilised by proteins, the oral processes involved during their consumption (and consumption of emulsions in general) as well as how these affect their sensory attributes. Finally, the latest developments in instrumental methods used to relate emulsion properties, as exhibited during oral processes, and their sensory perception will be considered.

9.2 PROCESSING AND STABILITY OF EMULSIONS

As emulsions are thermodynamically unstable systems, a lot of effort has been devoted towards obtaining an understanding of the mechanisms and kinetics of instabilities, properties, as well as processing routes. Although these phenomena have been mainly studied in the context of processing and storage, they would be directly applicable to the phenomena occurring in the mouth.

9.2.1 Instabilities in emulsions

In order to understand the function of proteins, in terms of the stability they impart to oil-in-water emulsions, it is useful to briefly discuss the main instabilities usually associated with these systems.

9.2.1.1 *Coalescence*

Coalescence is the irreversible joining of two or more emulsion droplets to form a single larger droplet. There are two mechanistic steps that should take place for coalescence to occur: film thinning and film rupture. Film thinning is a result of surface distortion between two (or more) approaching droplets, which leads to the formation of thin liquid lamellae between their surfaces. The rate and extent of film thinning depend on the hydrodynamics of film flow and on the colloidal forces acting across the film. Emulsion droplets will not coalesce if the thickness of the formed lamella remains above a certain critical value. In the case where the thickness of the lamella is reduced below this critical value, random surface fluctuations can result in rupture of the interfacial layer (film rupture), leading to coalescence. The kinetics of rupture depends on the extent of these fluctuations and on the viscoelastic properties of the adsorbed protein layer.

9.2.1.2 *Flocculation*

Flocculation is the aggregation of two (or more) emulsion droplets without the occurrence of any interfacial rupture events. Flocculation can

broadly be classed into two categories: depletion and bridging flocculation. Depletion flocculation is driven by an osmotic pressure gradient caused by the exclusion of a non-adsorbing 'depleting' agent from the space between two (or more) approaching droplets. Depletion flocculation is considered as a weak, reversible type of flocculation, since the formed flocs can be easily broken down by mild shearing. Bridging flocculation on the other hand is the linking of two or more droplets at the droplet interface to form a bridge, for example due to electrostatic interactions, and can effectively be an irreversible process. Bridging flocculation can also take place during emulsification when the emulsifier concentration is not sufficient enough to completely cover the available oil–water interfaces in the system. Under such conditions, emulsifier molecules may be 'shared' by more than one droplet, forming a 'bridge' between them.

9.2.1.3 *Creaming*

Creaming is the motion of droplets under the influence of gravitational forces to form a concentrated layer at the top of an oil-in-water emulsion; the same process is known as sedimentation in the case of water-in-oil emulsions, where the concentrated layer of (water) droplets is formed at the bottom of the system. The creaming rate is affected by the density difference between the oil and the water phases, the size of the emulsion droplets and the rheological properties of the continuous phase.

The creaming rate can be calculated by the Stokes–Einstein equation:

$$v_s = \frac{2g \cdot R^2(\rho_0 - \rho)}{9\eta_0} \tag{9.1}$$

where v_s is the creaming speed, g is the acceleration due to gravity, R is the radius of a spherical droplet, ρ_0 and η_0 are the density and Newtonian shear viscosity of the continuous phase, respectively, and ρ is the density of the dispersed phase (Binks, 1998).

What should be stressed at this point is that all the types of emulsion instabilities briefly described above are interrelated. For example flocculation will result in an increased creaming rate. Also, creaming can potentially accelerate coalescence events in the system due to the close proximity of the emulsion droplets in the cream layer. It is therefore of great importance, when considering potential routes of eliminating/reducing the occurrence of a specific instability, to also take into account the effect of such action on the other types of emulsion instabilities. For instance, addition of biopolymers to the continuous phase of an oil-in-water emulsion, in order to increase its viscosity and thus reduce the rate of creaming, can result in depletion flocculation.

9.2.2 Protein functionality at liquid interfaces

Proteins have been extensively used to assist the formation of oil-in-water emulsions and also to stabilise their bulk microstructure. This dual functionality of proteins in emulsions stems from their surface-active nature, and thus their ability to adsorb at the oil–water interface, but is also a direct consequence of their relatively 'large' molecular size, in comparison to the smaller emulsifiers used in foods (e.g. Tweens), which renders the interfaces they adsorb onto to be much 'thicker'.

By doing so, proteins lower the interfacial tension of the fluid interfaces (that they absorb onto) and thus aid the formation of oil-in-water emulsions by facilitating droplet break-up during emulsification. The equilibrium interfacial tension of protein-stabilised interfaces, depending on the type of the oil phase, is roughly between 10–25 mN/m for both flexible (e.g. β-casein) and globular proteins (e.g. ovalbumin, bovine serum albumin) (Beverung *et al.*, 1999).

In terms of their ability to lower the interfacial tension of oil-in-water emulsions, proteins are less effective when compared to low molecular weight (*lmw*) surfactants. Nonetheless, proteins are far more superior in stabilising the formed emulsion droplets, with respect to droplet coalescence and flocculation, than *lmw* surfactants (van Aken *et al*., 2003). Although *lmw* surfactants have higher adsorption energies per square metre than proteins, the latter can adsorb at the interface with several segments, and changes in their conformation allow for even more segments to adsorb. Therefore, because of their overall high energy of adsorption, proteins, forming a saturated monolayer covering the emulsion droplets, can be considered as being irreversibly bound to the oil–water interface.

The protein concentration required to provide a saturated monolayer covering the emulsion droplets (surface concentration) usually depends on the pH and ionic strength of the system; surface concentration increases at pH values close to the isoelectric point of the protein (Graham and Phillips, 1979). Surface concentration also depends on the type of protein; saturation for flexible proteins occurs at values of 2–3 mg/m^2, whereas for globular proteins, it is usually in the range of 1–2 mg/m^2 (Beverung *et al.*, 1999). In both cases, the thickness of the resulting interfacial films is between 5 and 6 nm (Graham and Phillips, 1979).

Further adsorption of protein molecules, on the initially formed protein monolayer, can take place but will only affect the thickness of the interfacial film and not its interfacial properties (interfacial tension). Although protein molecules are now reversibly adsorbed, with respect to aqueous substrate exchange, the thickness of the interfacial film can increase to more than 10 nm (Graham and Phillips, 1979). It is the thickness of these protein-saturated interfaces that provides a sterically

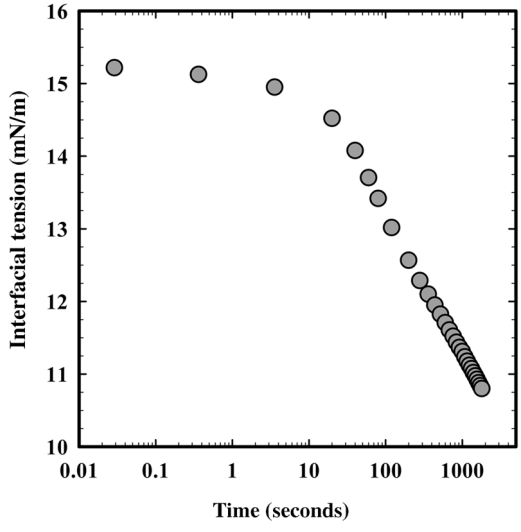

Fig. 9.1 Dynamic interfacial tension data of an oil–water interface stabilised by sodium caseinate. The change in the interfacial tension with time relates to the rate of protein adsorption and protein conformational changes at the interface.

stabilised film (Srinivasan, 2005), which serves to initially 'protect' the formed emulsion droplets against immediate re-coalescence (during the emulsification process) but also provides long-term stability (post-production) against droplet coalescence and potentially flocculation.

The rate of protein adsorption at the oil–water interface is also crucial in terms of emulsion stability during emulsification. Under these conditions, there is a sudden increase in the total surface of the newly formed emulsion droplets due to the decrease of their size and increase of their number. It is therefore the rate of protein adsorption that will determine the stability of the newly formed droplets against re-coalescence events.

Information on the kinetics of protein adsorption at an oil–water interface can be obtained from dynamic interfacial tension measurements (Beverung *et al.*, 1999). Protein adsorption displays three distinct regimes. Initially, there is an induction period where interfacial tension is only marginally reduced (Fig. 9.1) and the duration of which is controlled by diffusion and protein interfacial affinity. The second regime is defined by the continual rearrangement of the proteins at the interface. During this stage, a sudden reduction in interfacial tension takes place (Fig. 9.1), as more protein molecules adsorb at the interface and the number of interfacial contacts per protein molecule is increased. The final regime occurs upon monolayer coverage and is attributed to the continued relaxation of the adsorbed layer and the possible build-up of multilayers towards the latter stages. It is at this stage, and after monolayer coverage, that equilibrium interfacial conformation can be achieved.

The rate and mechanism of adsorption also depends on the type of protein (Beverung *et al.*, 1999). Flexible proteins (e.g. β-casein) display overall more rapid adsorption dynamics than globular proteins (e.g. ovalbumin) and also the ability to attain an apparent equilibrium interfacial tension sooner; equilibrium interfacial conformation in oil-in-water emulsions stabilised by globular proteins (e.g. ovalbumin) takes place after significantly long times. Because of their rapid adsorption at the interface, flexible proteins usually do not display a diffusional induction period (the first regime in the protein adsorption mechanism), unless they are present in the system at very low concentrations. The adsorption dynamics of flexible proteins may be explained by their disordered structure in solution, which promotes rapid adsorption and tension equilibration in the second and third regimes. Conversely, the slow interfacial unfolding and rearrangement of the globular proteins are the molecular processes that dominate the adsorption kinetics beyond the induction regime.

9.2.2.1 *Protein displacement*

Although protein adsorption at the oil–water interface can be regarded as an irreversible process, protein desorption can take place due to protein displacement by either other proteins or surfactants subsequently adsorbing at the same interface. Mutual displacement of proteins by other proteins relates to the difference in the ability of each of them to change their conformation upon adsorption. Since flexible proteins undergo conformational changes more easily and rapidly than globular proteins, the former tend to displace the latter from an interface (Arai and Norde, 1990a, 1990b).

The displacement of proteins by *lmw* surfactants, from both solid and liquid surfaces, usually takes place by 'solubilisation' of the protein or 'direct replacement' (Mackie *et al.*, 1999). One of the most interesting areas in this field has been the interaction between proteins and emulsifiers (including surfactants and lipids). The reason for this is that although both proteins and emulsifiers can stabilise foams and emulsions alone, their individual mechanisms of stabilisation are incompatible, often resulting in dramatic destabilisation when both species are present at the interface. This process is commonly known as competitive destabilisation (Wilde *et al.*, 2004). Water-soluble *lmw* surfactant can bind to proteins and form a soluble protein–surfactant complex, which desorbs from the interface to the bulk. This mechanism does not require the *lmw* surfactant to adsorb at the interface, but it must have a strong tendency to interact with the protein. Displacement by direct replacement occurs due to the fact that the interfacial energy (interfacial tension) for the surfactant is lower than that for the protein. Protein replacement

requires for the *lmw* surfactant to have a strong tendency to adsorb at the interface, but not necessarily to interact with the protein.

9.2.2.2 *Properties of protein-stabilised interfaces*

Another function that proteins impart on the oil–water interfaces they adsorb onto is a certain degree of viscoelasticity (Bos and van Vliet, 2001). Once at the interface, proteins, unlike *lmw* surfactants, can increase interfacial viscosity via non-covalent intermolecular interactions or covalent intermolecular disulphide cross-linking. The viscoelastic properties of the protein-stabilised interface depend on the type of protein, with globular protein films displaying two to three orders of magnitude larger viscosities than that of films stabilised by flexible proteins (Bos and van Vliet, 2001). The difference in viscoelastic properties, displayed by interfaces stabilised by globular or flexible proteins, has been attributed to the larger flexibility of the disordered/flexible protein molecules (Beverung *et al.*, 1999).

9.2.2.3 *Protein denaturation*

Once proteins adsorb at the oil–water interface, they may undergo considerable changes in their structure/conformation, a process usually referred to as 'surface denaturation'. In aqueous solutions, protein molecules adopt a characteristic 'folded' structure which allows them to expose their hydrophilic segments to the aqueous environment, while, at the same time, 'hide' their hydrophobic segments within the core of the molecular arrangement. Upon adsorption at the oil–water interface, the protein's molecular 'surroundings' change, as the structure is now exposed to both an aqueous and an oil environment. It is this change of environment that drives 'surface denaturation' as the molecule unfolds, exposing its hydrophobic residues, in order to maximise the number of favourable interactions and minimise the number of unfavourable interactions (Wilde, 2000b).

The dynamics of protein adsorption and conformational rearrangement depend, to a great extent, on the structure of the 'native' protein molecule (Freer *et al.,* 2004). Proteins with a flexible/random native configuration (e.g. β-casein) undergo relatively rapid conformational changes, with time scales of minutes to a few hours. On the other hand, for globular proteins (e.g. lysozyme), changes in conformation at the oil–water interface are extremely slow, often found to occur over time scales of days at both the air–water and oil–water interfaces (Freer *et al.,* 2004).

Denaturation of proteins can also occur prior to or post adsorption at the oil–water interface due to processing conditions (e.g. heat,

pressure, termed thermal or pressure denaturation) during emulsification (e.g. homogenisation) (Galazka *et al*., 1996; Kim *et al*., 2002; Rampon *et al*., 2003). Galazka *et al*. (1996) investigated the effect of high pressure on the emulsifying behaviour of β-lactoglobulin and reported that oil-in-water emulsions stabilised by protein that was pressure-treated were less stable than those stabilised by the native protein. More interestingly, high-pressure treatment of emulsions prepared with the native protein only slightly affected their stability, which suggests that the structure of the partially unfolded β-lactoglobulin (adsorbed at the oil–water interface) was more or less unaffected by the induced pressure.

In addition, emulsions stabilised by globular proteins are particularly sensitive to thermal treatments. This is because, when the temperature of the system is increased above a certain critical value, these proteins tend to unfold and expose reactive groups originally located in the interior of their native molecular arrangement. These reactive groups increase the likelihood of (attractive) interactions between proteins adsorbed on the same or different droplets, thus giving rise to emulsion instabilities, such as droplet flocculation and coalescence. Emulsion stability is further compromised when salt is also present in the system, since this results in screening of the electrostatic repulsion between the protein-stabilised droplets. Kim *et al*. (2002) have shown that when β-lactoglobulin-stabilised emulsions are heated above ~70°C (above the denaturation temperature of the native protein) in the presence of salt (NaCl), protein unfolding becomes much more extensive (than in the absence of salt), leading to a higher degree of droplet flocculation. A very interesting finding from the same study was that droplet flocculation can be significantly reduced when β-lactoglobulin-stabilised emulsions are heated in the absence of salt, and then salt is added later, after the system is brought down to room temperature (Kim *et al*., 2002).

Emulsion properties such as interfacial tension, interfacial concentration, and interfacial rheology are all directly affected by the denaturation of the adsorbed protein molecules. The molecular characteristics of the non-adsorbed proteins are also known to alter bulk physicochemical properties of oil-in-water emulsions. The fact that the structure of adsorbed and/or non-adsorbed proteins may be modified/altered during emulsion preparation can lead to very different surface and emulsification properties, which would, without a doubt, have important implications on the stability of oil-in-water emulsions.

9.2.3 Protein-stabilised oil-in-water emulsions – Effect of aqueous phase composition

In practice, protein functionality may have to be exhibited in oil-in-water emulsion-based products that have a wide range of different pH values

and ionic strengths, but also in the presence of other proteins, surfactants and biopolymers. Gaining insight into the effect of the abovementioned parameters on the stability of protein-stabilised oil-in-water emulsions is therefore of great importance.

9.2.3.1 *Effect of pH and ionic strength*

Most protein molecules usually exist in solution as charged species, and consequently, the interfacial membranes they form around droplets are also generally charged. As a result, another important mechanism by which stability of protein-stabilised emulsions is induced is electrostatic repulsion (Claesson *et al*., 1995). Therefore, protein-stabilised emulsions are particularly sensitive to changes in the pH and ionic strength of the system. At pH values close to the proteins' isoelectric point and/or at ionic strengths above a certain critical value, electrostatic repulsion between the emulsion droplets is no longer sufficiently strong enough to induce stability, and thus these systems tend to flocculate and also have a tendency to display high rates of creaming (Kulmyrzaev and Schubert, 2004; Surh *et al*., 2006).

A range of strategies has been applied to tackle the instability effects induced in protein-stabilised emulsions through changes in the pH and/or the ionic strength of the system. These include, amongst others, the use of chelating agents (such as EDTA) that bind to multivalent counter-ions (Keowmaneechai and McClements, 2002), and the use of charged biopolymers (e.g. pectin) that adsorb at the surface of oppositely charged droplets, thus shifting the pH dependence of the system with regard to stability against flocculation (Surh *et al*., 2006).

9.2.3.2 *Effect of addition of surfactants*

It is common for protein-stabilised oil-in-water emulsion-based products to contain one or more types of surfactants, proteins and/or biopolymers. As previously discussed, addition of *lmw* surfactants can result in the displacement of proteins from what initially was a protein-stabilised oil–water interface (Wilde, 2000a). Such an event would mean that emulsion droplets are no longer covered by a steric (or in some cases even an electrostatic) protein film, and thus stability against droplet coalescence and/or flocculation would be highly compromised (Chen and Dickinson, 1995; Derkatch *et al*., 2007).

Even when surfactants do not induce protein desorption, their addition can be detrimental to emulsion stability. It has been shown that addition of an emulsifier at a concentration low enough so as to not cause protein displacement can interfere with inter-protein interactions within the protein layer. This can lead to a reduction in interfacial viscosity of the

protein film and may compromise emulsion stability against coalescence (Euston *et al*., 2001). Protein-stabilised emulsions containing an excess of unbound surfactant, present in the continuous phase in the form of micelles, have also been found to flocculate (Aronson, 1989). The surfactant micelles are excluded from the space between the emulsion droplets, thus promoting depletion flocculation.

9.2.3.3 *Effect of addition of proteins*

Protein-stabilised oil-in-water emulsion-based products can also contain one or more types of proteins, other than those used to stabilise the oil–water interface. As previously discussed, such addition may result in the displacement of proteins from the interface, an event that potentially can have a negative effect on the stability of the emulsion. Interestingly enough, it has also been shown that emulsion stability can be compromised at high concentrations of the very protein used to provide stability in the first place. Oil-in-water emulsions stabilised solely by sodium caseinate can exhibit depletion flocculation when the protein concentration is increased above a certain critical value (Dickinson *et al*., 1997). This 'self-induced' flocculation behaviour was attributed, by analogy with surfactant micellar systems, to the presence of casein micelles (formed by non-adsorbing protein molecules) in the continuous phase of the emulsions (Dickinson *et al*., 1997).

9.2.3.4 *Effect of addition of biopolymers*

Emulsion stability can also be affected by the presence of biopolymers, which are usually added to food formulations as thickening or gelling agents. These biopolymers may interact with the adsorbed proteins and, indirectly or directly, influence the stability of the oil-in-water emulsion (Dickinson, 2003).

The presence of non-adsorbing biopolymers (e.g. pectin), when added in sufficiently high concentrations in the aqueous phase of a protein-stabilised emulsion, have been found to promote depletion flocculation (Surh *et al*., 2006). The rate of flocculation has been found to greatly depend on the concentration of the added biopolymer. As the concentration of non-adsorbing biopolymer is progressively increased so does the rate of flocculation. Nonetheless, once the biopolymer concentration is increased above a certain critical value, the rate of flocculation decreases, since the viscosity of the continuous phase is also increased to such an extent that the movement of the droplet in the emulsion is restricted.

Charged biopolymers are capable of adsorbing to the surfaces of oppositely charged protein-stabilised emulsion droplets through

electrostatic interactions. Above a certain concentration of biopolymer, droplet aggregation via a bridging flocculation mechanism can be induced (Dickinson, 2003). Since the driving force is electrostatic in origin, emulsion stability can be affected by the pH and ionic strength conditions in the system. Bridging flocculation is most pronounced under conditions of partial protein coverage of the emulsion droplets.

9.2.4 Effect of processing

Under quiescent conditions, protein-stabilised emulsions are highly stable due to the protein interfacial film formed around the emulsion droplets (van Aken *et al*., 2003). Nevertheless, there are a number of situations where emulsion instabilities (usually droplet coalescence) may be promoted due to the application of mechanical stresses, e.g. during homogenisation (Mohan and Narsimhan, 1997).

During processing, the collision frequency between droplets will increase, which subsequently may also result in, for example, an increase in the probability and frequency of coalescence events in the system. If the protein concentration in the system is not sufficient enough to provide full coverage of all the 'naked' oil–water interfaces created during processing, then coalescence is more likely to occur due to the protein 'gaps' on the surface of the droplets. Even in the case when the protein concentration is high enough to provide full coverage of the oil–water interfaces being created during processing, these conditions of high stress can still cause emulsion instability. This is because, during processing, oil–water interfaces can be subjected to sufficiently large stresses that can result in 'stretching' of the protein interfacial films. Stretching of these films may result in the creation of protein-rich and protein-depleted interfacial regions at the surface of the emulsion droplets in the system (Windhab *et al.,* 2005). If the protein-depleted interfacial regions of two (or more) droplets come into contact (or even into close proximity), then coalescence can take place. This type of coalescence event is more pronounced where protein adsorption is a relatively slow process compared to the duration of the applied stress, as unadsorbed protein molecules from the bulk do not have sufficient time to adsorb at the droplet surfaces and cover the protein-depleted gaps (Tornberg and Hermansson, 1977).

9.3 ORAL PROCESSES

Interest in the processes experienced by emulsions has been recently extended to include those occurring in the mouth during their consumption. Although the conventional processes used during the formulation

of emulsions are crucial in terms of the achieved microstructure and its stability during storage, what has become clear is that oral processes are equally (if not more) important. The reason for this is that it is the interplay between oral processing and the structure of the food emulsion that determine its sensory attributes and thus consumer acceptance. This section will concentrate on the in-mouth behaviour of emulsions in general and, to an extent, how this affects their perception.

The mouth is a device where digestive processes commence, and despite being used every day, very few people appreciate the complexity of the oral cavity and of the processes occurring during mastication. Traditionally, this area of work has appeared in physiology and dentistry journals with sporadic and non-conclusive information on the physicochemical transformations of food in the oral cavity. Recently, there has been an appreciation that a thorough understanding of the in-mouth behaviour of food products is required to be able to design novel food products and also develop respective instrumental methods with which to test them. As such, journal articles and book chapters have recently appeared in the food-related literature (Chen, 2009; Van Der Bilt, 2009; van Vliet *et al*., 2009).

In Fig. 9.2, a schematic diagram of the oral cavity is shown. In principle, the oral cavity is similar for all individuals, but significant differences do exist based on gender, age or health status; a normal mouthful of water for male adults is 30 $\pm$ 10.1 g and 25.2 $\pm$ 8.1 g for females (Hiiemae *et al*., 1996). The amount of food decreases when moving from liquids to soft solids and to hard solids; for example, the average mouthful for males is 13.1 $\pm$ 4.0 g and 5.5 $\pm$ 2.3 g for bananas and peanuts, respectively. The reason for this is probably due to the increased difficulty of breakdown.

Eating is a mixture of complex coordinated movements involving the complex coordinated motions of the jaw, tongue and inner cheeks (Lund, 1991). Chewing patterns are rhythmic-periodic differing between individuals, resulting in three-dimensional motions of the ingested foods.

9.3.1 Different stages and phenomena during oral processing

Significant efforts have been devoted towards understanding the physiological mechanisms occurring during eating. Oral processing of foods is highly dependent upon the structure/consistency of the food products themselves. For solid products, discrete stages in the mastication have been identified (Hiiemae and Palmer, 1999): *stage I transport*, in which food is ingested and positioned on the occlusal table, where reduction to an appropriate size, if required, is achieved; *stage II transport*, in which a bolus is formed by moving food distally through the pillars and lastly the *hypopharyngeal transit time*, in which the bolus is swallowed. Using

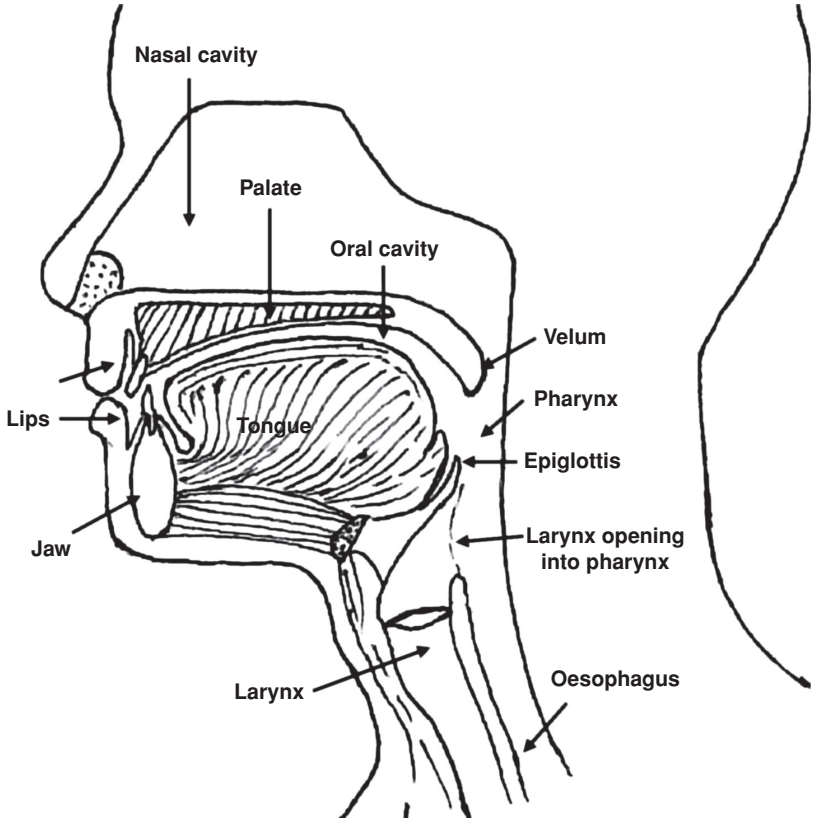

Fig. 9.2 Schematic representation of the oral cavity. Reprinted from Chen (2009), copyright 2009, with permission from Elsevier.

videofluorographic studies, the time spent for different types of foods has been measured. Irrespective of the food type, stage I transport lasted for about 2 seconds; stage II, depending on the product type, lasted between 8 and 20 seconds, with the time increasing with the 'hardness' of the product (Hiiemae and Palmer, 1999).

Hutchings and Lillford (1988) introduced a 'mouth process model' for analysing the breakdown of typical foods during eating. The authors identified criteria for swallowing based on the degree of structure reduction and lubrication. It appears that the overall preference within a class of foods (e.g. baked products) relates to samples that are swallowed in the smallest time.

In-mouth behaviour of soft solids (agar and gelatin gels) was investigated in humans by Arai and Yamada (1993). It was found that by increasing the hardness of the tested samples, oral manipulation changed from compression, between the tongue and hard palate, to shearing,

using the dentition. The threshold of hardness was 0.08 kg (force) for the agar gel and 0.03 kg (force) for the gelatine gel.

Oral management of liquid food products is similar, but processing in the mouth is not required, so typically only the preparatory and propulsive stages exist. Hiiemae and Palmer (1999) reported the relevant times for both processes as being in the order of a few seconds. Again, one of the difficulties in this area is the fact that literature seems to originate from the medical field and thus focuses on understanding clinical conditions (Silva *et al*., 2008) and does not focus on understanding oral behaviour of food structures and their changes during eating.

One of the difficulties in studying phenomena occurring *in vivo* is related to the challenge and the limited number of experimental techniques available. Videofluorographic studies have been used in the past (Hiiemae and Palmer, 1999). Recent advances in medical imaging have allowed the use of functional magnetic resonance imaging (fMRI) to study phenomena during eating. Felton *et al*. (2007) studied tongue movements and strain rates during swallowing of water. The authors have found that swallowing requires a range of coordinated compressive and expansive movements that last in the order of 500 ms. From the obtained images, the strain rates experienced on the tongue have been estimated and found to be both positive and negative with a magnitude of about 0.2 per second. Developing fMRI techniques to study phenomena occurring during eating is an active area of research, but conclusive quantitative results have not been published yet (Barkhausen *et al*., 2002; Humbert and Robbins, 2007). A technique based on video rate endoscopy has also been developed and used to investigate the interactions between food material and oral surfaces, with an emphasis on food residues remaining in the mouth after swallowing; for example, the same study demonstrated that the material remaining onto the surfaces in the mouth after swallowing increased exponentially with increasing viscosity of the food (Watson *et al*., 2002; Adams *et al*., 2007; Pivk *et al*., 2008).

9.3.2 Fluid dynamics during oral processing

Behaviour of emulsions under application of forces has been an active field of study (Windhab *et al*., 2005). During oral processing, large shear and elongational forces are applied to the food materials. This has a profound effect on the structure and has an effect on consumer perception. As oral movements are not only complex but also variable, obtaining a concise understanding of the flow fields and the forces and deformation experienced from the food material is challenging to say the least. Recently, effort has been devoted to estimate clearance times and shear rates during oral processing (Nicosia and Robbins, 2001).

The authors used a simplified squeeze flow to predict clearance times as a function of viscosity and estimated shear rates as high as 15 000 per second. This has lead to the development of thin film rheology and tribology in order to evaluate behaviour of structured fluids at high shear rates (Malone *et al.*, 2003; Davies and Stokes, 2008). This type of technique will be discussed in more detail in the later parts of this chapter.

9.3.3 Interactions with saliva

Saliva is a complex biological fluid providing, among other things, lubrication and protection of the oral surfaces. It is mainly composed of water (99.5%), proteins (0.3%) and inorganic and trace substances (Humphrey and Williamson, 2001). Over 1050 proteins have been identified in saliva, including glycoproteins and peptides. The majority of saliva (90%) is secreted from three pairs of glands, the paired parotid gland, the sublingual gland and the ubmandibular gland (Aps and Martens, 2005). The remaining 10% is secreted from minor glands such as the gingival crevicular sulci, Ebner's glands and buccal mucosae. The rate of saliva secretion ranges from 0.3 to 7 mL/min, depending on the stimulus type, individual, etc. Characterisation of saliva is extremely challenging as it is biochemically unstable and can contain relatively large particles, such as epithelial cells. Saliva has the characteristics of a weak gel (Glantz, 1997) and has a strong time-dependent viscoelastic behaviour, which in turn depends, among other parameters, on the type of stimulation (Stokes and Davies, 2007). The lubrication characteristics of saliva and its molecular structure have been an area of active research (Bongaerts *et al*., 2007b; Sajewicz, 2009). Although some of the unique properties of saliva are attributed to the high molecular weight of mucin (Strous and Dekker, 1992), it has been also shown that the performance of a simple mucin solution is different to that of saliva itself (Raynal *et al*., 2002).

Part of the structural changes that emulsions undergo during oral processing are a direct result of mixing with saliva; for example, flocculation of emulsion droplets within time scales relevant to eating have been observed *in vitro* and *in vivo* (Silletti *et al*., 2007; van Aken *et al*., 2007; van Vliet *et al*., 2009). Overall, these structural changes are considered to be a result of depletion flocculation, electrostatic and van der Waals interactions. Surface charge appears to have a strong effect on the mechanism of flocculation in emulsions under oral processing (Silletti *et al*., 2007). For highly negatively charged o/w emulsions, stabilised by sodium dodecyl sulphate (SDS), no flocculation was observed upon mixing with saliva. For weakly negatively charged emulsions (charged with β-lactoglubulin or Tween 20), reversible flocculation was observed,

indicating a depletion flocculation mechanism (Silletti *et al*., 2007). Flocculation was also observed for Na–caseinate emulsions in mixing with both saliva as well as a model mucin (pig gastric mucin). A sharply defined mucin concentration was required, while the observed aggregates were reversible upon dilution, an indication of a depletion flocculation mechanism (Vingerhoeds *et al*., 2005). The concentration of model mucin required to induce flocculation was much higher (0.4 wt%) than the average concentration in saliva (0.02 wt%). The flocculation phenomena that have been observed upon mixing with saliva could also be attributed to the presence of large aggregates in salivary mucin (Wickstrom *et al*., 2000; Soares *et al.*, 2004). Upon mixing of emulsions (stabilised by Tween 20, WPI- and β-lg) with saliva from certain individuals, irreversible flocculation was observed, implying that other flocculation mechanisms such as bridging might be of importance.

Besides the effect of the saliva-induced flocculation on the structure of protein-stabilised emulsions, it has been postulated that these flocculation events also have an effect on the emulsions' sensory attributes. As flocculation is a result of mixing with saliva, it will be more pronounced close to the oral surfaces, where saliva concentrations are higher. This would lead to a locally higher viscosity that, in turn, could be responsible for the smooth, velvety perception characterising these emulsions (van Vliet *et al.*, 2009).

9.3.4 Interaction with oral surfaces

Although mouthfeel and a number of sensory attributes have been related to emulsion bulk rheological properties, interactions with oral surfaces might also have a profound effect (Kokini, 1987; van Aken *et al*., 2007). One of the reasons for this is that all the oral processes that determine mouthfeel, such as temperature changes, mixing and interaction with saliva, will be more pronounced close to the oral surfaces. Efforts have been devoted to studying interactions of food formulations with oral surfaces. Watson *et al*. (2002) and Adams *et al*. (2007) have developed a fluorescent-based endoscopy technique to study the retention of food materials *in vivo*. Results have demonstrated that increasing the viscosity of CMC solutions resulted in an increase in the amount retained in the mouth after swallowing. Salivary flow rate was also found to influence the time at which material was consecutively removed.

One of the important attributes of multiphase (fat-containing) food products is that they cover oral surfaces, resulting in a thin, fat-based film. The existence of this thin film is believed to be responsible for part of the sensory characteristics attributed to many emulsion-based systems. Dresselhuis *et al*. (2008c) have studied the mechanisms by which emulsions stabilised with WPI reduce friction, and the resultant effect of

saliva. The authors concluded that the ability of an emulsion to first adhere to the surface of the tongue and later form a stable film determines the ability to reduce friction. Although saliva has a significant effect in removing oil from the hydrophobic tongue, emulsions that are prone to coalescence during oral processing appear to adhere more strongly and spread more easily on the surface of the tongue. This would have a direct effect on the perception attributes of these systems, a hypothesis confirmed by sensory studies which have shown that emulsions with a higher sensitivity to coalescence are perceived as more fatty and creamy (Dresselhuis *et al.*, 2008c).

Therefore, another 'tool' for succussfully designing functional foods is the introduction of (a level of) mucoadhesive properties into food formulations, as this could allow for the control of food transit time (e.g. delay) and manipulation of the coverage of oral surfaces. Malone *et al*. (2003) formulated chitosan stabilised o/w emulsions that could adhere to the mucus layer, resulting in absorption, even after 5 minutes. A result of the chitosan absorbing onto the oral mucosa, though, is an astringent mouthfeel, attributed to complexation and precipitation of salivary proteins (Rossetti *et al*., 2008).

9.4 *IN VITRO* MEASUREMENTS OF SENSORY PERCEPTION

It has been established that there are links between the sensory attributes of foods and their physical properties, usually in the form of (both bulk and thin film) rheological properties. However, it should be stressed that these links tend to be limited to specific products or individual attributes. This is partly due to the fact that the range of shear rates experienced in the mouth during oral processing, as reported in the available literature, is very wide, mainly due to the complexity of the system under investigation and also because the very nature of oral processing is quite material-specific. An example of this can be found in the early study by Shama and Sherman (1973), which demonstrated that the perceived thickness of a variety of foods could be correlated with bulk rheology as measured for a shear rate range from 10 to 1000 per second, depending on the material tested; however, correlations were subject to exceptions at high viscosities for non-Newtonian foods. Work on emulsions by Akhtar *et al*. (2005) studied the effects on sensory perception introduced by changes in the emulsions' oil content and droplet size. Perception did correlate with fat content and viscosity, but fat content only at high viscosities and not in the presence of thickeners, thus leaving the conclusions uncertain. Droplet sizes and emulsifier type

seemed to have no effect on the range of the tested samples. Similarly for smoothness, Kokini (1987) correlated the thin film rheology and friction of foods to creaminess and thickness (viscosity and large-scale rheology).

Physical measurements on the structure of emulsions can be greatly affected in the case of a time-dependent behaviour. The stability of an emulsion is an important factor in categorising its behaviour. Measurements of interfacial rheology in emulsions stabilised by proteins have been shown to relate to droplet stability, to creaming and coalescence phenomena, but also to the actual texture of the emulsion (Murray and Dickinson, 1996). Links to actual perception of bulk rheological properties are not yet established. However, work in understanding these interfaces could lead to a better understanding of emulsion behaviour and even sensory characteristics (Moore *et al*., 1998; Murray, 2002).

Recent work in emulsions has related fat perception, in the form of slipperiness or mouth lubrication, to properties measured using thin-film rheology and tribology, since bulk rheology failed to give reliable predictions for the overall mouthfeel of these systems. Tribology measurements consist of measuring the friction between two surfaces (with either one or both of these in motions) separated by a thin film of lubricating material. Commonly in food research, soft surfaces such as Poly-di-methyl-siloxane (PDMS) or silicone are used to give comparable 'oral-like' surfaces for friction measurement (de Vicente *et al*., 2006; Bongaerts *et al*., 2007a). The most frequently used configuration, during tribology experiments, consists of a rotating sphere loaded at an angle onto a rotating disc, creating a small contact point between the surfaces. Traditionally, lubrication properties are represented using a Stribeck curve, where the measured friction (or traction) coefficient data are plotted for a range of entrainment speeds of a lubricant (Fig. 9.3). The Stribeck curve can be divided into three main sections, which correspond to different lubrication regimes and also to films (as formed between the two surfaces) of different thicknesses. At low entrainment speeds, the system is within the boundary regime, where very little or no lubricant is entrained by the rotating surfaces and so the measured (high) friction is mainly due to surface-to-surface contacts. As speed is increased, the system enters the mixed regime, where now a thin film of material is present between the surfaces, partly separating them, and as a result, the measured friction is significantly reduced. Further increases in speed will finally move the system into the elasto-hydrodynamic regime, where the surfaces become completely separated from each other and the bulk (rheological) properties of the lubricant now determine the measured friction (Czichos, 1978). The behaviour, schematically represented in Fig. 9.3, is only exhibited by materials where there is no physical change taking place. For time-dependant materials, such as

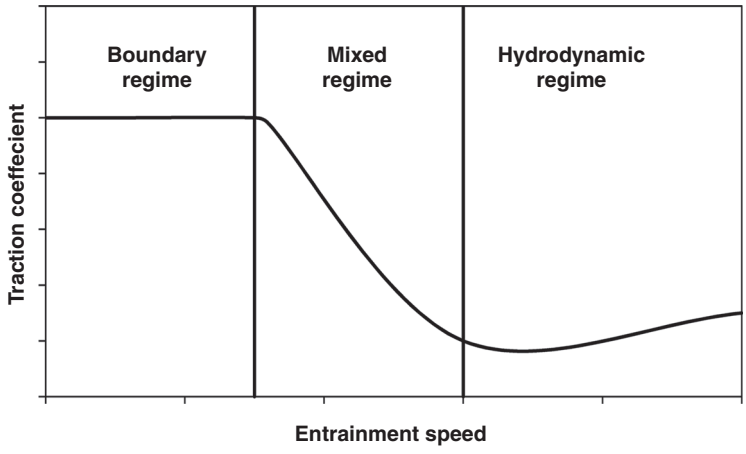

Fig. 9.3 Schematic of a Stribeck curve showing the different lubrication regimes.

un-stabilised emulsions, tribological experiments under constant speeds should be carried out instead, as these would allow determination of the behaviour of these systems under 'mouth-like' conditions.

In vitro measurements, such as tribology, can also prove extremely useful for the evaluation of fat-replacement approaches in food products (via an emulsion route), where the main concern is that the consumer might perceive the reduction in oil content as a reduction in the overall 'fattiness' of the product. Work carried out by Malone *et al*. (2003) investigated the tribological behaviour and sensory perception of simple oil-in-water emulsions of varying fat content and compared these to pure oil. The obtained Stribeck curves showed differences between samples of varying oil content. Below 15% oil content, the curves obtained overlapped that of pure water, thus showing a water-continuous contact under all stages of lubrication. The behaviour of systems containing between 15 and 30% oil was only found to, more or less, overlap that of pure oil in the boundary and mixed regimes and to follow that of pure water in the hydrodynamic regime. Finally for the emulsions containing 55% of oil, the obtained behaviour matches that of pure oil throughout the three lubrication regimes.

The sensory part of this work was equally interesting. Malone *et al*. (2003) showed that samples with oil content between 15 and 30% were difficult to be distinguished and received similar scores, which is in agreement with the fact that the friction results for these systems overlap within the boundary and mixed regimes. This further indicates that it is these lubrication regions that reflect the lubrication as it occurs between the tongue and palate during oral processing/assessment. The work also showed that the 55% oil-containing emulsion received a higher score

than the other emulsions (in terms of fattiness), when it was only found to be different in fraction measured above 100 mm/second, thus suggesting that a sensorial difference can be detected at these speeds. As all samples had the same bulk viscosity, results indicate that tribology measurements are a more relevant descriptor. Fat perception, however, does not just relate to the lubrication experienced in the mouth; this is evident in the sensory scores for the emulsion containing 1% oil, which are different to those for pure water (0% oil). This is attributed to flavours and volatiles present in the oil phase, which can be detected in the mouth even though the actual lubrication sensation remains the same.

Further to this work, Vingerhoeds *et al*. (2008) looked more extensively into the sensory response of different oils and oil contents in emulsions. In this study, increasing the fat content led to an increasing perception of fat-related attributes, but this is believed to be mostly due to viscosity increases between systems, as stated by Mela *et al*. (1994). This is somewhat confirmed by results gathered from guar-thickened emulsions of matched viscosities; panellists gave the same fattiness scores to a guar-thickened 10% oil-containing emulsion and an un-thickened 40% oil-containing emulsion. However, this result affected other attributes, making the thickened sample, for example, appear 'slimier'.

In order to determine whether tribology can indeed be used as a tool for the evaluation of emulsions processed under oral conditions, Dresselhuis *et al*. (2008a) carried out a series of experiments focusing on the different measuring aspects of the technique itself. Initially, the study compared PDMS and a biological tissue material (tongue from pig) in terms of their efficiency for use as the surfaces in contact during the tribology experiments, in other words, to determine which type of surface best reflects the characteristics of oral surfaces during food oral processing. The findings of this work revealed that there are certain issues associated with the use of the PDMS surface, namely the differences in roughness and hardness between the actual oral surfaces and PDMS. However, the practical implications of using biological materials for this type of experimentation render their use rather problematic and therefore an artificial surface would be more preferable, although in need of some improvement (Dresselhuis *et al*., 2008a). Another study by Ranc *et al*. (2006), looking at modified PDMS surfaces in tribology, showed that there is potential to make this type of surfaces more representative of the mouth, which is extremely important, since the frictions measured during such a test have been shown to be affected by the surfaces used. Regardless of this though, good correlations can still be obtained between sensory and friction measurements even when relatively rough PDMS surfaces are used (Ranc *et al*. (2006)). The set-up of the equipment used in this work was different to what is commonly used; here a lower glass plate moves over the 'tongue' or PDMS surface and as such

the range of speeds that can be obtained is fairly limited. This means that traditional Stribeck curves are not easy to obtain, and therefore, only timed experiments at a fixed speed can be carried out.

In their study, Ranc *et al*. (2006) further investigated the lubrication behaviour of emulsions undergoing time-dependent structural changes and analysed the effect on perception. A range of emulsions were studied, both *in vivo* and *in vitro*, with the obtained results suggesting that those more prone to coalescence were perceived as more fatty and had reduced friction (Dresselhuis *et al*., 2008b). This can be explained by the fact that coalescence increases the size of the emulsion droplets, which makes them adhere and spread more easily on the tribometer surfaces, thus leading to a lower friction value. In reality, this happens only at low speeds, since above a certain (high) critical speed, emulsion droplets are re-emulsified, and therefore, measured friction is increased as they are expelled from between the surfaces. The modified tribometer set-up, used by Ranc *et al*. (2006), was also adopted in a recent study by Chojnicka (2009), where the frictional and sensory properties of milk of varying fat content were investigated. Correlations with multiple attributes, including perceived creaminess, were obtained for fat contents between 1 and 4%, systems that also exhibited a reduced friction at low speeds, within the mixed and boundary regimes. The observed friction reduction was again attributed to coalescence events between the oil droplets during measurement. Individuals were able to distinguish between samples of different levels of fat, but this is probably due to the differences in the viscosities between the samples. What further supports this argument is the fact that the perceived differences between the samples correlated with the differences in their viscosities (Chojnicka, 2009).

9.5 FUTURE PERSPECTIVES

Design, processing and properties of emulsions have been extensively investigated over the years. In the area of foods, proteins have been commonly used to stabilise emulsions, and as such there is an interest in trying to understand the ways proteins stabilise emulsion systems and the properties they impart on them. Currently, there is a need to design functional food products and more specifically lower fat alternatives without compromising sensory properties. This has created a strong interest towards understanding the ways that emulsion systems behave under oral processing and the resulting sensory attributes.

Obtaining an understanding of oral processes and the changes these induce to emulsion structures is an active area of research, but a significant amount of work is still required to allow for the design of functional

emulsions. In this area, it is necessary to obtain an understanding of the phenomena occurring at all relevant scales ranging from *cm* to *nm*. Mixing and kinetics of food interaction with saliva and the shear and elongational forces associated with these will have to be quantified in an engineering context. This will require development and application of novel *in vitro* methods.

Oral processing of emulsions includes destabilisation phenomena, such as depletion flocculation, as a result of interactions with saliva and oral surfaces. Investigation of the interactions between emulsions and saliva/mucin under oral condition with an emphasis on phenomena occurring at the interface of the emulsions will be required. Significant challenges in this area are a result of the biological and variable nature of the materials involved as well as the dynamic nature of the materials and the interfacial phenomena.

A number of sensory properties, such as smoothness and creaminess, have already been linked with bulk rheological properties of fluids and soft solids. Empirical correlations have been made using viscosity measurements at conditions 'relevant' to oral processes. A better understanding of the relation between structure and structural changes, under oral processing, and sensory perception is required to design functional materials.

A potentially powerful tool towards achieving this could be the development and use of *in vitro* and *in silico* models, which would allow for more detailed studies of emulsions under conditions relevant to oral processing. This, albeit challenging, will provide the opportunity to evaluate the performance of new structures. Recent developments in instrumental measurements have demonstrated, for example, the possibility of using tribological techniques to understand the behaviour of emulsions in narrow gaps and then relate this measured response to their sensory properties.

REFERENCES

Adams, S., Singleton, S., Adamsa, S., Singletonb, S., Juskaitisc, R. and Wilsonc, T. (2007) In-vivo visualisation of mouth-material interactions by video rate endoscopy. *Food Hydrocolloids* **21**(5–6), 986–995.

Akhtar, M., Stenzel, J., Akhtar, M., Stenzel, J., Murray, B.S. and Dickinson, E. (2005) Factors affecting the perception of creaminess of oil-in-water emulsions. *Food Hydrocolloids* **19**(3), 521–526.

Aps, J.K.M. and Martens, L.C. (2005) Review: the physiology of saliva and transfer of drugs into saliva. *Forensic Science International* **150**(2–3), 119–131.

Arai, E. and Yamada, Y. (1993) Effect of the texture of food on the masticatory process. *Japan Journal of Oral Biology* **35**, 10.

Arai, T. and Norde, W. (1990a) The behavior of some model proteins at solid-liquid interfaces 1. Adsorption from single protein solutions. *Colloids and Surfaces* **51**, 1–15.

Arai, T. and Norde, W. (1990b) The behavior of some model proteins at solid–liquid interfaces 2. Sequential and competitive adsorption. *Colloids and Surfaces* **51**, 17–28.

Aronson, M.P. (1989) The role of free surfactant in destabilizing oil-in-water emulsions. *Langmuir* **5**(2), 494–501.

Barkhausen, J., Goyen, M., von Winterfeld F., Lauenstein T., Arweiler-Harbeck D. and Debatin J.F. (2002) Visualization of swallowing using real-time TrueFISP MR fluoroscopy. *European Radiology* **12**(1), 129–133.

Beverung, C.J., Radke, C.J. and Blanch H.W. (1999) Protein adsorption at the oil/water interface: characterization of adsorption kinetics by dynamic interfacial tension measurements. *Biophysical Chemistry* **81**(1), 59–80.

Binks, B.P. (1998) *Modern Aspects of Emulsion Science*. Cambridge: Royal Society of Chemistry.

Bongaerts, J.H.H., Fourtouni, K. and Stokes J.R. (2007a) Soft-tribology: lubrication in a compliant PDMS-PDMS contact. *Tribology International* **40**(10–12), 1531–1542.

Bongaerts, J.H.H., Rossetti, D. and Stokes J.R. (2007b) The lubricating properties of human whole saliva. *Tribology Letters* **27**(3), 277–287.

Bos, M.A. and van Vliet, T. (2001) Interfacial rheological properties of adsorbed protein layers and surfactants: a review. *Advances in Colloid and Interface Science* **91**(3), 437–471.

Chen, J. (2009) Food oral processing–a review. *Food Hydrocolloids* **23**(1), 1–25.

Chen, J. and Dickinson, E. (1995) Protein/surfactant interfacial interactions part 1. Flocculation of emulsions containing mixed protein + surfactant. *Colloids and Surfaces A: Physicochemical and Engineering Aspects* **100**, 255–265.

Chojnicka, A. (2009) Sensory perception and friction coefficient of milk with increasing fat content (submitted).

Claesson, P.M., Blomberg, E., Fröberg, J.C., Nylander, T. and Arnebrant, T. (1995) Protein interactions at solid surfaces. *Advances in Colloid and Interface Science* **57**, 161–227.

Czichos, H. (1978) *Tribology: A Systems Approach to the Science and Technology of Friction, Lubrication, and Wear*. Amsterdam, The Netherlands: Elsevier.

Davies, G.A. and Stokes, J.R. (2008) Thin film and high shear rheology of multiphase complex fluids. *Journal of Non-Newtonian Fluid Mechanics* **148**(1–3), 73–87.

Derkatch, S.R., Levachov, S.M., Kuhkushkina, A.N., Novosyolova, N.V., Kharlov, A.E. and Matveenko, V.N. (2007) Rheological properties of concentrated emulsions stabilized by globular protein in the presence of nonionic surfactant. *Colloids and Surfaces A: Physicochemical and Engineering Aspects* **298**(3), 225–234.

de Vicente, J., Stokes, J.R. and Spikes H.A. (2006) Soft lubrication of model hydrocolloids. *Food Hydrocolloids* **20**(4), 483–491.

Dickinson, E. (2003) Hydrocolloids at interfaces and the influence on the properties of dispersed systems. *Food Hydrocolloids* **17**(1), 25–39.

Dickinson, E., Golding, M. and Povey, M.J.W. (1997) Creaming and flocculation of oil-in-water emulsions containing sodium caseinate. *Journal of Colloid and Interface Science* **185**(2), 515–529.

Dresselhuis, D.M., de Hoog, E.H.A., Cohen Stuart, M.A. and van Aken G.A. (2008a) Application of oral tissue in tribological measurements in an emulsion perception context. *Food Hydrocolloids* **22**(2), 323–335.

Dresselhuis, D.M., de Hoog, E.H.A., Cohen Stuart, M.A., Vingerhoeds, M.H. and van Aken, G.A. (2008b) The occurrence of in-mouth coalescence of emulsion droplets in relation to perception of fat. *Food Hydrocolloids* **22**(6), 1170–1183.

Dresselhuis, D.M., Cohen Stuart, M.A., van Aken, G.A., Schipper, R.J. and de Hoog, E.H.A. (2008c) Fat retention at the tongue and the role of saliva: Adhesion and spreading of 'protein-poor' versus 'protein-rich' emulsions. *Journal of Colloid and Interface Science* **321**(1), 21–29.

Euston, S.R., Finnigan, S.R., Finnigan, S.R. and Hirst, R.L. (2001) Aggregation kinetics of heated whey protein-stabilised emulsions: effect of low-molecular weight emulsifiers. *Food Hydrocolloids* **15**(3), 253–262.

Felton, S.M., Gaige, T.A., Reese, T.G., Wedeen, V.J. and Gilbert, R.J. (2007) Mechanical basis for lingual deformation during the propulsive phase of swallowing as determined by phase-contrast magnetic resonance imaging. *J Appl Physiol* **103**(1), 255–265.

Freer, E.M., Yim, K.S., Fuller, G.G. and Radke, C.J. (2004) Interfacial rheology of globular and flexible proteins at the hexadecane/water interface: comparison of shear and dlatation deformation. *The Journal of Physical Chemistry B* **108**(12), 3835–3844.

Galazka, V.B., Dickinson, E., Dickinson, E. and Ledward, D.A. (1996) Effect of high pressure on the emulsifying behaviour of [beta]-lactoglobulin. *Food Hydrocolloids* **10**(2), 213–219.

Glantz, P.-O. (1997) Interfacial phenomena in the oral cavity. *Colloids and Surfaces A: Physicochemical and Engineering Aspects* **123–124**, 657–670.

Graham, D.E. and Phillips, M.C. (1979) Proteins at liquid interfaces: II. Adsorption isotherms. *Journal of Colloid and Interface Science* **70**(3), 415–426.

Hiiemae, K., Heath, M.R., Heath, G., Kazazoglu, E., Murray, J., Sapper, D. and Hamblett, K. (1996) Natural bites, food consistency and feeding behaviour in man. *Archives of Oral Biology* **41**(2), 175–189.

Hiiemae, K.M. and Palmer, J.B. (1999) Food transport and bolus formation during complete feeding sequences on foods of different initial consistency. *Dysphagia* **14**(1), 31–42.

Humbert, I. and Robbins, J. (2007) Normal swallowing and functional magnetic resonance imaging: a systematic review. *Dysphagia* **22**(3), 266–275.

Humphrey, S.P. and Williamson, R.T. (2001) A review of saliva: Normal composition, flow, and function. *The Journal of Prosthetic Dentistry* **85**(2), 162–169.

Hutchings, J.B. and Lillford, P.J. (1988) The perception of food texture – the philosophy of the breakdown path. *Journal of Texture Studies* **19**(2), 103–115.

Keowmaneechai, E. and McClements, D.J. (2002) Influence of EDTA and citrate on physicochemical properties of whey protein-stabilized oil-in-water emulsions containing CaCl2. *Journal of Agricultural and Food Chemistry* **50**(24), 7145–7153.

Kim, H.J., Decker, E.A. and McClements, D.J. (2002) Role of postadsorption conformation changes of $\hat{I}^2$-lactoglobulin on its ability to stabilize oil droplets against flocculation during heating at neutral pH. *Langmuir* **18**(20), 7577–7583.

Kokini, J.L. (1987) The physical basis of liquid food texture and texture-taste interactions. *Journal of Food Engineering* **6**(1), 51–81.

Kulmyrzaev, A.A. and Schubert, H. (2004) Influence of KCl on the physicochemical properties of whey protein stabilized emulsions. *Food Hydrocolloids* **18**(1), 13–19.

Lund, J.P. (1991) Mastication and its control by the brain stem. *Critical Reviews in Oral Biology & Medicine* **2**(1), 33–64.

Mackie, A.R., Gunning, A.P., Ridout, M.J., Wilde, P.J. and Morris, V.J. (1999) Orogenic displacement of protein from the oil/water interface. *Langmuir* **16**(5), 2242–2247.

Malone, M.E., Appelqvist, I.A.M. and Norton, I.T. (2003) Oral behaviour of food hydrocolloids and emulsions. Part 1. Lubrication and deposition considerations. *Food Hydrocolloids* **17**(6), 763–773.

Mela, D.J., Langley, K.R. and Martin, A. (1994) Sensory assessment of fat content: effect of emulsion and subject characteristics. *Appetite* **22**(1), 67–81.

Mohan, S. and Narsimhan, G. (1997) Coalescence of protein-stabilized emulsions in a high-pressure homogenizer. *Journal of Colloid and Interface Science* **192**(1), 1–15.

Moore, P.B., Langley, K., Wilde, P.J., Fillery-Travis, A. and Mela , D.J. (1998) Effect of emulsifier type on sensory properties of oil-in-water emulsions. *Journal of the Science of Food and Agriculture* **76**(3), 469–476.

Murray, B.S. (2002) Interfacial rheology of food emulsifiers and proteins. *Current Opinion in Colloid & Interface Science* **7**(5–6), 426–431.

Murray, B.S. and Dickinson, E. (1996) Interfacial rheology and the dynamic properties of adsorbed films of food proteins and surfactants. *Food Science and Technology International, Tokyo* **2**(3), 131–145.

Nicosia, M.A. and Robbins, J. (2001) The fluid mechanics of bolus ejection from the oral cavity. *Journal of Biomechanics* **34**(12), 1537–1544.

Norton, I., Fryer, P. and Moore, S. (2006). Product/process integration in food manufacture: engineering sustained health. *Aiche Journal* **52**(5), 1632–1640.

Pivk, U., Godinot, N., Keller, C., Antille, N., Juillerat, M. and Raspor, P. (2008) Lipid deposition on the tongue after oral processing of medium-chain triglycerides and impact on the perception of mouthfeel. *Journal of Agricultural and Food Chemistry* **56**(3), 1058–1064.

Rampon, V., Riaublanc, A., Anton, M., Genot, C. and McClements, D.J.V. (2003) Evidence that homogenization of BSA-stabilized hexadecane-in-water emulsions induces structure modification of the nonadsorbed protein. *Journal of Agricultural and Food Chemistry* **51**(20), 5900–5905.

Ranc, H., Servais, C., Chauvy, P.-F., Debaud, S. and Mischler, S. (2006) Effect of surface structure on frictional behaviour of a tongue/palate tribological system. *Tribology International* **39**(12), 1518–1526.

Raynal, B.D.E., Hardingham, T.E., Hardingham, T.E., Thornton, D.J. and Sheehan, J.K. (2002) Concentrated solutions of salivary MUC5B mucin do not replicate the gel-forming properties of saliva. *Biochemical Journal* **362**(2), 289–296.

Rossetti, D., Yakubov, G.E., Stokes, J.R., Williamson, A.-M., Fuller, G.G. (2008) Interaction of human whole saliva and astringent dietary compounds investigated by interfacial shear rheology. *Food Hydrocolloids* **22**(6), 1068–1078.

Sajewicz, E. (2009) Effect of saliva viscosity on tribological behaviour of tooth enamel. *Tribology International* **42**(2), 327–332.

Shama, F. and Sherman, P. (1973) Identification of stimuli controlling the sensory evaluation of viscosity II. Oral methods. *Journal of Texture Studies* **4**(1), 111–118.

Silletti, E., Vingerhoeds, M.H., Norde, W. and van Aken, G.A. (2007) The role of electrostatics in saliva-induced emulsion flocculation. *Food Hydrocolloids* **21**(4), 596–606.

Silva, A., Fabio, S., Fabio, S.R.C. and Dantas, R.O. (2008) A scintigraphic study of oral, pharyngeal, and esophageal transit in patients with stroke. *Dysphagia* **23**(2), 165–171.

Soares, R.V., Lin, T., Siqueira, C.C., Bruno, L.S., Li, X., Oppenheim, F.G., Offner, G. and Troxler, R.F. (2004) Salivary micelles: identification of complexes containing MG2, sIgA, lactoferrin, amylase, glycosylated proline-rich protein and lysozyme. *Archives of Oral Biology* **49**(5), 337–343.

Srinivasan, D. (2005) Protein stabilization of emulsions and foams. *Journal of Food Science* **70**(3), R54–R66.

Stokes, J.R. and Davies, G.A. (2007) Viscoelasticity of human whole saliva collected after acid and mechanical stimulation. *Biorheology* **44**(3), 141–160.

Strous, G.J. and Dekker, J. (1992) Mucin-type glycoproteins. *Critical Reviews in Biochemistry and Molecular Biology* **27**(1–2), 57–92.

Surh, J., Decker, E.A. and McClements, D.J. (2006) Influence of pH and pectin type on properties and stability of sodium-caseinate stabilized oil-in-water emulsions. *Food Hydrocolloids* **20**(5), 607–618.

Tornberg, E. and Hermansson, A.M. (1977) Functional characterization of protein stabilized emulsions: effect of processing. *Journal of Food Science* **42**(2), 468–472.

van Aken, G.A., Blijdenstein, T.B.J., Blijdenstein, T.B.J. and Hotrum, N.E. (2003) Colloidal destabilisation mechanisms in protein-stabilised emulsions. *Current Opinion in Colloid & Interface Science* **8**(4–5), 371–379.

van Aken, G.A., Vingerhoeds, M.H., Vingerhoeds, M.H. and de Hoog, E.H.A. (2007) Food colloids under oral conditions. *Current Opinion in Colloid & Interface Science* **12**(4–5), 251–262.

Van Der Bilt, A. (2009) Oral physiology, mastication and food perception. In: McClements, D.J. and Decker, E.A., editors. *Designing Functional Foods: Measuring and Controlling Food Structure Breakdown and Nutrient Absorption*. Oxford: Woodhead Publishing Limited, pp. 3–29.

van Vliet, T., van Aken, G.A., de Jongh, H.H.J. and Hamer, R.J. (2009) Colloidal aspects of texture perception. *Advances in Colloid and Interface Science* **150**(1), 27–40.

Vingerhoeds, M.H., Blijdenstein, T.B.J., Zoet, F.D. and van Aken, G.A. (2005) Emulsion flocculation induced by saliva and mucin. *Food Hydrocolloids* **19**(5), 915–922.

Vingerhoeds, M.H., de Wijk, R.A., Zoet, F.D., Nixdorf, R.R. and van Aken, G.A. (2008) How emulsion composition and structure affect sensory perception of low-viscosity model emulsions. *Food Hydrocolloids* **22**(4), 631–646.

Watson, T.F., Neil, M.A.A., Juškaitis, R., Cook, R.J. and Wilson, T. (2002) Video-rate confocal endoscopy. *Journal of Microscopy* **207**(1), 37–42.

Wickstrom, C., Christersson, C., Davies, J.R. and Carlstedt, I. (2000) Macromolecular organization of saliva: identification of 'insoluble' MUC5B assemblies and non-mucin proteins in the gel phase. *Biochemical Journal* **351**, 421–428.

Wilde, P., Mackie, A., Husband, F., Gunning, P. and Morris, M. (2004) Proteins and emulsifiers at liquid interfaces. *Advances in Colloid and Interface Science* **108–109**, 63–71.

Wilde, P.J. (2000a) Interfaces: their role in foam and emulsion behaviour. *Current Opinion in Colloid & Interface Science* **5**(3–4), 176–181.

Wilde, P.J. (2000b) Physically modified proteins. In: Doxastakis, G. and Kiosseoglou, V., editors. *Developments in Food Science*, Volume **41**. Cambridge: Elsevier, pp. 161–180.

Windhab, E.J., Dressler, M., Fischer, F.P., Megias-Alguacil, D. (2005) Emulsion processing – from single-drop deformation to design of complex processes and products. *Chemical Engineering Science* **60**(8–9), 2101–2113.

10 Rheological Control and Understanding Necessary to Formulate Healthy Everyday Foods

Ian T. Norton, Abigail B. Norton, Fotios Spyropoulos, Benjamin J. D. Le Révérend and Philip Cox

10.1 INTRODUCTION

There is clear evidence that the consumption of high calorific and/or salty diets leads to chronic diseases such as obesity, type II diabetes and hypertension (Dahl, 2005). However, most people are reluctant to change their dietary habits.

This gives the formulation scientist (microstructural engineer) an opportunity to develop the science and understanding necessary to produce high quality everyday foods with lower calories and salt, but with all the qualities and consumer perception of the unhealthy food (Le Révérend *et al*., 2009; Norton *et al*., 2006b). One of the major tools available is rheological measurements/materials measurement. However, in order to understand the product and redesign it to be healthier and still acceptable to the consumer, no one technique can be used alone. So, from a practical standpoint, a range of techniques are used to get an understanding of the products and how different parameters relate to consumer response. For instance, in order to understand what happens in the mouth, we need to use tribology, rheology, viscosity at a range of temperatures, yield values (creep compliance), Young's modulus and failure stress and strain. For spreading, we need rheology, thin-film behaviour (tribology) and compression tests; if a product is to be cooked, we need to measure the relevant material properties at a range of temperatures.

A good example of the approach necessary to understand and then gain detailed control of the rheological properties of food can be given by considering mayonnaise. On the face of it, this is a simple food. However, in order to formulate a product that can be considered to be a healthy everyday food, what do we need to do? There are many low-fat mayonnaise formulations in the market. However, they suffer in terms of their acceptability because their textures are significantly different from

Practical Food Rheology: An Interpretive Approach
Edited by Ian T. Norton, Fotios Spyropoulos and Philip Cox
 ISBN: 978-1-405-19978-0

the full-fat original. The reason is that in most cases, the reformulation has been tackled by using starch to replace some of the fat. The starch is present as swollen granules or in a hydrolysed format. Unfortunately, the starch used does not sufficiently resemble fat to fool the mouth, and so the products are generally described as having a 'pasty' feel. The microstructural explanation for this is that the fat in mayonnaise exists in soft spherical droplets with an average size of about 5 μm. The starches used by the manufactures are gelatinised to various states, but always have dimensions of between 10 and 100 μm. The consumer easily identifies the resulting rheological changes and the products are described as thick and gloopy.

An alternative has been developed, which can reduce the amount of fat in emulsion-based water-continuous products without changing their sensory properties. This is a microstructure approach, which is used to design 'droplets' based on alternative materials or emulsion structures. Even using this approach, it is impossible to remove all of the fat, as doing so has a detrimental effect on flavour release (Le Révérend *et al.*, 2009), but it is possible to remove a significant proportion of the fat. So what is the microstructure approach? In principle, this is shown in Fig. 10.1. This schematic implies that the microstructure determines the physical properties of the product and thus the consumer response. In addition, we need to consider the temperature profile for storage and then cooking and eating. On the other hand, the schematic implies that the microstructure is determined by both the process and the materials used. These hypotheses will be considered throughout this chapter.

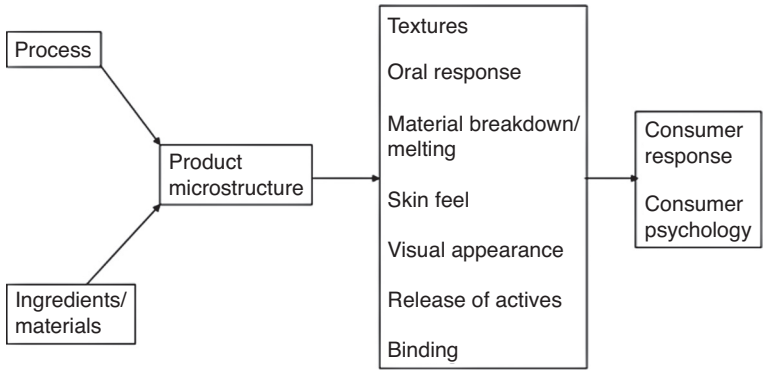

Fig. 10.1 Schematic representation of the microstructure approach, showing typical material properties and consumer aspects that are impacted by product microstructure along with which parameters can be used (i.e. process and starting materials/ingredients) to design the product microstructure.

10.2 DESIGN AND CONTROL OF MATERIAL PROPERTIES OF FOODS INSIDE PEOPLE

If we are to construct healthy everyday foods, we need to start out by considering what happens inside the body. The three major stages worth considering are the mouth, the stomach, and the intestine. The processes that occur and the rheological considerations that need to be made are different for these three stages.

10.2.1 Oral perception of foods

Once food has entered the mouth, it is comminuted by mastication and chewing, which allows the release of flavour and for the texture to be experienced. As this breakdown proceeds, the coupling of mechanical, thermal and chemical reactions, as well as wetting by saliva, leads to the formation of a food bolus (Hutchings and Lillford, 1988). The bolus is processed until a threshold of size distribution and lubrication is achieved (Lillford, 2000). This processing not only occurs upon ingestion of solids, where its effect is rather intuitive (reduction of particle size distribution (Peyron *et al*., 2004), lubrication and hydration (Bongaerts *et al*., 2007)), but also occurs upon ingestion of soft solids and liquids, where the effects are more related to the tasting of aroma and the perception of texture(Kokini and Cussler, 1983).

Kokini and others (Kokini, 1987; Kokini, 1994; Kokini and Cussler, 1983) developed a creaminess 'equation' linking the perception of creaminess (intuitively related to fat content) with other sensory attributes from trained panellists such as thickness (related to the rheological properties), smoothness (related to the particle size in the system) and slipperiness (related to the friction properties). This relationship has been formulated in two studies (Kokini and Cussler, 1983; Kokini, 1994) as follows:

$$\text{Creaminess} \propto \text{thickness}^{0.54} \cdot \text{smoothness}^{0.82} \tag{10.1}$$

or

$$\begin{aligned}\text{Creaminess} = {} & 0.54 \cdot \log(\text{thickness}) + 1.56 \cdot \log(\text{smoothness}) \\ & + 0.32 \cdot \log(\text{slipperiness})\end{aligned} \tag{10.2}$$

The fact that a strongly hedonic sensory attribute such as creaminess can be explained by these attributes suggests that creaminess is not only controlled by the rheology of the product (Malone *et al*., 2003a; Akhtar

et al., 2005; Akhtar *et al*., 2006), but also by its lubricating properties. This is consistent with the observations from a study by Lillford (2000), in which it is indicated that, in the mouth, food is subject to not only a range of shear rates, but also to extensional flow; for more theory on this matter, the reader is directed to Steffe (1992).

On the other hand, astringency seems to be related to an increase in the friction coefficient (Malone *et al*., 2003a; de Hoog *et al*., 2006). In recent work (Bongaerts *et al*., 2007; Stokes *et al*., 2008), the injection of a typically astringent compound, epigallocatechin gallate (ECGC), a polyphenol extracted from green tea, was used while measuring the friction coefficient of saliva and was found to increase the friction coefficient from around 0.1 to 20. Under similar conditions, addition of water to the system also increased the friction coefficient, but to a lesser extent. The main difference rising from the introduction of ECGC is the rate at which the friction coefficient increases. Such data seems to confirm the original work from Malone *et al*. (2003a), in which astringency is related to the flocculation of the material in contact with the oral mucosa.

In conclusion, the various attempts made to formulate low-fat products by only matching their viscosity (to that of the full-fat equivalent) have failed because of the lack of understanding of oral processing, as well as the microstructure of the product. Indeed, it appears that, as suggested by Lillford (2000), *'texture is a consequence of the microstructure'*.

In terms of rheological response, the mouth is therefore very interesting (Chen, 2009). Here processes that are involved are a combination of the following: fracture as the material is broken, mixing with saliva, the viscosity effects that are obtained as the material breaks down and is diluted, and thin-film behaviour as the mouth works the material. Each of these is an interesting process and forms the basis of significant amounts of past and present research in foods (Aguilera and Lillford, 2007). The most recent addition to the toolbox of measurement techniques is tribology, which can be used to estimate, *in vitro*, the in-mouth lubricating properties of a food, allowing the food technologist to partially predict the performance of a designed formulation, which can be correlated with consumer response. It is now becoming a routine technique and as such is a very interesting measurement for the design and product development of everyday foods. However, the surfaces need to be adapted to more closely mimic the bio-surfaces of the mouth. This requirement has resulted in two different adaptations of the technique: the first is to have soft rubber surfaces in a pin or ball on plate technique (Malone *et al*., 2003a) and the other is the use of pig tongues (Dresselhuis *et al*., 2008).

Malone *et al*. (2003a) carried out the original piece of work in this field, where they studied a range of emulsions with different fat contents.

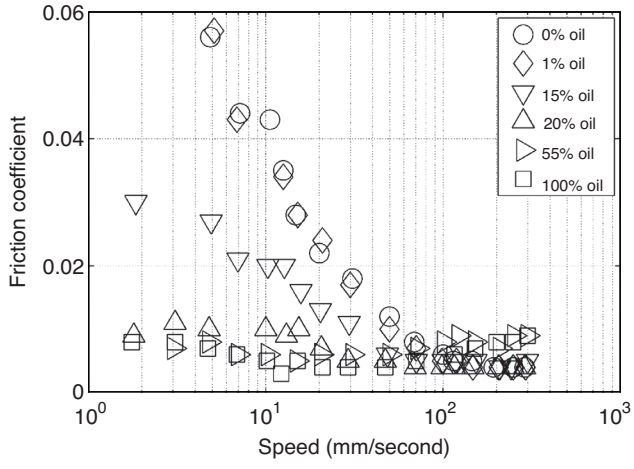

Fig. 10.2 Tribometer curves for o/w emulsions containing different levels of fat at 35°C. All emulsions were made to have the same viscosity at a shear rate of 100 per second.

All the emulsions were made iso-viscous at a shear rate of 100 per second. This work showed that the physical sensation of fat tends to be one of a mixture of thin-film (tribology) and hydrodynamic behaviour, i.e. the mixed regime. Fig. 10.2 shows how the frictional coefficient changes for a range of samples (emulsions with oil levels between 1 and 55%, the data obtained for the aqueous phase used and pure vegetable oil are included for comparision (Malone *et al.*, 2003a). As can be seen, at low rotational speeds (the tribological region – where the gap between the ball-and-plate is the smallest), the pure water and 1% fat emulsion have a much higher frictional coefficient than that of emulsions with 20% oil or more. The emulsion with 15% oil falls between these two sets of curves. As the rotational speed of the disc increases, the gap between the ball-and-plate increases and the flow becomes what is known as a mixed regime (hydrodynamic and tribological). In these conditions, emulsions with greater than 20% oil match the pure oil. Finally, at very high speeds, where the gap is greatest (the hydrodynamic regime), the emulsions with the lowest fat levels give the lowest friction. This is expected as they contain higher levels of hydrocolloids in this experiment, as the authors constructed the emulsions to be iso-viscous at 100 per second.

By comparing this data with sensory perception data (from a trained panel), it has been shown that the best correlation between the rheological measurement and the human sensation occurs with speeds between 10 and 100 mm/second (the mixed regime) (Malone *et al.*, 2003a). When considering the eating action and the dimensions of the human mouth, these speeds seem to be realistic. This data suggests that a lower

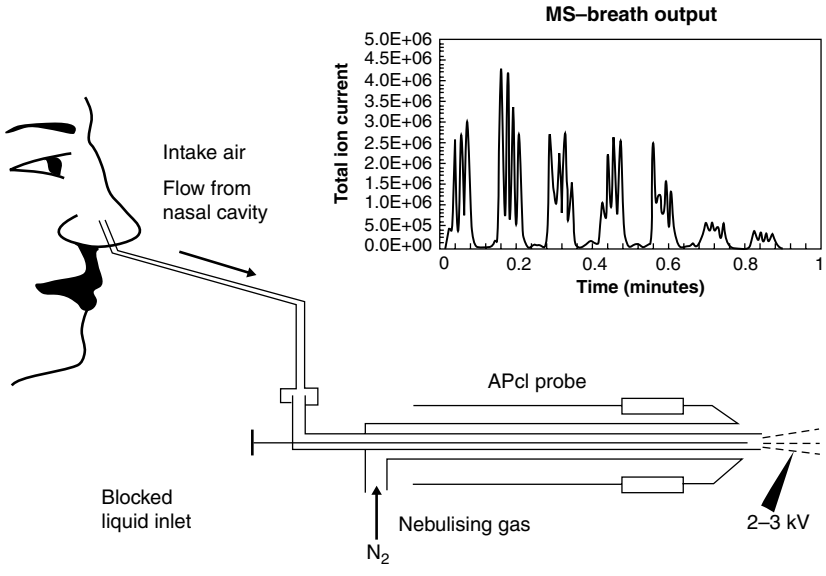

Fig. 10.3 Schematic representation of the experimental set-up for measuring in-mouth flavour release using APcI. Reproduced from Lian *et al.* (2004). Copyright 2004, with permission from Elsevier.

limit of fat content in emulsion-based products of between 15 and 20% gives acceptable performance on consumption. However, in the future, it is to be expected that microstrucural elements such as particles of gel or air-filled emulsion droplets will be designed to act like oil droplets, allowing these limits to be changed. This is discussed more fully later in the chapter.

The use of tribology should not be seen as a replacement for other rheological and material measurements of what happens within the human mouth, although the use of viscosity at 100 per second seems to be of limited value for most food products, even though it has been used extensively in the past.

The other aspect of the eating process that deserves consideration from a material structure and rheological control point of view is flavour release. If healthy everyday foods are to be acceptable to the consumer, we need to control the flavour release and the after-taste of the reformulate food.

The material properties and the detailed food microstructure and its breakdown in the mouth have been shown to affect the flavour of foods (Hutchings and Lillford, 1988; Lillford, 2000). More recently, Lian *et al*. (2004) have started to develop models for the release process and attempted to explain how the viscosity of a food influenced the mixing in the mouth and subsequent flavour release. This was studied using the MS breath technique, a schematic of which is shown in Fig. 10.3. In

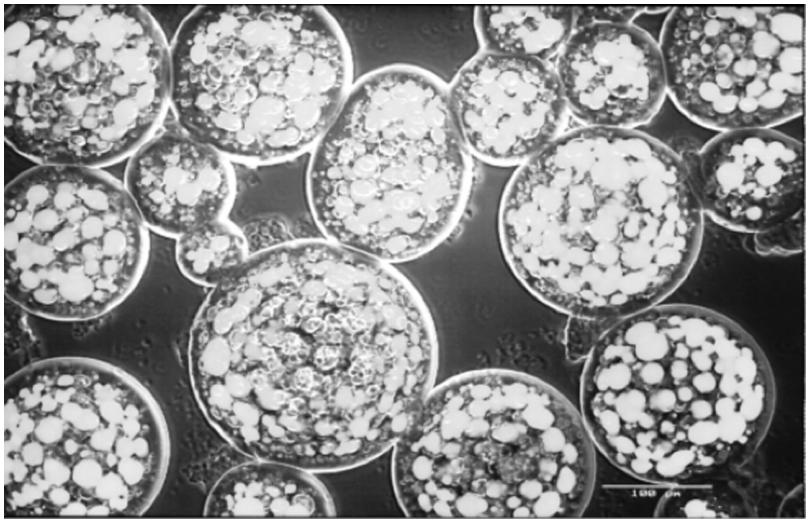

Fig. 10.4 Designed gel beads with included oil droplets to control flavour release of oil-soluble flavours. The photomicrograph shows oil droplets (the small white droplets) inside an alginate gel beads (which were designed to be soft and elastic) within a continuous aqueous phase (scale bar is 100 μm).

this experiment, a subject is asked to chew a food while the headspace within their nose is removed and analysed for the aroma compounds in real time.

An important aspect that emerges from this type of study is that the mouth is a mixer, which dilutes and mixes to a scale of about 10 μm. With this as background knowledge, it is possible to design and modify the release of tastes and flavours from foods. This requires the researcher to think about the mixing dimensions and how to build structures that can change these mixing dimensions. An example of how this can work can be illustrated for low-fat products. It has been reported (Malone *et al*., 2003b) that the flavour release of a 3% fat emulsion can match a 40% fat emulsion if the fat is included inside gel beads with dimensions of 100 or greater microns (Fig. 10.4). Flavour release from the fat droplets is then delayed as it needs to be transported to the edge of the gel bead before it can enter the saliva and ultimately the head space. This causes the flavour to be released more gradually and gives the impression of the product having a much greater fat content.

It has been proposed (Vliet *et al*., 2009) that particles of food broken down during the mastication process can not only form a bolus by adhering to one another, but can also adhere to the oral mucosa and stay in the oral cavity after the bolus has been swallowed. The same situation is also likely to occur with liquid that could be excluded from

the food bolus upon compression during swallowing, for example. These in-mouth residues are then largely contributing to the after-taste that can be perceived post-swallowing.

To control such phenomenon, a microstructural approach using polymers that bind to the oral mucosa, such as amidated pectins and chitosans alginates (Sigurdsson *et al*., 2006; Sriamornsak *et al*., 2008; Thirawong *et al*., 2008; Andrews *et al*., 2009), can be applied. A successful demonstration of this approach has been given by the pharmaceutical industry for controlled drug delivery not only on the oral mucosa, but also on other mucus-covered surfaces (Smart, 2005; Andrews *et al*., 2009). Such materials can therefore be manipulated to offer taste enhancement by prolonging the release of sapid molecules after swallowing.

Again, for this matter, the friction properties of the food bolus against the tongue and palate of the consumer should be important, as high friction will promote the deposition and adhesion of such residues. Tribological characterisation of food boluses in mouth-like condition appears then to be a key aspect to establish for future new product development.

10.2.2 Food in the stomach

The stomach offers a harsh and surprisingly complex environment for the research to consider or study. This complexity is in terms of its anatomy, physical and chemical environments, enzymology and psychology. The stomach is divided into four main parts: the fundus, body, antrum and pylorus, as presented in Fig. 10.5.

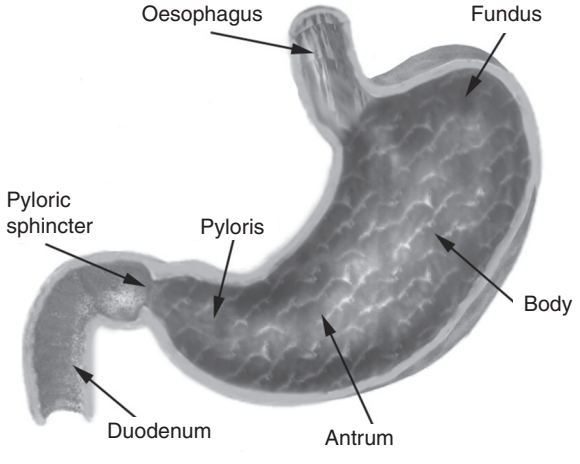

Fig. 10.5 Schematic of the human stomach.

These parts function in such a way as to allow storage of undigested food for primary digestion, mixing and comminution of the contents and then to propel the digested chyme to the intestine for further digestion and absorption. Although in terms of chronology, the processes in the antrum are towards the end of the process, it nevertheless provides the most important area when considering the breakdown of solid material. Food enters the stomach in a masticated form and has a variety of sizes and structural characteristics. Even though it will become diluted with gastric secretions, it is the physical actions of the antrum, which grinds, mixes and sieves the food (Kong and Singh, 2008), that reduces the particle sizes of the ingested food, and this is modulated by the release of material through the pylorus. The size reduction of food particles (as initiated by mastication) then exposes fresh surface area for dissolution or enzymatic attack.

The low pH of gastric juice has two practical evolutionary reasons and essentially only one digestive purpose. The evolutionary reasons are firstly, the acidic environment kills possible pathogens or parasites and secondly, it will rapidly dissolve potentially harmful bone fragments. The digestive purpose is that the low pH assists in the break-up of food structures and the molecular degradation of the food ingredients. The presence and secretion rate of gastric juice is itself modulated by the stomach contents and will rise from 1 mL/minute to 10–50 mL/minute upon food ingestion (Jalan *et al*., 1979; Versantvoort *et al*., 2005), in turn, this affects the pH of the stomach contents with a fasted stomach being in a range of pH 1.3–2.5 and a postprandial range of typically pH 4.5–5.8, which then falls rapidly. Similarly, stomach volume changes with the fasting state to full volume ranging from 25 mL to as much as 4 L (Kong and Singh, 2008). However, it is worth mentioning that the expectation of eating (i.e. a psychological response) will also affect gastric secretion as most famously shown by Pavlov (Pavlov and Gantt, 1928).

The other major constituents of gastric juice are pepsinogen/pepsin ($\sim$1 mg/mL) and suspended mucin removed from its protective position at the stomach wall. All of these components combine to produce a rheologically dynamic stomach content with a complex and changing rheological profile (Versantvoort *et al*., 2005). As previously mentioned, the antrum comminutes food particles and these are typically in the region of 1–2 mm, and these particles become suspended in the gastric juice, further complicating the gastric rheology. However, the emptying rate of the stomach is dependent upon the composition of the contents. The review of Kong and Singh (2008) highlights the differences between the stomach emptying rates for liquid and solid meals and correlates observed emptying rates with meal composition and calorific value. Most interestingly, they describe the dilution of initially viscous meals

with gastric juice and this reduces the satiation potentially provided by a thickened liquid.

A number of attempts have been made to model the behaviour of the human stomach (Wickham *et al*., 2009). These models are based on mixed tanks, which are run in sequence to mimic the behaviour of different parts of the stomach, i.e. the upper stomach, the lower stomach and even the small intestine. However, the approach has been used to investigate the digestive process and to a large extent to ignore the impact that food structure has on the flow and mixing behaviour, which would be observed in the real human stomach. These models do help from a nutritional aspect, including the molecular breakdown of components, but for the food engineer, there really needs to be further investigation to help design food material properties, including rheology for specific behaviour in the human GI tract.

Many people (de Wijk *et al*., 2008) have studied the effect of viscosity on the eating frequency of foods. In addition, they have investigated energy (sugar) update changes as a consequence of the meal viscosity (Spiller, 1994).

Other investigations (Marciani *et al*., 1998a, 1998b) have attempted to study food inside people using MRI. These researchers have investigated the effect of viscosity on gastric emptying and their results have shown only a slight effect for changes in viscosity to levels that are unpalatable. So far the effect of increasing the viscosity of a food has not resulted in changes on satiety in the range required to have a significant effect on dietary intake of food. So if control is to be obtained, then we need to have a rheological control beyond viscosity. This has introduced the idea of self-structuring systems discussed in detail later.

10.2.3 Food in the intestine

Studies in the intestine are very difficult and until recently have received virtually no attention at all for the healthy human.

In order to build a model of the human intestine, one would need to consider mass transfer, mixing and molecular degradation. A model intestine (Fig. 10.6) has been developed to study the chemical engineering aspects of the process (Thakaran *et al*., 2007). The machine has two cuffs that can be inflated either together or independently. These are designed to give the pulse flow, which is present within the human intestine. The extent of squeezing and timescale for the pulses can be varied.

The other part of the design is to have a semi-permeable membrane as an inner tube, which is then enclosed in a non-permeable membrane as the outer wall. This allows the transport of material to be measured

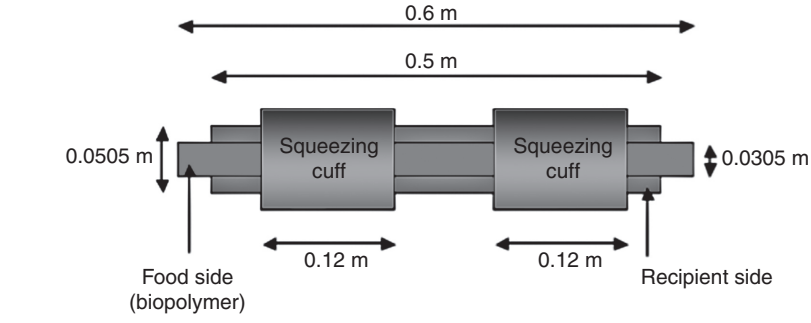

(a)

(b)

Fig. 10.6 A schematic (a) of the experimental set-up (b). For a colour version of this figure, please see the colour plate section.

during the experiment to simulate the transport of low molecular weight material across the gut wall into the blood stream.

Although in an early stage of development, this machine is starting to reveal some interesting results. They suggest that rheological measurements and understanding are important for what happens in the human intestine and that the human intestine is amenable to chemical engineering measurements and models. This is demonstrated in Fig. 10.7, which shows how the mass transport of sugar is affected by different guar concentrations under different flow and mixing conditions. This data shows how the squeezing mechanism increases transport at low guar concentrations (low viscosities), but as the concentration is increased (higher viscosities), there is little or no effect of flow rate or squeezing action (Thakaran *et al*., 2010).

Although this is an interesting development, there is a long way to go in terms of making it match the processes that occur in the flow of foods within the intestine and in terms of the transport mechanisms that occur across the membrane in a healthy individual. Future developments are planned, whereby a live intestine (pig) is the membrane and where techniques such as PEPT (Seville *et al*., 2005) are used to study the

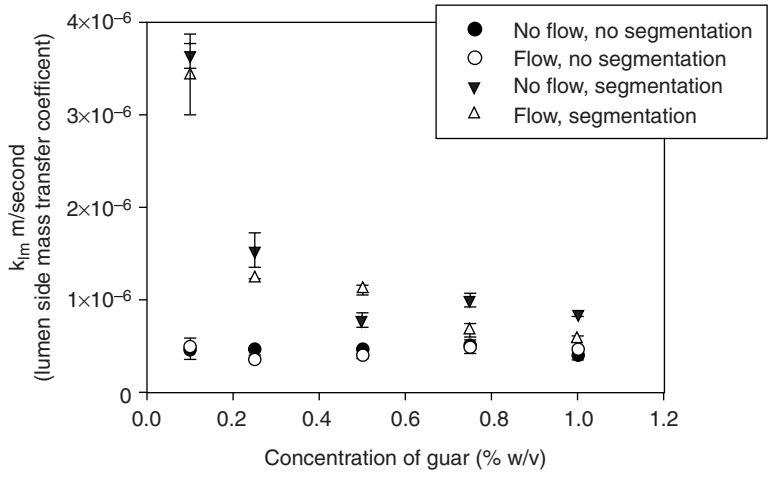

Fig. 10.7 Lumen mass transfer coefficient for a concentration of guar gums.

flow patterns when *villi* are present. This will be carried out in a way that keeps the intestine alive for a period of time so that studies can be carried out with an active membrane. Much more is expected from this approach in the near to medium term.

10.3 RECONSTRUCTING FOODS TO BE HEALTHY AND CONTROL DIETARY INTAKE

So how do you reconstruct a food for healthy everyday living?

The first thing that has to be developed is an understanding of how the current foods behave and how the behaviour is linked to the microstructure (see introduction). Having developed this understanding, then the alternative structures have to be designed and need to be constructed, which give similar physical properties, including material properties. This is not as simple as it first sounds: we need to consider the size of the element, rheology/fracture and flow properties and the way they interact with the rest of the structure. This needs to be done for storage, cooking and consumption. By way of example, let us consider what we need to do if we want to replace a fat droplet. Firstly, we need to have a particle, which is the same size as the oil droplet and has the same rheological properties of the oil particle that it is replacing. If we want to replace a saturated fat that forms a crystal network, then we need to construct a network, which has approximately the same crystal size and similar properties to the one that is being replaced. We then need to make sure that the new particle is placed into the food matrix in the same

way as the oil droplet it replaces and is then connected to the structure with the same strength of bonding and thermal liability.

We will now illustrate the approach by considering a number of successful applications:

10.3.1 Use of emulsions as partial fat replacement

The first approach is to replace pure fat with an emulsion. By doing this, the calorific value of the food will be reduced. Here, there is a whole new area of rheology that needs to be considered: interfacial rheology. This can be a consequence of low molecular weight surfactants assembling at an interface, thus imparting a change in interfacial rheology or it can be where large molecular weight material is adsorbed or where there is low molecular weight material aggregate due to the increased concentration. These then lead to a surface modulus or even a gel-like structure. This imparts a surface elasticity, which needs to be considered when designing our healthy everyday foods. If this is to be used in a practical sense, a rheological issue is raised, which needs to be considered; in terms of the measurement and control of interfacial rheology, and in practical terms, how does the practitioner/product developer measure this physical property accurately and reliably? This question will need to be addressed in the future.

One step further is to use particles at the interface (Pickering stabilisation). One way to use these is to construct emulsions which allow the addition of water to products where it is generally considered to be impossible because it causes dramatic changes in the material properties, often as a result of the solubility of sugar in water, for example chocolate. So if this is to be done, a totally new way of thinking about structures is required. Recent work (Norton *et al*., 2009) has approached this by moving into the area of Pickering stabilisation of emulsions. However, a simple Pickering emulsion would not work, as the water would be free to move out of the droplets to solubilise the sugar. What the authors did in order to try and overcome this effect was to place crystals at the interface to build an intact shell (Fig. 10.8), thus offering protection against water movement. The figure shows an electron microscope picture of the cocoa butter emulsion. The shell of fat crystals around the water droplet can clearly be seen. It appears as if the crystals have sintered together and the structure appears to be fairly smooth. Of course, this requires the production of a crystalline shell with no defects. More recent work has been carried out with gelling of the aqueous phase to address this issue. This would give further strength to the structure, but the advantage of gelatin is that it melts at the same temperature as the fat phase, thus anything obtained in the droplets will be released on consumption. No doubt more revelations will emerge from this group in the future.

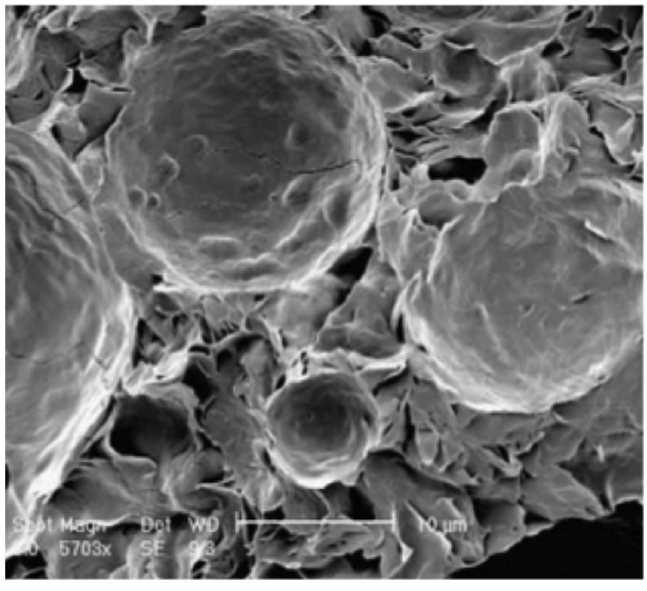

Fig. 10.8 Electron microscope picture of a cocoa butter emulsion with 30% included water, showing the microstructure of a continuous fat phase incorporating oil and triglyceride crystals and water droplets which have a fat crystal shell around them (scale bar is 10 μm). Reproduced from Norton *et al.* (2009). Copyright 2009, with permission from Elsevier.

One of the advantages of shells is that they cause scattering of the cracks when the structure is broken. Thus, they can be used to hide material from the rest of the structure, i.e. water which is not seen by the materials in the continuous phase of the chocolate matrix, but also salt in sauces soups, etc. This is discussed in a later section of this chapter.

10.3.2 Duplex emulsions

So what is a duplex (or double) emulsion? An example is given in Fig. 10.9, in which a primary emulsion of water in oil was produced using PGPR as the emulsifier. This particular emulsifier is often used for oil-continuous emulsions, as it is polymeric in nature and gives a very stable elastic interface. Once formed, the primary emulsion is then used as the included phase in the production of an oil-in-water emulsion. This is achieved by using a second emulsifier (often a low molecular weight material). By doing this, a duplex (or double) emulsion is produced.

One of the problems with duplex emulsions that has limited their application in real foods is that they are inherently unstable. This is because there are two oil/water interfaces, which have different curvatures.

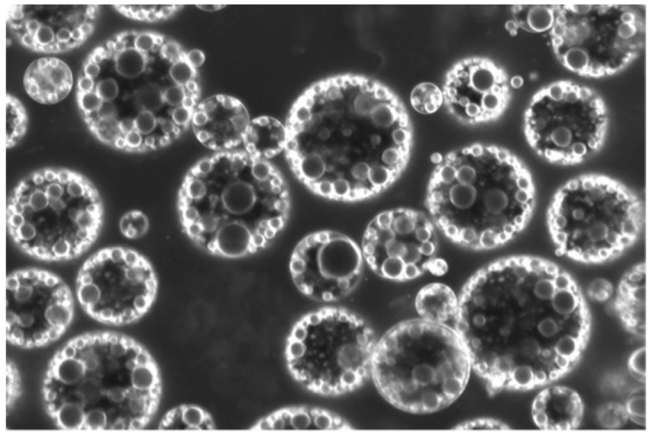

Fig. 10.9 A photomicrograph of a w/o/w duplex emulsion stabilised with PGPR. The inner droplets are approximately 10 μm and the secondary emulsion has droplets of approximately 100 μm.

As the emulsifier moves between interfaces, they become identical and the structure collapses. The most common way of stopping this from happening is to have a large emulsifier which aggregates at one of the interfaces to give gel-like structures, hence the reason that PGPR is used in studies on duplex emulsions for foods. The second problem that exists is that the primary emulsion is damaged in the second emulsification process. This results in various levels of release of the contents of the primary emulsion contents during the process. Again, it has been shown that PGPR is a good emulsifier to use, as it is very stable in the process.

So duplex emulsions can be made, but the use of PGPR is not ideal as it is not generally allowed in foods, although its use is allowed in chocolate. Even if PGPR was more widely allowed in foods, duplex emulsions produced with this emulsifier are not stable for the shelf life of a product. On storage, droplets tend to change size as a consequence of osmotic pressure differences between different phases.

10.3.2.1 *Fat replacement*

For fat replacement, the use of duplex emulsions has some inherent advantages. The most significant one is that if the primary emulsion is constructed to remain stable throughout the lifetime of the product, at least until it is within the human stomach, then the product will be perceived to have a much higher fat content than is actually present. However, if this dream is to be realised, then a duplex emulsion has to be made that is stable throughout the shelf life and usage of the product and only using food-allowed materials.

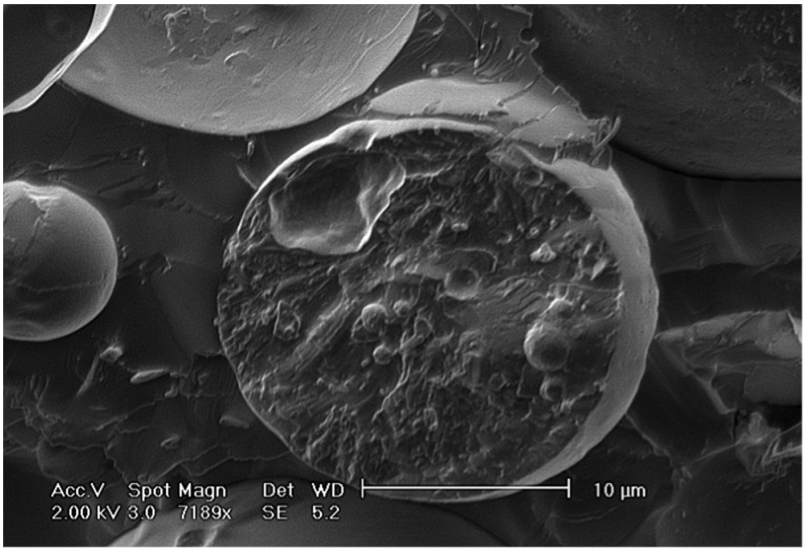

Fig. 10.10 Photomicrograph of a duplex emulsion with the inner interface stabilised by crystals (shell).

Very recently new work using shells has been carried out by Frasch-Melnik *et al*. (2009). This work involved the use of crystallising triglycerides that are placed at the interface for Pickering stabilisation and then sintered together to produce an intact structure surrounding the droplet (Fig. 10.10). As can be seen in this figure, the primary emulsion has been produced to have a sub-micron size and then the secondary emulsion has a droplet size of about 10 μm. The crystalline structure, which has been produced via a combination of crystallising mono- and triglycerides, can be seen within the secondary droplets. Crystalline shells can be seen around the primary droplets.

10.3.2.2 *Salt reduction*

One of the advantages of a duplex emulsion is that we can design in two different water phases, i.e. w/o/w emulsion. This potentially gives a structure that, for instance, could contain salt in the outer water phase and no salt or KCl in the inner phase. The idea of the design is that the consumer would be able to taste the salt contained in the outer water phase when the food is eaten, while the inner water phase would go undetected. This would result in a product, which is perceived as having a higher salt content than is actually present. The extent of salt reduction possible would depend on the ratio of the inner and outer water phases.

Some initial work by Malone *et al*. (2003b) demonstrated the potential for this approach, although this work was in controlling acid perception.

It showed that the perceived acidity was related to the outer water phase and not to the overall content of acid in the product. This finding suggests that if the structures can be made, then they will have the desired properties.

As discussed earlier, recent work (Frasch-Melnik *et al*., 2009) has shown that shells can be produced around the inner droplets. It has been shown that if the shells are controlled carefully, they result in an intact structure. These perfect shells then resist the osmotic pressure differences of having 1% salt in one water phase and 0% salt in the other. These structures have been demonstrated to be stable for greater than 6 months with less than 5% leakage of the salt between the phases. The potential of duplex emulsions for salt reduction in wet products (i.e. the difficult task) will be tested in the near future.

10.3.3 Fat replacement with air-filled emulsion

Another stratagem is to replace the fat droplets in an emulsified product with stabilised air cells that physically (size and shape) and rheologically resemble the fat droplets they are replacing.

The first question is whether air can change the lubrication and mouth-feel properties of a product? Recently, there has been some research in this field. Heuer and Norton (unpublished data) investigated the role of air in tribology using dairy cream alternatives. They studied the effect of taking fat out of a product and then compared this when air was whipped in. As Fig. 10.11 shows, air has increased the lubrication of the low-fat emulsion. The authors argue that this is a consequence of increasing the proportion of an included phase. This has the effect of

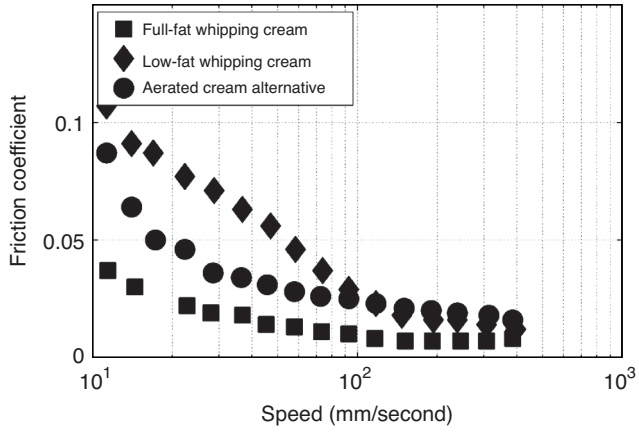

Fig. 10.11 Stribeck curves for a full-fat whipping cream (■), a low-fat whipping cream alternative (◇) and an aerated cream alternative (●).

moving the included phase volume back towards the full-fat version. Not surprisingly, the low-fat alternative does not provide the same level of lubrication as the full-fat original.

Clearly, this approach has not resulted in the air totally replacing the fat droplets in terms of lubrication and probably not in terms of consumer perception either. However, the air cells whipped into the dairy cream alternatives were much larger than the oil droplets that they replaced (at least an order of magnitude larger). So the question is what would have happened if the air cells were in the same size range as the oil droplets? The work required to make air cells so small is not trivial, and then stabilising them against ripening needs a whole new science area. This is the science area of air-filled emulsions, which has recently been established. The initial work reported in 2009 (Tchuenbou-Magaia *et al*., 2009) used a novel group of proteins (hydrophobins), which are found ubiquitously across all genera of filamentous fungi. Because of their molecular make up and tertiary structure, they present some fascinating physical properties. For instance, these proteins assemble at air–water interfaces, and once there, they rearrange and aggregate to give what is essentially a protein skin (Kisko *et al*., 2009). The gel-like network seems to give elasticity to the interface (de Vocht, 2001), and the mechanism of action is as if this elastic interface imparts a restoring force, so as air tries to move via Ostwald ripening, the protein resists this movement and keeps the air droplet size originally made in the process. Hydrophobins will not only stabilise air–water interfaces, but they behave in the same way at oil–water interfaces. The relevance of this will be discussed shortly.

The approach reported so far involves the production of very small air cells (less than 10 μm) using sonication. By doing this, the researchers report that air-filled emulsion droplets can be constructed to give physical properties similar to the oil-filled droplets they replace. This approach obviously offers an exciting new route for reducing the fat content of foods.

The initial work from A. Cox (Cox *et al*., 2007) was limited from a microstructural design point of view as they produced large air cells specifically targeted for use in stabilising ice creams. More recent work reported by Tchuenbou-Magaia *et al*. (2009) has shown that air cells can be produced of the same size as oil droplets in a traditional oil/water emulsion, i.e. 10 μm, and which are stable for months using this type of protein. This shows the remarkable nature of hydrophobins when we consider the ripening forces acting on such small air cells. In addition, by understanding the molecular and rheological behaviour of hydrophobins at air/water interfaces, the P. Cox group has developed ways to use alternative proteins to give the same interfacial rheological properties. It has been shown that these alternatives can be used to impart the same

properties to air-filled droplets as those observed for hydrophobins (Cox *et al.*, in press).

Having produced air-filled emulsions, which is one step on the road to using them in foods, it is also necessary for complex food formulations to have the stability in the presence of oil droplets. Oil is an antifoam in aerated products as it normally adds a level of mobility to the air/water interface. This allows the surfactants to move and cause film drainage, allowing the air to escape within a few minutes or hours. However, as fat is a carrier of flavour in many products, there will be a need to have some oil present. This means that we will have to construct a triphasic system. So, again, can rheological understanding and control give us a route to overcome this obstacle?

As discussed earlier, the initial work was performed using hydrophobin proteins and alternatives have been developed. The reason for developing alternatives was two-fold. The first was that hydrophobins are currently scarce and expensive. The second reason is that the kinetics of structuring at the interface is hard to control, and once the proteins are aggregated at the interface, any further application of shear in the process causes the proteins to detach from the interface and become inactive. The alternatives are food grade proteins that are thermally denaturing at the interface using sonication, which produces small air cells at the same time (Fig. 10.12). The proteins, which are applicable, are high in cysteine residues so that they covalently cross-link to form an elastic robust interface. It has been shown (de Vocht, 2001) that the kinetics of ordering and the point at which cross-linking occurs within the process can more easily be controlled than for the hydrophobins.

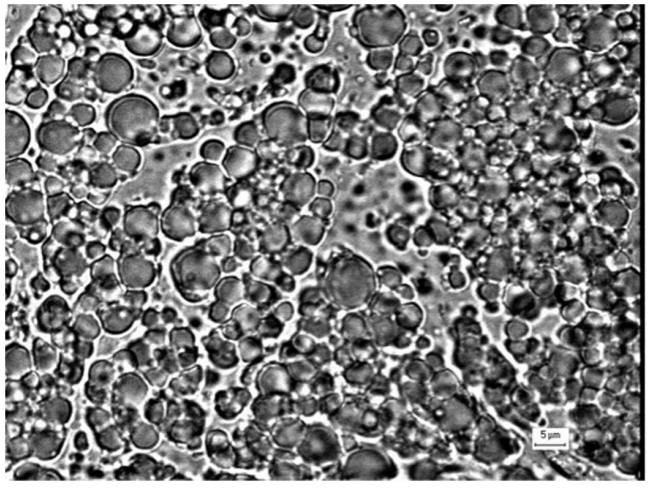

Fig. 10.12 A light photomicrograph of a BSA-stabilised air-filled emulsion. This sample is 140 days old and showed almost no Ostwald ripening over this time.

However, once formed, these structures are incredibly robust and due to their interfacial rheology are resistant to Ostwald ripening even when the air cells are micron sized.

10.3.4 Sheared gels (fluid gels)

So having considered how to rebuild structures using water or air in emulsions and multiple emulsions, are there alternative routes which do not require the use of 'emulsions'? An example of how oil droplets in an emulsion product can be replaced using the design rules established from a microstructural approach is the development of sheared gels, for example agar, carrageenan, alginate, etc. (Norton *et al*., 1999). So what happens when you take a gelling biopolymer and shear it during the gelation process? The result is gel particles, which if the shear is sufficient are spherical (Gabriele *et al*., 2009). Each particle has the same rheology as the bulk gel from which they were produced.

It has been shown how the particles and rheological parameters depend on the processing conditions and how different sheared gels can be produced (Wolf *et al*., 2000). An example of the ongoing work in the field has recently been published (Gabriele *et al.*, 2010). In this work, it was shown how the rate of cooling at a set shear rate in the process influences the sheared gel obtained (Fig. 10.13). This figure gives a good example of how these sorts of material behave. As can be seen, agarose

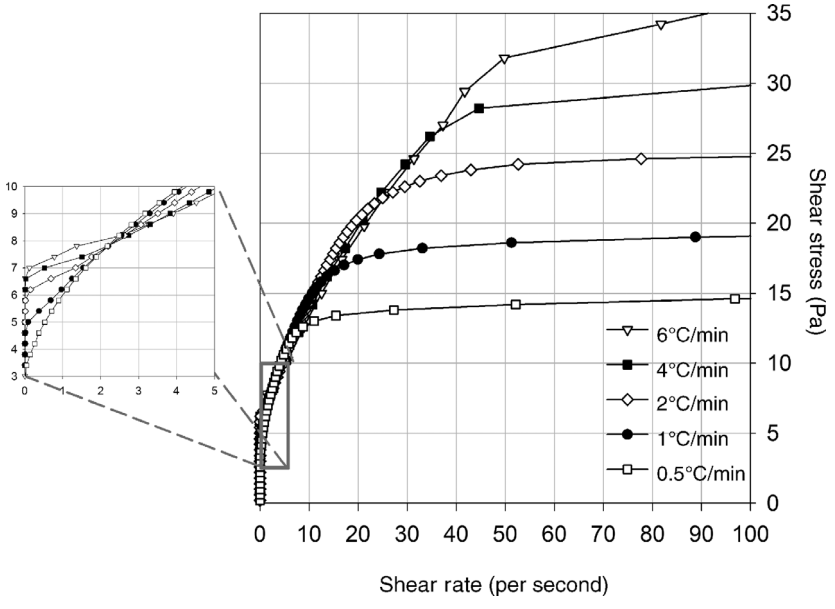

Fig. 10.13 Stress/shear rate curves of 1% agarose sheared gels produced at a constant shear rate, but with different cooling profiles (adapted from Gabriele *et al*., 2010).

fluid gels produced at a single polymer concentration, but at different cooling rates, can behave quite differently in terms of their rheology. Samples produced at the lower cooling rates have greater interaction when the sample is at rest and thus show the highest yield stress. However, once the samples are flowing, the fluid gels produced at the higher cooling rates have the highest viscosity. This is probably because the particles are larger and have a more irregular shape.

As this example shows, there are many parameters that can be changed in the formation of the gel particles. These not only change the shape and size of the particle, but also manipulate the extent of bridging between them and hence parameters like yield stress. Other parameters which need to be considered and will be discussed later are the type and concentration of the hydrocolloid used.

So having obtained sheared gel particles and having developed an understanding of their material properties, the question becomes, how do they behave in the mouth? As can be seen from Fig. 10.13, parameters like yield stress and viscosity at a shear rate of 100 per second can be manipulated. However, if we are to consider the use of these gel particles as replacement for fat in an emulsion, we need to consider how they behave in terms of lubrication in the mouth. Here again we turn our attention to the thin film behaviour. Investigations of the tribology of fluid gels are just beginning (Gabriele *et al.*, 2010), but are showing some very interesting results.

Fig. 10.14 shows the tribological response from two concentrations of agarose. At 1% agarose, there is a hysteresis between the ramp up and the ramp down. It seems that on the ramp up, the particles are initially excluded from the gap, but as the speed is increased, particles

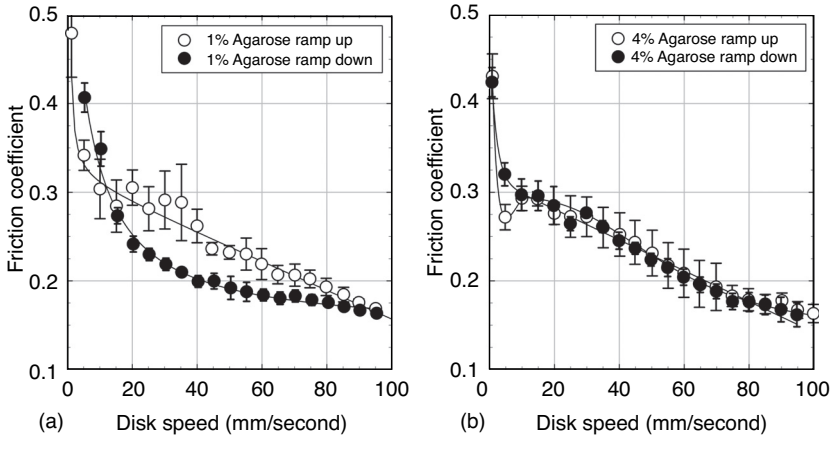

Fig. 10.14 Difference in the friction ramps for different fluid gels with different agarose concentrations. The load *W* is constant to 4 N for all the experiments (adapted from Gabriele *et al.*, 2010).

are entrained into the gap. As they are reasonably soft, they are distorted by the applied normal force and so, in effect, their presence is a narrowing of the gap, i.e. they allow less flow of the liquid through the gap. This results in the friction remaining constant for a significant range of rotation speeds (in this example from approximately 10 to 35 mm/s). As the speed is increased further, the force of fluid and fluid gel entering the gap causes the ball-and-plate gap to widen and the friction decreases. On decreasing the rotational speed of the plate, gel particles are being entrained at all stages so the friction is lower than the up ramp when they were excluded. At the higher polymer concentration, this hysteresis is not observed and the up and down ramps overlay each other. It would seem that this is due to the modulus of the gel particle: at an applied normal force of 4 N, the particles are not distorted, so when they are entrained, they immediately lead to the lowering of the friction. This finding has been shown to be reproducible and, as such, is very interesting as it raises questions about what happens within the mouth and whether soft particles will still have lubrication properties.

So how is this used to replace fat in a product? We turn our attention again to mayonnaise. If the majority of the oil droplets in a mayonnaise are replaced by soft elastic spherical gel particles, then the overall bulk rheology of the mayonnaise can be matched (as in Fig. 10.15). In this figure, we have shown a flow curve for a full-fat mayonnaise and compared it with a reduced-fat (3% compared to 80% in the full-fat version) emulsion in which the oil droplets have been replaced by sheared agar gel (5%), assembled as a particulate gel. This combination

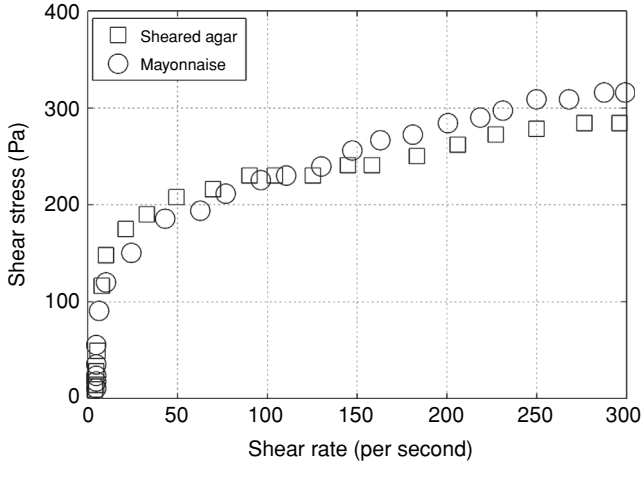

Fig. 10.15 Stress/shear rate curve for a 5% sheared agar (○) with 3% phase volume of oil droplets (droplet size ~1 μm) compared to a full-fat Hellman's mayonnaise (□) using a roughened cone-and-plate geometry on a Rheometrics instrument.

of oil droplets and gel droplets has provided a yield stress and flow behaviour which are similar (although still not an exact rheological match) to the full-fat emulsion and with a close match in sensory properties when tested by a consumer panel. The tribology data discussed above suggests that at 5% polymer concentration, the thin-film behaviour will be significantly affected and thus give an improved lubrication score in sensory scores, although no such data has yet been reported in the open literature.

10.3.5 Water-in-water emulsions

The next level of complexity is to have mixed biopolymers in which the two or more molecular structures lead to phase separation. The simplest way to consider these is to regard them as composites where one of the components forms a continuous network across the entire system and the other serves as a gel filler, i.e. resembling an oil/water or water/oil system. A typical photomicrograph is shown in Fig. 10.16. This figure shows different water-in-water emulsion structures and how they are influenced by the amount of the phases. So Fig. 10.16a shows the single phase observed for the protein phase with LBG at a level that is miscible. Fig. 10.16b then shows the microstructure obtained when 25% of the LBG phase is present. In this picture, the droplets of LBG can be seen as a dark phase included in the protein continuous phase. Fig. 10.16c shows the bi-continuous structure, which occurs when 50:50 mixtures are used. This is the condition when both phases are capable of being continuous and the confused system is obtained. This type of structure persists for quite a concentration range around the 50:50 mix as discussed by Norton and Frith (2001). Once a dominant phase volume of the LBG phase inversion of the structure has occurred, we can see protein phase included in a continuous LBG phase.

As can be seen from this set of photomicrographs, the mixed biopolymer systems behave like a water-in-oil mixture in which the phase with the highest phase volume dominates. When a 50:50 mixture is present, the structure attempts to be bi-continuous. In mixed biopolymer systems, this bi-continuous region can and does persist over a far wider concentration range. The design principles for these types of system have been described before (Norton and Frith, 2001). The way that they behave in flow has been described and from this came the name of water-in-water emulsions (Spyropoulos *et al*., 2007, 2008a, 2008b). So if these systems behave as water-in-water emulsions, can they be induced to phase invert in shear? Phase inversion was originally talked about some time ago (Kasapis *et al*., 1993a, 1993b, 1993c, 1993d) for the gelatin/maltodextrin mixture in which both polymers were gelling. It was argued that inversion was a consequence of the molecular weight

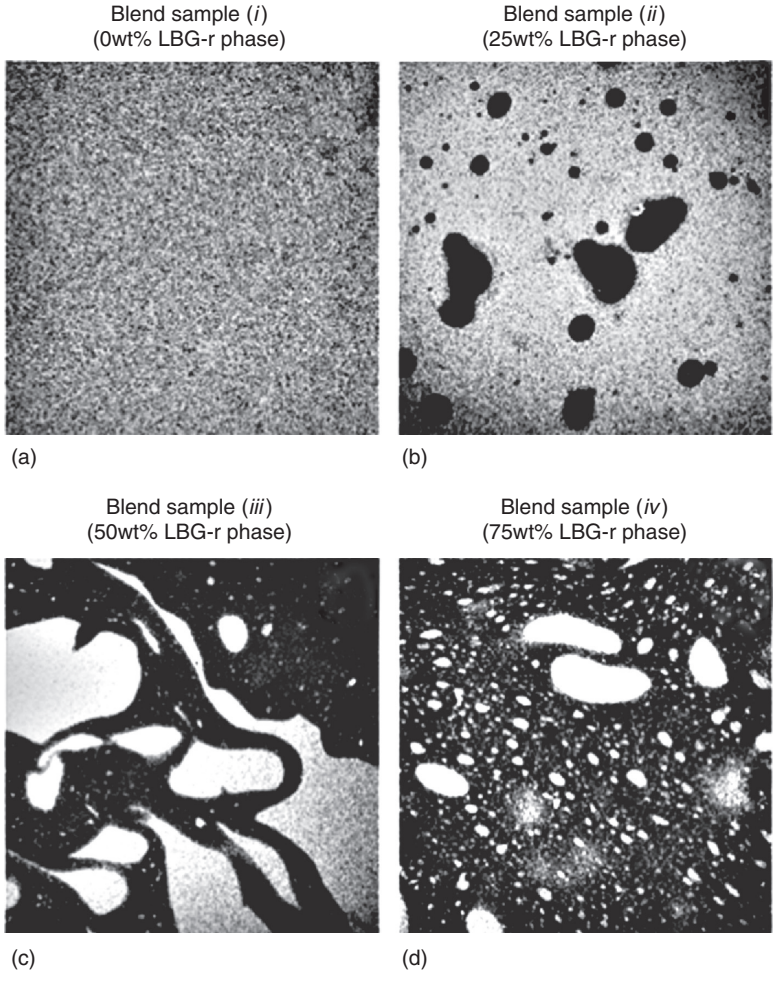

Fig. 10.16 Showing photomicrographs of caseinate/LBG mixtures in the presence of sucrose. Reproduced from Spyropoulos *et al*. (2010). Copyright 2010, with permission from Elsevier.

increase of the maltodextrin phase. More recently, the inversion of non-gelling systems has been reported (Portsch *et al*., 2009).

Fig. 10.17 shows data collected for the caseinate/LBG mixture with different volumes of the two phases. When no LBG is present (i.e. the pure caseinate phase), the viscosity simply reduces with shear rate as would be expected. This is also true when 25% of the included LBG phase is present. However, when 50% of both phases are present, then at higher shear rates of 100 per second, the viscosity shows an increase with shear rate. This is more clearly shown when 75% of the LBG phase is present. It has been argued by the authors that this shows a phase inversion in shear, so as the applied forces increase, the system

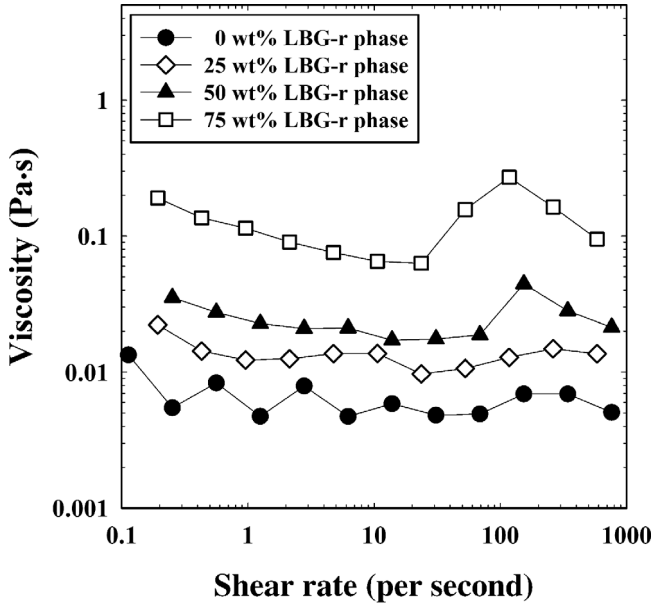

Fig. 10.17 Viscosity verses shear rate for mixtures of LBG/caseinate for different phase volumes of the two phases (adapted from Spyropoulos *et al.*, 2010).

starts to invert, resulting in an effective increased phase volume of the included phase, as would be expected, giving a higher overall viscosity to the system. On further increasing the applied forces, the materials totally phase invert so that the viscosity is seen to decrease significantly. In this inverted form, the included phase now has a greater phase volume than the continuous phase, although the continuous phase has a lower viscosity. This results in the overall system having a viscosity close to the non-inverted state for this particular mixture of biopolymers.

The remaining question, which is by and large still unanswered, is, can these systems be emulsified using a molecule or a particle as an interfacial material? Although this is not as yet clear, there has been some work (Simon *et al.*, 2007; Firoozmand *et al.*, 2009) to investigate this. The suggestion at the moment is that low molecular weight materials (e.g. oligosaccharides) probably go to the interface as a consequence of their increased solubility (over the polymers) in the second phase. There is a need to investigate this further, as the use of molecular surfactants, if available, will make the design of different structures possible.

Water-in-water emulsions constructed in the right way have been shown to have all the rheological properties of spreads and margarines. This means that they can be used to produce products that are not just low in fat, but are zero fat. Again, the design strategy is to create a microstructure that mimics that of the high-fat product and thus gives the

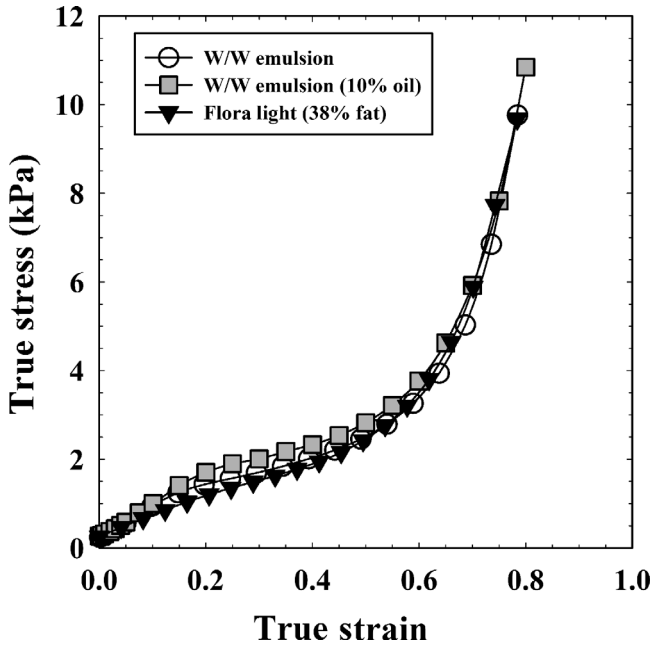

Fig. 10.18 Compression stress/strain curves obtained for a low-fat spread (Flora) and water-in-water emulsions (20% maltodextrin/4% gelatin/0.1 m NaCl) contained 0 or 10% oil (emulsified with 0.5% (w/w) Tween 80, droplet size ~5μm) using an Instron material tester.

material properties, mouth-feel and sensory properties of a full-fat product. An ingredient which has been used very successfully is low dextrose equivalent maltodextrin gels, which when used in mixed biopolymer systems can mimic the organoleptic properties (failure, melting, etc.) and material properties (e.g. spreading, scooping, etc.) of the high-fat products. Fig. 10.18 shows some gelatin/maltodextrin water-in-water emulsions in which liquid oil has been added to produce a low or very low fat spread with virtually no saturated fatty acids (SAFA). These mixtures were designed to have properties similar to fat-continuous spreads (butter alternatives); as demonstrated in the figure, these water-in-water emulsions can be constructed to give material properties very similar to the original high-fat SAFA-containing emulsion (e.g. low-fat Flora). As would be expected, the addition of oil has little effect, as it acts as a soft filler. The material properties of the water-in-water emulsion depend upon the continuous phase and, as such, depend on the bloom strength of the gelatin which is present both as droplets in the water-in-water emulsion and in the continuous maltodextrin phase. The major reason that maltodextrin works in this system is that, as an oligosaccharide, it forms aggregates which are crystalline in nature. These crystals then interact to produce a crystal network. This network has properties that

are similar to the triglyceride crystal structure and network in the low-fat spread.

Although most of the work carried out on water-in-water emulsions has been directed at soft products, which are used from chill or ambient temperatures, they can also be used in products that are cooked, for example meat products such as low-fat sausages (Baumanis *et al.*, 1995). This is again possible as a result of using crystallising biopolymers, which are used to replace the crystalline structure produced by saturated fats.

10.3.6 Self-structuring systems

As discussed earlier in this chapter, an area of research interest is to understand and control the rheological behaviour of foods inside the human gastrointestinal tract. The problem is that viscosity alone seems to have a marginal effect on people's food intake. So how do we go beyond this? The idea is to have systems that self-assemble inside the stomach to give a rigid three-dimensional structure. If this is to be achieved, then we need to have the ability to use environmental changes, which occur on entering the stomach and control the rate and extent of structuring.

As an approach, this seems to stand a chance as demonstrated from work carried out by Marciani *et al*. (2000, 2001a, 2001b). In this study, they fed already gelled beads to their participants and then visualised how they behaved in the stomach and how this affected their feelings of hunger. The particles used were large (cm) and were swallowed intact by the volunteer. These particles were shown to affect gastric emptying rates. More recently, smaller particles have been studied by Rayment *et al*. (2009) and Hoad *et al*. (2009) followed on from an idea put forward by Norton *et al*. (2006a) in which these authors suggested that one way to get stomach structuring was to use sheared calcium-set alginate gels that then partially unfold and rearrange as a consequence of the acidity in the stomach.

10.3.6.1 *Alginate*

So if rheological control of the stomach contents offers a way to control the eating habits and calorific intake of the general population, what materials are available to test the idea and achieve the goal? There is a whole area of science on self-structuring systems using a range of different materials including polymers (Norton *et al*., 2006a).

However, none of these are food allowed. More recently, however, researchers have started to consider the physical and chemical aspects of the stomach and intestine and how pH changes, enzymes, etc. can

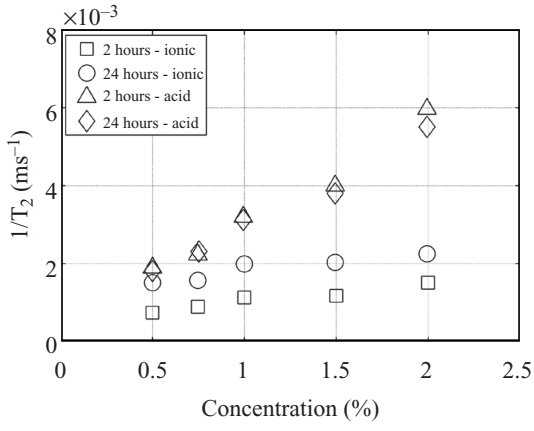

Fig. 10.19 Comparison of the concentration dependence of T_2 relaxation time (i.e. extent of ordering) of ionic and acid gels, together with how these properties change with time after the gels had been formed (adapted from Norton *et al.*, 2006a).

be used to induce self-structuring of food-grade hydrocolloids (Norton *et al*., 2006a). A number of different polysaccharides are known to be acid sensitive and so could be used to form structures as they enter the stomach. However, in order to make them applicable, it will be necessary to control the structure produced, the rate of structuring and the structural breakdown of the materials used throughout the human GI tract.

Acid gelation of alginate in environments close to stomach conditions have been studied and compared with simple viscosifying systems (Fig. 10.19). This figure shows that when guar is used, the stomach contents become diluted and more water-like with time. However, when alginate is used, the T_2 becomes shorter with time in the acid conditions, indicating an increased amount of structuring. In principle, the design idea is to have systems that undergo self-structuring in the stomach to gel the whole stomach contents. The work by Rayment *et al*. (2009) has in principle tried to investigate this, but unfortunately there was no attempt to control acid gelation rates or even when gel beads were used, cross-linking of the beads in acid conditions was also not considered. This meant that in both studies, no real control of stomach gelling was obtained and as a consequence, no real difference between meals with or without alginate was observed.

One of the major problems with alginate is gaining control of the gelation kinetics. This is proving very difficult even with selected or modified alginates. However, control is likely in the fullness of time. As a consequence of these difficulties, investigators have started to look at other materials. One of the best candidates is gellan.

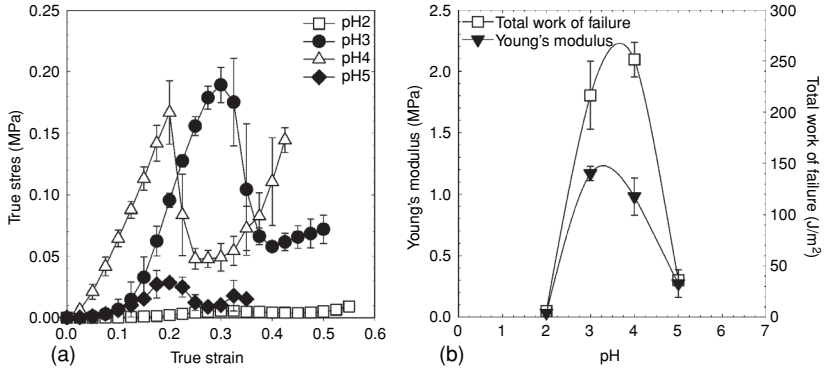

Fig. 10.20 Effect of pH on the structure of a 2% gellan gel. (a) True stress–true strain curves and (b) Young's modulus and total work of failure given as a function of pH (adapted from Norton *et al.*, submitted).

10.3.6.2 *Gellan*

Recently, work has been reported on the acid gelation of gellan as a route for causing self-structuring of the stomach. The advantage of gellan is that the acid range required for gelation is very close to those observed in the human stomach. In addition, and probably much more importantly, the rate of gelation is slower than that observed for alginate. Some recent work (Norton *et al.*, submitted) has shown that by slowly adding hydrochloric acid, gellan will gel at pH 4 and below. A maximum in gel strength is observed between pH 3 and 4 (Fig. 10.20). As can be seen from the figure, the pH affects gelation: the stiffness of the structures (Young's Modulus) and the total energy required for these structures to 'fail' (Total Work of Failure) both gave maximum values between pH 3 and pH 4 (Fig. 10.20b). Acid gels produced at either lower or higher pH values (pH 2 or pH 5) were considerably weaker (Fig. 10.20a). As the pH is reduced further, extensive aggregation of the gellan chains was observed. This was seen as the gels, which at higher pHs were clear, became very turbid. The aggregation resulted in weaker gels and gels in which water could be squeezed out (Fig. 10.21) as if they were sponges.

These authors showed that, as would be expected for hydrocolloid gels, both the gel strength and the work of failure increase with the gellan concentration (Fig. 10.20) and with a lowering of pH to 3. These curves are shown to be linear and have a critical concentration (i.e. there is a finite concentration to form a gel) with the strongest gel always occurring at approximately pH 3. What was very clear was that the material properties had a linear dependency on polymer concentration for the pHs studied. This indicates that acid gels are behaving in a way

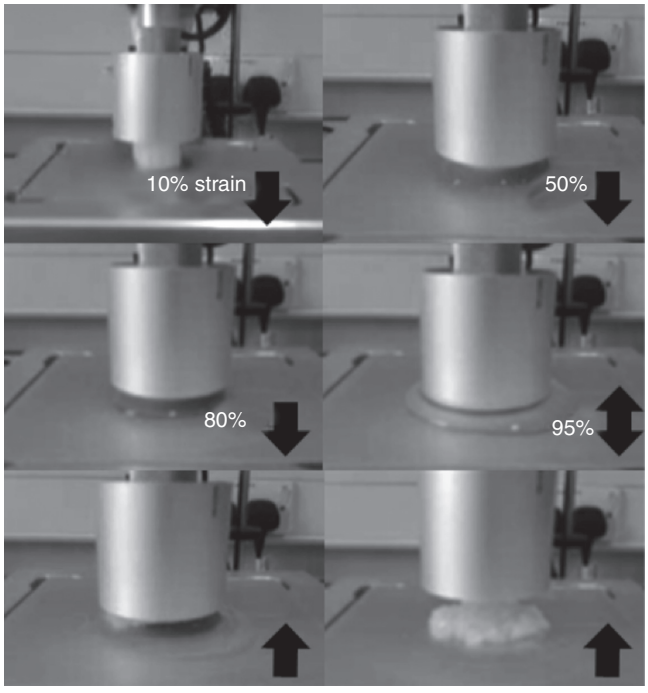

Fig. 10.21 Showing photographs from video. Water squeezed out and then sucked in.

previously observed (Clark and Ross-Murphy, 2009) for many different salt-induced hydrocolloid gels.

At pH below 3, the type of behaviour changes as the polymer chains become uncharged so that extensive aggregation occurs. This results in a cloudy appearance (scattering caused by the large aggregates). At the same time, gels become sponge-like so that water can be squeezed out. This has previously been reported for a number of cryogels of hydrocolloids (Lozinsky *et al*., 2003). This is demonstrated in Fig. 10.21. On initial compression of the gel at pH 2, the gel starts to look wet and a small amount of water appears to have been squeezed out. On further compression, significant amounts of water are squeezed out, and as the extent of strain reaches approximately 95%, the water can be seen around the probe. As the compression is removed, the gel is seen to spring back to some extent, although the cracks in the gel are clearly visible. The water, which has been squeezed out on compression, is sucked back into the gel so that after a few seconds no water can be seen. This sequence of photographs helps explain the compression test, i.e., at pH 2, the gel has paste-like rheology and a sponge-like consistency. As mentioned earlier, these are similar to the cryogels previously studied and reported by Lozinsky *et al*. (2003). The explanation put forward for

cryogels was that the ice formed caused the polymer network into large aggregates with large pores between them.

One of the main objectives for self-structuring is that the structure produced to stop gastric emptying must eventually be removed from the stomach to allow the next regular meal to be consumed. From the work reported on gellan, it seems that aggregation caused the gel strength to decrease as the pH goes below 3 and that the gel became a sponge-like structure. This type of behaviour is potentially very important when materials are being designed for self-structuring in the human stomach. A gelling system that responds to acid to produce a strong elastic gel and then changes structure as the acidity drops below pH 2 to give a sponge-like structure could potentially lead to system that gives fullness originally and then allow compression and compaction as the stomach empties after digestion of the meal.

10.4 CONCLUSIONS

As this review has demonstrated, the use of practical rheology can help in formulating healthy everyday foods, as long as the techniques are used in combination and as tools to understand how microstructures can be developed to give specific performance. By doing this, it is likely that significant progress will be made in the next few years in the development of healthier foods that fit into a normal everyday diet. This is most likely to be for self-structuring systems for manipulation of eating patterns, the use of tribology to understand the performance of materials in the mouth and how consumers respond to reformulation of foods, and in the development of duplex emulsions and their material properties. The latter has promised such potential in the past but never delivered due to production and stabilisation issues. However, recent advances seem to offer hope for their future use in everyday foods.

REFERENCES

Aguilera, J.M. and Lillford, P.J. (2007) *Food Materials Science: Principles and Practice (Food Engineering Series)*, 1st Edition. New York: Springer.

Akhtar, M., Stenzel, J., Murray, B.S. and Dickinson, E. (2005) Factors affecting the perception of creaminess of oil-in-water emulsions. *Food Hydrocolloids* **19**(3), 521–526.

Akhtar, M., Murray, B.S. and Dickinson, E. (2006) Perception of creaminess of model oil-in-water dairy emulsions: Influence of the shear-thinning nature of a viscosity-controlling hydrocolloid. *Food Hydrocolloids* **20**(6), 839–847.

Andrews, G.P., Laverty, T.P. and Jones, D.S. (2009) Mucoadhesive polymeric platforms for controlled drug delivery. *European Journal of Pharmaceutics and Biopharmaceutics* **71**(3), 505–518.

Baumanis, P., Norton, I., Brown, C.T. and Underdown, J. (1995) Meat Products containing gelling agents. US Patent No. 5,413,802. Washington, DC: US Patent and Trademark Office.

Bongaerts, J., Rossetti, D. and Stokes, J. (2007) The lubricating properties of human whole saliva. *Tribology Letters* **27**(3), 277–287.

Chen, J. (2009) Food oral processing – A review. *Food Hydrocolloids* **23**(1), 1–25.

Clark, A.H. and Ross-Murphy, S.B. (2009) *Biopolymer Network Assembly: Measurement and Theory, in Modern Biopolymer Science*. San Diego: Academic Press, pp. 1–27.

Cox, A.R., Cagnol, F., Russell, A.B. and Izzard, M.J. (2007) Surface properties of class II hydrophobins from trichoderma reesei and influence on bubble stability. *Langmuir* **23**(15), 7995–8002.

Cox, P., Tchuenbou-Magaia, F. and Norton, I. PB123335WO ZSR 705 Author.

Dahl, L.K. (2005) Possible role of salt intake in the development of essential hypertension. *International Journal of Epidemiology* **34**, 967–972.

de Vocht, M.L. (2001) Structural changes that accompany the self-assembly of hydrophobins. Ph.D. Thesis, University of Groningen.

de Wijk, R., Zijlstra, N., Mars, M., de Graaf, C. and Prinz, J. (2008) The effects of food viscosity on bite size, bite effort and food intake. *Physiology & Behavior* **95**(3), 527–532.

Dresselhuis, D., de Hoog, E., Cohen Stuart, M. and van Aken, G. (2008) Application of oral tissue in tribological measurements in an emulsion perception context. *Food Hydrocolloids* **22**(2), 323–335.

Firoozmand, H., Murray, B.S. and Dickinson, E. (2009) Interfacial structuring in a phase-separating mixed biopolymer solution containing colloidal particles. *Langmuir* **25**(3), 1300–1305.

Frasch-Melnik, S., Spyropoulos, F. and Norton, I.T. (2009) Fat crystal-stabilized w/o emulsions for controlled salt release. ISFRS, pp. 530–531.

Gabriele, A., Spyropoulos, F. and Norton, I.T. (2010) A conceptual model for fluid gel lubrication, *Soft Matter*, DOI: 10.1039/c001907k

Gabriele, A., Spyropoulos, F. and Norton, I.T. (2009) Kinetic study of fluid gel formation and viscoelastic response with kappa-carrageenan. *Food Hydrocolloids* **23**(8), 2054–2061.

Hoad, C., Rayment, P., Cox, E., Wright, P., Butler, M., Spiller, R. and Gowland, P. (2009) Investigation of alginate beads for gastro-intestinal functionality, Part 2: In vivo characterisation. *Food Hydrocolloids* **23**(3), 833–839.

de Hoog, E.H.A., Prinz, J.F., Huntjens, L., Dresselhuis, D.M. and van Aken, G.A. (2006) Lubrication of oral surfaces by food emulsions: the importance of surface characteristics. *Journal of Food Science* **71**(7), E337–E341.

Hutchings, J.B. and Lillford, P.J. (1988) The perception of food texture – the philosophy of the food breakdown path. *Journal of Texture Studies* **19**(2), 103–115.

Jalan, K., Mahalanabis, D., Maitra, T. and Agarwal, S. (1979) Gastric acid secretion rate and buffer content of the stomach after a rice- and a wheat-based meal in normal subjects and patients with duodenal ulcer. *Gut* **20**(5), 389–393.

Kasapis, S., Morris, E.R., Norton, I.T. and Brown, C.T. (1993a) Phase equilibria and gelation in gelatin/maltodextrin systems – Part III: phase separation in mixed gels. *Carbohydrate Polymers* **21**(4), 261–268.

Kasapis, S., Morris, E.R., Norton, I.T. and Clark, A.H. (1993b) Phase equilibria and gelation in gelatin/maltodextrin systems – Part I: gelation of individual components. *Carbohydrate Polymers* **21**(4), 243–248.

Kasapis, S., Morris, E.R., Norton, I.T. and Clark, A.H. (1993c) Phase equilibria and gelation in gelatin/maltodextrin systems – Part IV: composition-dependence of mixed-gel moduli. *Carbohydrate Polymers* **21**(4), 269–276.

Kasapis, S., Morris, E.R., Norton, I.T. and Gidley, M.J. (1993d) Phase equilibria and gelation in gelatin/maltodextrin systems – Part II: polymer incompatibility in solution. *Carbohydrate Polymers* **21**(4), 249–259.

Kisko, K., Szilvay, G.R., Vuorimaa, E., Lemmetyinen, H., Linder, M.B., Torkkeli, M. and Serimaa, R. (2009) Self-assembled films of hydrophobin proteins HFBI and HFBII studied in situ at the air/water interface. *Langmuir* **25**(3), 1612–1619.

Kokini, J. (1994) Predicting the rheology of food biopolymers using constitutive models. *Carbohydrate Polymers* **25**(4), 319–329.

Kokini, J.L. (1987) The physical basis of liquid food texture and texture-taste interactions. *Journal of Food Engineering* **6**(1), 51–81.

Kokini, J.L. and Cussler, E.L. (1983) Predicting the texture of liquid and melting semi-solid foods. *Journal of Food Science* **48**(4), 1221–1225.

Kong, F. and Singh, R. (2008) Disintegration of solid foods in human stomach. *Journal of Food Science* **73**(5), R67–R80.

Le Révérend, B.J.D., Norton, I.T., Cox, P.W., Spyropoulos, F. (2009) Colloidal aspects of eating. *Current Opinion in Colloid and Interface Science* **15**, 84–89.

Lian, G., Malone, M.E., Homan, J.E. and Norton, I.T. (2004) A mathematical model of volatile release in mouth from the dispersion of gelled emulsion particles. *Journal of Controlled Release* **98**(1), 139–155.

Lillford, P.J. (2000) The materials science of eating and food breakdown. *MRS BULLETIN* **25**(12), 38–43.

Lozinsky, V.I., Galaev, I.Y., Plieva, F.M., Savina, I.N., Jungvid, H. and Mattiasson, B. (2003) Polymeric cryogels as promising materials of biotechnological interest. *Trends in Biotechnology* **21**(10), 445–451.

Malone, M.E., Appelqvist, I.A.M. and Norton, I.T. (2003a) Oral behaviour of food hydrocolloids and emulsions. Part 1. Lubrication and deposition considerations. *Food Hydrocolloids* **17**(6), 763–773.

Malone, M.E., Appelqvist, I.A.M. and Norton, I.T. (2003b) Oral behaviour of food hydrocolloids and emulsions. Part 2. Taste and aroma release. *Food Hydrocolloids* **17**(6), 775–784.

Marciani, L., Manoj, P., Hills, B.P., Moore, R.J., Young, P., Fillery-Travis, A., Spiller, R.C. and Gowland, P.A. (1998a) Echo-planar imaging relaxometry to measure the viscosity of a model meal. *Journal of Magnetic Resonance* **135**(1), 82–86.

Marciani, L., Wright, J., Manoj, P., Moore, R., Young, P., Bush, D., Al-Sahab, S., Fillery-Travis, A., Gowland, P.A. and Spiller, R.C. (1998b) Noninvasive echo-planar imaging (EPI) monitoring of intragastric viscosity, dilution and emptying of viscous meals in normal subjects. *Gastroenterology* **114**(Supplement 1), A798.

Marciani, L., Gowland, P.A., Spiller, R.C., Manoj, P., Moore, R.J., Young, P., Al-Sahab, S., Bush, D., Wright, J. and Fillery-Travis, A.J. (2000) Gastric response to increased meal viscosity assessed by echo-planar magnetic resonance imaging in humans. *Journal of Nutrition* **130**(1), 122–127.

Marciani, L., Gowland, P.A., Fillery-Travis, A., Manoj, P., Wright, J., Smith, A., Young, P., Moore, R. and Spiller, R.C. (2001a) Assessment of antral grinding of a model solid meal with echo-planar imaging. *American Journal of Physiology Gastrointestinal and Liver Physiology* **280**(5), G844–849.

Marciani, L., Gowland, P.A., Spiller, R.C., Manoj, P., Moore, R.J., Young, P. and Fillery-Travis, A.J. (2001b) Effect of meal viscosity and nutrients on satiety, intragastric dilution, and emptying assessed by MRI. *American Journal of Physiology Gastrointestinal and Liver Physiology* **280**(6), G1227–1233.

Norton, A.B., Cox, P.W. and Spyropoulos, F. Acid gelation of low acyl gellan gum relevant to self-structuring in the human stomach, *Food Hydrocolloid*, submitted.

Norton, I.T. and Frith, W.J. (2001) Microstructure design in mixed biopolymer composites. *Food Hydrocolloids* **15**(4–6), 543–553.

Norton, I.T., Jarvis, D.A. and Foster, T.J. (1999) A molecular model for the formation and properties of fluid gels. *International Journal of Biological Macromolecules* **26**(4), 255–261.

Norton, I.T., Frith, W. and Ablett, S. (2006a) Fluid gels, mixed fluid gels and satiety. *Food Hydrocolloids* **20**(2–3), 229–239.

Norton, I.T., Fryer, P. and Moore, S. (2006b) Product/process integration in food manufacture: engineering sustained health. *AIChE Journal* **52**(5), 1632–1640.

Norton, J.E., Fryer, P., Parkinson, J. and Cox, P.W. (2009) Development and characterisation of tempered cocoa butter emulsions containing up to 60% water. *Journal of Food Engineering* **95**(1), 172–178.

Pavlov, I.P. and Gantt, W.H. (1928) *Lectures on Conditioned Reflexes*. New York: International Publishers.

Peyron, M., Mishellany, A. and Woda, A. (2004) Particle size distribution of food boluses after mastication of six natural foods. *Journal of Dental Research* **83**(7), 578–582.

Portsch, A., Spyropoulos, F. and Norton, I.T. (2009) Phase equilibria and rheological behaviour of polysaccharide/protein mixtures in the presence of sugars. ISFRS, pp. 530–531.

Rayment, P., Wright, P., Hoad, C., Ciampi, E., Haydock, D., Gowland, P. and Butler, M.F. (2009) Investigation of alginate beads for gastro-intestinal functionality, Part 1: in vitro characterisation. *Food Hydrocolloids* **23**(3), 816–822.

Seville, J., Ingram, A. and Parker, D. (2005) Probing processes using positrons. *Chemical Engineering Research and Design* **83**(7), 788–793.

Sigurdsson, H.H., Loftsson, T. and Lehr, C. (2006) Assessment of mucoadhesion by a resonant mirror biosensor. *International Journal of Pharmaceutics* **325**(1–2), 75–81.

Simon, K.A., Sejwal, P., Gerecht, R.B. and Luk, Y. (2007) Water-in-water emulsions stabilized by non-amphiphilic interactions: polymer-dispersed lyotropic liquid crystals. *Langmuir* **23**(3), 1453–1458.

Smart, J.D. (2005) The basics and underlying mechanisms of mucoadhesion. *Advanced Drug Delivery Reviews* **57**(11), 1556–1568.

Spiller, R. (1994) Pharmacology of dietary fibre. *Pharmacology & Therapeutics* **62**(3), 407–427.

Spyropoulos, F., Frith, W.J., Norton, I.T., Wolf, B. and Pacek, A.W. (2007) Morphology and shear viscosity of aqueous two-phase biopolymer-surfactant mixtures. *Journal of Rheology* **51**(5), 867–881.

Spyropoulos, F., Ding, P., Frith, W., Norton, I.T., Wolf, B. and Pacek, A.W. (2008a) Interfacial tension in aqueous biopolymer-surfactant mixtures. *Journal of Colloid and Interface Science* **317**(2), 604–610.

Spyropoulos, F., Frith, W., Norton, I.T., Wolf, B. and Pacek, A. (2008b) Sheared aqueous two-phase biopolymer-surfactant mixtures. *Food Hydrocolloids* **22**(1), 121–129.

Spyropoulos, F., Portsch, A. and Norton, I.T. (2010) Effect of sucrose on the phase and flow behaviour of polysaccharide/protein aqueous two-phase systems. *Food Hydrocolloids* **24**, 217–226.

Sriamornsak, P., Wattanakorn, N., Nunthanid, J. and Puttipipatkhachorn, S. (2008) Mucoadhesion of pectin as evidence by wettability and chain interpenetration. *Carbohydrate Polymers* **74**(3), 458–467.

Steffe, J.F. (1992) *Rheological Methods in Food Process Engineering*. Freeman Press., Retrieved April 21, 2009, from http://www.egr.msu.edu/~steffe/freebook/offer.html.

Stokes, J.R., Davies, G.A., Macakova, L., Yakubov, G., Bongaerts, J. and Rossetti, D. (2008) From rheology to tribology: multiscale dynamics of biofluids, food emulsions and soft matter. In: *THE XV INTERNATIONAL CONGRESS ON RHEOLOGY: The Society of Rheology 80th Annual Meeting, AIP*, Monterey (California), pp. 1171–1173. Retrieved May 15, 2009, from http://link.aip.org/link/?APC/1027/1171/1.

Tchuenbou-Magaia, F., Norton, I.T. and Cox, P.W. (2009) Hydrophobins stabilised air-filled emulsions for the food industry. *Food Hydrocolloids* **23**(7), 1877–1885.

Thakaran, A., Norton, I.T., Fryer, P.J. and Bakalis, S. Mass transfer and nutrient absorption in a simulated model of small intestine. *Journal of Food Science*, doi: 10.1111/j.1750-3841.2010.01659.x, E1-E8.

Thakaran, A., Rayment, P., Fryer, P.J. and Norton, I.T. (2007) Modelling of physical and chemical processes in the small intestine. In: *European Congress of Chemical Engineering*. Copenhagen.

Thirawong, N., Kennedy, R.A. and Sriamornsak, P. (2008) Viscometric study of pectin-mucin interaction and its mucoadhesive bond strength. *Carbohydrate Polymers* **71**(2), 170–179.

Versantvoort, C.H.M., Oomen, A.G., Van de Kamp, E., Rompelberg, C.J.M. and Sips, A.J.A.M. (2005) Applicability of an in vitro digestion model in assessing the bioaccessibility of mycotoxins from food. *Food and Chemical Toxicology: An International Journal Published for the British Industrial Biological Research Association* **43**(1), 31–40.

Vliet, T.V., Aken, G.A.V., Jongh, H.H.D. and Hamer, R.J. (2009) Colloidal aspects of texture perception. *Advances in Colloid and Interface Science* **150**(1), 27–40.

Wickham, M., Faulks, R. and Mills, C. (2009) In vitro digestion methods for assessing the effect of food structure on allergen breakdown. *Molecular Nutrition & Food Research* **53**(8), 952–958.

Wolf, B., Scirocco, R., Frith, W.J. and Norton, I.T. (2000) Shear-induced anisotropic microstructure in phase-separated biopolymer mixtures. *Food Hydrocolloids* **14**(3), 217–225.

Index

Note: Page numbers with Italicised *f*'s and *t*'s refer to figures and tables.

acid gelation, 246–7
acids, 95–9
  effect on protein-stabilised emulsions, 201
  xanthan gum and, 95–9
    pH sensitivity of solution viscosity, 96–8
    stability at low pH, 98–9
activation energy, 145*f*
additives, 122–8
  appetite control, 127–8
  encapsulation, 125
  film-forming agent, 125
  gelling agent, 123–4
  immobilisation, 126
  stabiliser, 126–7
  thickening agent, 124–5
adiabatic compressibility, 42
agar, 62*t*
agarose, 73–4, 239
age-thickening process, 135
air-filled emulsion, 235–8
alginate, 113–29. *See also* gelation
  alginic acid, 119–20
  biosynthesis of, 114–15
  derivatives, 115
  enzymatically tailored, 121–2
  as food additives, 122–8
    appetite control, 127–8
    encapsulation, 125
    film-forming agent, 125
    gelling agent, 123–4
    key functions in food products, 123*t*
    stabiliser, 126–7
    texturisation of vegetative materials, 126
    thickening agent, 124–5
  gelling conditions, 62*t*
  hydrogels, 115–19
  molecular structure, 62*t*, 114–15, 114*f*
  self-structuring systems, 245–6
  shear-thinning behaviour, 121*f*
  solutions, 120–21
  sources of, 113–14
  thickening conditions, 62*t*
alginic acid, 119–20
amylopectin, 62*t*
amylose, 62*t*
antrum, 226*f*
apparent viscosity, 135, 145
appetite control, 127–8
applied rheology, 10
Arrhenius equation, 145
Ascophyllum nodosum, 113
aspiration, 106
associated phase separation, 78
astringency, 222
attenuation, 42
Azobacter vinelandii, 114, 121

backscattering, 43–5
Bagley correction, 22
bentonite suspension, 33*t*
Bingham model, 12, 12*t*, 135–6
bolus, 225

Practical Food Rheology: An Interpretive Approach
Edited by Ian T. Norton, Fotios Spyropoulos and Philip Cox

 ISBN: 978-1-405-19978-0

bridging flocculation, 195
bulk modulus of elasticity, 42

capillary rheometer, 21–2
capillary rheometry, 26
capillary tube rheometer, 9
Carbopol solution, 33*t*, 50–51
carrageenan, 62*t*, 70, 73
Carreau model, 137
Carreau-Yasuda model, 137
casein, 147, 153–4
casein micelles, 143
cassia gum, 86
Casson model, 12*t*, 14
castor oil, 32*t*
cellulose fibre suspension, 32*t*
cellulose pulp, 33*t*
cellulosics, 62*t*
cheddar cheese, 150, 156
cheese, 147–59. *See also* fluid milk; semi-solid dairy foods
  creep test, 157–8
  large strain rheological analysis, 152–7
    cutting with wire, 156–7
    torsion test, 155–6
    uniaxial compression, 152–4
    uniaxial tension, 154–5
    vane method, 155–6
  small amplitude oscillatory tests, 148–51
  stress relaxation test, 158–9
  texture of, 153
cheese sauce, 32*t*
cheese whey, 134
chewing, 221
chocolate, 32*t*
coalescence, 194
cocoa butter, 32*t*
cocoa butter emulsion, 232*f*
complex shear compliance, 17
complex shear modulus, 16–17
complex viscosity, 16, 138
concentric cylinder rheometry, 25
condensation, 42
cone-and-plate rheometry, 9, 23–4
conformational states, 91–2
consistency index, 12
corn syrup solution, 33*t*
Cox-Merz rule, 138–9
cream cheese, 163
creaminess, 221
creaming, 195
creep test, 157–8
Cross model, 66–7
cross-linking, 165, 237
crossover frequency, 19
crossover modulus, 148

dairy systems, 133–67
  cheese, 147–59
    creep test, 157–8
    cutting with wire, 156–7
    large strain rheological analysis, 152–7
    small amplitude oscillatory tests, 148–51
    stress relaxation test, 158–9
    torsion test, 155–6
    uniaxial compression, 152–4
    uniaxial tension, 154–5
  fluid milk, 134–47
    age-thickening process, 135
    apparent viscosity, 135–6
    falling sphere method, 139
    fat globules, 142
    Herschel-Bulkley yield stress, 136
    mathematical models, 143–4
    measurements of rheological properties, 137–41
    milk composition, 141–3
    Newtonian behaviour of, 134
    process engineering calculation, 146–7
    rheological properties of, 134–9
    rotational viscometers, 141
    sensory perceptions and, 145–6
    shear-thinning behaviour, 135
    temperature, 144–5
    U-tube capillary viscometers, 140–41
  semi-solid dairy foods, 159–65
    flow properties, 159–63
    hysteresis loop, 160–61

dairy systems (*Continued*)
time-dependent flow behaviour characterisation, 159–63
viscoelastic properties of, 164–5
yield stress, 163–4
texture perception, 165–7
deformation, 10
denaturation, 199–200
depletion flocculation, 195
dextran solutions, 63
dilation, 42
dispersion, 12
Doppler angle, 40–41
Doppler ultrasound-based rheology, 29–54
acoustic properties, 41–5
attenuation, 42
backscattering, 43–5
propagation, 41–2
scattering, 43
sound velocity, 42–3
Carbopol solution, 50–51
Doppler angle, 40–41
electronics, 45
flow adapters, 39–40
fluids and suspensions used, 32–3*t*
measurement parameters, 34–5*t*
models, 46–8
gradient method, 46–7
Herschel-Bulkley fluid model, 48
point-wise rheological characterisation, 46–7
power law fluid model, 47–8
profile estimation, 45
publications, 31–8
rheometry, 49–50
averaging effects at pipe wall, 49
fitting, 49
gradient method, 50
signal processing, 45
software, 45–6
suspension of polyamide in rapeseed oil, 52–4
transducers, 38–9
duodenum, 226*f*
duplex emulsions, 232–5. *See also* emulsions
fat replacement, 233–4
salt reduction, 234–5
dynamic shear, 10
dynamic viscosity, 16
dysphagia, 106

Eilers equation, 144
Einstein equation, 144
elastic modulus, 68, 137, 148
Ellis model, 12*t*
emulsions, 193–214
air-filled, 235–8
aqueous phase composition, 200–203
duplex, 232–5
fat replacement, 233–4
salt reduction, 233–4
future perspectives, 213–14
in vitro measurements of sensory perception, 209–13
instabilities in, 194–5
coalescence, 194
creaming, 195
flocculation, 194–5
oral processing of, 203–9
fluid dynamics, 206–7
interactions with oral surfaces, 208–9
interactions with saliva, 207–8
stages and phenomena, 204–6
overview, 193
as partial fat replacement, 231–2
protein functionality at liquid interfaces, 196–200
protein denaturation, 199–200
protein displacement, 198–9
protein-stabilised interfaces, 199
protein-stabilised, 200–203
addition of biopolymers, 202–3
addition of proteins, 202
addition of surfactants, 201–2
effect of processing, 203
pH and ionic strength, 201
water-in-water, 241–5
xanthan gum, 104–5
encapsulation, 125
epigallocatechin gallate (ECGC), 222
external gelation, 116–17, 118*f*
Eyring model, 12*t*

falling sphere method, 138–9
fast Fourier transformation (FFT), 45
fat blends, 33*t*
fat globules, 142
fat replacement, 233–4
  air-filled emulsion, 235–8
  duplex emulsions, 232–5
  partial, 231–2
fat suspension, 32*t*
feta cheese, 153
film-forming agent, 125
flavour perception, 176–9
flocculation, 104, 194–5
flow behaviour index, 12
flow curves, 11*f*
flow velocity, 46–8
fluid gels, 238–41
  age-thickening process, 135
  apparent viscosity, 135–6
  fat globules, 142
  Herschel-Bulkley yield stress, 136
  measurements of rheological properties, 139–41
    falling sphere method, 139
    rotational viscometers, 141
    U-tube capillary viscometers, 140–41
  Newtonian behaviour of, 134
  rheological properties of, 134–9
    mathematical models, 143–4
    milk composition, 141–3
    sensory perceptions and, 145–6
    temperature, 144–5
  shear-thinning behaviour, 135
fluids, 8
food additives, 122–8
  appetite control, 127–8
  encapsulation, 125
  film-forming agent, 125
  gelling agent, 123–4
  immobilisation, 126
  stabiliser, 126–7
  texturisation of vegetative materials, 126
  thickening agent, 124–5
food formulation, 219–49
  duplex emulsions, 232–5
  emulsions as partial fat replacement, 231–2
  fat replacement with air-filled emulsion, 235–8
  microstructure approach, 220–30
    food in the intestine, 228–30
    food in the stomach, 226–8
    oral perception of foods, 221–6
    schematic representation of, 220
  overview, 219, 230
  self-structuring systems, 245–9
    alginate, 245–6
    gellan, 247–9
  sheared gels, 238–41
  water-in-water emulsions, 241–5
food pastes, 20–21
food processing, 101–3
  freezing, 103
  homogenisation, 102
  thermal treatment, 101–2
food rheology, 8
  case study, 3–5
  fluid milk, 134–9
    mathematical models, 143–4
    milk composition, 141–3
    sensory perceptions and, 145–6
    temperature, 144–5
  gel, 68–9
  literature, 7–8
  measurements, 139–41
    effect of oral processing, 165–7
    falling sphere method, 139
    rotational viscometers, 141
    U-tube capillary viscometers, 140–41
  perception and, 173–90
    flavour, 176–9
    gels, 185–7
    in vitro measurements of, 209–13
    microstructure and, 181–3
    mixing and, 179–80
    mouthfeel, 184–5
    shear rheology and, 187–90
    thickness, 174–6
food structures, 104–5
  emulsions, 104–5
  gels, 105
foods
  oral perception of, 221–6
  in the stomach, 226–8
frequency sweep, 148–9

fruit jams, 33*t*
functional magnetic resonance imaging (fMRI), 206
fundus, 226*f*

galactomannan, 71–2, 78, 86–7
galactose, 62*t*
gastric juice, 227
Gaviscon, 119
gelatin, 185–7
gelation, 68–9. *See also* hydrocolloid gums
  acid, 246–7
  alginate, 246
  bead size, 118
  calcium ions in, 115–16
  egg box model, 115
  external, 116–17, 118*f*
  gellan, 247–9
  internal, 116–17
gellan gum, 73–4
  gelling conditions, 62*t*
  molecular structure, 62*t*
  self-structuring systems, 247–9
  thickening conditions, 62*t*
gelling agent, 123–4
gels, 185–7
  fluid, 238–41
  sheared, 238–41
  xanthan gum, 105
gluco-δ-lactone (GDL), 3–5
glucose, 62*t*
glucose syrup, 32*t*, 175
glucuronic acid, 62*t*
glycerin, 32*t*
glycerol, 32*t*
glycomannan, 138
Gouda cheese, 152–3
Grace curve, 188
gradient method, 46–7
guar gum, 87
  galactomannans, 72
  gelling conditions, 62*t*
  lumen mass transfer coefficient, 230*f*
  molecular structure, 62*t*
  as thickeners, 106
  thickening conditions, 62*t*
guluronate, 115, 121
guluronic acid, 73, 120*f*
gum Arabic, 75

haematocrit, 44
Haug triangle, 64*f*
Herschel-Bulkley fluid model, 48
Herschel-Bulkley model, 12*t*, 13, 67, 135–6, 161
heterotypic junction zones, 71
high temperature-short time (HTST) pasteurisation, 102
high-ester pectin, 3–5
high-shear viscosity, 67
homogenisation, 102, 200
Hooke, Robert, 7
Hooke solid, 137
Hookean spring, 9
hydrocolloid gums, 61–79
  behaviour in solution, 61–8
  in foods, 77–9
  gel rheology, 68–9
  gelation, 68–9
  gelling conditions, 62*t*
  hydrocolloid-hydrocolloid interactions, 69–77
  molecular structure, 62*t*
  overview, 61
  role and interactions, 77–9
  as thickeners, 160
  thickening conditions, 62*t*
hydrogels, 115–19
hydroxypropyl guar gum, 32*t*
hydroxypropylmethyl cellulose (HPMC), 177–9, 189
hypopharyngeal transit time, 204
hysteresis loop, 160–61
  shear stress decay, 161–3

ice cream, 78
infinite-shear viscosity, 67, 137
internal gelation, 116–17
interpenetration networks, 73–4
intestine, food in, 228–30
intrinsic viscosity, 63–4
ionic strength, 201

kaolin suspension, 33*t*
Kokini oral shear stress, 175*f*, 178
konjac glucomannan, 71–2, 90

LabVIEW, 46
Laminaria hyperborea, 113
large strain rheological analysis, 152–7
  cutting with wire, 156–7
  torsion test, 155–6
  uniaxial compression, 152–4
  uniaxial tension, 154–5
  vane method, 155–6
limiting viscosity, 13
linear viscoelastic region (LVR), 17, 148–50
locust bean gum (LBG)
  flow behaviour, 86–7
  gelation, 70
  gelling conditions, 62*t*
  konjac glucomannan and, 71–2
  in milk beverages, 138
  molecular structure, 62*t*
  thickening conditions, 62*t*
  xanthan and, 78, 90–91, 94–5
loss modulus, 17, 19, 68, 137, 148
low molecular weight surfactants, 196
lumen mass transfer coefficient, 230*f*

Macrocystis pyrifera, 113
macrorheology, 9
maltodextrin, 75, 244
mannose, 62*t*
mannuronan epimerases, 121
mannuronate, 114, 121
mannuronic acid, 62*t*
Maras ice cream, 78
Mark-Houwink parameter, 64
marmalades, 33*t*
mastication, 221
MATLAB, 46
maximum compliance, 158
mayonnaise, 32*t*, 219–20, 240
measuring instruments, 23–6
methoxy pectin, 73
micelles, 143
microstructure, 20, 181–3
microstructure approach, 220–30
  food in the intestine, 228–30
  food in the stomach, 226–8
  oral perception of foods, 221–6
  schematic representation of, 220
milk, 134–47
  age-thickening process, 135
  apparent viscosity, 135–6
  fat globules, 142
  Herschel-Bulkley yield stress, 136
  measurements of rheological properties, 139–41
    falling sphere method, 139
    rotational viscometers, 141
    U-tube capillary viscometers, 140–41
  Newtonian behaviour of, 134
  nonfat dry milk, 146
  process engineering calculation, 146–7
  rheological properties of, 137–9
    mathematical models, 143–4
    milk composition, 141–3
    sensory perceptions and, 145–6
    temperature, 144–5
milk fat, 142
milk protein, 78
mineral slurries, 32*t*
mixing, 179–80
mouth process model, 205
mouthfeel, 184–5
  oral processes, 203–9
    fluid dynamics, 206–7
    interactions with oral surfaces, 208–9
    interactions with saliva, 207–8
    stages and phenomena, 204–6
mozzarella cheese, 150–51, 153–5, 158*f*
mucin, 208, 227

NaCl, 94–5
National Dysphagia Diet project, 106
Newton, Isaac, 7
Newtonian behaviour, 8
Newtonian dashpots, 9
Newtonian model, 12*t*, 13, 134
Newtonian viscosity, 134, 145
nonfat dry milk (NDM), 146
non-Newtonian behaviour, 8, 12

oesophagus, 226*f*
oil-in-water emulsions, 200–203. *See also* emulsions
  addition of biopolymers, 202–3
  addition of proteins, 202
  addition of surfactants, 201–2
  effect of processing, 203
  instabilities in, 194–5
    coalescence, 194
    creaming, 195
    flocculation, 194–5
  pH and ionic strength, 201
  protein functionality at liquid interfaces, 196–200
    protein denaturation, 199–200
    protein displacement, 198–9
    protein-stabilised interfaces, 199
oil-water interfaces, 198–9
oligosaccharides, 244
oral cavity, 205*f*
oral mucosa, 225–6
oral processes, 203–9. *See also* sensory perception
  fluid dynamics, 206–7
  interactions with oral surfaces, 208–9
  interactions with saliva, 207–8
  stages and phenomena, 204–6
oscillation, 16–17
oscillatory shear, 10
oscillatory testing, 18–20
Ostwald-de Waele behaviour, 66
ovalbumin, 198

parallel plate rheometry, 24–5
partial fat replacement, 231–2
pasta sauce, 33*t*
pastes, 20–21
pasteurisation, 102
pectin, 3–5, 62*t*
pepsin, 227
pepsinogen, 227
perception, 173–90
  flavour, 176–9
  food formulation and, 221–6
  gels, 185–7
  in vitro measurements of, 209–13
  microstructure and, 181–3
  mixing and, 179–80
  mouthfeel, 184–5
  oral processing and, 165–7
  rheological properties of milk and, 145–6
  shear rheology and, 187–90
  thickness, 174–6
pH, 95–9
  effect on protein-stabilised emulsions, 201
  xanthan gum and, 95–9
    pH sensitivity of solution viscosity, 96–8
    stability at low pH, 98–9
phase angle, 16–17, 137, 148
phase lag, 18–19
phase separation, 71, 75–6
phenomenological rheology, 9
Pickering stabilisation, 231, 234
Plexiglas, 40
point-wise rheological characterisation, 46–7
polyacrylamide, 32*t*
polyamide, 52–4
poly-β-D-mannuronate, 121
polydimethylsiloxane, 33*t*
polydimethylsiloxane (PDMS), 210, 212
polygalacturonic acid, 62*t*
polyglycerol polyricinolate (PGPR), 232–3
polymannuronate, 115
polymer exclusion, 71
polysaccharides, 161, 165, 184
power law, 12, 12*t*
power law fluid model, 47–8, 134–5
Powell-Eyring model, 12*t*
Prandtl model, 12*t*
pressure denaturation, 200
pressure drop, 29–30, 46
Principia, 7
propagation, 41–2
propylene glycol alginate (PGA), 115
proteins, 99–100
  adsorption at oil-water interface, 197–8
  cross-linking, 165, 237

denaturation, 199–200
displacement, 198–9
functionality at liquid interfaces, 196–200
milk proteins, 99–100
xanthans and, 99–100
protein-stabilised emulsions, 200–203. *See also* emulsions
addition of biopolymers, 202–3
addition of proteins, 202
addition of surfactants, 201–2
effect of processing, 203
pH and ionic strength, 201
proteolysis, 150
Pseudomonas aeruginosa, 114
pulsed ultrasound, 29
pyloric sphincter, 226*f*
pyloris, 226*f*
pyruvate, 89

Rabinowitch correction, 22
rapeseed oil, 33*t*, 52–4
relative hysteresis, 161
relative viscosity, 140
rheological analysis, large-strain
cutting with wire, 156–7
torsion test, 155–6
uniaxial compression, 152–4
uniaxial tension, 154–5
vane method, 155–6
rheology, 1–3
aims, 2
applied, 10
case study, 3–5
criteria, 2–3
definition of, 1–2, 10
gel, 68–9
interpretive approach in, 1
literature, 7–8
measurements, 139–41
falling sphere method, 139
rotational viscometers, 141
U-tube capillary viscometers, 140–41
microstructure and, 20
perception and, 173–90
flavour, 176–9
gels, 185–7
in vitro measurements of, 209–13
microstructure and, 181–3
mixing and, 179–80
mouthfeel, 184–5
shear rheology and, 187–90
thickness, 174–6
phenomenological, 9
results, 3
of soft solids, 20–23
structural, 9
rheology, Doppler ultrasound-based, 29–54
acoustic properties, 41–5
attenuation, 42
backscattering, 43–5
propagation, 41–2
scattering, 43
sound velocity, 42–3
Carbopol solution, 50–51
Doppler angle, 40–41
electronics, 45
flow adapters, 39–40
fluids and suspensions used, 32–3*t*
measurement parameters, 34–5*t*
models, 46–8
gradient method, 46–7
Herschel-Bulkley fluid model, 48
point-wise rheological characterisation, 46–7
power law fluid model, 47–8
profile estimation, 45
publications, 31–8
rheometry, 49–50
averaging effects at pipe wall, 49
fitting, 49
gradient method, 50
signal processing, 45
software, 45–6
suspension of polyamide in rapeseed oil, 52–4
transducers, 38–9
rheometers, 21–3
capillary, 21–2
controlled stress vs. controlled strain, 24*f*
squeeze flow, 22–3

rheometry, 9–10, 23–6
  capillary, 26
  concentric cylinder, 25
  cone-and-plate, 23–4
  in Doppler ultrasound-based rheology, 49–50
    averaging effects at pipe wall, 49
    fitting, 49
    gradient method, 50
  dynamic/oscillatory shear, 10
  parallel plate, 24–5
  steady shear characterization, 10
  vane, 25–6, 25*f*
rheopexy, 14
rotational viscometers, 141

Saccharina japonica, 113
salad dressings, 104–5
Salep glycomannan, 138
saliva, 207–8
salt reduction, 234–5
salts, 93–5
saturated fatty acids (SAFA), 244
scattering, 43
seafood chowder, 33*t*
sedimentation, 195
segregative phase separation, 78
self-structuring systems, 245–9
  alginate, 245–6
  gellan, 247–9
semi-fluids, 8
semi-solid dairy foods, 159–65. *See also* cheese; fluid milk
  flow properties, 159–63
  hysteresis loop, 160–61
  time-dependent flow behaviour characterisation, 159–63
  viscoelastic properties of, 164–5
  yield stress, 163–4
sensory perception, 173–90
  flavour, 176–9
  food formulation and, 221–6
  gels, 185–7
  in vitro measurements of, 209–13
  microstructure and, 181–3
  mixing and, 179–80
  mouthfeel, 184–5
  oral processing and, 165–7, 203–9
    fluid dynamics, 206–7
    interactions with oral surfaces, 208–9
    interactions with saliva, 207–8
    stages and phenomena, 204–6
  rheological properties of milk and, 145–6
  shear rheology and, 187–90
  thickness, 174–6
shampoo, viscosity of, 2
shear, 10
shear flow, 10–16
  rheological models, 11–15
    time-dependent flow models, 14–15
    time-independent flow models, 11–14
  wall slip, 15–16
shear loss compliance, 17
shear loss modulus, 17
shear rate, 11*f*, 12, 13*f*, 46, 137, 160–61
shear storage compliance, 17
shear storage modulus, 16–17
shear strain, 68
shear stress, 11*f*, 12, 13*f*, 68
  correction, 22
  wall, 21–2
shear stress amplitude, 18
shear stress decay, 161–3
sheared gels, 238–41
shear-thinning, 13, 135, 137
Sisko model, 12*t*, 13–14
skim milk, viscosity of, 142–3
small amplitude oscillatory tests, 148–51
smoothness, 221
Snell's law, 41
soft solids, 20–23, 204
sound velocity, 42–3
squeeze flow rheometers, 22–3
stabiliser, 126–7
stage I transport, 204
stage II transport, 204
starch, 62*t*, 101, 106–8, 178–9
steel pipes, 40
sterilisation, 101–2
Stokes-Einstein equation, 195
stomach, food in, 226–8
storage and dispatch, 17
storage modulus, 17, 19, 68, 148

strawberry yoghurt, 33*t*
stress relaxation test, 158–9
Stribeck curve, 210–11
structural kinetic model, 162–3
structural rheology, 9
surface denaturation, 199
surfactants, 32*t*, 196, 201–2
Swedish Institute for Food and Biotechnology, 36–7
Swiss Federal Institute of Technology, 36

tan delta, 17
tara gum, 86
tensile testing, 154–5
texture perception, 165–7
texturisation of vegetative materials, 126
thermal denaturation, 200
thickeners, 106–8
thickening agent, 124–5
thickness, 221
thickness perception, 174–6
thixotropy, 14, 160–61
time-dependent flow models, 14–15
time-independent flow models, 11–14
tomato sauce, 33*t*
torsion test, 155–6
transducers, 38–9
tribology, 223–4
Trouton's law, 68
time sweep, 149

ultra high temperature (UHT) sterilisation, 102
ultrasonic velocimetry, history of, 30–31
ultrasonic velocity profiling (UVP), 29–30
  history of, 30–31
  literature, 31–8
ultrasonic velocity profiling (UVP)-pressure drop (PD) method, 29–54
  acoustic properties, 41–5
    attenuation, 42
    backscattering, 43–5
    propagation, 41–2
    scattering, 43
    sound velocity, 42–3
  Carbopol solution, 50–51
  Doppler angle, 40–41
  electronics, 45
  flow adapters, 39–40
  fluids and suspensions used, 32–3*t*
  measurement parameters, 34–5*t*
  models, 46–8
    gradient method, 46–7
    Herschel-Bulkley fluid model, 48
    point-wise rheological characterisation, 46–7
    power law fluid model, 47–8
  profile estimation, 45
  rheometry, 49–50
    averaging effects at pipe wall, 49
    fitting, 49
    gradient method, 50
  signal processing, 45
  software, 45–6
  suspension of polyamide in rapeseed oil, 52–4
  transducers, 38–9
uniaxial compression, 152–4
uniaxial tension, 154–5
Urick equation, 43
uronic acid, 114
U-tube capillary viscometers, 140–41

vane method, 156
vane rheometry, 25–6, 25*f*
vegetable sauces, 33*t*
vegetative materials, texturisation of, 126
viscoelasticity, 16–17
  measurement of, 137–8
  oscillatory testing, 18–20
viscometer, 9
viscometers
  falling sphere method, 139
  rotational, 141
  U-tube capillary, 140–41
viscosity, 10–16
  apparent, 135, 145
  complex, 16, 138
  definition of, 10
  dynamic, 16

viscosity (*Continued*)
infinite-shear, 67, 137
intrinsic, 63–4
limiting, 13
Newtonian, 134, 145
relative, 140
rheological models, 11–15
time-dependent flow models, 14–15
time-independent flow models, 11–14
wall slip, 15–16
zero-shear, 67, 137
viscous flow, 10
voxel, 44

wall shear rate, 21–2
wall shear stress, 21–2
wall slip, 15–16
water-in-water emulsions, 241–5. *See also* emulsions
Weltmann model, 161–2
whey proteins, 143, 165
Williamson model, 12*t*
wine gums, 3–5
wire cutting test, 156–7
Wood equation, 43

xanthan gum, 85–110
applications, 106–8
conformational states of, 91–2
food ingredients and effects on functionality, 93–103
acids, 95–9
proteins, 99–100
salts, 93–5
starch, 101
food processing and, 101–3
freezing, 103
homogenisation, 102
thermal treatment, 101–2
food structures, 104–5
emulsions, 104–5
gels, 105
future trends, 108–10
gel strength with locust bean gum, 90–91
gelling conditions, 62*t*
guar galactomannan and, 78
interactions with galactomannans, 86–7, 91
molecular structure, 62*t*, 85–91
primary structure, 89*f*
pyruvate content, 89
rheology and, 85–6
trisaccharide side chain, 88
pH and, 95–9
pH sensitivity of solution viscosity, 96–8
stability at low pH, 98–9
synergistic interactions, 70–71
thickening conditions, 62*t*
Xanthomonas campestris, 85, 90
xyloglucan, 72

Yasuda constant, 137
yield stress, 10–11, 161–3
yoghurt, 160–61
Young modulus, 152

zero-shear viscosity, 67, 137

Food Science and Technology

WILEY-BLACKWELL

GENERAL FOOD SCIENCE & TECHNOLOGY AND FOOD PROCESSING

Food Flavour Technology 2E	Taylor	9781405185431
Food Mixing: Principles and Applications	Cullen	9781405177542
Functional Food Product Development	Smith	9781405178761
Confectionery and Chocolate Engineering	Mohos	9781405194709
Industrial Chocolate Manufacture and Use (4th Edition)	Beckett	9781405139496
Chocolate Science and Technology	Afoakwa	9781405199063
Essentials of Thermal Processing	Tucker	9781405190589
Calorimetry in Food Processing: Analysis and Design of Food Systems	Kaletunc	9780813814834
Fruit and Vegetable Phytochemicals	de la Rosa	9780813803203
Water Properties in Food, Health, Pharma and Biological Systems	Reid	9780813812731
Nutraceuticals,Glycemic Health and Type 2 Diabetes	Pasupuleti	9780813829333
Nutrigenomics and Proteomics in Health and Disease	Mine	9780813800332
Food Science and Technology (textbook)	Campbell-Platt	9780632064212
IFIS Dictionary of Food Science and Technology 2nd Edition	IFIS	9781405187404
Sensory Evaluation: A Practical Handbook	Kemp	9781405162104
Statistical Methods for Food Science	Bower	9781405167642
Drying Technologies in Food Processing	Chen	9781405157636
Biotechnology in Flavor Production	Havkin-Frenkel	9781405156493
Frozen Food Science and Technology	Evans	9781405154789
Sustainability in the Food Industry	Baldwin	9780813808468
Kosher Food Production 2nd Edition	Blech	9780813820934
Dictionary of Flavors 2nd Edition	DeRovira	9780813821351
Whey Processing, Functionality and Health Benefits	Onwulata	9780813809038
Nondestructive Testing of Food Quality	Irudayaraj	9780813828855
High Pressure Processing of Foods	Doona	9780813809441
Concept Research in Food Product Design and Development	Moskowitz	9780813824246
Water Activity in Foods	Barbosa-Canovas	9780813824086
Food and Agricultural Wastewater Utilization and Treatment	Liu	9780813814230
Multivariate and Probabilistic Analyses of Sensory Science Problems	Meullenet	9780813801780
Applications of Fluidisation in Food Processing	Smith	9780632064564
Encapsulation and Controlled Release Technologies in Food Systems	Lakkis	9780813828558
Accelerating New Food Product Design and Development	Beckley	9780813808093
Chemical Physics of Food	Belton	9781405121279
Handbook of Organic and Fair Trade Food Marketing	Wright	9781405150583
Sensory and Consumer Research in Food Product Design and Development	Moskowitz	9780813816326
Sensory Discrimination Tests and Measurements	Bi	9780813811116
Food Biochemistry and Food Processing	Hui	9780813803784
Handbook of Fruits and Fruit Processing	Hui	9780813819815
Food Processing - Principles and Applications	Smith	9780813819426
Food Supply Chain Management	Bourlakis	9781405101684

SEAFOOD, MEAT AND POULTRY

Handbook of Seafood Quality, Safety and Health Effects	Alasalvar	9781405180702
Fish Canning Handbook	Bratt	9781405180993
Fish Processing – Sustainability and New Opportunities	Hall	9781405190473
Fishery Products: Quality, safety and authenticity	Rehbein	9781405141628
Thermal Processing for Ready-to-Eat Meat Products	Knipe	9780813801483
Handbook of Meat Processing	Toldra	9780813821825
Handbook of Meat, Poultry and Seafood Quality	Nollet	9780813824468

BEVERAGES & FERMENTED FOODS/BEVERAGES

Beverage Industry Microfiltration	Starbard	9780813812717
Wine Quality: Tasting and Selection	Grainger	9781405113663
Handbook of Fermented Meat and Poultry	Toldra	9780813814773
Microbiology and Technology of Fermented Foods	Hutkins	9780813800189
Carbonated Soft Drinks	Steen	9781405134354
Brewing Yeast and Fermentation	Boulton	9781405152686
Food, Fermentation and Micro-organisms	Bamforth	9780632059874
Wine Production	Grainger	9781405113656
Chemistry and Technology of Soft Drinks and Fruit Juices 2nd Edition	Ashurst	9781405122863
Technology of Bottled Water 2nd Edition	Senior	9781405120388
Wine Flavour Chemistry	Clarke	9781405105309

BAKERY & CEREALS

Whole Grains and Health	Marquart	9780813807775
Gluten-Free Food Science and Technology	Gallagher	9781405159159
Baked Products - Science,Technology and Practice	Cauvain	9781405127028
Bakery Products Science and Technology	Hui	9780813801872
Bakery Food Manufacture and Quality 2nd Edition	Cauvain	9780632053278
Pasta and Semolina Technology	Kill	9780632053490

For further details and ordering information, please visit www.wiley.com/go/food

Food Science and Technology from Wiley-Blackwell

FOOD SAFETY, QUALITY AND MICROBIOLOGY		
The Microbiology of Safe Food 2nd Edition	Forsythe	9781405140058
Food Safety for the 21st Century	Wallace	9781405189118
Microbial Safety of Fresh Produce	Fan	9780813804163
Biotechnology of Lactic Acid Bacteria: Novel Applications	Mozzi	9780813815831
HACCP and ISO 22000 - Application to Foods of Animal Origin	Arvanitoyannis	9781405153669
Food Microbiology: An Introduction 2nd Edition	Montville	9781405189132
Management of Food Allergens	Coutts	9781405167581
Campylobacter	Bell	9781405156288
Bioactive Compounds in Foods	Gilbert	9781405158756
Color Atlas of Postharvest Quality of Fruits and Vegetables	Nunes	9780813817521
Microbiological Safety of Food in Health Care Settings	Lund	9781405122207
Control of Food Biodeterioration	Tucker	9781405154178
Advances in Thermal and Nonthermal Food Preservation	Tewari	9780813829685
Biofilms in the Food Environment	Blaschek	9780813820583
Food Irradiation Research and Technology	Sommers	9780813808826
Preventing Foreign Material Contamination of Foods	Pearlso	9780813816395
Aviation Food Safety	Sheward	9781405115810
Food Microbiology and Laboratory Practice	Bell	9780632063819
Listeria 2nd Edition	Bell	9781405106184
Preharvest and Postharvest Food Safety	Beier	9780813808840
Shelf Life	Man	9780632056743
HACCP	Mortimore	9780632056484
Salmonella	Bell	9780632055197
PACKAGING		
Packaging Research in Food Product Design and Development	Moskowitz	9780813812229
Packaging for Nonthermal Processing of Food	Han	9780813819440
Packaging Closures and Sealing Systems	Theobald	9781841273372
Modified Atmospheric Processing and Packaging of Fish	Otwell	9780813807683
Paper and Paperboard Packaging Technology	Kirwan	9781405125031
Food Packaging Technology	Coles	9781841272214
Canmaking for Can Fillers	Turner	9781841272207
DAIRY FOODS		
Technology of Cheesemaking 2nd Edition	Law	9781405182980
Dairy Fats	Tamime	9781405150903
Bioactive Components in Milk and Dairy Products	Park	9780813819822
Milk Processing and Quality Management	Tamime	9781405145305
Dairy Powders and Concentrated Products	Tamime	9781405157643
Cleaning in Place	Tamime	9781405155038
Advanced Dairy Technology	Britz	9781405136181
Dairy Processing and Quality Assurance	Chandan	9780813827568
Structure of Dairy Products	Tamime	9781405129756
Brined Cheeses	Tamime	9781405124607
Fermented Milks	Tamime	9780632064588
Manufacturing Yogurt and Fermented Milks	Chandan	9780813823041
Handbook of Milk of Non-Bovine Mammals	Park	9780813820514
Probiotic Dairy Products	Tamime	9781405121248
INGREDIENTS		
Enzymes in Food Technology 2nd Edition	Whitehurst	9781405183666
Food Stabilisers, Thickeners and Gelling Agents	Imeson	9781405132671
Glucose Syrups - Technology and Applications	Hull	9781405175562
Handbook of Vanilla Science and Technology	Havkin-Frenkel	9781405193252
Fish Oils	Rossell	9781905224630
Weight Control and Slimming Ingredients in Food Technology	Cho	9780813813233
Prebiotics and Probiotics Handbook	Jardine	9781905224524
Food Colours	Emerton	9781905224449
Sweeteners	Wilson	9781905224425
Sweeteners and Sugar Alternatives in Food Technology	Mitchell	9781405134347
Emulsifiers in Food Technology	Whitehurst	9781405118026
Food Additives Data Book	Smith	9780632063956
FOOD LAWS & REGULATIONS		
BRC Global Standard – Food	Kill	9781405157964
Food Labeling Compliance Review 4th Edition	Summers	9780813821818
Guide to Food Laws and Regulations	Curtis	9780813819464
Regulation of Functional Foods and Nutraceuticals	Hasler	9780813811772
OILS & FATS		
Trans Fatty Acids	Dijkstra	9781405156912
Rapeseed and Canola Oil - Production, Processing, Properties and Uses	Gunstone	9781405116251
Vegetable Oils in Food Technology	Gunstone	9781841273310
Fats in Food Technology	Rajah	9781841272252
Edible Oil Processing	Hamm	9781841270388

For further details and ordering information, please visit www.wiley.com/go/food